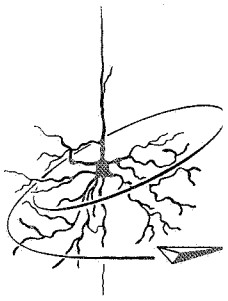

First Quarterly Report

FORMULATION OF THEORETICAL BASIS FOR ANALYSIS AND SYNTHESIS OF ADVANCED SELF-ORGANIZING CONTROL SYSTEMS

Contract No.: NAS5-10149

Prepared for

Goddard Space Flight Center
Greenbelt, Maryland

ADAPTRONICS, INC
WESTGATE RESEARCH PARK
7700 OLD SPRINGHOUSE ROAD • McLEAN, VIRGINIA 22101

First Quarterly Report

FORMULATION OF THEORETICAL BASIS FOR ANALYSIS AND SYNTHESIS OF ADVANCED SELF-ORGANIZING CONTROL SYSTEMS

(17 Mar., 1966 - 16 Jun., 1966)

Contract No.: NAS5-10149

L. O. Gilstrap, Jr., S. Schalkowsky
R. M. McKechnie, III, R. L. Barron, C. W. Armstrong

Prepared by

ADAPTRONICS, Inc.
Westgate Research Park
7700 Old Springhouse Road
McLean, Virginia 22101

for

Goddard Space Flight Center
Greenbelt, Maryland 20771

FOREWORD

This is the first quarterly technical report prepared by Adaptronics, Inc., McLean, Virginia under the terms of National Aeronautics and Space Administration Contract No. NAS5-10149.

L. O. Gilstrap, Jr. has been the principal author of this report. To him is due the material in Section 2 and Appendix II, dealing with pulse density code theory and its application to mathematical modeling of the self-organizing controller. R. M. McKechnie, III performed the analog computer simulations and hardware tests described in Section 3 and is the author of that section; in his work he was assisted by D. Cleveland and G. Mowles. S. Schalkowsky prepared the Bayesian formulation of statistical source behavior that is presented in Section 4; he authored most of that section, except for the Monte Carlo simulations, which were performed by C. W. Armstrong, and the further hardware experiments, which were conducted by McKechnie. H. J. Cook authored Appendix I. Mr. R. F. Snyder has participated in some of the numerical analysis tasks. R. L. Barron, project manager for Adaptronics, Inc. is responsible for the general content of this report and the work it describes.

The authors are indebted to Mr. James A. Gatlin of Goddard Space Flight Center, Greenbelt, Maryland, who has served as project monitor for NASA and has made innumerable valuable suggestions in the course of this research. His many important contributions and those of Mr. Clarence Cantor, also with GSFC, are gratefully acknowledged.

This investigation has indirectly benefitted from a related research program in self-organizing control systems theory engaged in by Adaptronics, Inc. for the United States Air Force under Contract No. AF 33(615)-3673, sponsored by the Bionics Branch, Avionics Laboratory (RTD), Air Force Systems Command, Wright-Patterson Air Force Base, Ohio.

ABSTRACT

This first quarterly report presents the development of a mathematical model of Probability State Variable (PSV) conditioning logic of a type used in self-organizing control systems. Results of analog computer simulations of the model are provided and these results are compared with those obtained using the hardware PSV controller. Behavior of the mathematical model is shown to be in close agreement with the behavior of the PSV controller.

TABLE OF CONTENTS

TABLE OF CONTENTS
(Continued)

LIST OF FIGURES

LIST OF FIGURES
(Continued)

LIST OF FIGURES
(Continued)

LIST OF FIGURES
(Continued)

LIST OF FIGURES
(Continued)

LIST OF TABLES

1. INTRODUCTION AND SUMMARY

1.1 Scope

This is the first quarterly progress report under Goddard Space Flight Center contract NAS5-10149 covering the study of self-organizing control systems for spacecraft applications. As defined in Article 1 of the contract, submission of the first quarterly report is associated with the completion of Phase I of the program dealing with the development of "a mathematical model of a Probability State Variable (PSV) in terms of input/output characteristics; that is, as an isolated element". This report describes the mathematical model evolved during the past three months to define the principal functional characteristics of PSV conditioning logic. Results of simulations of this model are presented and it is shown that the behavior of the model is in close agreement with the behavior of PSV hardware.

1.2 Background

Reference 1 describes the results of an investigation of a self-organizing controller (SOC) developed for piloted aircraft. Extensive simulations were conducted in the program using laboratory experimental SOC equipment. Work is now in progress at Adaptronics to fabricate this SOC for flight testing next year in a high-performance aircraft. This work is sponsored by the Air Force Flight Dynamics and Avionics Laboratories, Research and Technology Division, Air Force Systems Command, Wright-Patterson Air Force Base, Ohio, under contract AF 33(615)-5141.

The present study of SOC systems for spacecraft applications partly parallels research work at Adaptronics sponsored by the Air Force Avionics Laboratory under Contract AF 33(615)-3673. The Air Force Research program is a three-year effort planned to involve primarily advanced SOC synthesis studies, simulations and analyses of single-axis and multiple-axis SOC systems (with emphasis on aeronautical applications), development of the theory of parameter space search, and development of performance assessment techniques (Ref. 2). Generally speaking, this Air Force sponsored research relates to self-organizing systems for operational employment in about five to ten years, whereas work on the subject contract can be related to systems for operational use at an earlier time.

The investigation described in the present report has as its point of departure an existing design of self-organizing controller which, in past evaluations, has demonstrated a number of desirable characteristics. Furthermore, the projection of demonstrated performance and design features to control applications of greater complexity than those tried to date indicates a potential not available in current control system designs.

Self-organizing control is fundamentally different from self-adaptive control, although the two approaches have some elements of theory and practice in common. A detailed contrastive analysis of self-adaptive and self-organizing control is beyond the scope of the investigation but Reference 3 describes some of the common origins of these two forms. The Adaptronics self-organizing controller was designed with the recognition that the sine qua non of good control is the proper signal to an actuator, and not information as to the parameters of the plant or of the

controller. With high-speed digital techniques available, there is little difficulty in performing the necessary control processing to generate actuator excitation signals using the SOC approach. The digital mechanization helps achieve satisfactory control in the presence of high sensor noise, while use of the PSV (directed) random search process tends to increase efficiency of the SOC in comparison with conventional multiple-variable controllers. Furthermore, the random processed used in the Adaptronics SOC serve to break up the periodicity of limit cycles, and the amplitude of any plant limit-cycle activity with the SOC tends to decay to within approximately the expected sensor noise levels.

1.3 Objectives of the Modeling

The objective of the effort leading to this first quarterly report has been to provide mathematical models of the PSV unit and the functional components which make up this unit. Analysis of the performance assessment unit which, with the PSV unit, makes up a complete self-organizing controller, has been defined by monitoring personnel to be outside the scope of the Phase I (first-quarter) study. Specific system configurations and application aspects have thus far entered into the investigation only by way of basic simulations performed to evaluate validity of the PSV model.

In more specific terms, the functions which have been modeled in this study are all those of the PSV unit elements: the biasing logic, the p register, the statist'ical source, the feedback delay, and the u register. These elements are described in Appendix I; while the description in the first appendix does constitute a "model" of an SOC in that all functions and rules of operation are defined (hence, can be

simulated on a digital computer), the design engineer needs a simple model that will allow him to estimate total system performance in simulations and analyses of a variety of situations. Thus, our investigations have been oriented toward obtaining continuous approximations of the PSV elements, and of the PSV unit as a whole in terms of conventional multipliers, filters, relays, delays, saturating amplifiers, etc.

Whenever an attempt is made to model mathematically a physical process, a trade-off exists between the range of validity of the model and its complexity. For the purpose of this investigation, we have accepted one important limitation on the validity of the model, i.e., we have concerned ourselves chiefly with a single-PSV system. It is expected that the performance of multiple-PSV systems (using unified performance assessment means for the distribution of actuation signals) will prove to be superior to the performance which would be predicted by the present model for multivariable cases. Less noticeable, but also of great potential importance, might be the differences between the behavior of the model and of the PSV hardware in application to high-order and/or nonlinear plants, using either one or more PSV units. Here it is expected that the randomized "sliding mode" (see discussion) and steady-state behavior of the PSV hardware will prove to be superior to that indicated by the model.

1.4 Approaches Taken

The primary approach taken in this investigation has been the development of a theory of pulse density codes and application of this theory to modeling of elements in the PSV unit. The theoretical development has been supported by analog computer simulations of the pulse density model and comparison of the results so obtained with those of PSV hardware

units. In addition, several empirically-derived models have been simulated as a means of gaining further understanding of the PSV unit characteristics. These empirical models have consisted of (1) relay controllers, *(2)* a proportional controller with limiting, and (3) a "variable structure" controller which is described in the recent Soviet literature.

For most of the simulations, it has been desirable to consider closed-loop cases, and for this purpose a representative second-order plant was chosen. Other experiments have been conducted with PSV hardware in an open-loop configuration to obtain hardware input-output characteristics as an additional means of verifying the pulse density model.

1.5 Results Achieved

The pulse density model of the PSV unit has proven to be very tractable, consisting in the simplest case of only three elements, a multiplier, a lag filter, and a sign detector, with the latter two elements connected in a simple feedback loop around the multiplier as shown below in Figure 1.1. This simple model has been found to replicate closely the behavior of PSV hardware. It is concluded that the theoretically-derived model is valid subject only to the limitations indicated above (Section 1.3).

The pulse density model of the PSV unit should greatly facilitate application of design and analysis of self-organizing control systems for spacecraft. During Phase II of this work, models will be developed for single and multiple control loops which use the PSV unit as a key element.

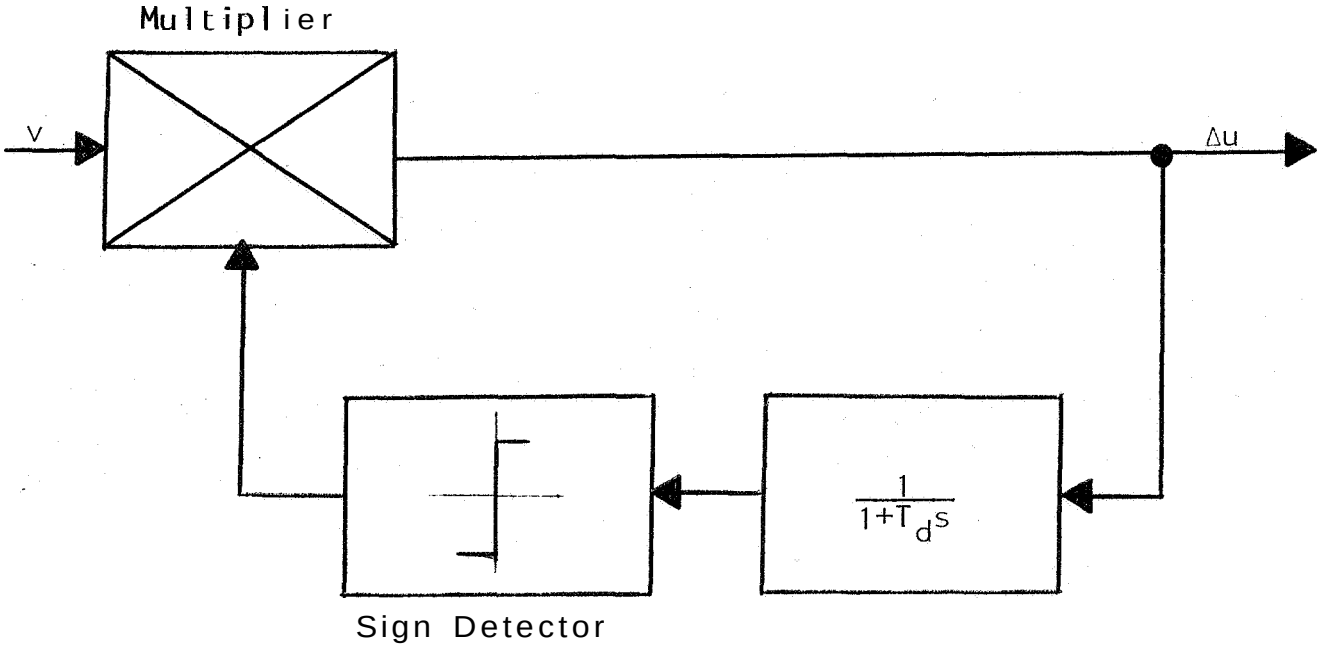

v = value-function signal (from performance assessment unit)

Δu = output of SOC

Figure 1.1: Simplest-Case Pulse Density Model of PSV Unit

1.6 Organization of this Report

Section 2 of this report presents the theoretical development of the pulse density model and a discussion of the mathematical properties of this model. In Section 3, the pulse density model is compared with several empirically-derived models and a physical interpretation of these models is given in terms of both regenerative/degenerative loop operation and the quasi-linear operation which is achieved by the dithering action. Section 3 emphasizes the simulation and bench tests conducted to evaluate the pulse density and empirical models and compares their performance with that of PSV hardware.

Because the models thus far developed do not explicitly involve the statistical source (inasmuch as the effects of

this source are negligible within the framework of the defined problem), Section 4 discusses the important role of the statistical source in both single and multiple PSV systems and presents the results of digital computer and hardware experiments performed to obtain an accurate characterization of the statistical source properties. Of particular interest in Section 4 is the theoretical application of Bayes' Theorem to analysis and design of the statistical source.

Recommendations and conclusions are presented in Sections 5 and 6.

Appendix I is a description of the PSV and performance assessment functions. Appendix II details the pulse density code theory underlying the development of the PSV model.

2. THEORETICAL DEVELOPMENT

It follows readily from Appendix II that the (high frequency) pulse train output of a digitally mechanized self-organizing controller is integrated out to an ordinary analog signal by any actuator with a lag characteristic. Thus, we can analyze SOC behavior in terms of the parameters of its pulse trains at various locations or stations throughout the device. From this, we can conclude that SOC analysis could follow conventional lines established for nonlinear control systems with noise, These methods include power density spectrum or autocorrelation function as well as such novel methods as statistical linearization (Ref. 4). Further, although it should be possible *to* synthesize self-organizing controllers by more familiar analog circuits, desirability of doing so is debatable in view of the simplicity and reliability of present day integrated logic devices.

The utility of pulse density signal theory in the analysis of self-organizing control is that it enables us to relate the functions of logic gates and other digital devices to the functions of more conventional analog components. However, pulse density signal theory, at this stage of development, is still based upon mean or expected values of pulse train parameters, and the role of noise and noise generators in control systems can presently only be imperfectly assessed and modeled.

Even though it is possible to develop a formal model of the PSV, complete mathematical analysis of the device is quite difficult for two reasons:

1. the PSV is a learning machine in that it acquires information about the environment and uses this acquired information in its primary function of control;

2. the PSV is highly nonlinear, and, in addition, uses noise in a direct manner as part of its excitation of the actuator.

The learning element in a PSV introduces a new dimension into control -- that of spontaneous, but carefully controlled, experimentation with the environment. The noise output of the statistical source, which produces the experimentation, continually drives the controller and produces a dynamic stability of apparently novel character. Although the effects of the statistical source can be simulated without noise in single-axis, single-PSV configurations, we have not yet been able to arrive at a simulation *of* its effects in the multiple-PSV case.

The strong nonlinearity in the PSV models constitutes a formidable obstacle to the development of satisfactory analytical treatment. However, as is noted in Section 3 of this report, simulated analog equivalents of the PSV elements provide control action that is quite similar to that of the PSV hardware under a variety of conditions. On the positive side, we conclude from this that the use of pulse train parameters is valid for the controllers under consideration and that, at least, the first step toward a satisfactory analytical treatment of self-organizing control has been completed.

2.1 PSV Elements and Model Assumptions

The major elements of the PSV can be considered to be:

1. the logic gates

2. the sampling gates for the p register

3. the p register

4. the statistical source

5. the Δu feedback delay

6. the u register

Since the u register serves primarily as a short transport lag or as a simple delay, it will be largely ignored in the material that follows and the PSV can be treated as consisting of the first five items in the above list. This point of view can be justified theoretically and it has been verified experimentally.

The objective in this section will be to summarize the transformations on the relative duty cycle of the input signal, v, through the PSV unit to the Δu output. Since this treatment is limited to the relative duty cycle parameters of the pulse trains, we will use a notation which is simplified for this purpose. Figure 2.1 shows the various locations *of* stations within the PSV. These station numbers will be used to subscript the pulse parameters of interest to'us.

The logic gating in the PSV, as described in Appendix I, is

$$v\Delta u + \overline{v\Delta u}$$

This gating is the complement of the exclusive "OR". As is shown in Appendix II, this gating logic provides the product

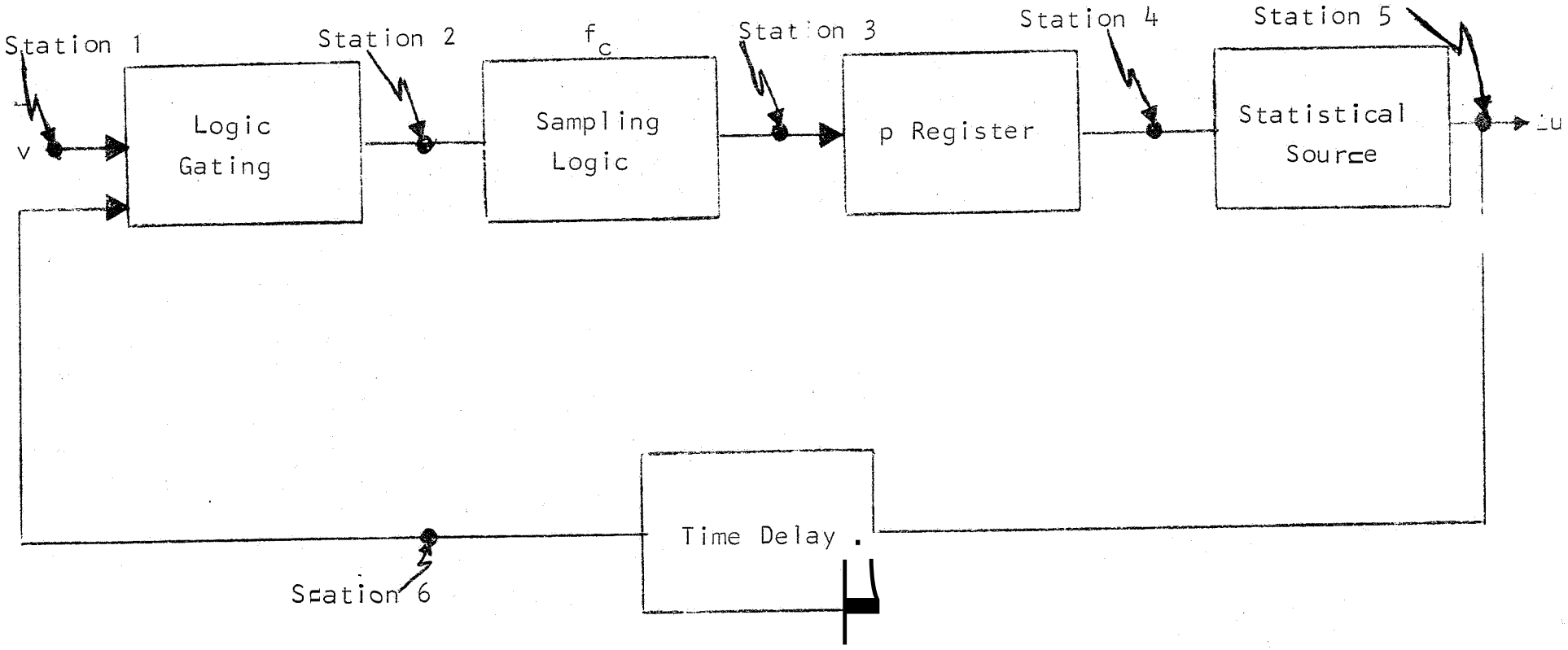

Figure 2 1: Diagram of Station Locations for Pulse Density Signal Analysis of PSV Unit

of the Z-parameters of its input variables:

$$Z_2 = Z_1 Z_6 \quad \text{.....} \quad 2:1$$

The sampling logic for the counter is the same as that for case 2b of Appendix II. However, the clock frequency, f_c, is extremely high with respect to the time constant of the actuator in most physically realizable systems, so that the normalized counter output, Z_4, becomes a multilevel pulse-width modulated signal identical to Z_2, except that it is delayed by about three clock pulses. Defining

$$T_P = 3T_c \quad \text{.....} \quad 2:2$$

as the delay introduced by the p register, we obtain

$$Z_4(t) = Z_2(t - T_p) \quad \text{.....} \quad 2:3$$

In other words, the p register acts primarily as a transport lag in the PSV.

The shift register which holds the Δu feedback from the statistical source for a period of time, T_d, is also a transport lag and can be represented by

$$Z_6(t) = Z_5(t - T_d) \quad \text{.....} \quad 2:4$$

where T_d is the delay introduced by the shift register.

The statistical source has several functions in the PSV. Its primary function is to produce the experimentation required in the learning process. The relative duty cycle of the statistical source output is a function of the input control voltage. The output should properly be represented by the sum of duty cycle and a noise signal.

$$Z_5 = f(Z_4) + n \quad \ldots\ldots\ldots\ldots\ldots\ldots\ldots \quad 2:5$$

For ease of analysis, we can assume linearity of the statistical source transfer function:" and set

$$f(Z_4) = Z_4 \quad \ldots\ldots\ldots\ldots\ldots\ldots\ldots \quad 2:6$$

which leads us to

$$Z_5 = Z_4 + n \quad \ldots\ldots\ldots\ldots\ldots\ldots\ldots\ldots\ldots 2:7$$

Combining Equations 2:1, 2:3, 2:4, and 2:7, in accordance with Figure 2.1, we get

$$Z_5(t) = Z_1(t - T_p)\, Z_5(t - T_p - T_d) + n \quad \ldots\ldots\ldots 2:8$$

Equation 2:8 is a fairly accurate equation for the PSV. It is not a mathematically simple model, since it involves transport lags and noise, but various approximations can be used for simulation.

The first step in simplifying Equation 2:8 is to assume that $T_p = 0$. On physical grounds, this assumption can be justified easily, since all controllers must, of necessity, introduce a small delay. Experimentally, it has been noted that there is no observable difference whether a small delay, corresponding to the $3T_c$ value, is used for T_p or whether Z_2 is fed directly to the output. If anything, performance of the controller can be "improved"' by taking out the p-register delay. Hence, a first simplification is

---

*See Section 4 of this report.

'Within the context of the mathematical model only (see later discussion).

$$Z_5(t) = Z_1(t)\, Z_5(t - T_d) + n \qquad \text{.....2:9}$$

However, Equation *2:9* is still not analytically tractable.

There is no possibility of setting T_d to zero, since T_d is the time required for signals to propagate through the environment and come back as value signals. The multiplier, which provides the product Z_1 Z_c, provides the correlation of trial states with results. Without the delay, there would be no correlation of cause and effect, and control action would not be possible. In connection with this correlation, we can note that the p register acts as a decision device which sums up the evidence of the degree of correlation and tends to reduce the incidence of false alarm. Thus, although the p-register lag can be dispensed with for simulation purposes, it serves the useful role of reducing the effects of environmental and sensor noise in the total system.

Figure *2.2* shows the diagram of a circuit which performs the functions in Equation 2:9. Although various approximations to the transport lag, such as the Pade or Stubbs-Single, could be used in a simulation, there is a still simpler circuit which can be used if we take into account the interactions of the noise, the transport lag in the feedback circuit, and the p-register behavior. We previously pointed out that the p-register level tends to move up and down rapidly with respect to the time constant of the plant, and that its output, and consequently, the output of the statistical source which is controlled by the p register, tends to follow the Z_2 signal with but a slight delay. What this means is that the p register tends to drive rapidly to one limit or the other, depending on the algebraic sign of Z_2. Even though there is a slight dependence *of* the p-register rate on the magnitude of Z_2, the sign information is, by far, the more important. Hence,

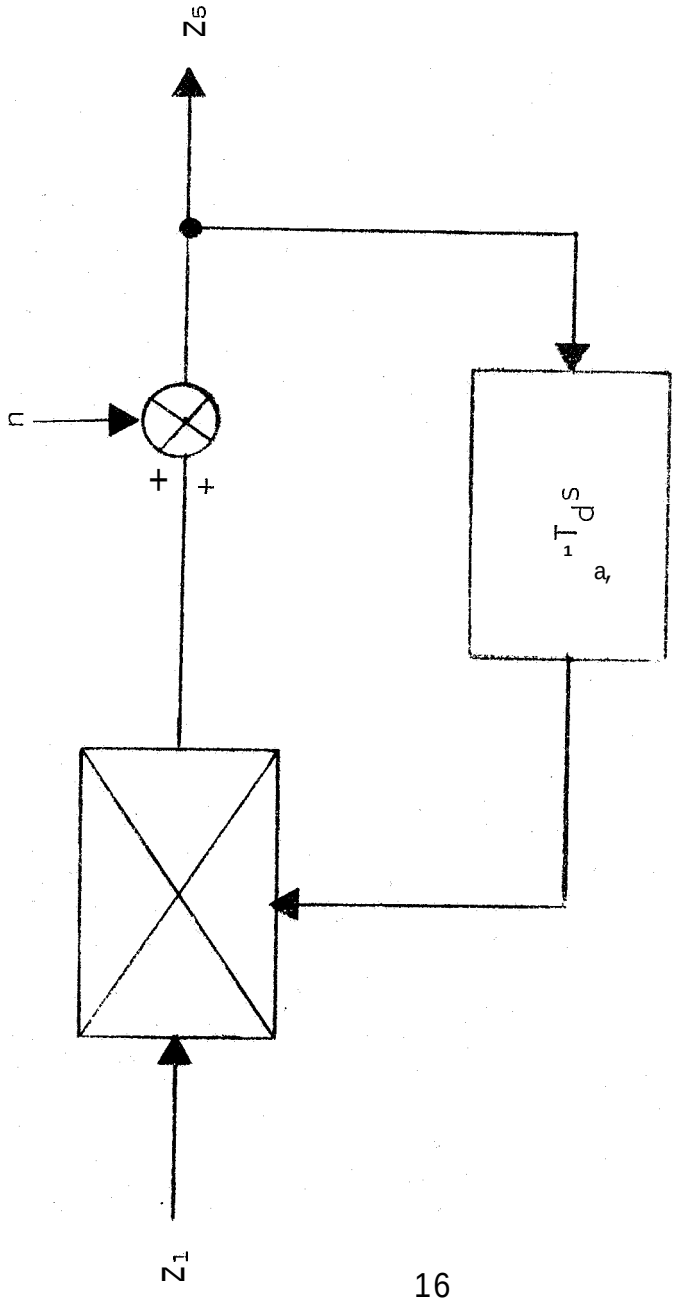

Figure 2.2: Simplified Transport-Lag Model of the PSV

we could insert a relay or hard limiter into the loop at station 2 to simulate this characteristic. However, putting the relay at station 2 would tend to exaggerate the effects of the p register. A better place to introduce the relay is at station 6 in the feedback loop as shown in Figure 2.3, since it still permits Z_5 to vary over a continuous range. There is a further benefit which can be obtained from placing the relay in the feedback circuit: the transport lag applies to the sign of Z_5 and not its magnitude, so that the combination of a first order lag and a relay constitute a fairly good transport lag.

One other feature of the model in Figure 2.2 should be noted. In the absence of noise, a Z_5 value of zero will remain at zero if the value propagates through the multiplier. The noise signal serves to prevent this "settling out" to a zero value. Again the hard limiter in the feedback loop serves a similar function in the PSV since it can take only the two values -1 and +1.

As is described in Section 4, the model in Figure 2.3 has been programmed on an analog computer. Variations of this model, which used lag circuits, $\frac{1}{1+T_p s}$ and $\frac{1}{1+T_u s}$, respectively, for the p-register and u-register delays, were also programmed. To check further on the effects of noise, it has been added to the input of the lag circuit corresponding to the p register. In all cases, excellent agreement has been obtained between the model behavior and PSV hardware behavior, provided that the model time constants were within one or two orders of magnitude of those required by pulse density theory.

2.2 Solution of the Model Equation

As a final point on the pulse density model of the PSV, it is possible to approximate Equation *2:9* to obtain analytical solutions.

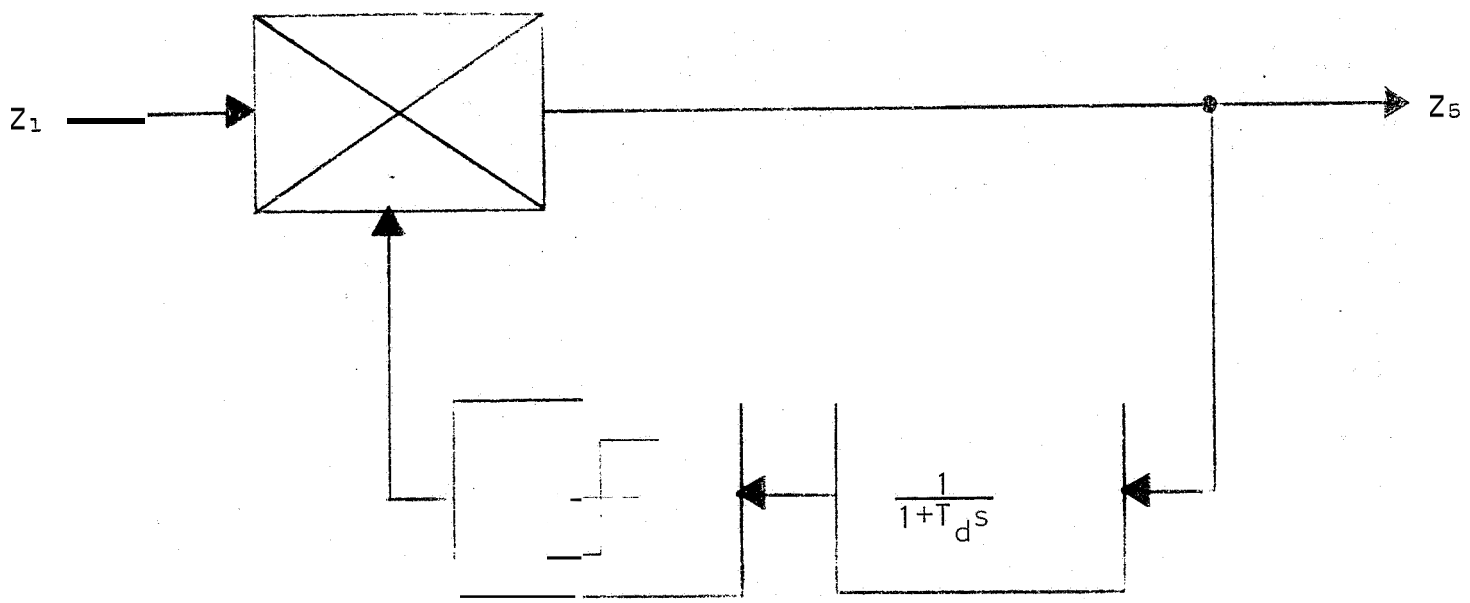

Figure 2.3: Simplified Model of the PSV with Lag Circuit and Relay

We will consider the two (important) special cases of $Z_1 = +1$ and $Z_1 = -1$. Since the expressions

$$Z_5(t) = Z_1(t)Z_5(t - T_d) \qquad \text{.....2:10}$$

and

$$Z_5(t + T_d) = Z_1(t + T_d)Z_5(t) \qquad \text{.....2:11}$$

mean the same, we can work with the second for simplicity.

Since $\dot{Z}_1 = 0$, $Z_1(t + T_d) = Z_1(t)$. Also

$$Z_5(t + T_d) \simeq Z_5(t) + T_d\dot{Z}_5(t) \qquad \text{.....2:12}$$

Hence,

$$Z_5 + T_d\dot{Z}_5 \sim Z_1Z_5 \qquad \text{.....2:13}$$

or

$$\dot{Z}_5 \simeq \frac{1}{T_d}Z_5(Z_1 - 1)$$

If $Z_1 = +1$, then $Z_5 \simeq 0$ or

$$Z_5 = Z_5|_{t=0} \qquad (Z_1 = +1) \qquad \text{.....2:14}$$

which indicates that Z_5 retains the value it had initially on a switch from a negative Z_1 to a value of $+1$. Putting it another way, the system (except for noise from the statistical source) tends to continue what it was previously doing.

If $Z_1 = -1$, then $\dot{Z}_5 \simeq -\frac{2}{T_d}Z_5$ or

$$Z_5 = Z_{5o}e^{-2t/T_d} \qquad (Z_1 = -1) \qquad \text{.....2:15}$$

which indicates that Z_5 decays to zero when Z_1 switches to a -1, regardless of the initial value of Z_5. Of course, the presence of the statistical source prevents Z_5 from remaining continuously at zero, and it will, in general, execute a rapid random walk with an average value of zero as seen by the plant.

In view of the assumptions required to obtain the above solutions, the quantitative significance of the solutions is debatable, even though qualitatively, they appear reasonably close, In particular, we know from experiments that when $Z_1 = +1$, the system tends to drive to a limit fairly rapidly, rather than remaining constant. The physical interpretation of the model is discussed further in the section which follows.

3. SIMULATIONS AND SOC HARDWARE TESTS

3.1 Open Loop Tests and Simulations

To insure completely that behavior of the PSV model adequately represents that of the hardware, it is necessary to perform open-loop and closed-loop tests and simulations. When sufficient proof is presented that the model behaves properly in each of these configurations, it becomes reasonable to assume that one has an adequate model.

For comparative purposes, similar tests and simulations have been performed on both the model and the hardware. Results of these tests and simulations are presented in this section as evidence that the model behavior is representative of PSV operation.

3.1.1 SOC Hardware

Figure 3.1 is a matrix of the PSV statistical decision device (SDD) internal signal-to-noise ratios, R, based on the p-register analog output voltage, or probability control voltage (PCV), and the noise-generator voltage. This ratio is useful in quantitative determination of "rich" vs. "lean" PSV noise. The ratio R is a pseudo signal-to-noise figure, because the PCV does not easily lend itself to measurement or calculation in the true RMS voltage sense. Therefore, maximum values of the PCV have been measured on a DC VTVM and transformed to a pseudo RMS value by means of the formula

$$RCV_{RMS} = \sqrt{\frac{V_{DC}^2}{2}}$$

where V_{DC} is a zero-to-peak measurement. The noise voltage

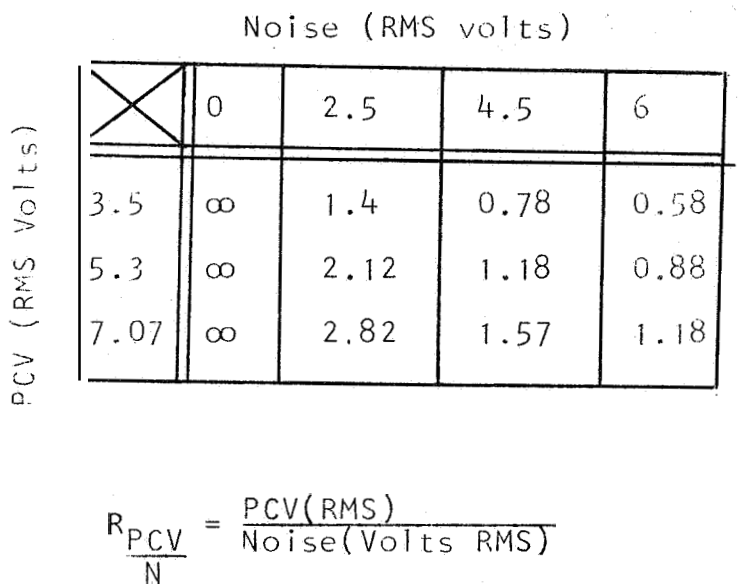

$$R_{\frac{PCV}{N}} = \frac{PCV(RMS)}{Noise(Volts\ RMS)}$$

Figure 3.1: SDD Signal to Noise Ratio, R

was measured on an RMS VTVM, and three RMS noise levels, 2.5, 4.5, and 6.0 volts, were used. Also three values of PCV were used: 3.5, 5.3, and 7.07 volts RMS. The test layout is shown in Figure 3.2. Using the previously described methods of measurement for PSV settings, tests were run on the SOC hardware and Table 3.1 is a description of the test program.

(a) Elementary SOC Configuration

The Elementary SOC configuration is shown by Figure 3.3 to consist of a simplified PA module that provides a sgn e_p output and a simplified PSV module without sgn Au feedback. This SOC configuration was shown in Reference 3 to be mathematically equivalent to the General Purpose SOC configuration for the case in which plant polarity is known a priori. Extensive tests have been performed to determine phase shift of the Elementary SOC as a function of input frequency, as described by Table 3.2; however, for brevity, only a selected group of results is presented in Figures 3.4 through 3.7. Tests have been performed with sinusoidal inputs of large amplitude (20 volts peak-to-peak) and small amplitude (4 volts peak-to-peak). Phase-shift vs. frequency diagrams are presented for various conditioning in Figures 3.8 through 3.15.

(b) General Purpose PSV Configuration

The General Purpose PSV configuration consists of either of two PSV module designs:

(i) PSV module with normal sgn Au feedback

(ii) PSV module with modified sgn Δu feedback

The difference between the two designs (above) is the point

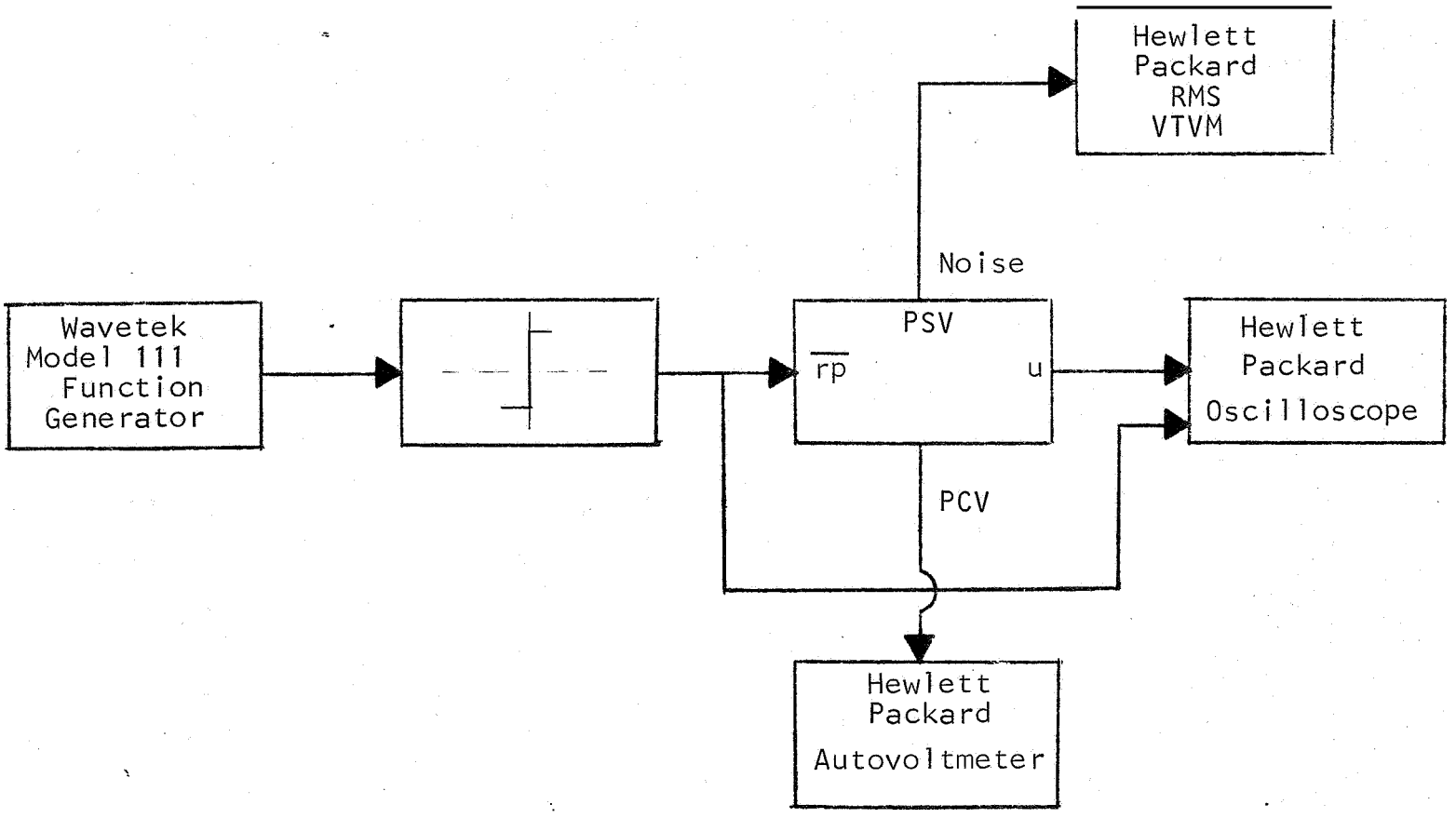

Figure 3.2: Test Equipment Layout for Experimental Program

Table 3 1: SOC Hardware Test Program

Object under Test	Input	Output	Looking for
1. "Elementary SOC" (PSV without sgn $\Delta\omega$ feedback)	Sinusoidal e(t) of various amplitudes and frequencies	$\omega(t)$	In/Out response curves (attn/phase)
2 (a) Entire PSV Module*	sgn v > 0($\overline{rp}$ = 1)	$\omega(t)$	Regenerative and Degenerative conditions in the Δu loop for: (i) Transient after sgn v change (ii) Steady states (iii) $\lvert E_n \rvert$ & $\lvert P_{max} \rvert$ effects
(b) Entire PSV Module* with sgn $\Delta u'$ logic	sgn v < 0($\overline{rp}$ = 0)		

*$\overline{\text{Centered p register}}$

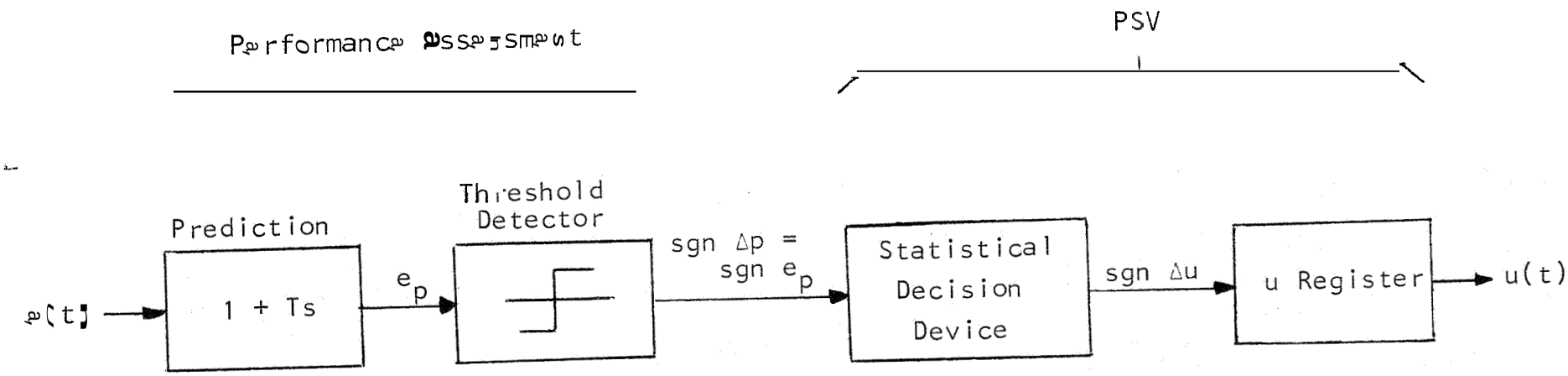

Figure 3 3: Elementary SOC Configuration (PSV without sgn as Feedback)

R	MCV (Volts, P.P.)	Noise (Volts, RMS)	T (Sec)	e(t) (Volts, P.P.)	Frequency of e(t) Sinusoidal Input (cps)					
					5	10	50	100	500	800
0.88	15	4.5	0.033	4	Fig. 3.4(b)	×	×	×	×	×
				20	Fig. 3.4(a)	×	×	×	×	×
			1.0	4	Fig. 3.5(b)	×	×	×	×	×
				20	Fig. 3.5(a)	×	×	×	×	×
1.18	15	6.0	0.033	4	×	×	×	×	×	×
				20	×	×	×	×	×	×
			1.0	4	Fig. 3.6(a)	×	Fig. 3.6(b)	Fig. 3.7(a)	×	Fig. 3.7(b)
				20	×	×	×	×	×	×
1.18	20	4.5	0.033	4	×	×	×	×	×	×
				20	×	×	×	×	×	×
			1.0	4	×	×	×	×	×	×
				20	×	×	×	×	×	×
1.57	20	6.0	0.033	4	×	×	×	×	×	×
				20	×	×	×	×	×	×
			1.0	4	×	×	×	×	×	×
				20	×	×	×	×	×	×

Note: 'x' Denotes conditions tested but not presented in figures

Table 3.2: Summary of Open-Loop Tests of Elementary SOC

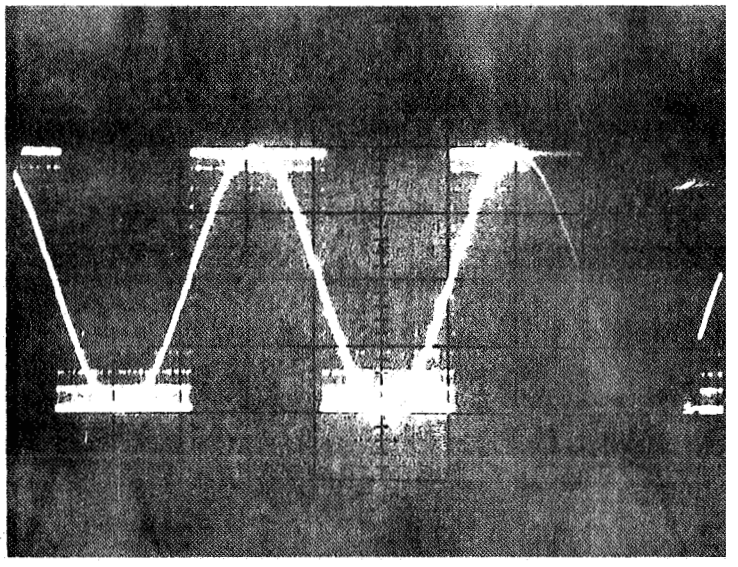

(a) Large Signal, 5 cps
R = 1.18

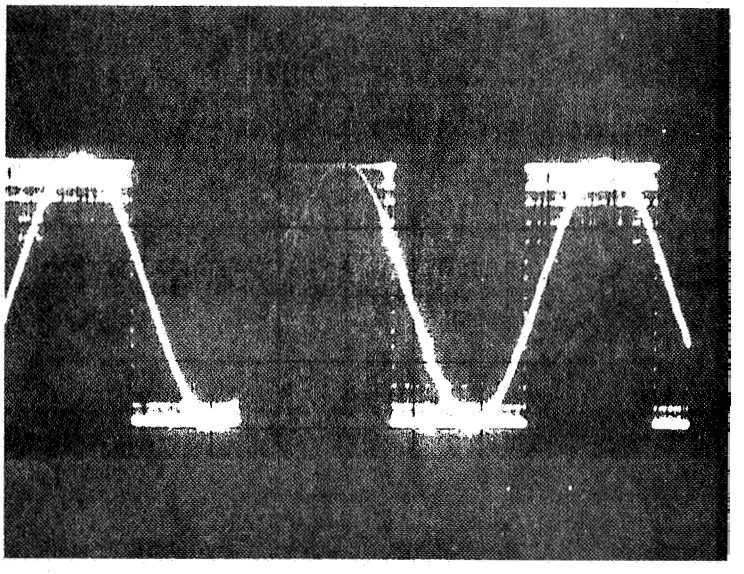

(b) Small Signal, 5 cps
R = 1.18

Figure 3.4 : Frequency Response, Elementary SOC, T = *0.033* Second

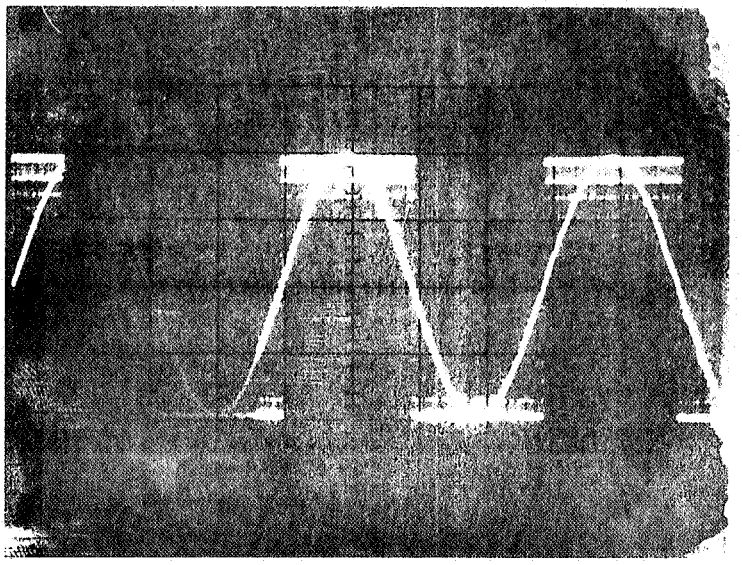

(a) Large Signal, 5 cps
R = 1.18

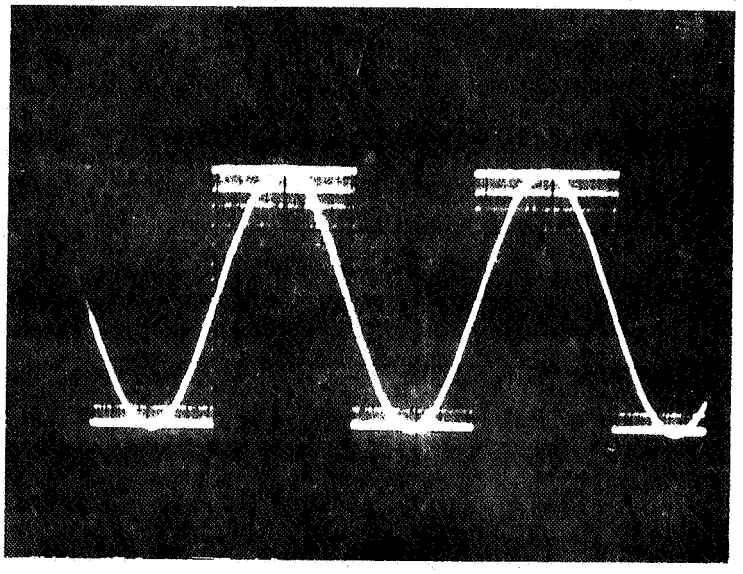

(b) Small Signal, 5 cps
R = 1.18

Figure 3.5 : Frequency Response, Elementary SOC, T = 1.0 Second

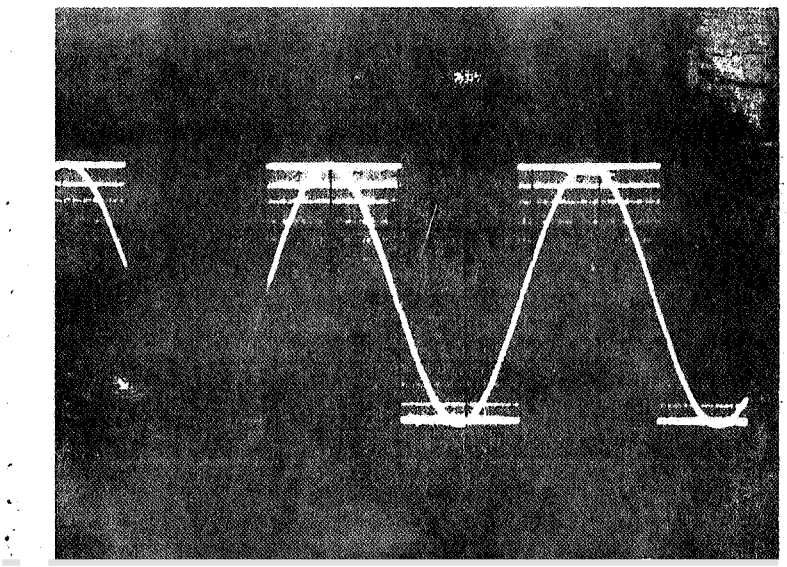

(a) 5 cps

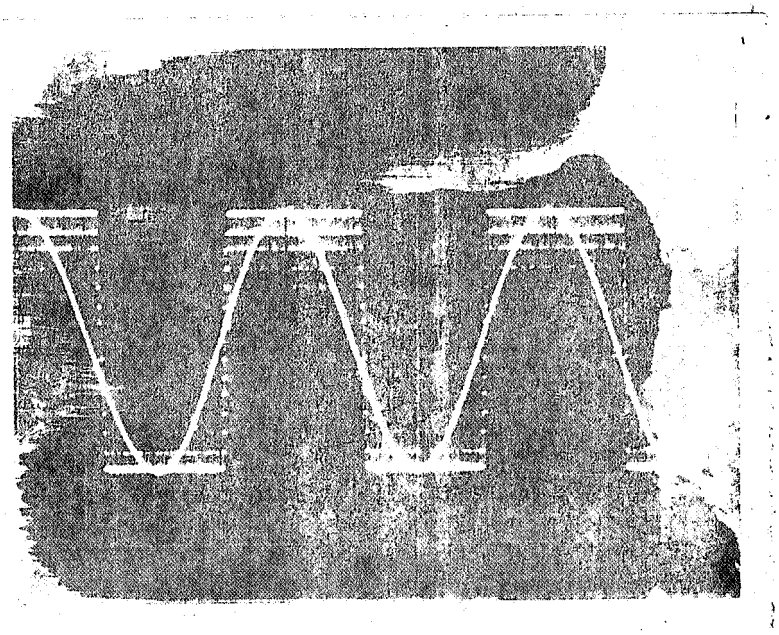

(b) 50 cps

Figure 3.6: Frequency Response, Elementary SOC, T = 1.0 Second, **Small** Signal, R = 0.88

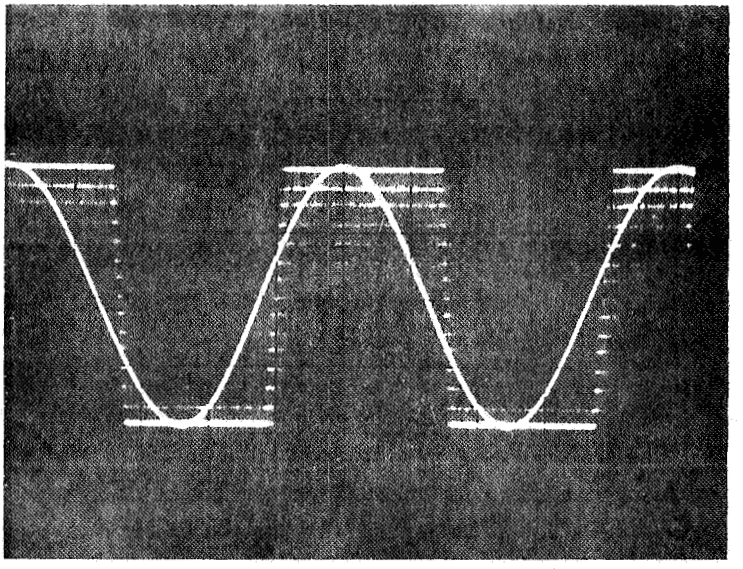

(a) 100 cps

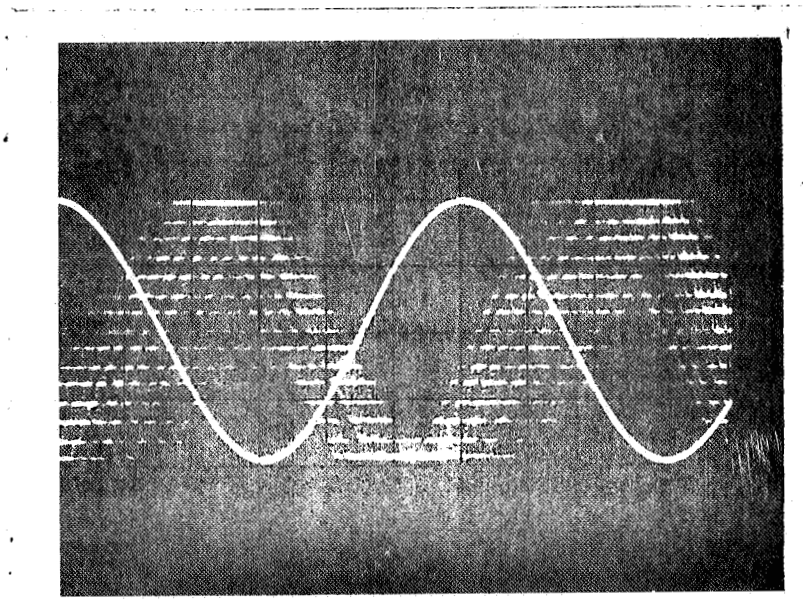

(b) 820 cps

Figure 3.7: Frequency Response, Elementary SOC, T = 1.0 Second, Small Signal, R = 0.88

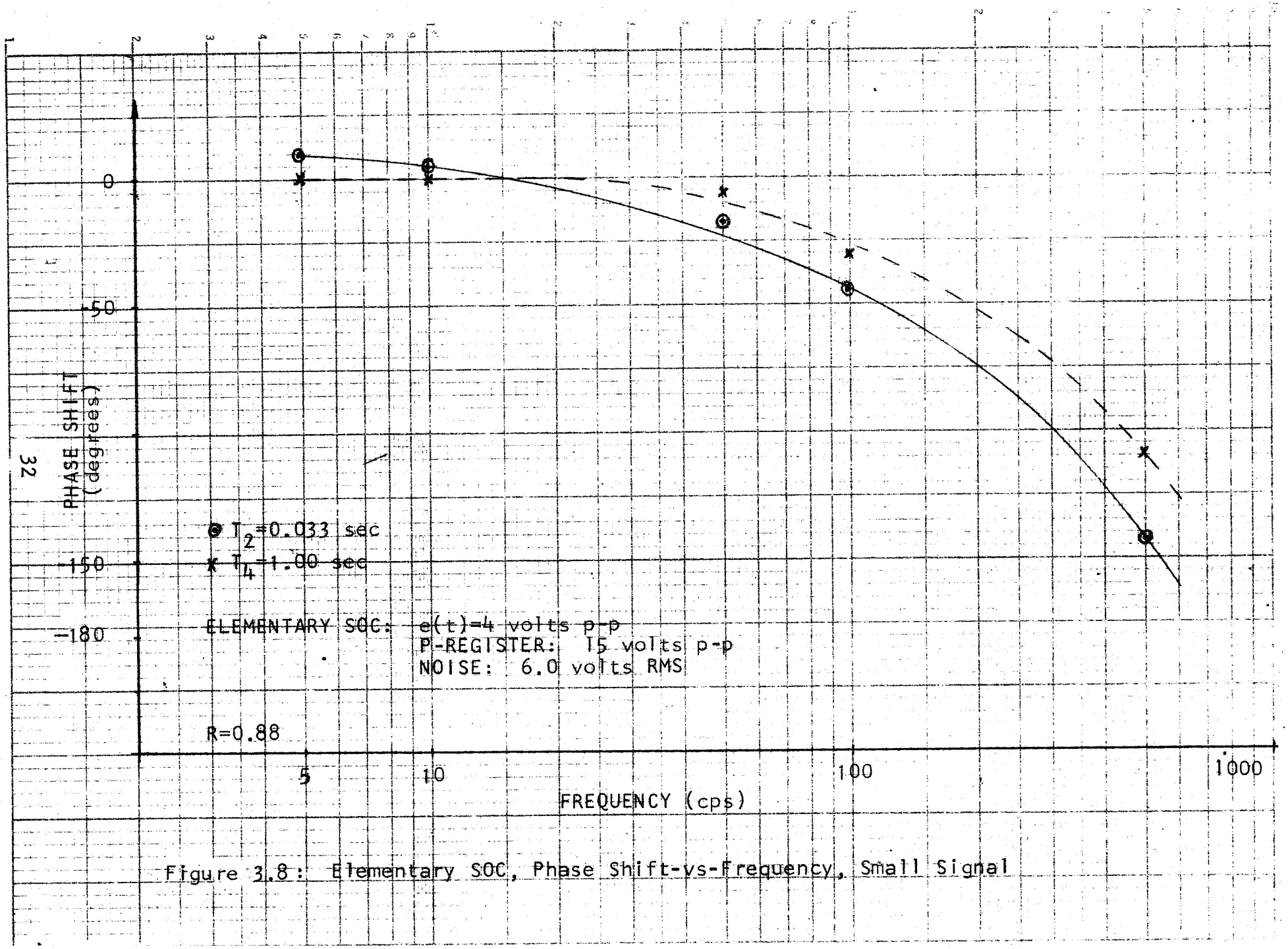

Figure 3.8: Elementary SOC, Phase Shift-vs-Frequency, Small Signal

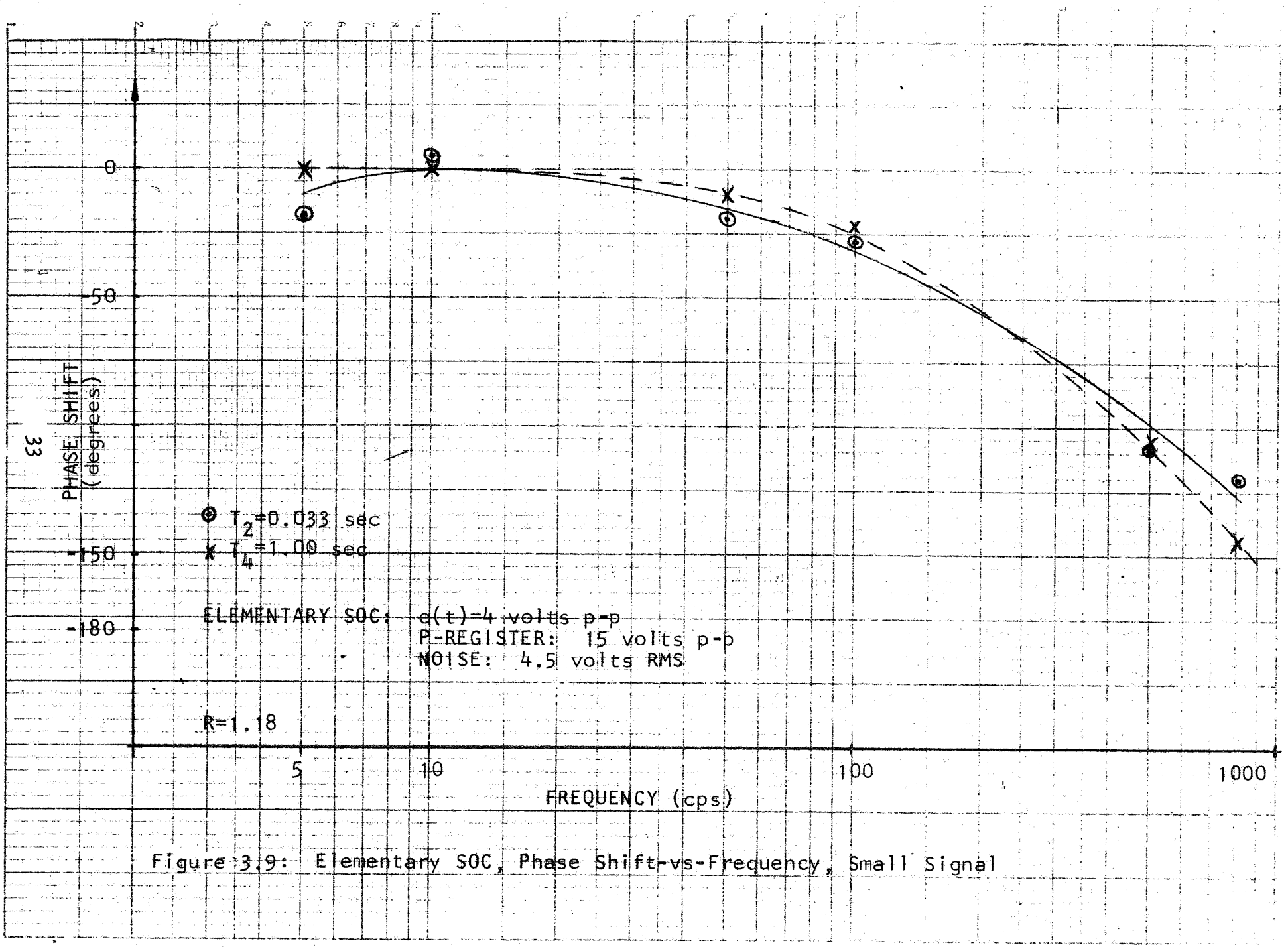

Figure 3.9: Elementary SOC, Phase Shift-vs-Frequency, Small Signal

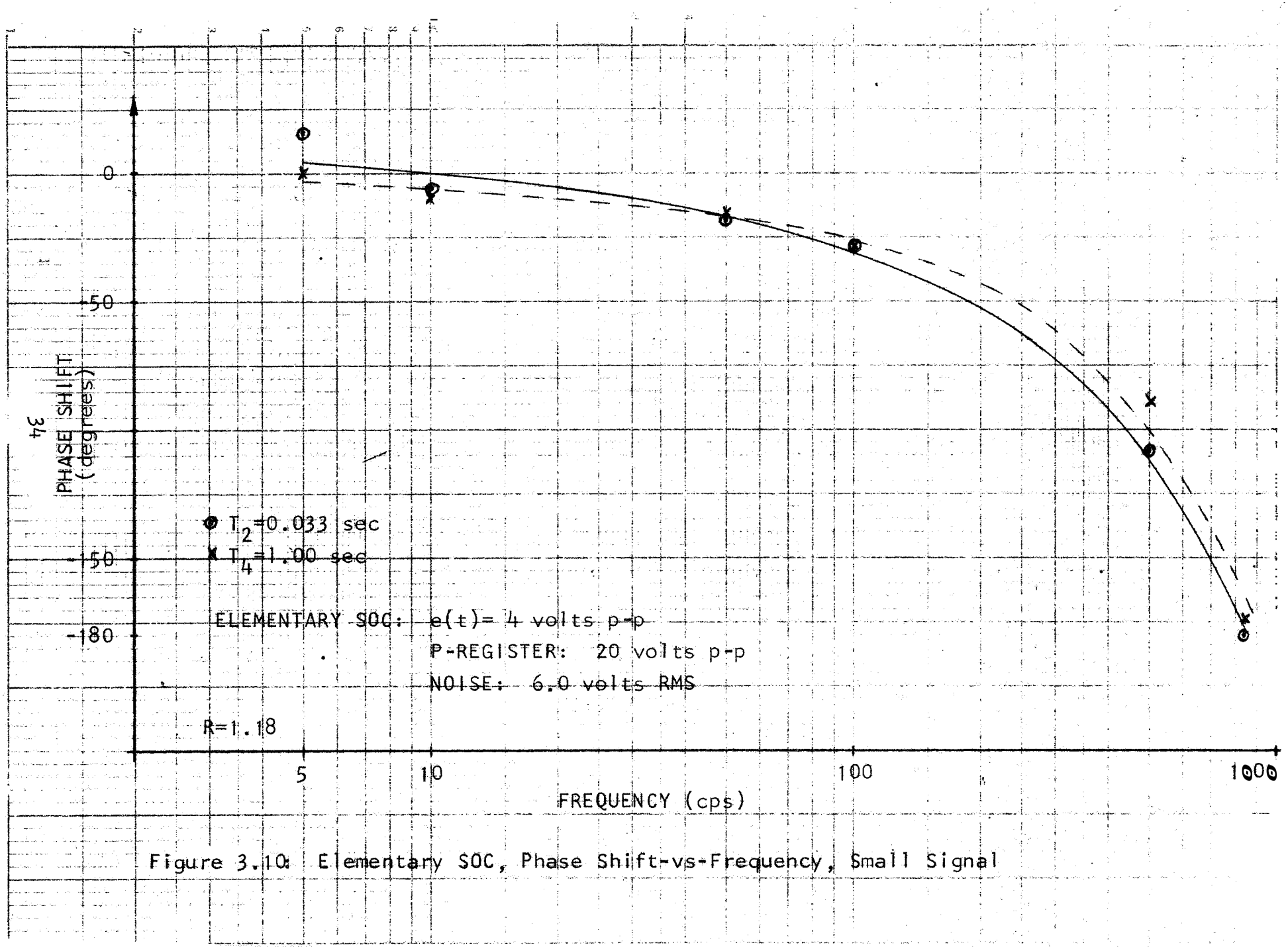

Figure 3.10: Elementary SOC, Phase Shift-vs-Frequency, Small Signal

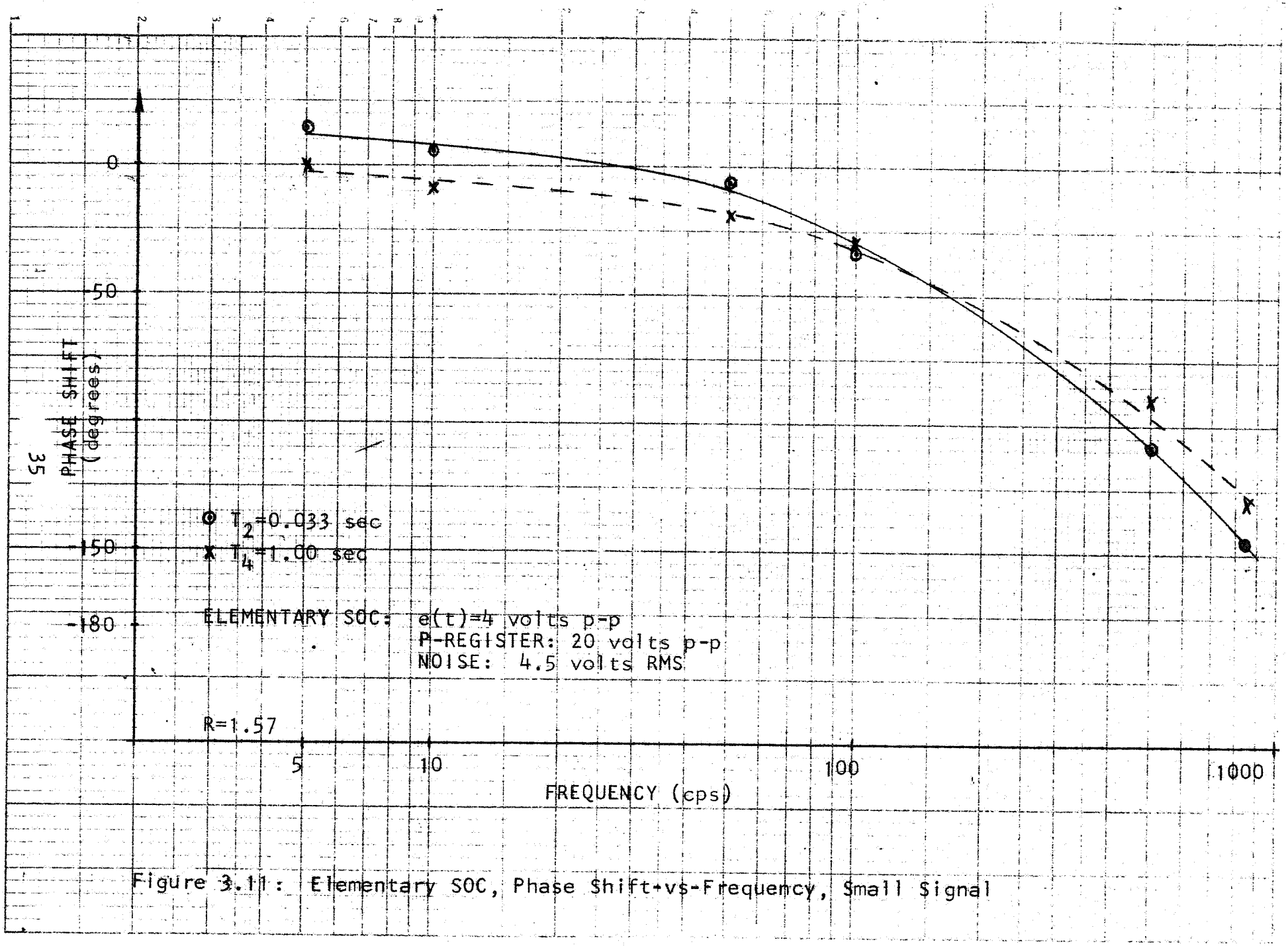

Figure 3.11: Elementary SOC, Phase Shift-vs-Frequency, Small Signal

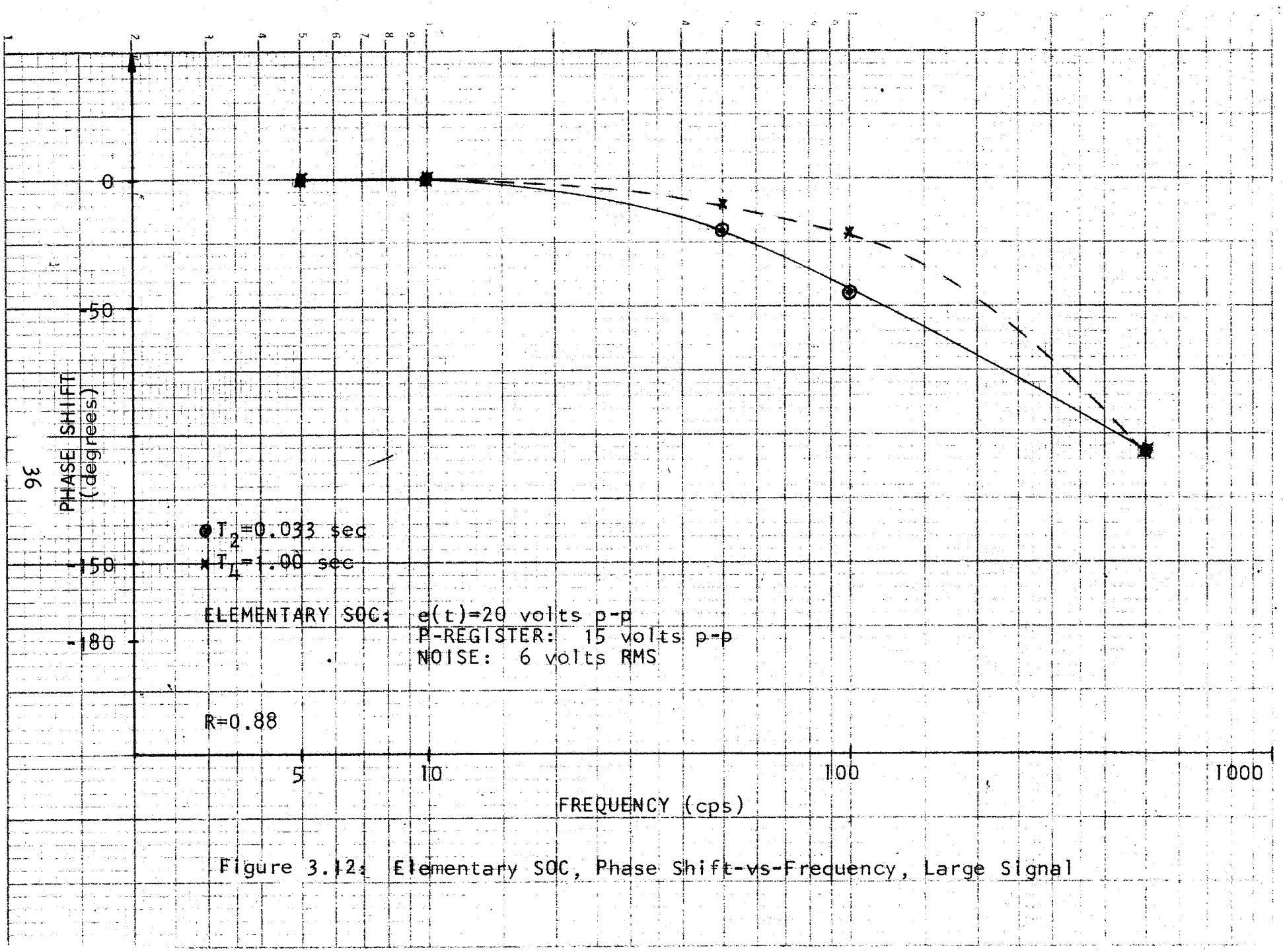

Figure 3.12: Elementary SOC, Phase Shift-vs-Frequency, Large Signal

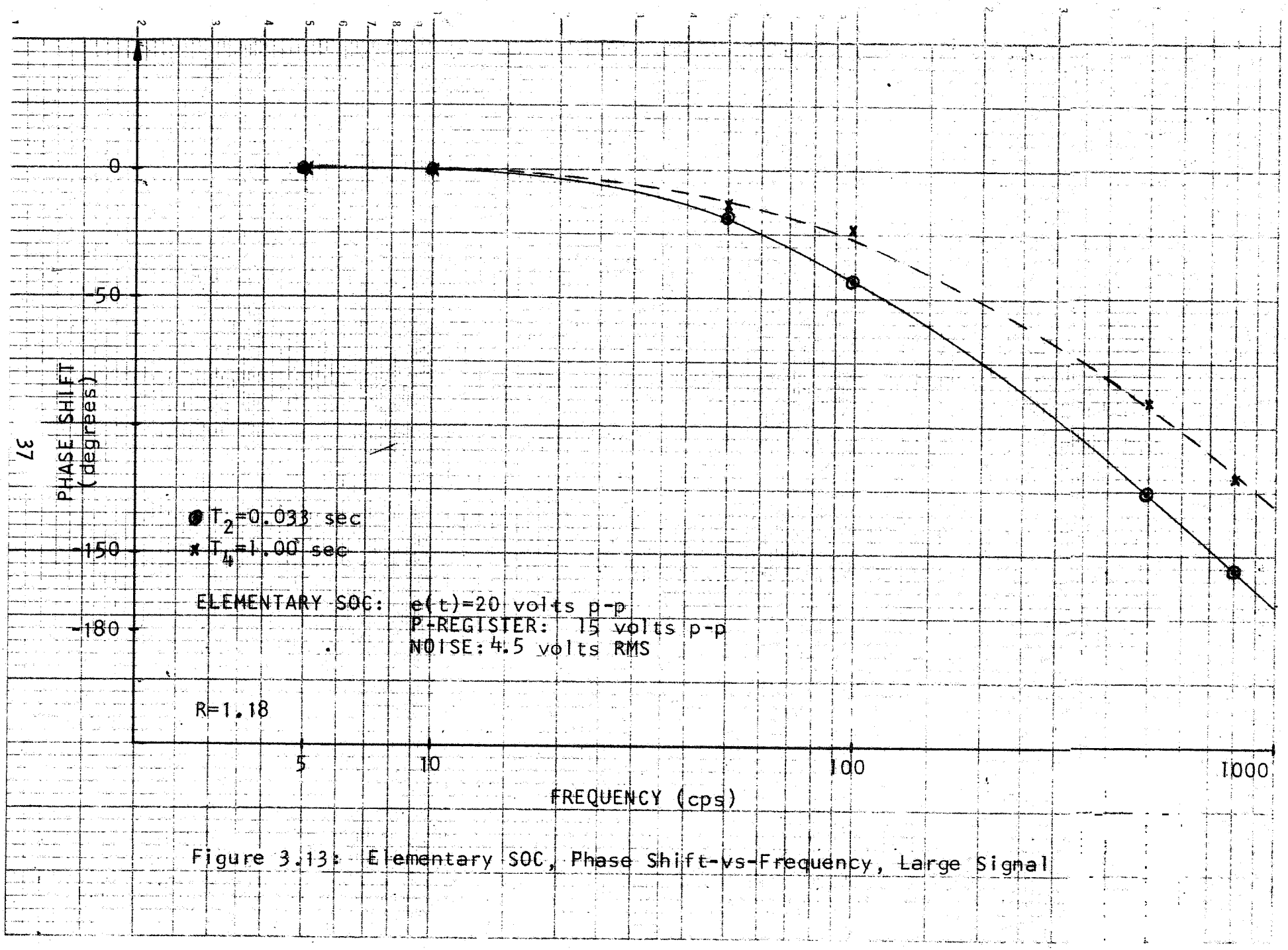

Figure 3.13: Elementary SOC, Phase Shift-vs-Frequency, Large Signal

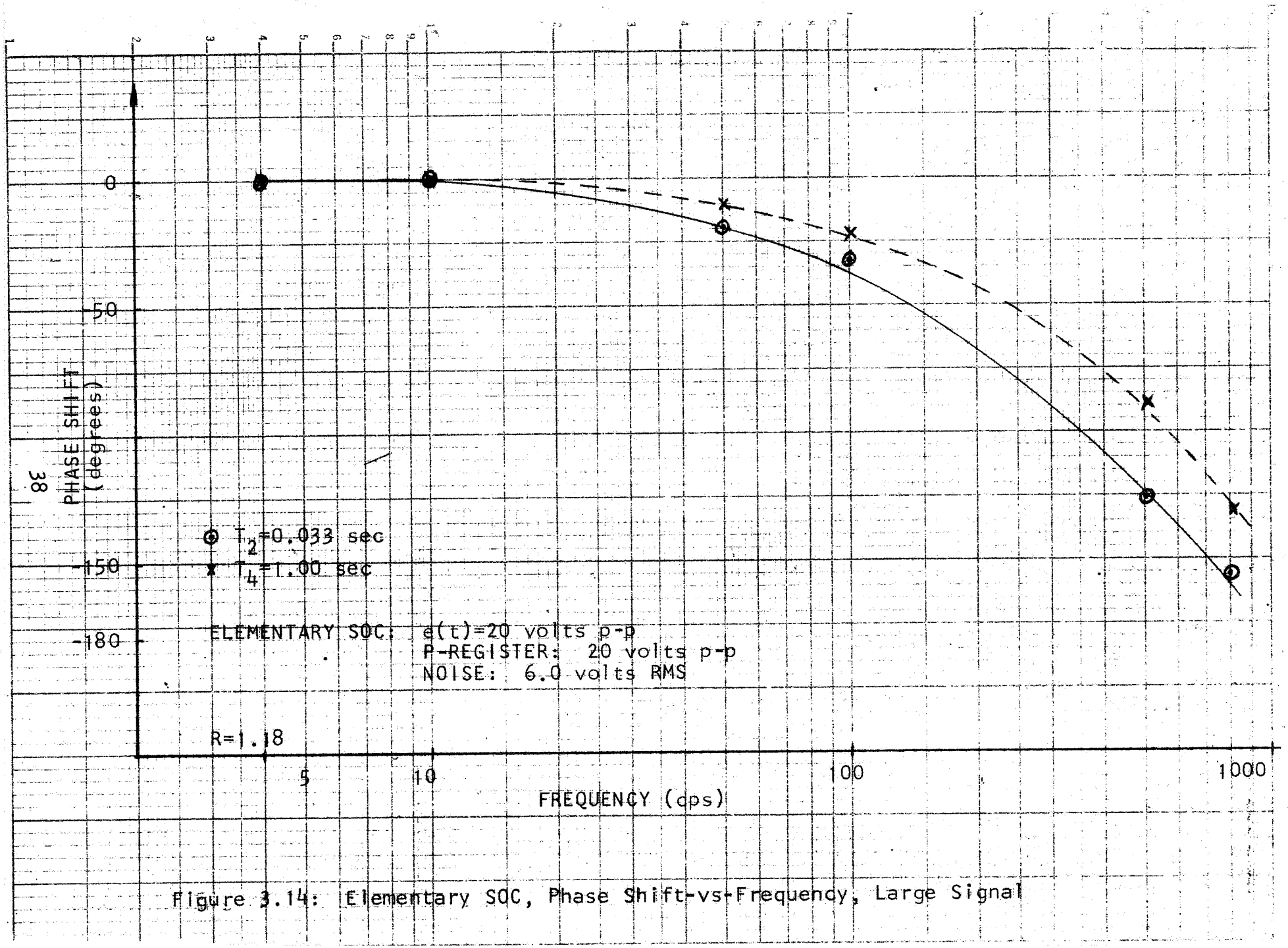

Figure 3.14: Elementary SOC, Phase Shift-vs-Frequency, Large Signal

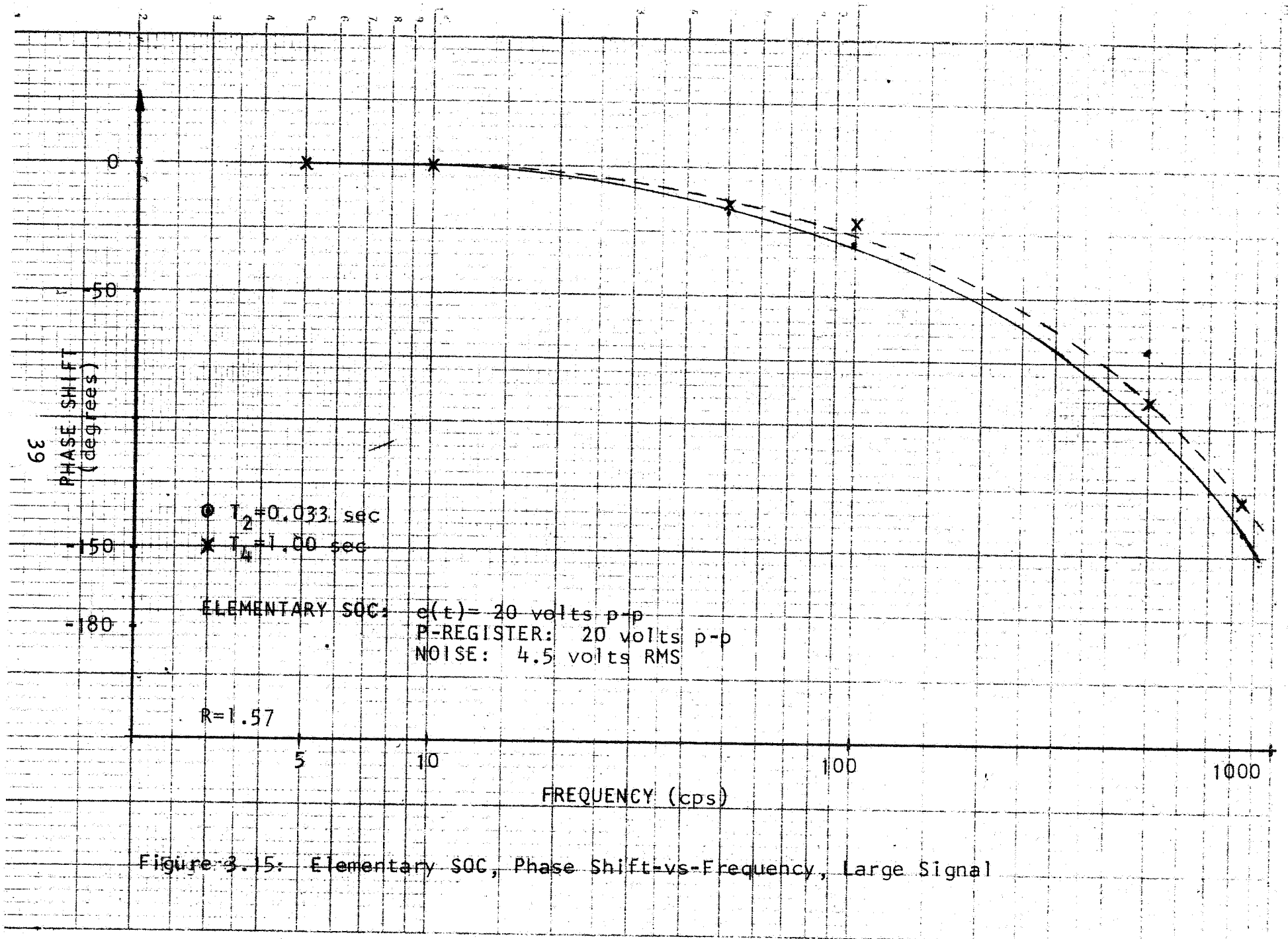

Figure 3.15: Elementary SOC, Phase Shift-vs-Frequency, Large Signal

of electrical connection used in the hardware to sense Au, as shown in Figures 3.16 and 3.17. The PSV with normal sgn Au feedback, Figure 3.16, and the PSV with modified sgn Δu feedback, Figure 3.17, are both General Purpose PSV modules. Tests, as indicated in parts 2(a) and 2(b) of Table 3.1, have been performed with both designs to determine the degree of correspondence between input and output waveforms for R values of 0.88, 1.18, and 1.57.

For the PSV with normal sgn Δu feedback, due to noise-center offset, the PCV was set to the range (-10 volts, +5 volts) for a 15 volts peak-to-peak PCV and to the range (-12.4 volts, + 7.4 volts) for a 20 volts peak-to-peak PCV. Using a 3 volt peak-to-peak, 20 cps, square wave input for sgn v, a series of oscilloscope photographs, Figures 3.18 and 3.19, was taken showing the u(t) response for the various R values. For this same PSV configuration, sgn Au response is recorded on an EAI Model 1120 X-Y Recorder for sgn v input frequencies of 0.1 cps and 1.0 cps and the R values given above. These results are presented in Figures 3.20 through 3.25. Higher input frequencies were not used because of the limited frequency response of the X-Y recorder. As described in Table 3.1, tests were performed to observe the degenerative and regenerative modes of PSV operation. The degenerative mode is observed as a sgn Au signal which rapidly switches logic levels when sgn v is a logical zero, while the regenerative mode is observed as a sgn Au signal which is nearly constant at logical one or logical zero when sgn v is at logical one. Figure 3.26(a) shown an example of the degenerative mode and Figure 3.26(b) shown an example of the regenerative mode. These photographs were obtained with a 4.5 volt RMS noise voltage (R = 1.18).

The PSV with modified sgn Au feedback was tested for different amounts of sgn Au memory shift, viz., 1Δt, 2Δt,

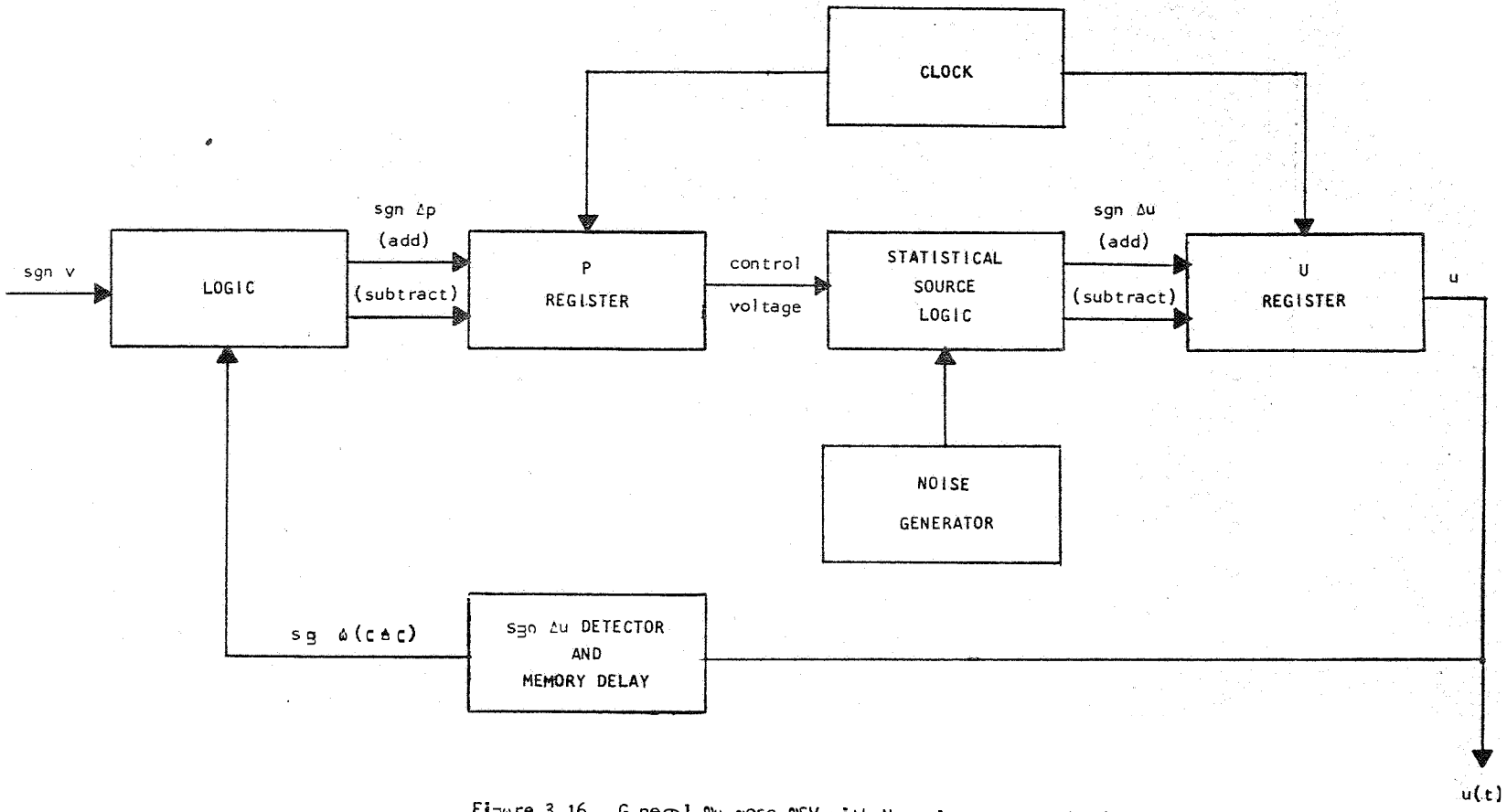

Figure 3.16 General purpose PSV with N-bit sign feedback

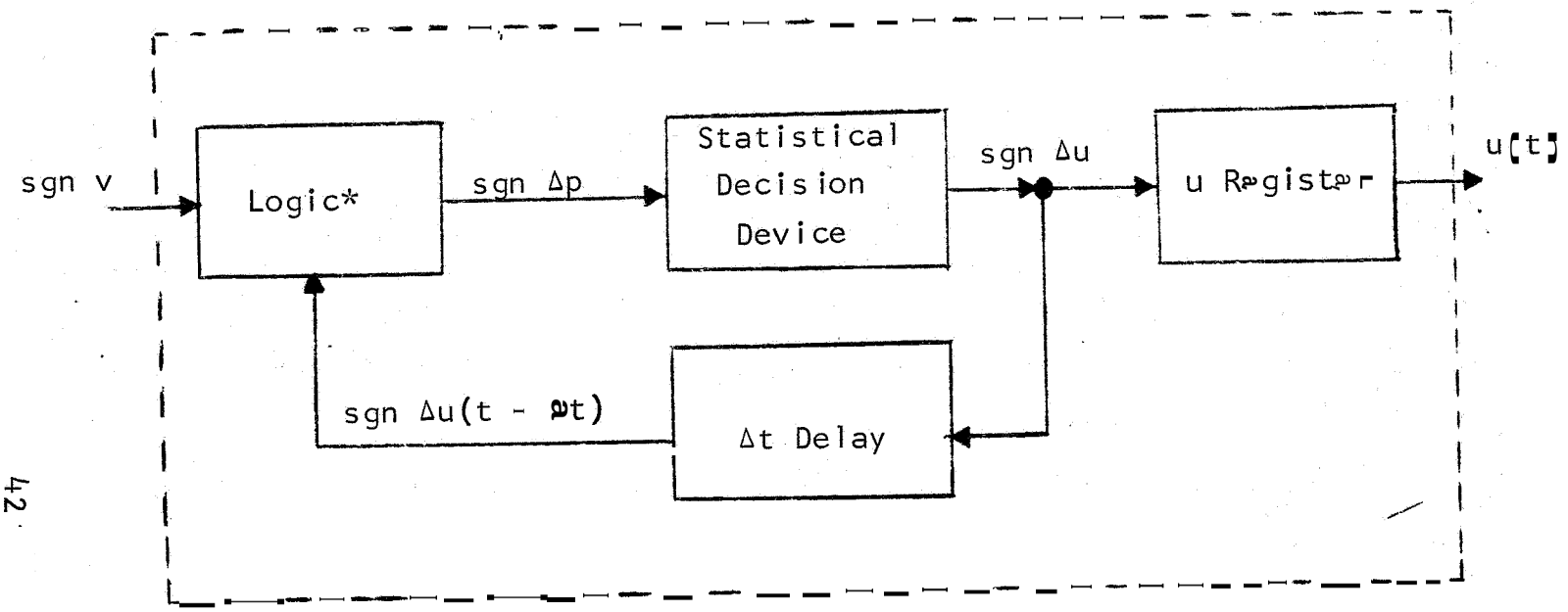

* sgn Δp = sgn v sgn Δu(t - Δt)

Figure 3.17 : General Purpose VSV with Modified sgn Δu Feedback

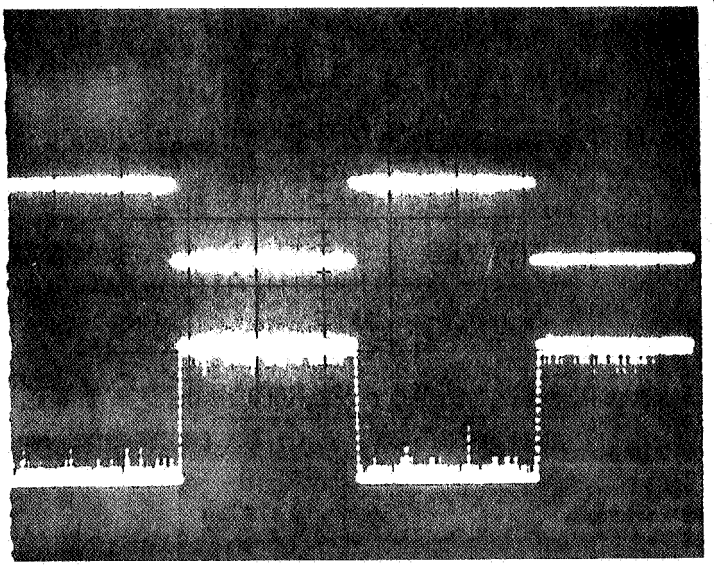

(a) R = 1.18, PCV = 15 Volts

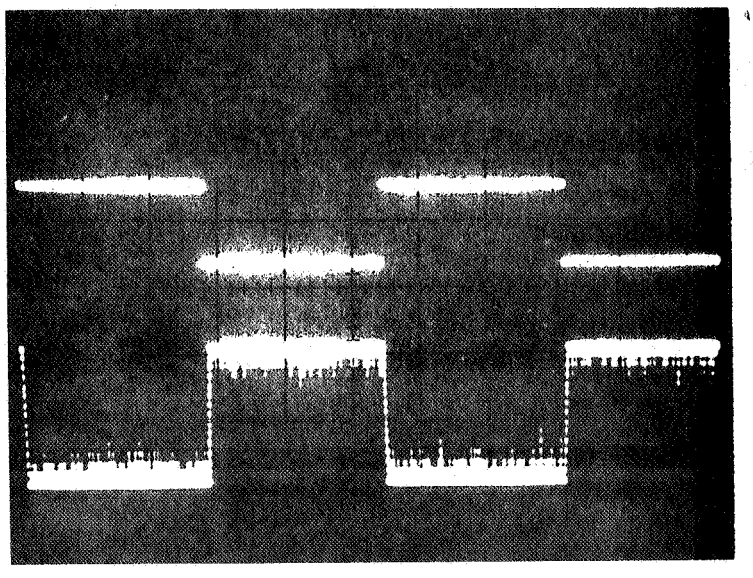

(b) R = 0.88, PCV = 15 Volts

Figure 3.18: Open Loop Response, General Purpose PSV (with normal sgn Δu feedback)

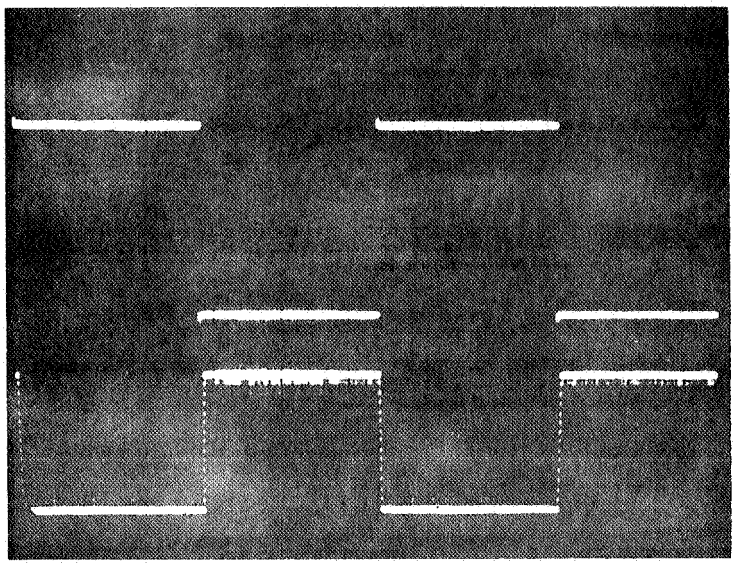

(a) R = 1.57, PCV = 20 Volts

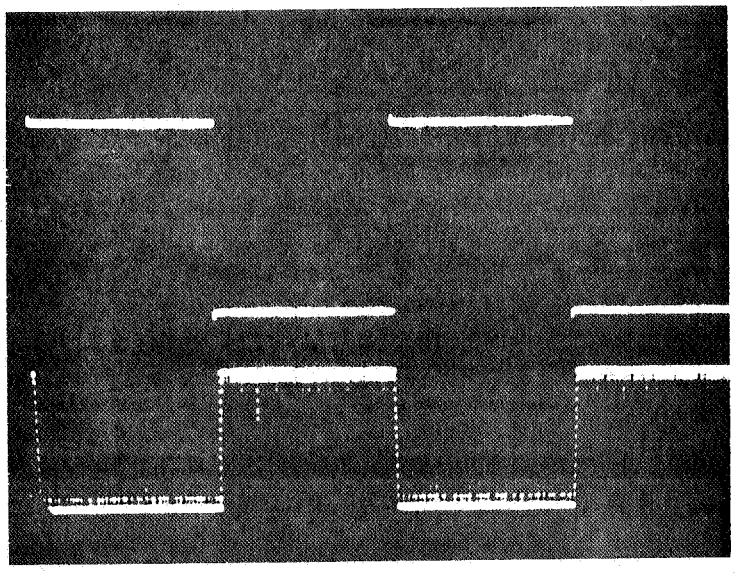

(b) R = 1.18, PCV = 20 Volts

Figure 3.19: Open Loop Response, General Purpose PSV (with normal sgn Δu feedback)

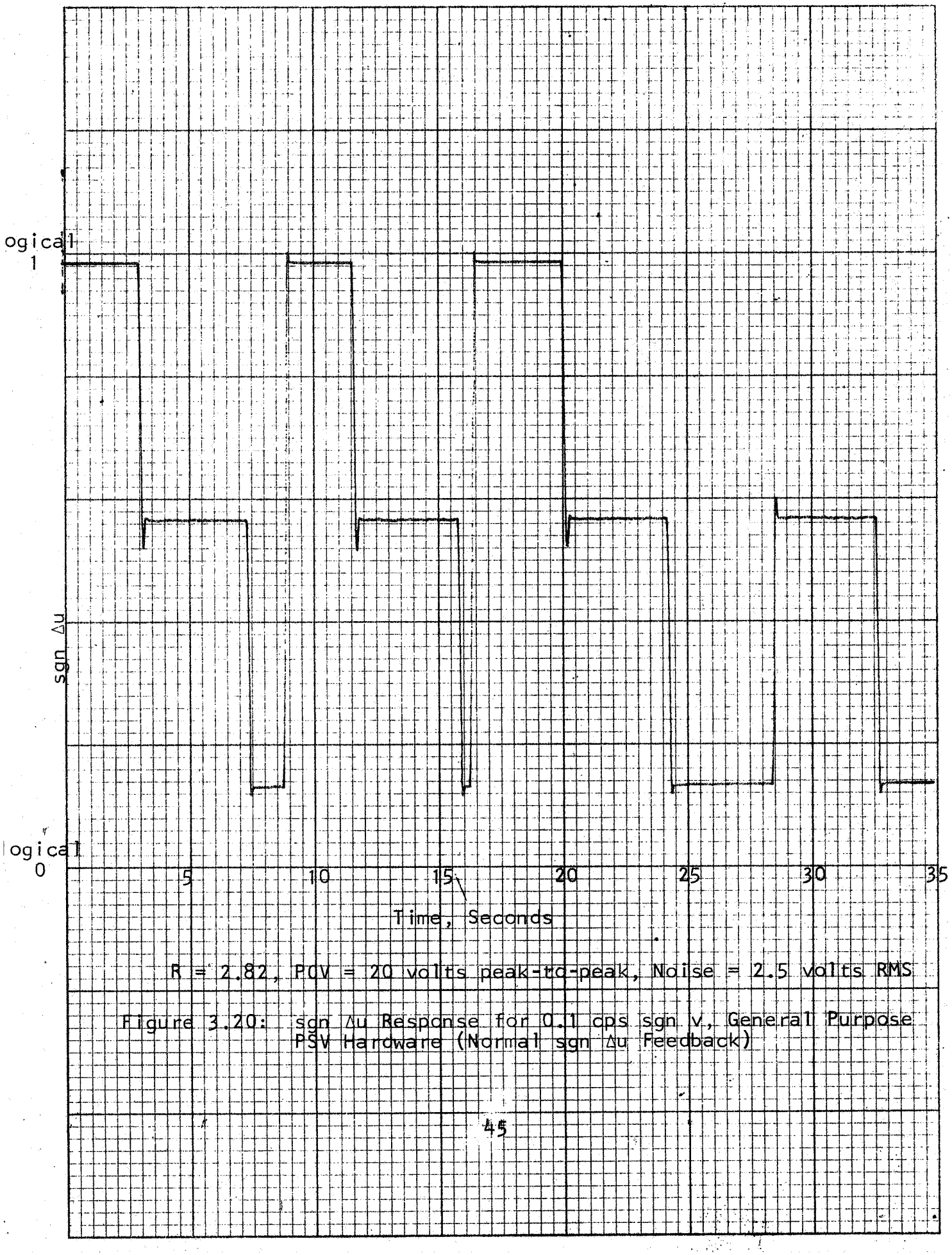

R = 2.82, PCV = 20 volts peak-to-peak, Noise = 2.5 volts RMS

Figure 3.20: sgn Δu Response for 0.1 cps sgn v, General Purpose PSV Hardware (Normal sgn Δu Feedback)

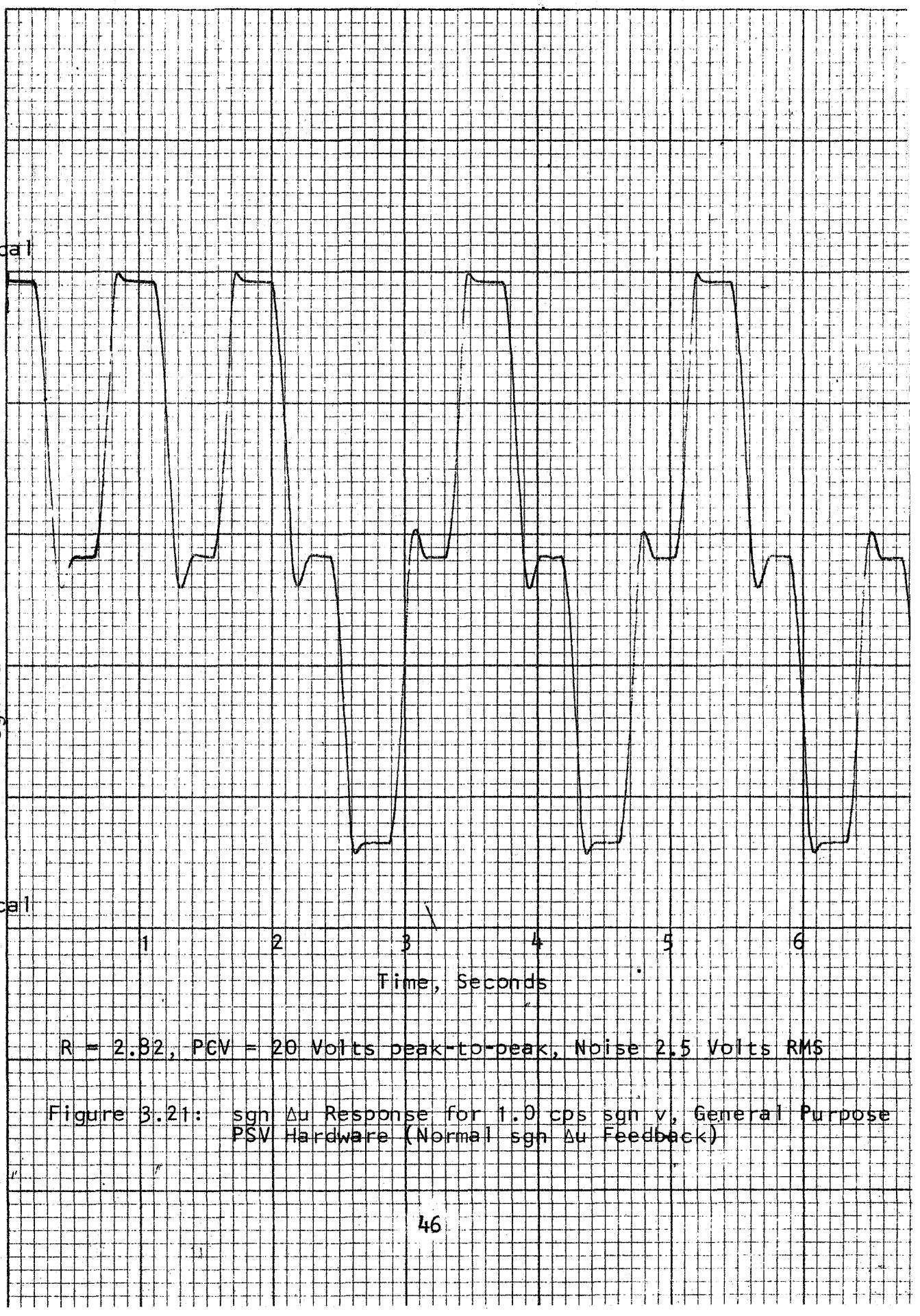

R = 2.82, PCV = 20 Volts peak-to-peak, Noise 2.5 Volts RMS

Figure 3.21: sgn Δu Response for 1.0 cps sgn v, General Purpose PSV Hardware (Normal sgn Δu Feedback)

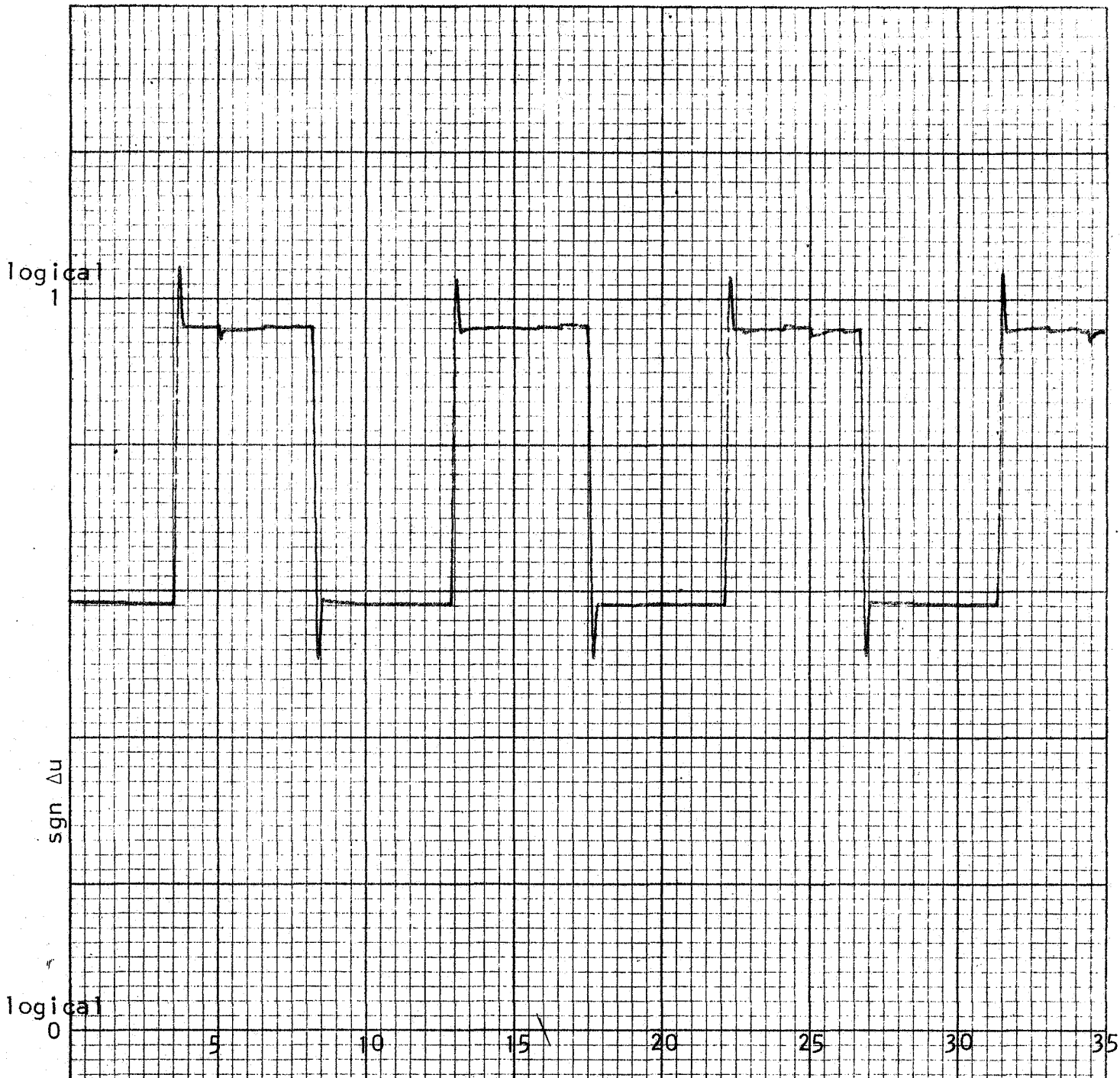

R = 1.18, PCV = 20 Volts peak-to-peak, Noise = 6.0 Volts RMS

Figure 3.22: sgn Δu Response for 0.1 cps sgn v, General Purpose PSV Hardware (Normal sgn Δu Feedback)

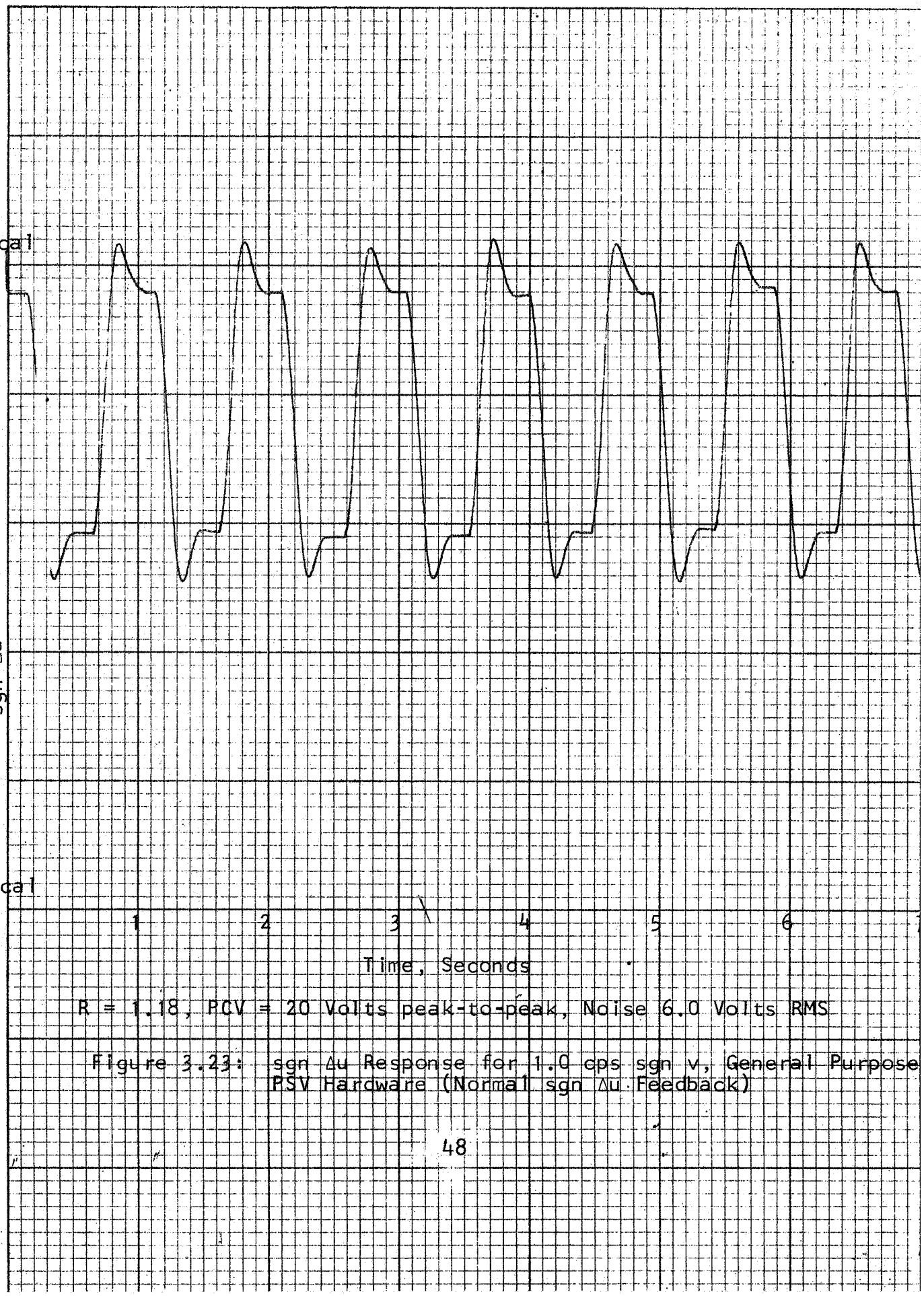

R = 1.18, PCV = 20 Volts peak-to-peak, Noise 6.0 Volts RMS

Figure 3.23: sgn Δu Response for 1.0 cps sgn v, General Purpose PSV Hardware (Normal sgn Δu Feedback)

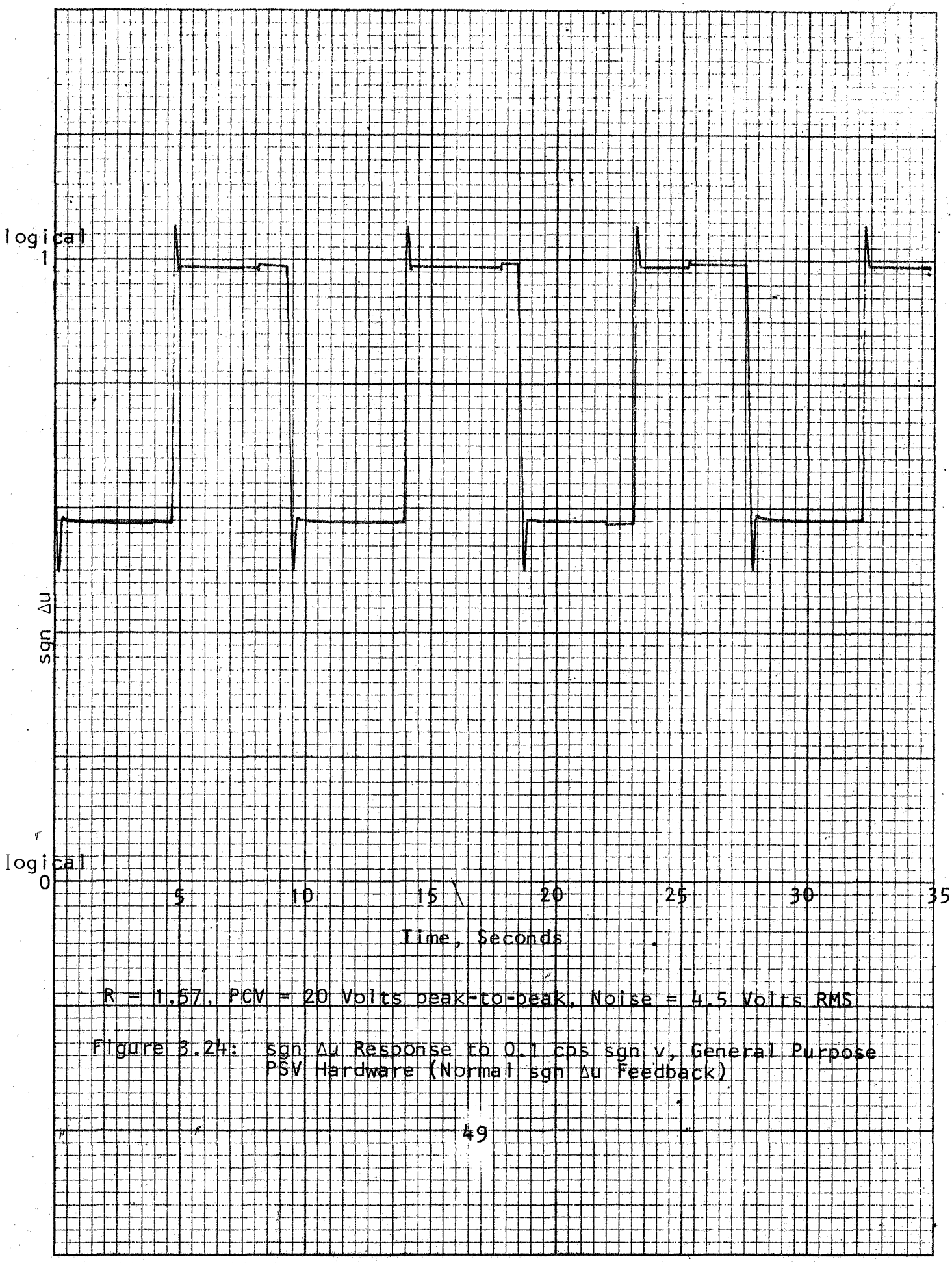

R = 1.57, PCV = 20 Volts peak-to-peak, Noise = 4.5 Volts RMS

Figure 3.24: sgn Δu Response to 0.1 cps sgn v, General Purpose PSV Hardware (Normal sgn Δu Feedback)

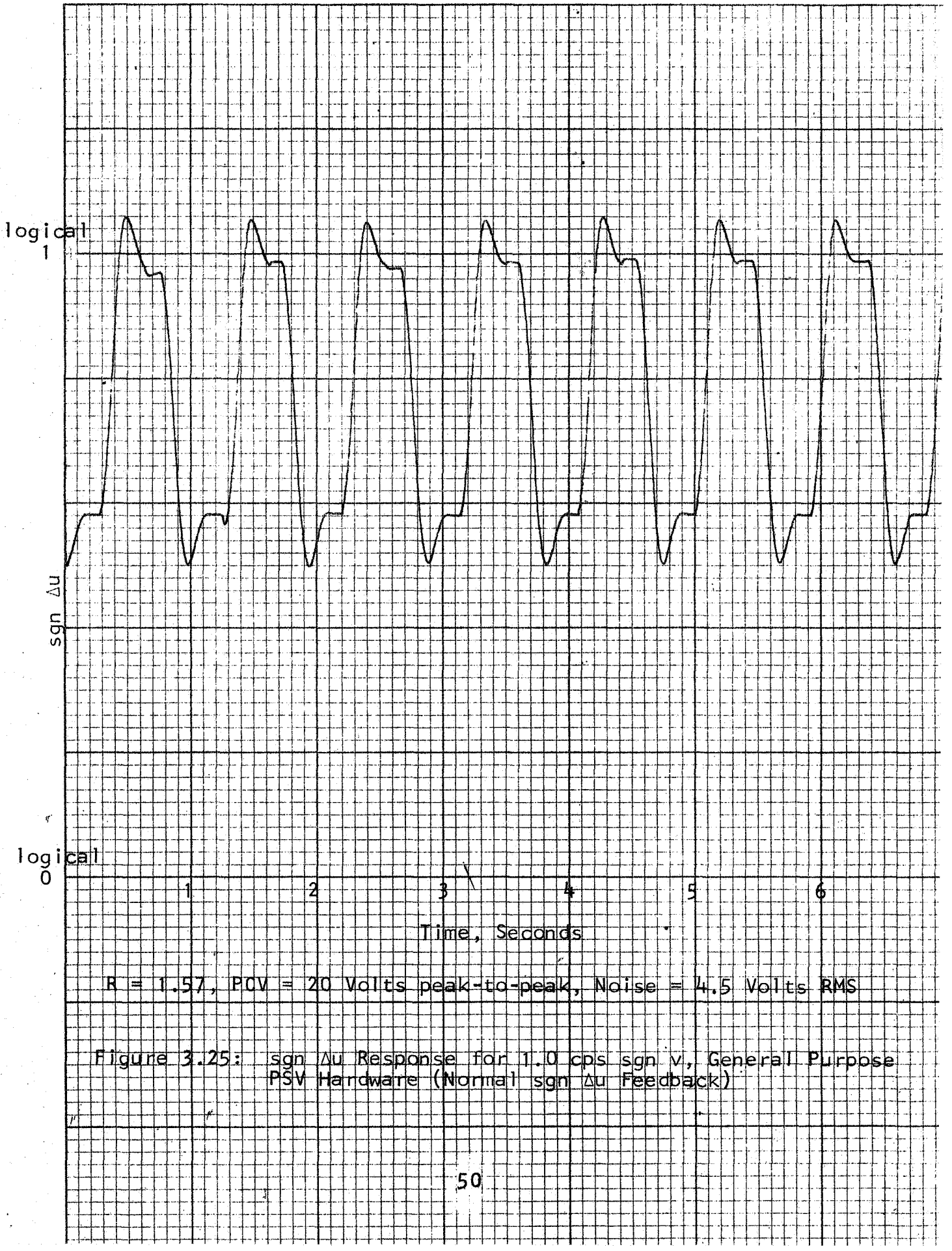

R = 1.57, PCV = 20 Volts peak-to-peak, Noise = 4.5 Volts RMS

Figure 3.25: sgn Δu Response for 1.0 cps sgn v, General Purpose PSV Hardware (Normal sgn Δu Feedback)

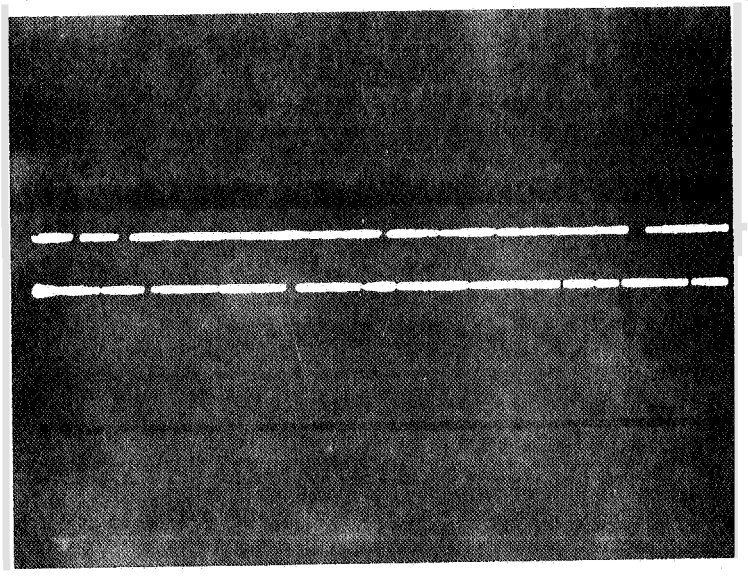

←·1 msec.→

(a) Degenerative Mode

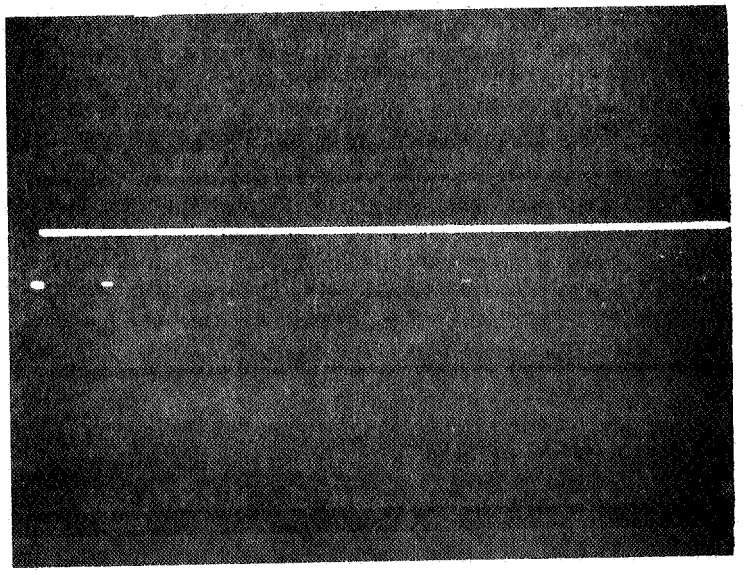

←·1 msec.→

(b) Regenerative Mode

Figure 3.26: General Purpose PSV Hardware, sgn Δu Modes.

$3\Delta t$, $4\Delta t$, and $5\Delta t$, as well as for the previously stated R values. The different memory shifts were used to show the point at which the PSV with modified sgn Au feedback corresponds to the PSV with normal sgn Δu feedback. From the figures, $1\Delta t$ and $2\Delta t$ are seen to exhibit close correspondence, a result which one would expect from the theory (Ref. 3). Table 3.3 is a summary of tests conducted with the modified sgn Au feedback and indicates which results were selected for presentation, (Figures 3.27 through 3.31).

3.1.2 Pulse Density Model of PSV

Figure 3.32 shows the pulse density model of the PSV unit as simulated on the EAI TR-48 analog computer. This simulation was time scaled to be 10-to-1 slower than real time; however, all results shown here have been transformed back and are therefore labelled with real-time coordinates. The open-loop experiments performed with the mathematical model are the same as those performed on the SOC hardware, as described in 3.1.1.

(a) PSV Model Only

An EAI X-Y recorder was used to record the sgn Au output of the model for sgn v input frequencies of 0.1 cps and 1.0 cps. This test is identical to the one made on the general purpose PSV (normal sgn Δu feedback), and the results are presented in Figures 3.33 and 3.34. As can be observed, the model response closely follows hardware results for R = 2.82, i.e., the case with "lean" noise (Figure 3.20).

(b) PSV Model with Hardware PA

With the pulse density model of the PSV connected to a hardware Type 2 PA module (see Appendix I), recordings were

Table 3: Summary of Test Conditions for SSV with Modified sgn Δu Feedback

PCV (Volts peak-peak)	R	Delay				
		1Δt	2Δt	3Δt	4Δt	5Δt
15	0.88	Fig. 3.27(a)	Fig. 3.27(b)	Fig. 3.28(a) ×	Fig. 3.28(b) ×	Fig. 3.29 ×
	1.18	Fig. 3.30(a)	Fig. 3.30(b)	---	---	---
20	1.18	Fig. 3.31(a)	Fig. 3.31(b)	×	×	×
	1.57	×	×	×	×	×

Note: × Denotes condition tested but not presented in figures

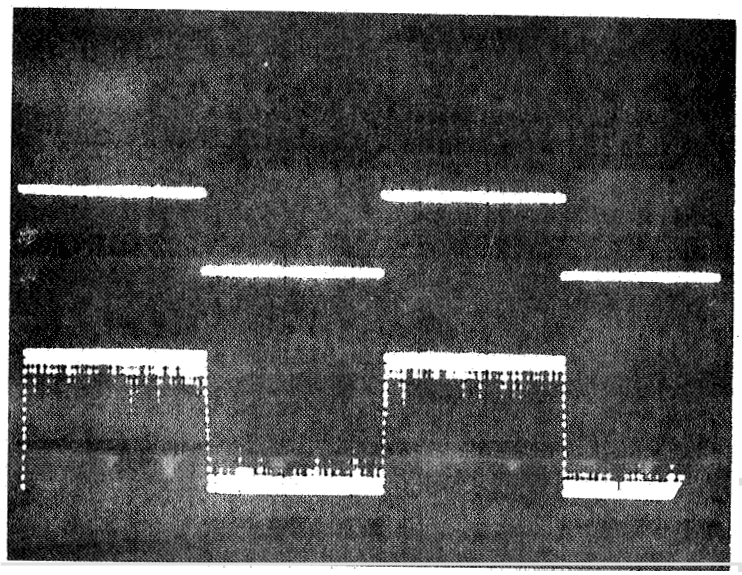

(a) 1 Δt delay

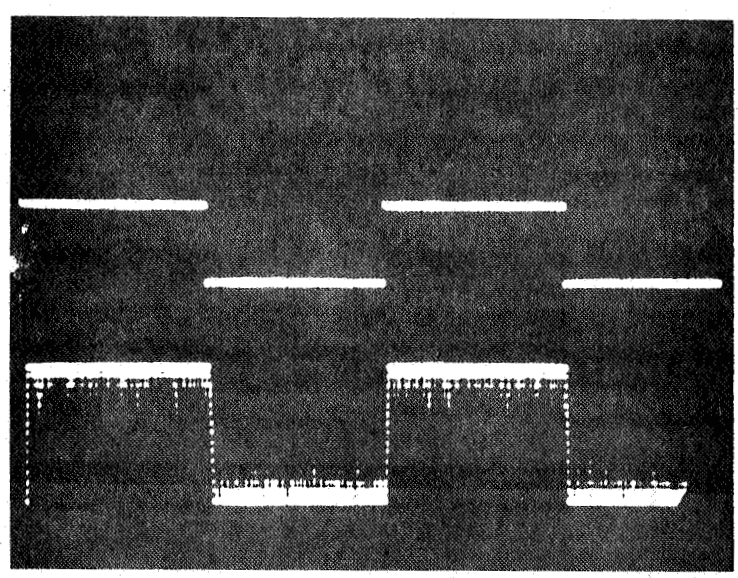

(b) 2 Δt delay

Figure 3.27 : Open Loop Response, General Purpose PSV (with modified sgn Δu feedback, 15 V **PCV**, *6.0* V RMS Noise, R = 0.88)

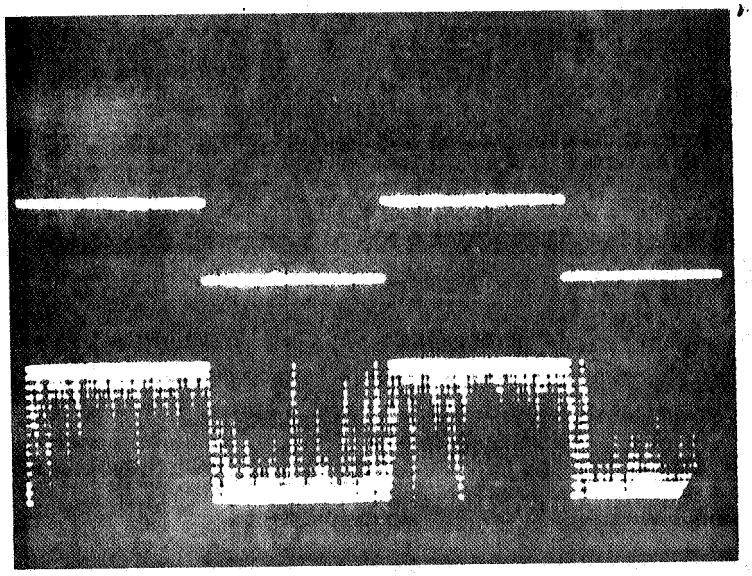

(a) 3 Δt delay

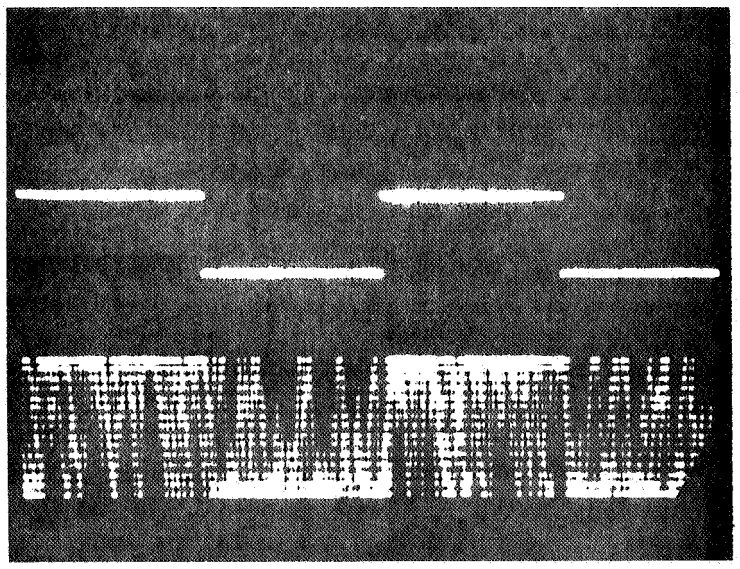

(b) 4 Δt delay

Figure 3.28: Open Loop Response, General Purpose PSV (with modified sgn Δu feedback, 15 V PCV, 6.0 V RMS Noise, R = 0.88)

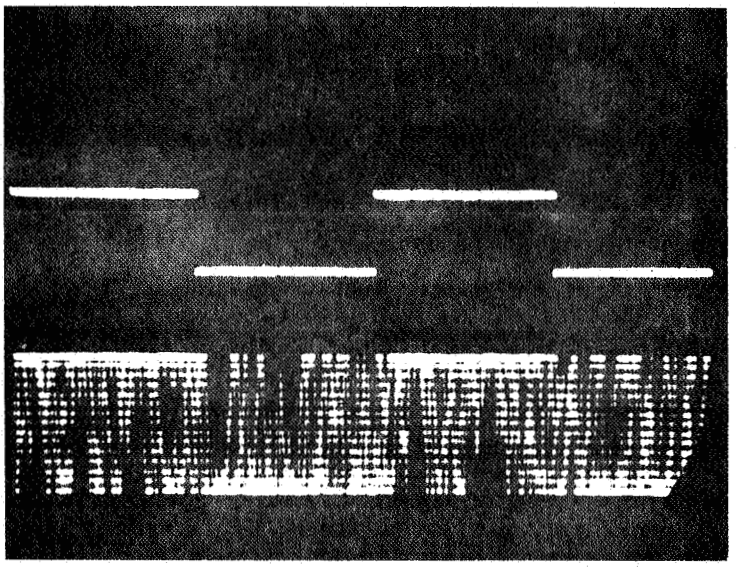

Figure 3.29: Open Loop Response, General Purpose PSV (with modified sgn Au feedback, 15 V PCV, 6.0 V RMS Noise, R = 0.88)

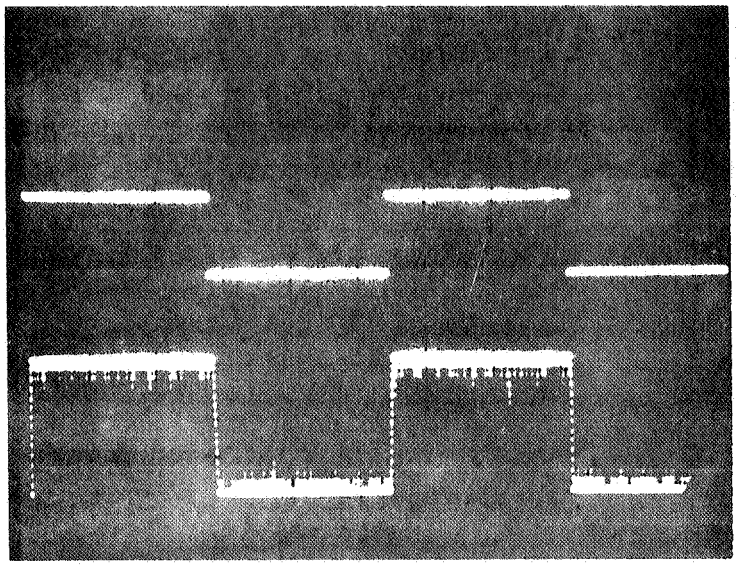

(a) 1 At delay

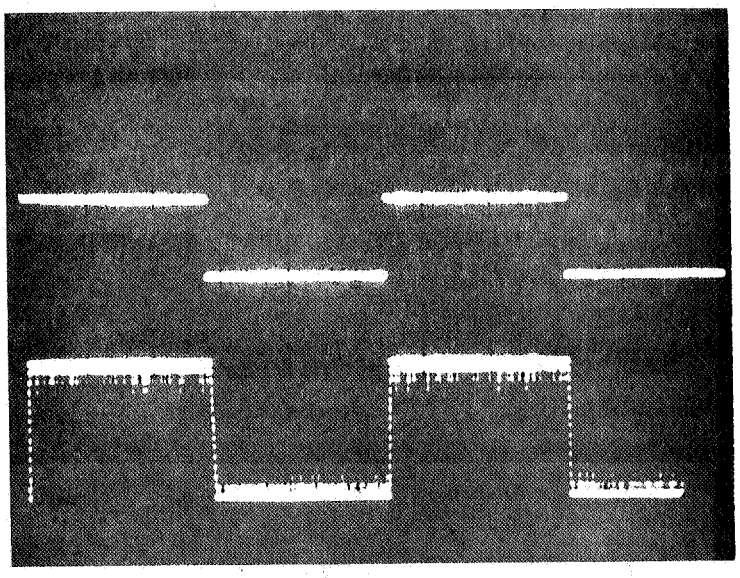

(b) 2 At delay

Figure 3.30: Open Loop Response General Purpose PSV (with modified sgn Au feedback, 15 V PCV, 4.5 V RMS Noise, R = 1.18)

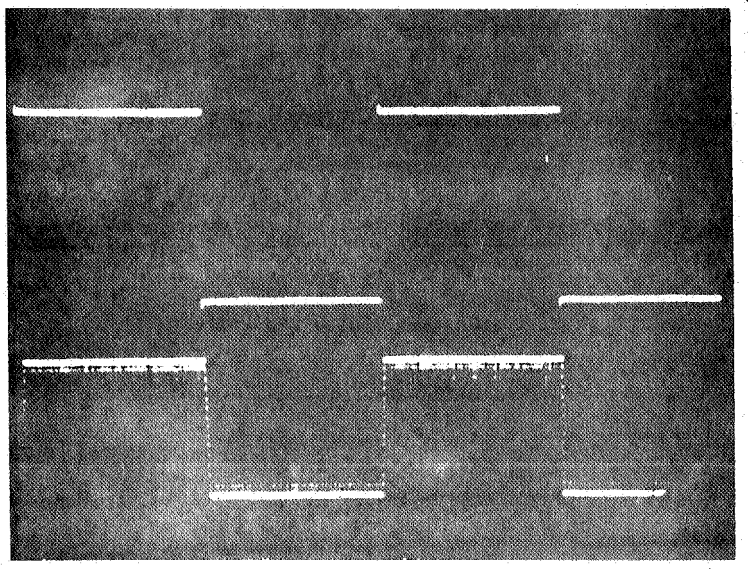

(a) 1 Δt delay

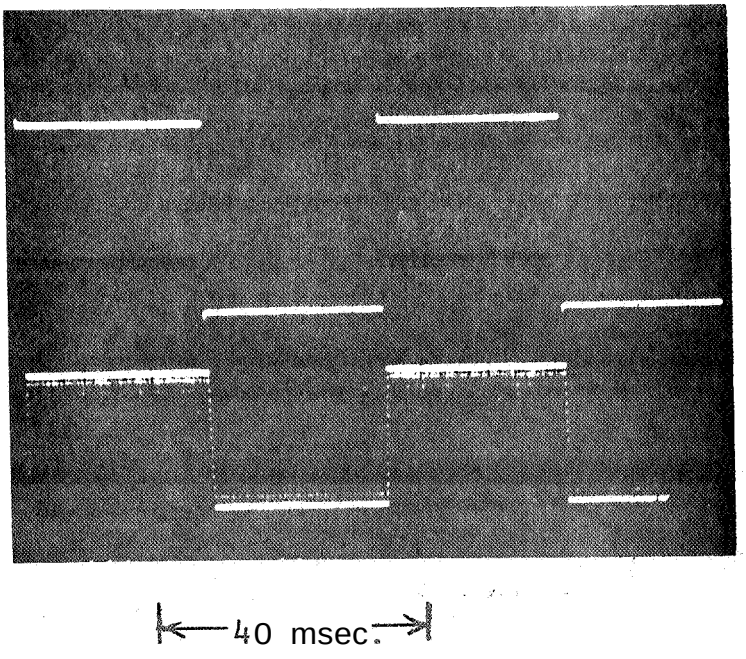

(b) 2 Δt delay

Figure 3.31 : Open Loop Response, General Purpose PSV (with modified sgn Δu feedback, 20 V PCV, 6.0 V RMS Noise, R = 1.18)

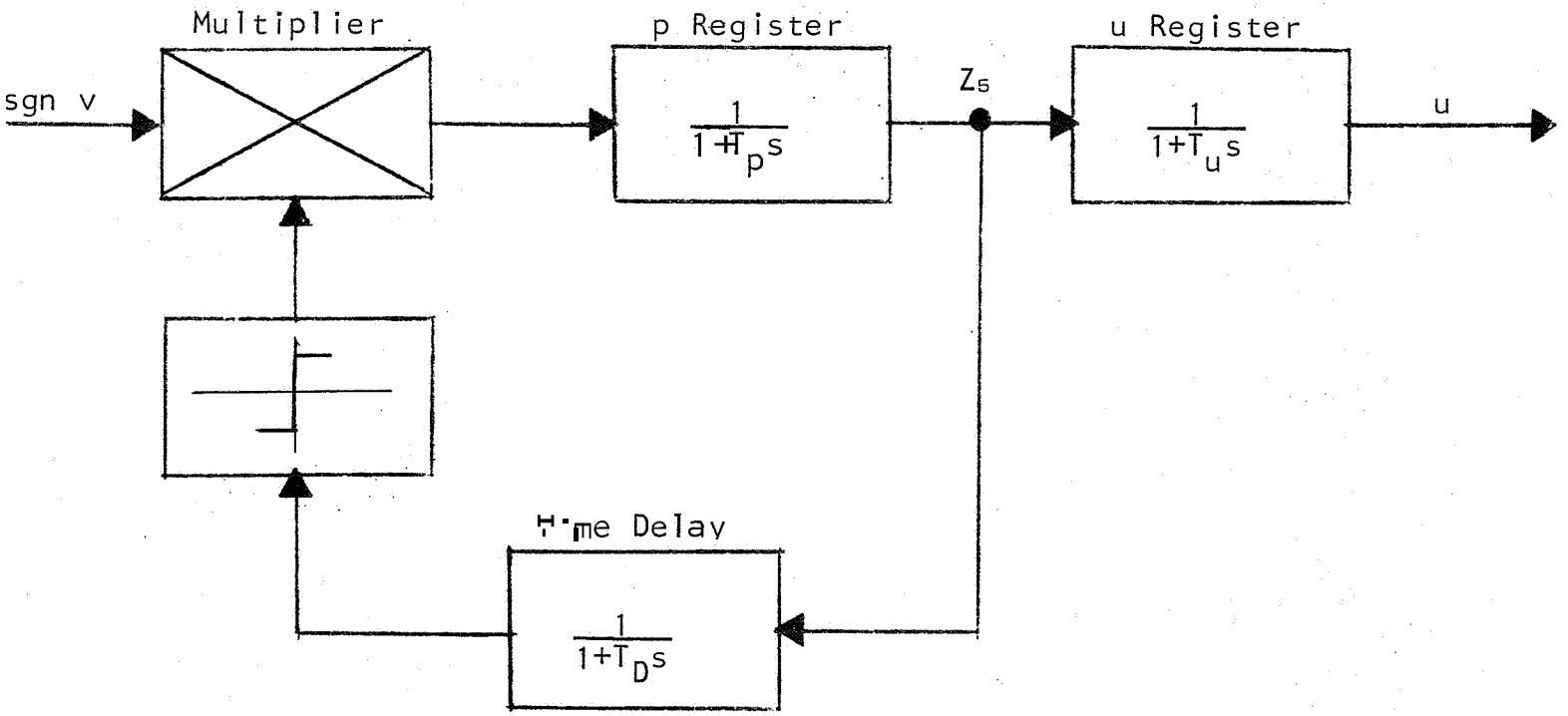

Figure 3.32: Pulse Density Model of PSV

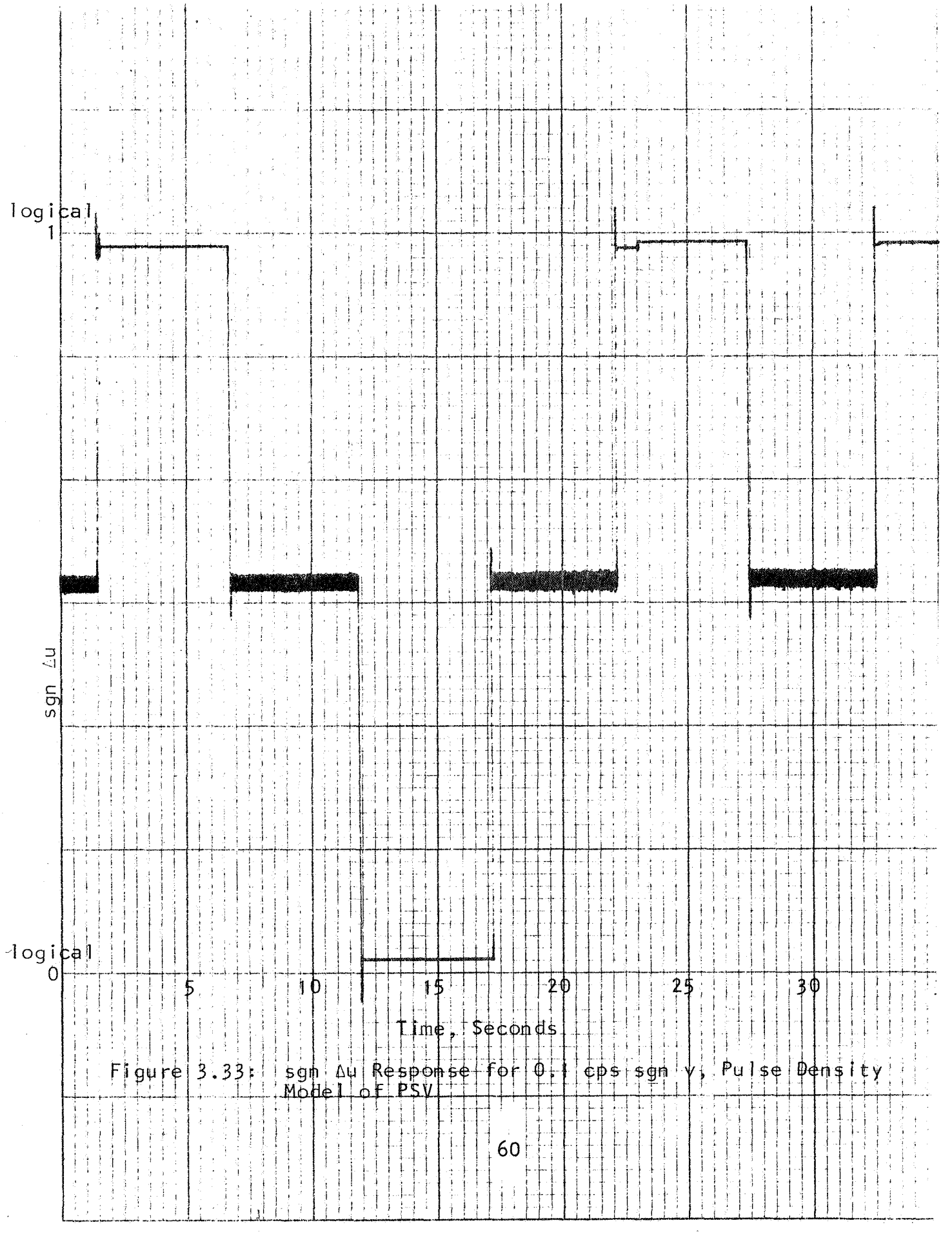

Figure 3.33: sgn Δu Response for 0.1 cps sgn v, Pulse Density Model of PSV

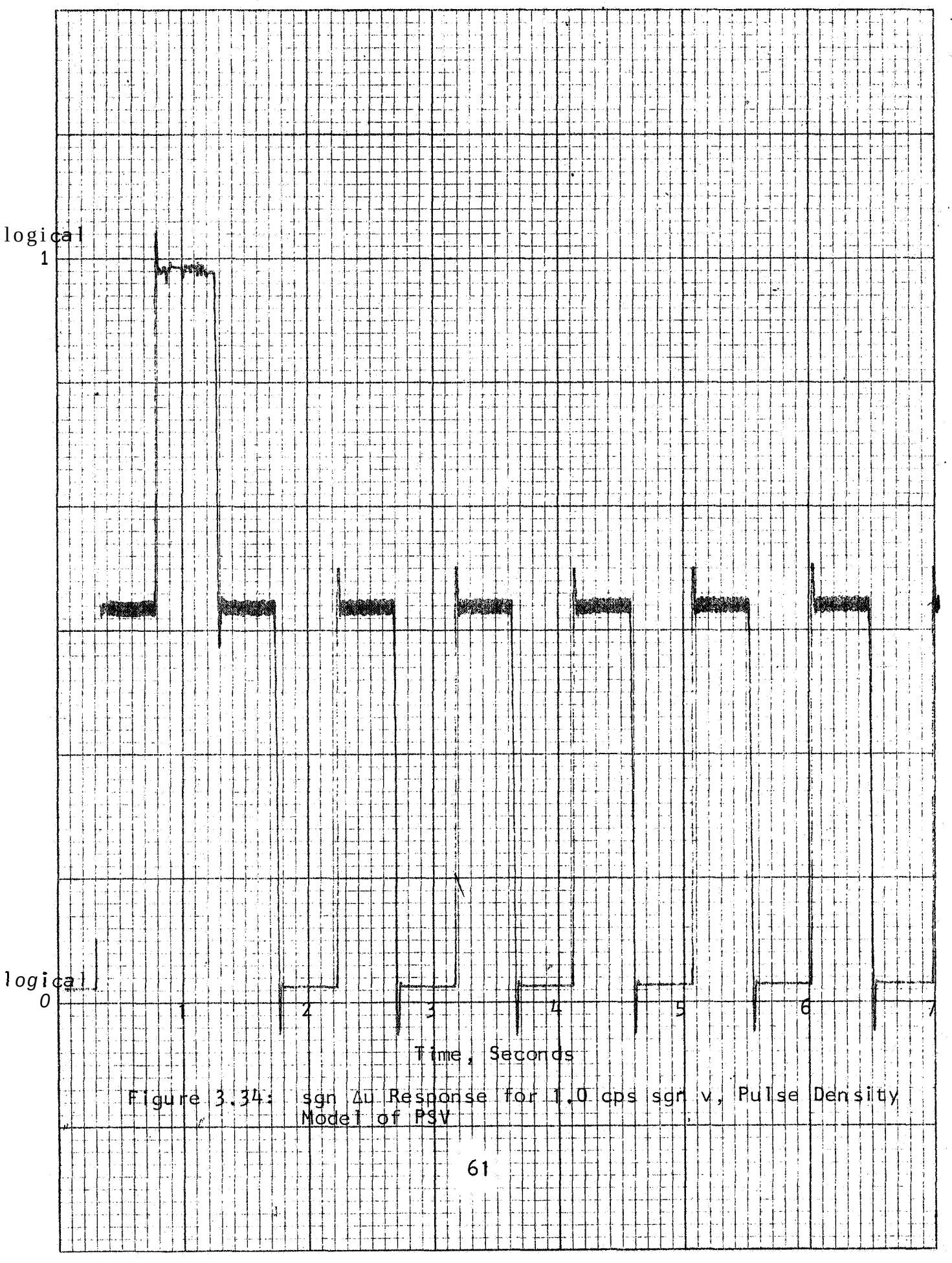

Figure 3.34: sgn Δu Response for 1.0 cps sgn v, Pulse Density Model of PSV

made to determine the waveforms of the u(t) signal generated by the PSV model. With PA prediction intervals of 0.33 second and 1.0 second, recordings were made for PA e(t) input signal frequencies of 0.1 cps and 1.0 cps, and tlie results of these experiments are shown in Figures 3.35 'through 3.38. Since this configuration of Type 2 PA and pulse density PSV model is mathematically equivalent to the Elementary SOC configuration, the results may be compared with the results of the hardware Elementary SOC tests found in Section 3.1.1. Such comparison indicates validity of the pulse density model.

3.1.3 Discussion of Open-Loop Performance with Constant v Input

When the PSV hardware is driven in an open-loop configuration by a constant logical zero v input, it behaves as a free-running multivibrator, with a frequency of oscillation equal to one-half the frequency of the p-register clock, provided the delay is set equal to one clock period. Increasing the time delay produces an oscillation of correspondingly longer period. Very similar behavior is noted in the analog computer simulations of the PSV model; the relay in the feedback also oscillates when the model is driven with a negative v input; the frequency, again, being a function of the delay in the feedback path.

These frequencies of oscillation are well above the cutoff frequency for the actuator and are integrated out to a zero signal; i.e., a negative Z_1 (or logical-zero v) produces, effectively, a $Z_5 = 0$. Viewed over a span of time, the Z_5 output will thus exhibit a decay to zero (degenerative mode) from its initial value starting at the instant Z_1 switches to a negative value. This result also is predicted by the solution for Z_5 under the assumption of $Z_1 = -1$, as developed in Section 2.

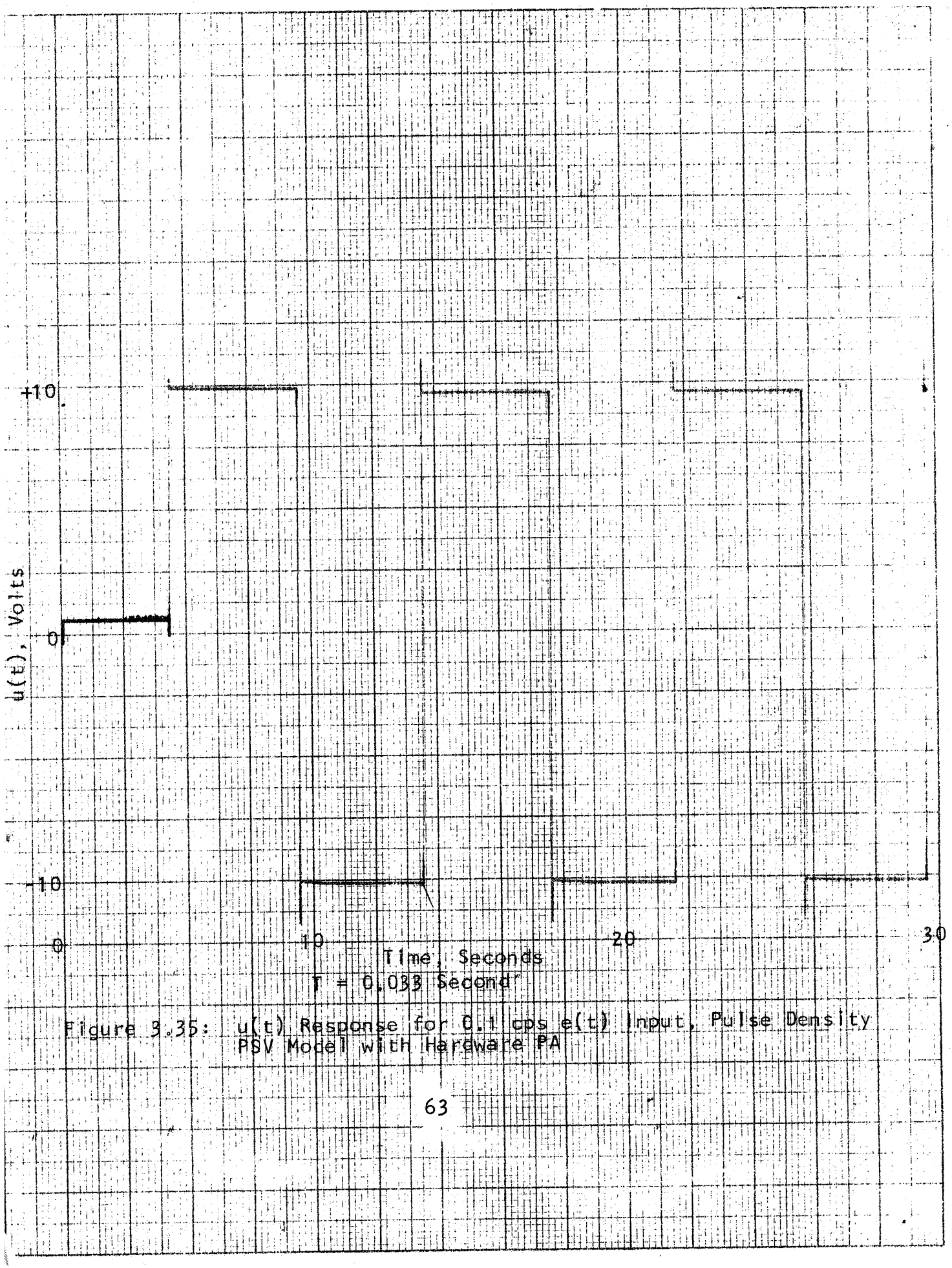

Figure 3.35: u(t) Response for 0.1 cps e(t) Input, Pulse Density PSV Model with Hardware PA

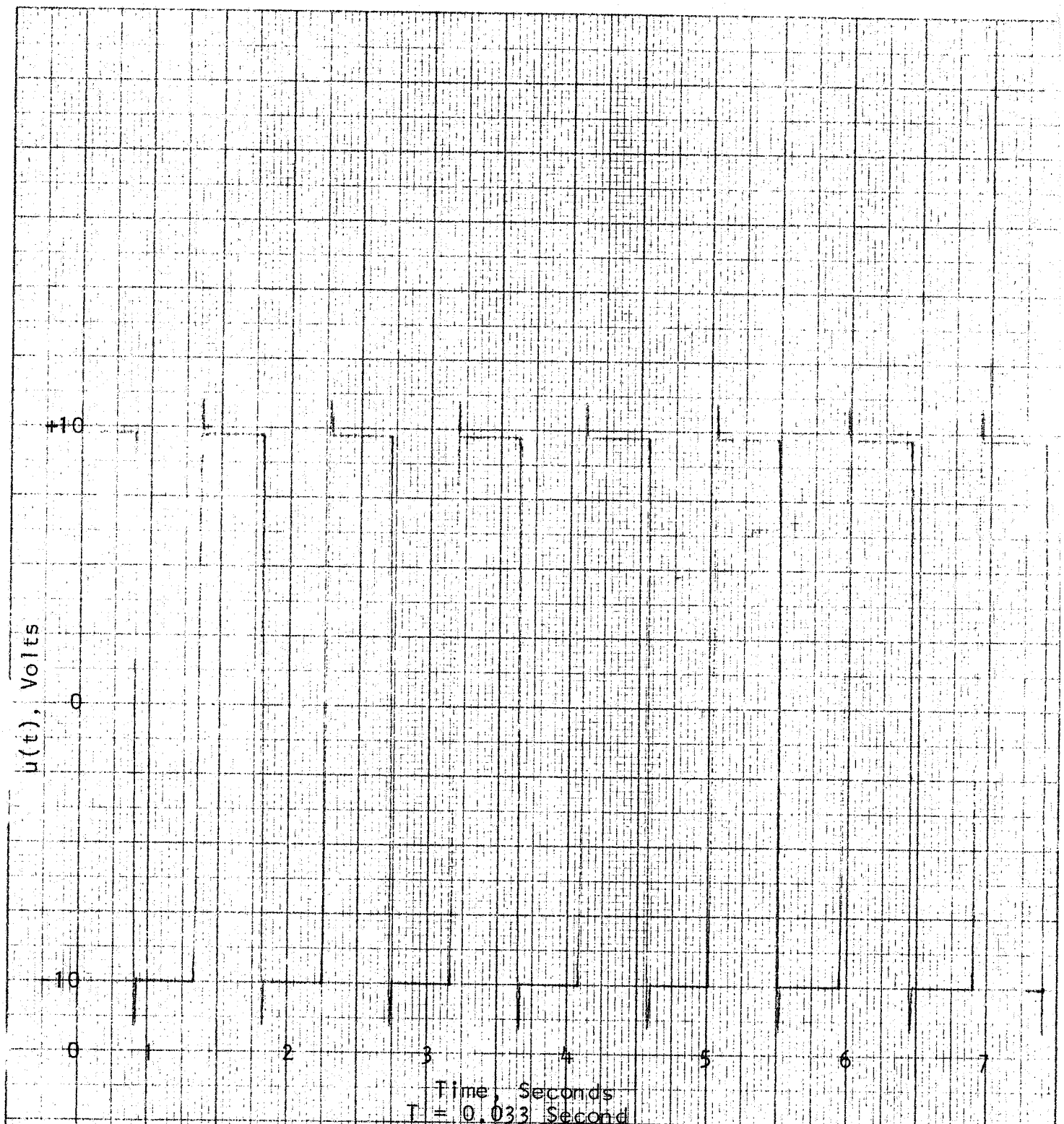

Figure 3.36: u(t) Response for 1.0 cps e(t) Input, Pulse Density PSV Model with Hardware PA

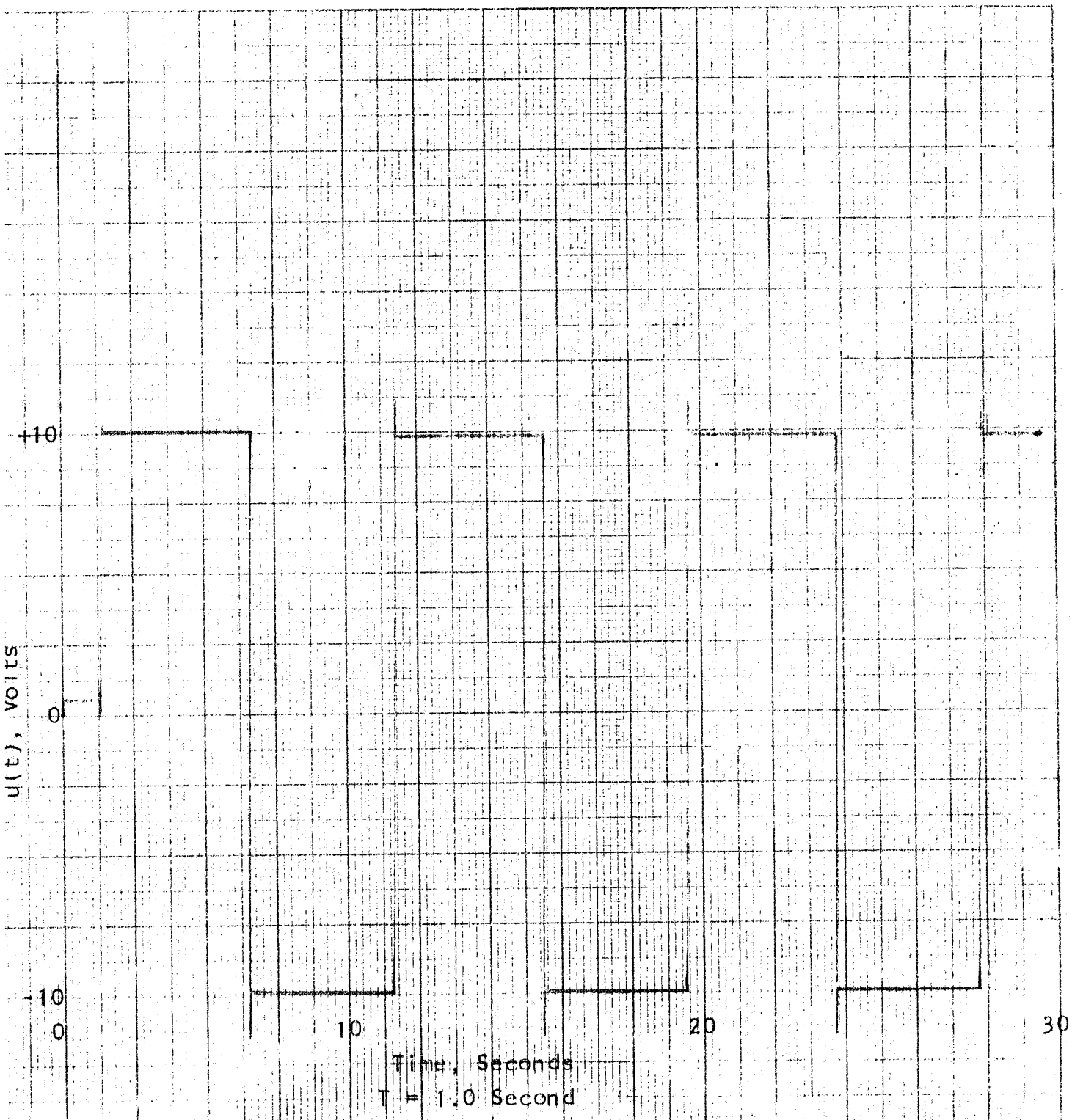

Figure 3.37: u(t) Response for 0.1 cps e(t) Input, Pulse Density PSV Model with Hardware PA

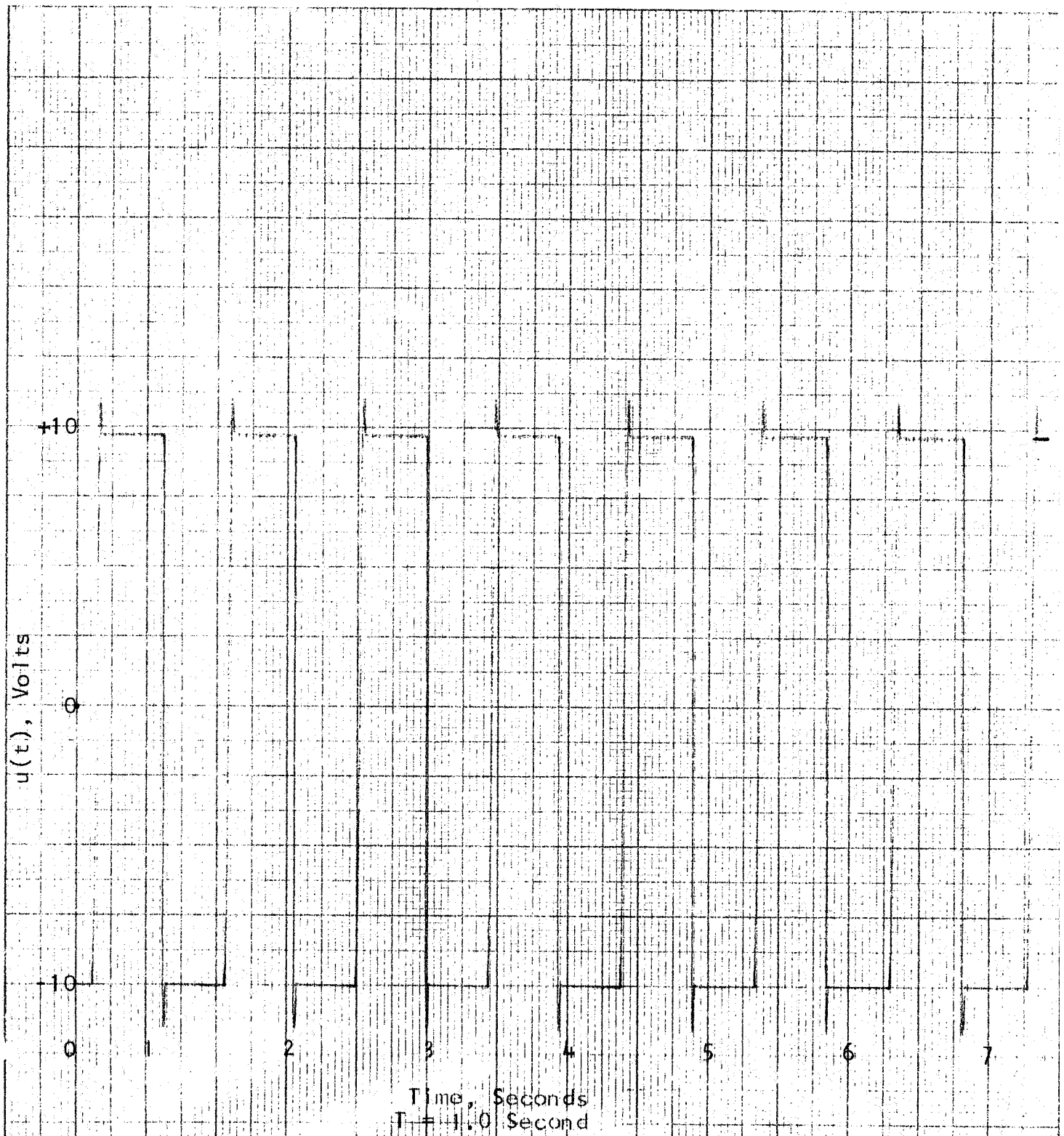

Figure 3.38: u(t) Response for 1.0 cps e(t) Input, Pulse Density PSV Model with Hardware PA

When Z_1 switches to a value of +1, the p register tends to remain at either its positive or negative limit, depending on which sign it has at the time Z_1 switches from -1 to +1. Hence, the previously obtained equation for this case, $Z_5 = 0$ (regenerative mode), appears to be correct in this respect. Sometimes the hardware PSV exhibits changes from one extreme to the other when $Z_1 = +1$, due to the noise in the statistical source. Mathematically, this is the case of $\dot{Z}_5 = n$, where n is simply a random noise signal. By reducing the RMS level of the noise in the statistical source to a value about one-fourth the value for normal operation, the hardware PSV is found to behave essentially as the noise-free mathematical solutions indicate.

It therefore appears that the theory, simulated PSV model, and the actual PSV hardware are substantially in agreement. The exception (noted above) is in the open-loop response for a very "rich" noise setting of the statistical source where, with v = 1, the model does not show the effects of the tendency of the hardware p register to vary from one of its extremes to the other. In deriving the model, we ignore the influence of the noise and have, furthermore, effectively limited the p register to two values, +1 and -1, so that the solution to the equation $\dot{Z}_5 = 0$ can have only one of these two values, which value must be the one existing at t = 0. Although this is apparently a justifiable solution, one might desire a somewhat more elegant solution which includes the noise effects and the integration action of the p register. But in view of the very high speed of operation of the p register, it behaves as a relay as far as the actuator is concerned, so that a more complex model would not add greatly to the solutions insofar as requirements of the Phase I program are concerned.

3.2 Closed-Loop Simulations

3.2.1 Description of Simulated Plant

The plant used in the analog computer simulation for closed-loop experiments is composed of a momentum wheel with the transfer function

$$\frac{Gs}{1+T_m s}$$

and a vehicle with the transfer function $1/s^2$. Combination of these two transfer functions yields

$$\frac{G}{s(1+T_m s)}$$

where G is the momentum-wheel gain factor (including the reciprocal of vehicle inertia if other than unity) and T_m is the momentum-wheel time constant. G = 1.64 and T_m = 20 seconds were used in this simulation.

3.2.2 Simulations of Pulse Density Model of PSV

The closed-loop simulation of the pulse density PSV model is shown in Figure 3.39. The scaled analog computer diagram is presented in Figure 3.40 and Table 3.4 gives the potentiometer values for the computer program.

(a) Without Noise

A phase-plane portrait for PA prediction intervals, T, of 0.4, 0.68, 1.0, 1.5, and 2.0 seconds is given by Figure 3.41 for a 4-degree command signal. This phase-plane

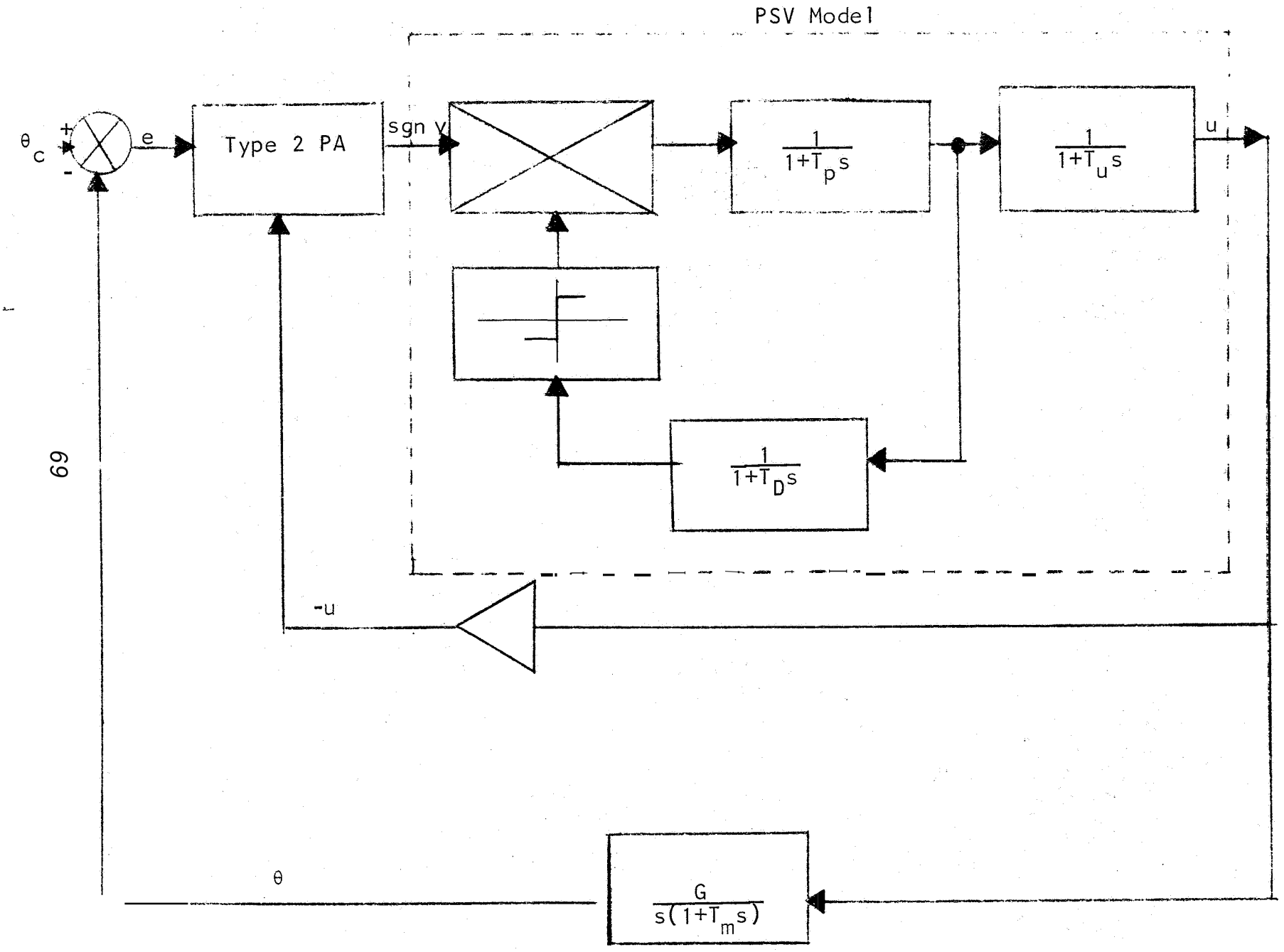

Figure 3 39: Block Diagram of Analog Computer Simulation Using Pulse Density Model for PSV

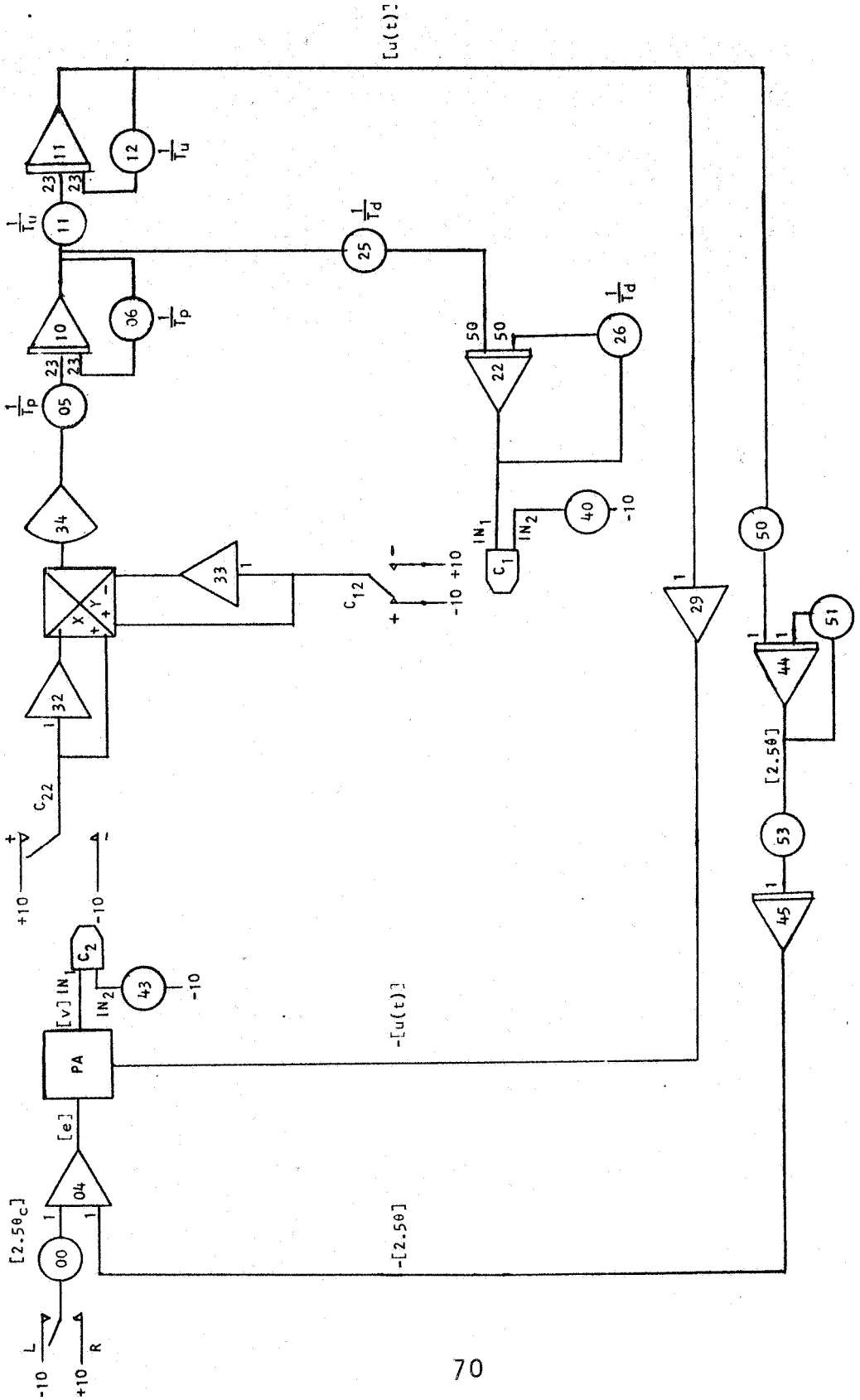

Figure 3.40: Analog Computer Program for Figure 3.39

Table 3.4: Potentiometer Settings for Pulse Density Model of PSV

Potentiometer Number	Setting	Function
00	1.0000	θ_c magnitude control
05	1.0000	$\frac{1}{T_P}$
06	1.0000	
11	1.0000	$\frac{1}{T_U}$
12	1.0000	
25	0.6030	$\frac{1}{T_d}$
26	1.0000	
40	0.1000	for p feedback comparison*
43	0.1010	for v comparison*
50	0.0819	10 G/T_m (0.3280)
51	0.0050	$1/T_m$ (0.0200)
53	0.1000	plant time-scale factor

*Offset here needed to balance comparator to zero.

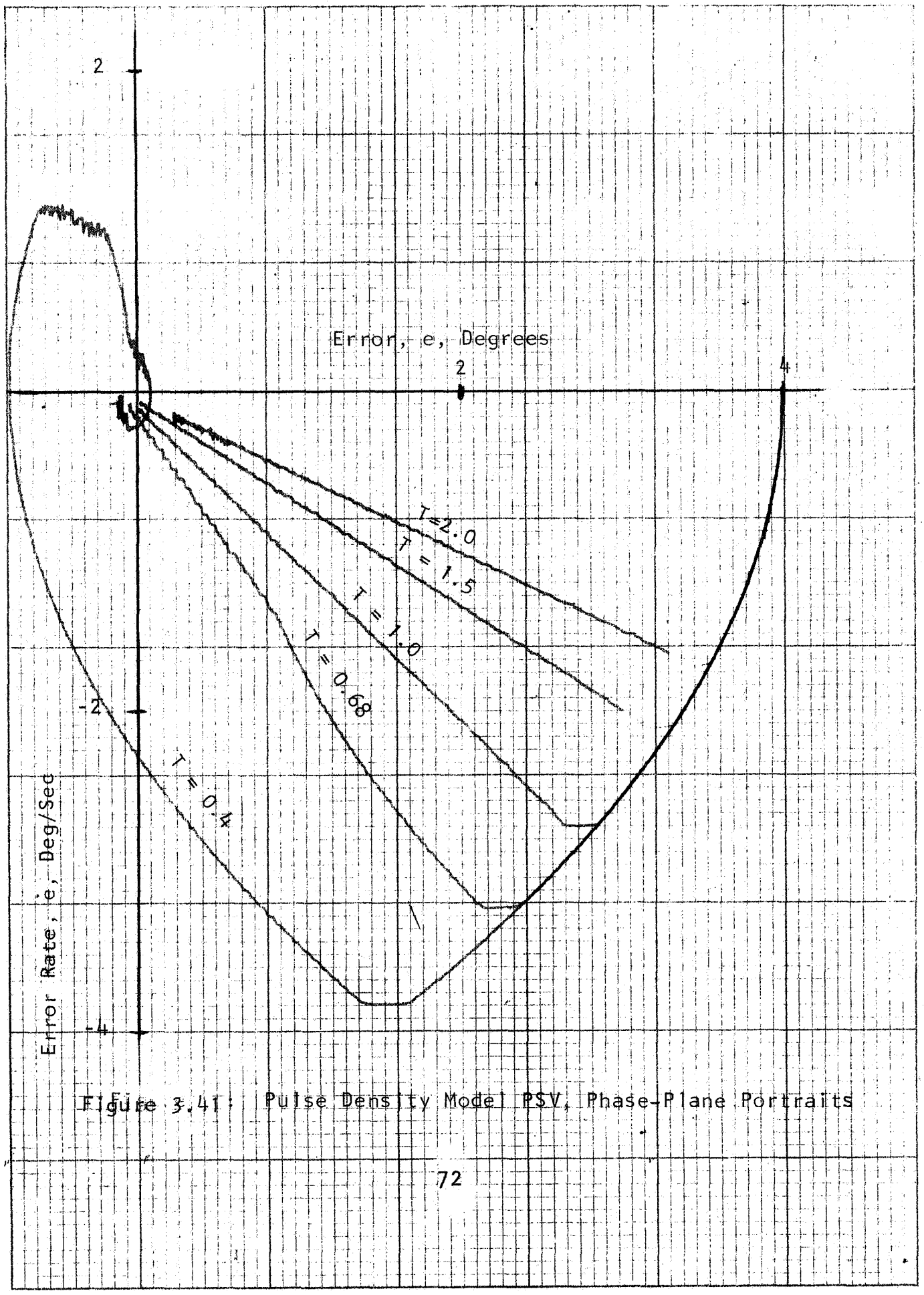

Figure 3.41: Pulse Density Model PSV, Phase-Plane Portraits

portrait illustrates the transient response and stability of the model. The response of error as a function of time for T = 1.5 seconds is given by Figure 3.42 to show the smoothness of the model response.

(b) With Noise

Noise with an equivalent bandwidth of 50 kc was injected at various points in the analog simulation. This noise had no effect on time response or phase-plane response when injected at input or output of the p register, amplifier 10 on Figure 3.40. Since the results of the simulation with noise were identical to previously presented results, they are not shown here in the interest of brevity.

3.2.3 Simulations of Empirical Models

Three different types of empirical models have been simulated:

(i) Relay controllers

(ii) Proportional controller with limiting

(iii) Variable structure controller

The simulation of these controllers were all run in real time. Figure 3.43 is the analog computer diagram for the relay controllers and the proportional controllers with limiting. Table 3.5 gives the potentiometer values and Table 3.6 describes the switch settings.

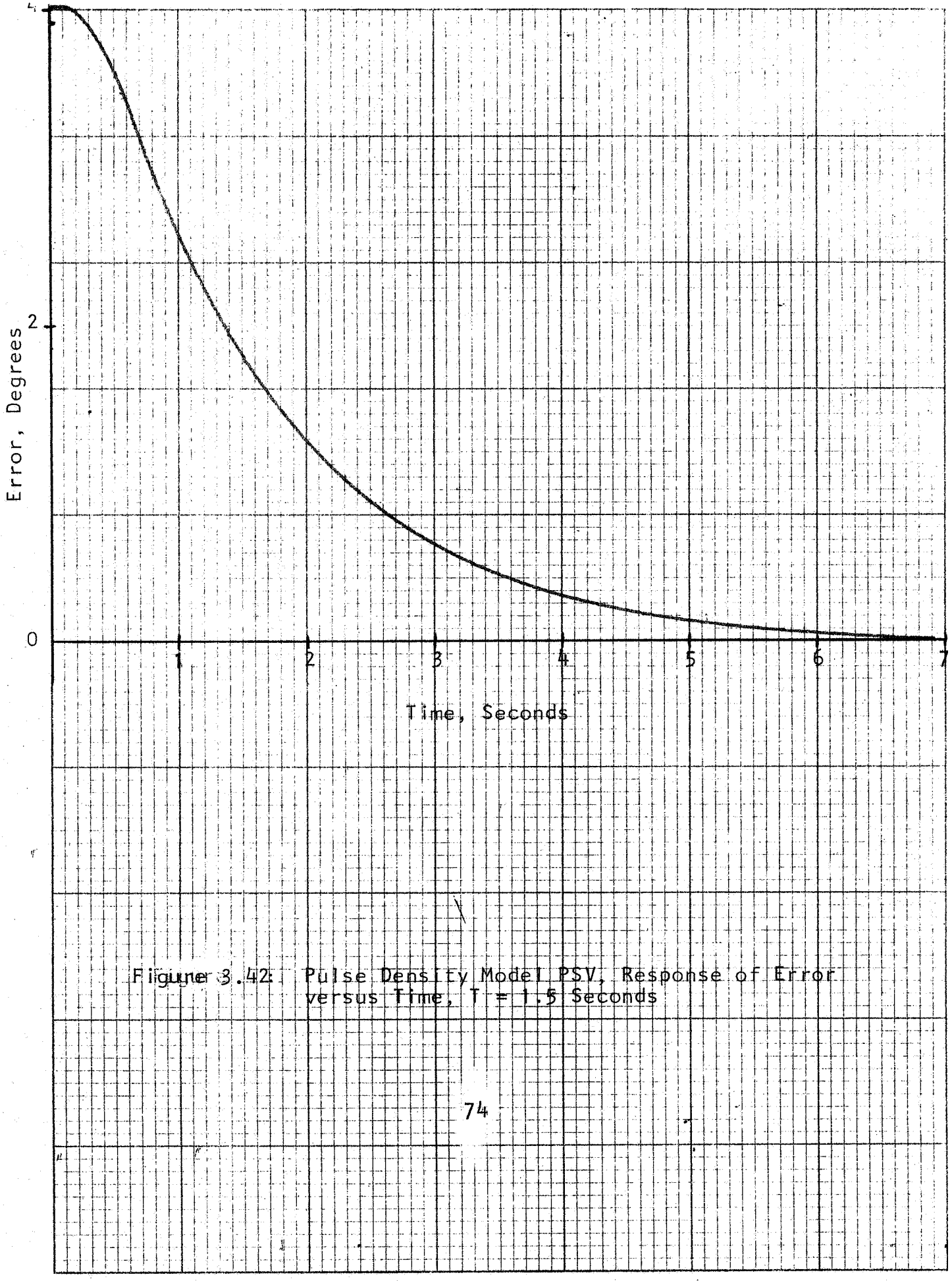

Figure 3.42: Pulse Density Model PSV, Response of Error versus Time, T = 1.5 Seconds

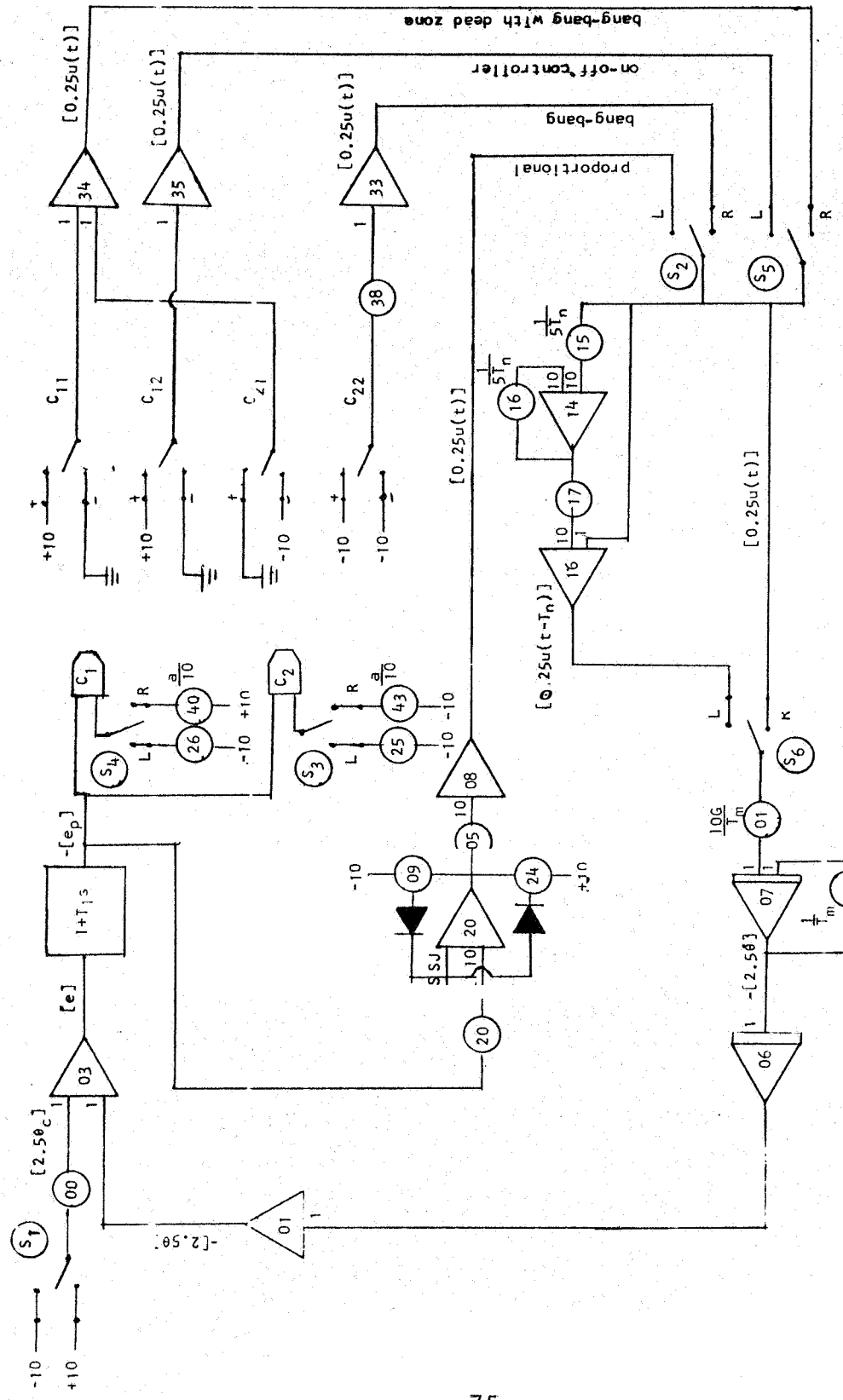

Figure 3.43: Analog Computer Diagram for Relay Controllers and Proportional Controller with Limiting

Table 3.5: Potentiometer Settings for Simulation of Empirical Models

Potentiometer Number	Setting	Function
00	1.0000	θ_c magnitude control
01	0.8200	$10G/T_m$ (0.3280)
02	0.0500	$1/T_m$ (0.0200)
05	0.3726	proportional controller gain control
09	0.1995	soft-limiter upper limit
15	0.2000	$\frac{1}{5T_n}$ time delay (T_n) control
16	0.2000	
17	0.2000	time-delay component
20	0.1568	proportional controller slope control
24	0.1955	soft-limiter lower limit
25	0.0316	C_{2a} bang-bang controller with deadzone*
26	0.0299	C_{1a} on-off controller*
38	1.0000	
40	0.1089	C_{11}
43	0.1792	C_{21} deadzone width

*Offset here needed to balance comparator.

Table 3.6: Description of Switch Positions for Empirical Model Simulation

Switch Number	Position		
	Left	Center	Right
1	θ_c = -4 deg	Open	θ_c = +4 deg
2	Proportional	Open	Bang-Bang, No Deadzone
3	Bang-Bang, No Deadzone	Open	Bang-Bang, with Deadzone
4	On-Off Controller	Open	Bang-Bang, with Deadzone
5	On-Off Controller	Open	Bang-Bang, with Deadzone
6	Time-Delay	Oper	No Time Delay

(a)' Relay Controllers

Two relay controllers were simulated, a pure bang-bang controller and a bang-bang controller with deadzone. The pure bang-bang controller is shown in Figure 3.44. It uses a comparator to detect zero crossings of e_p. The phase-plane portraits for prediction intervals, T, of 0.32, 0.4, 0.68, 1.0, 2.2, 3.2, and 10.0 seconds for the pure bang-bang controller are shown in Figure 3.45.

A deadzone of 1.4 degrees was used in the bang-bang controller with deadzone. The block diagram of this controller is presented in Figure 3.46, and its phase-plane performance is shown in Figure 3.47 for the same T values as used above with the pure bang-bang system. As can be observed, the deadzone produces a terminal error offset (actually the beginning of the limit cycle), but the controller with deadzone exhibits a much smoother response than does the pure bang-bang controller.

(b) Proportional Controllers with Limiting

Figure 3.48 is the block diagram of the proportional controller with limiting. The phase-plane portraits for this system are shown in Figure 3.49 for the same T values used with the relay controllers. The proportional controller with limiting appears to have a smoother response than was produced by either of the relay controllers simulated.

(c) Variable Structure Controller

The block diagram of a Variable Structure Controller (VSC) is shown in Figure 3.50, with the associated analog

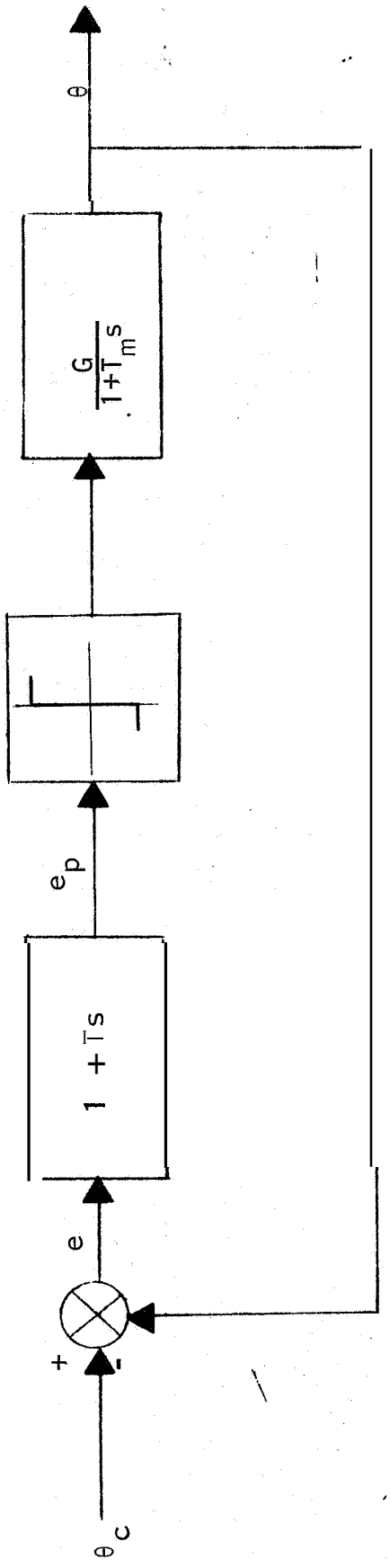

Figure 3.4: Bang-Bang Controller

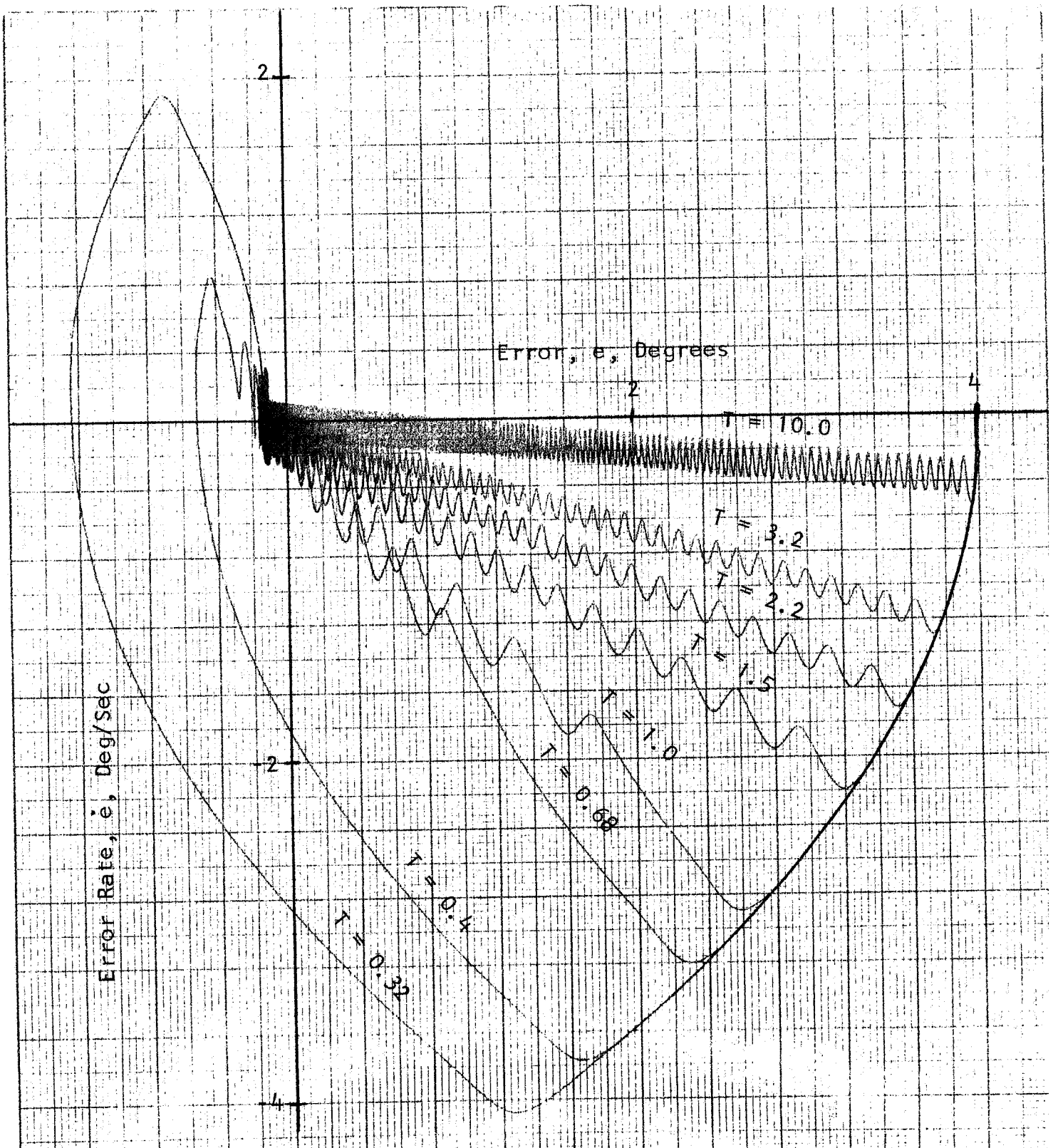

Figure 3.45: Bang-Bang Controller, Phase-Plane Portraits

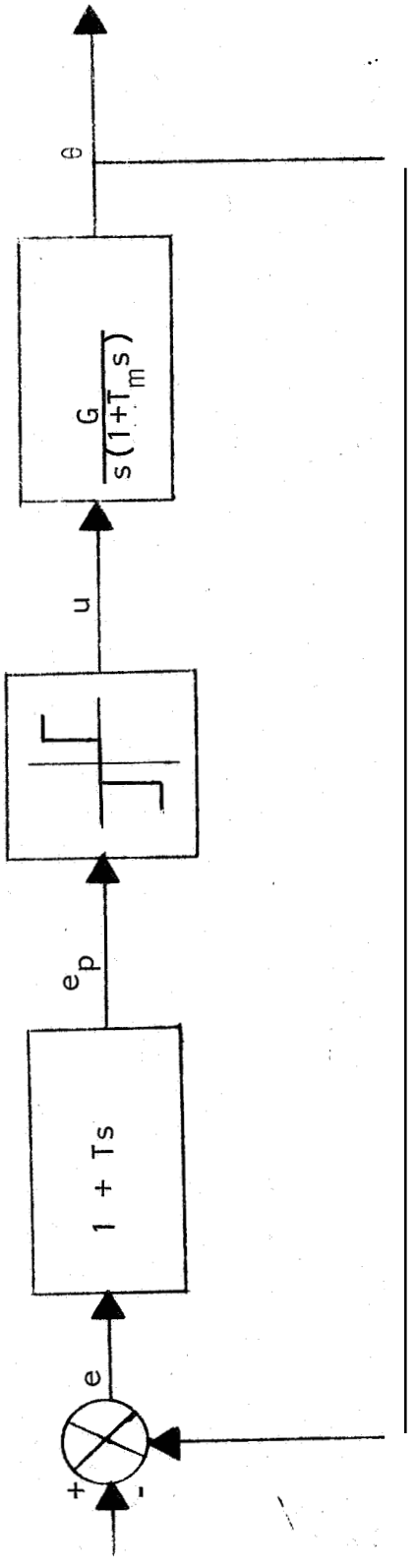

Figure 3.46: Bang-Bang Controller with Deadzone

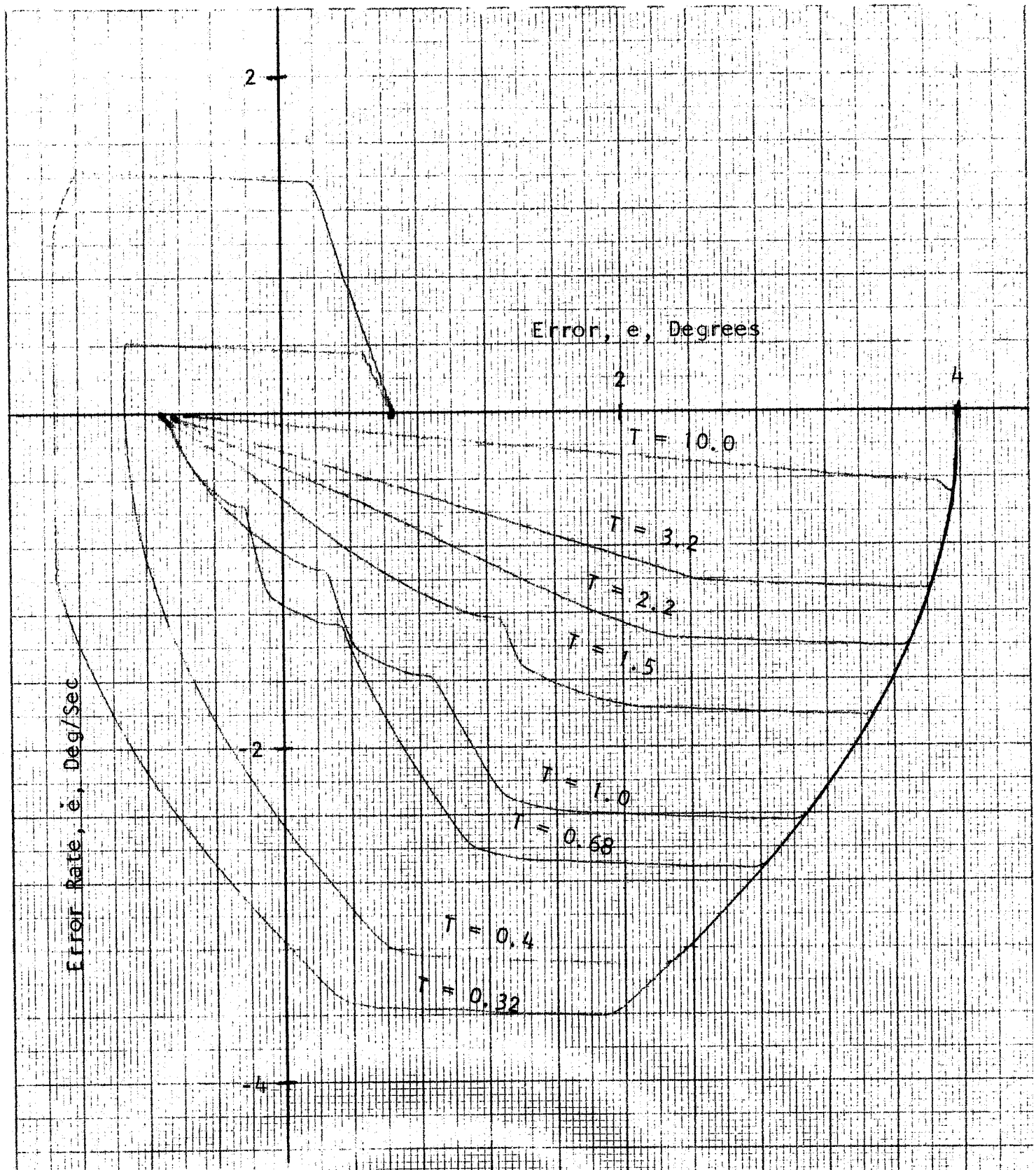

Figure 3.47: Bang-Bang Controller with Deadzone, Phase-Plane Portraits

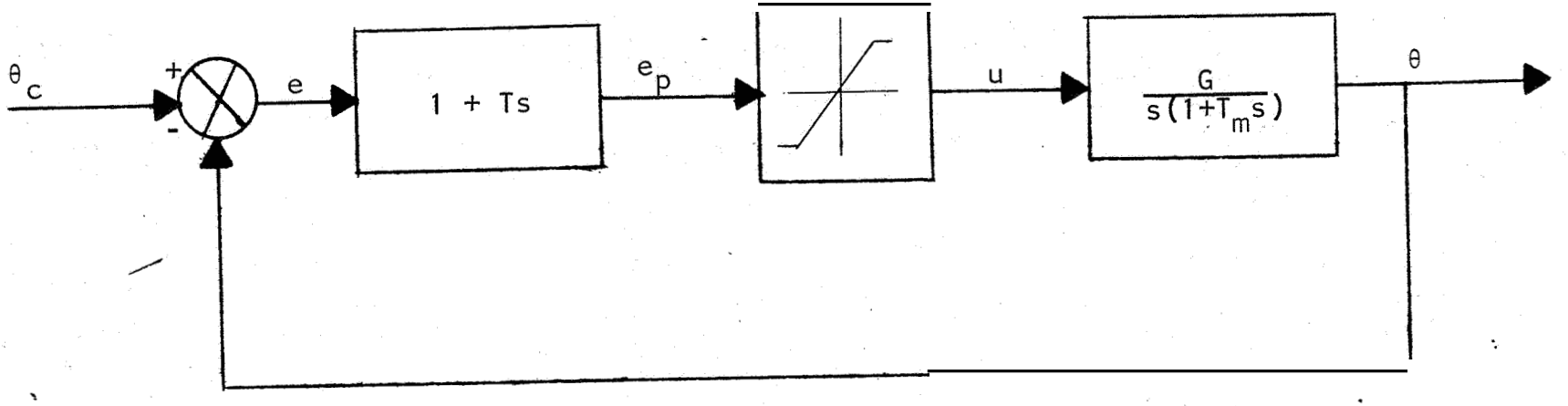

Figure 3.48 : Proportional Controller with Limits

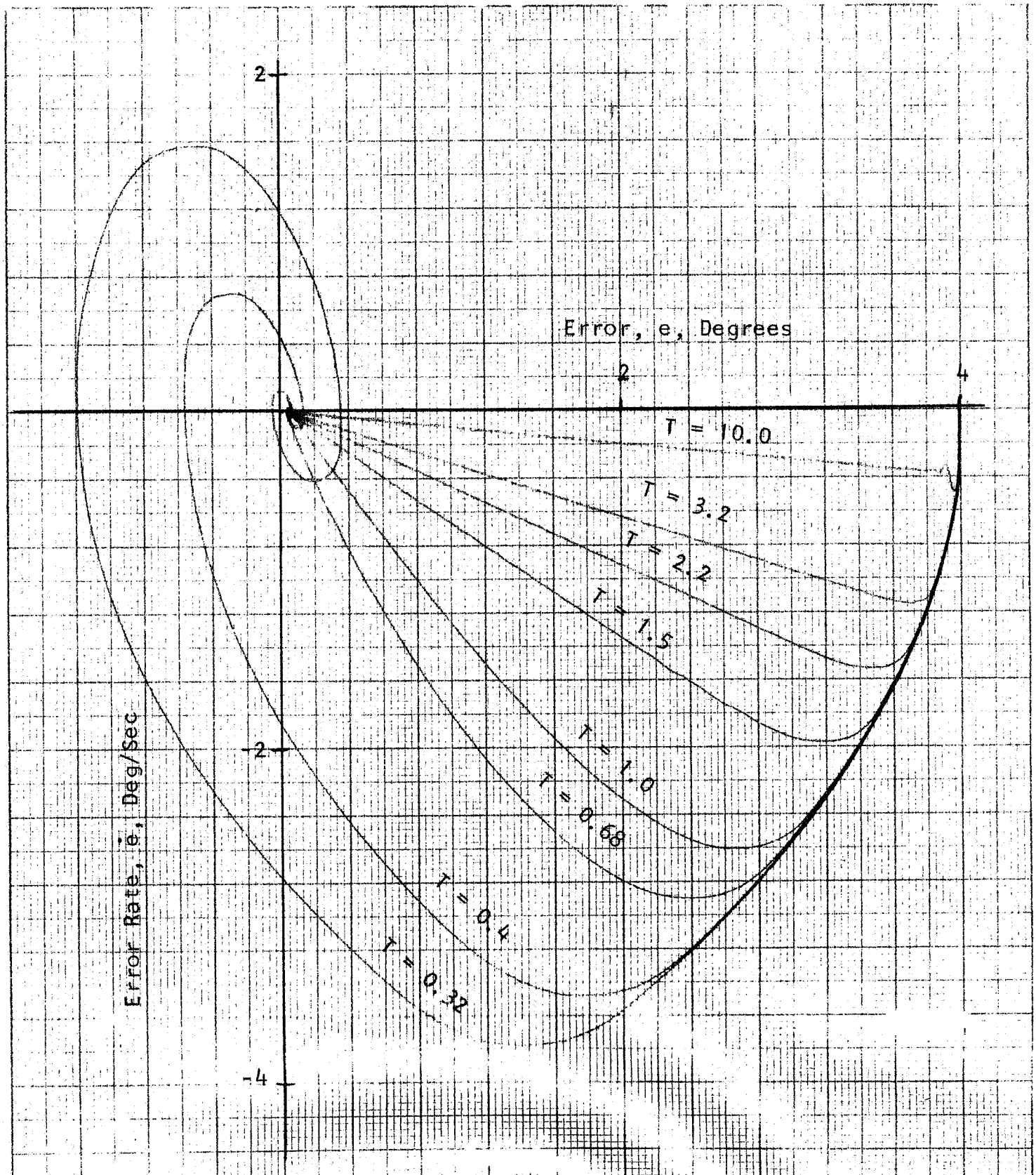

Figure 3.49 : Proportional Controller with Limits, Phase-Plane Portraits

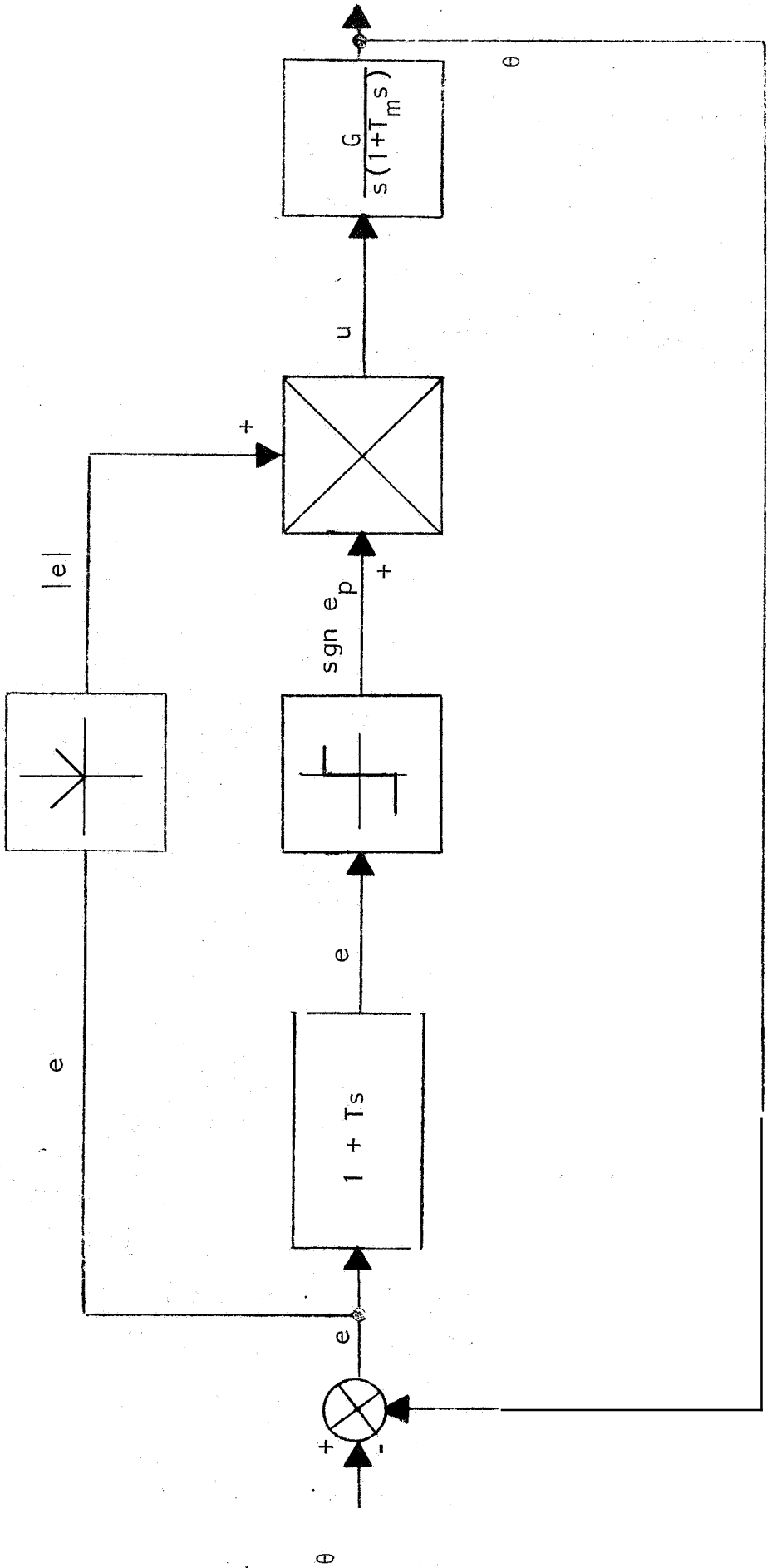

Figure 3.50 : Variable Structure Controller

computer diagram given in Figure 3.51, An extensive discussion of the theory and operation of the Variable Structure Controller is available in References 5 and 6. This simulation used the same plant dynamics as were employed in the other closed-loop experiments. Plant simulation potentiometers were set as follows.

Potentiometer No.	Setting
05	0.8200
06	0.0500
07	1.0000

The phase-plane response of the VSC for T = 3.2 seconds, Figure 3.52, exhibits a stable response much like that of the other empirical models; however, the VSC response is much different when T = 1.0 second, as shown by Figure 3.53. The VSC error response for the case of T = 1.0 second is recorded vs. time in Figure 3.54. The latter figure exhibits the oscillatory motion very clearly.

3.2.4 Simulations with SOC hardware

Simulations using SOC hardware were performed for Elementary SOC and Type 1 PA/General Purpose PSV controller as discussed below.

(a) Elementary SOC Configuration

The block diagram for simulation with the Elementary SOC is shown by Figure 3.55. The phase-plane portraits for this configuration are given by Figure 3.56 for T values of 0.32, 0.4, 0.68, 1.0, 1.5, 3.2, and 10.0 seconds. Except for X-Y recorder internal noise problems accompanying the

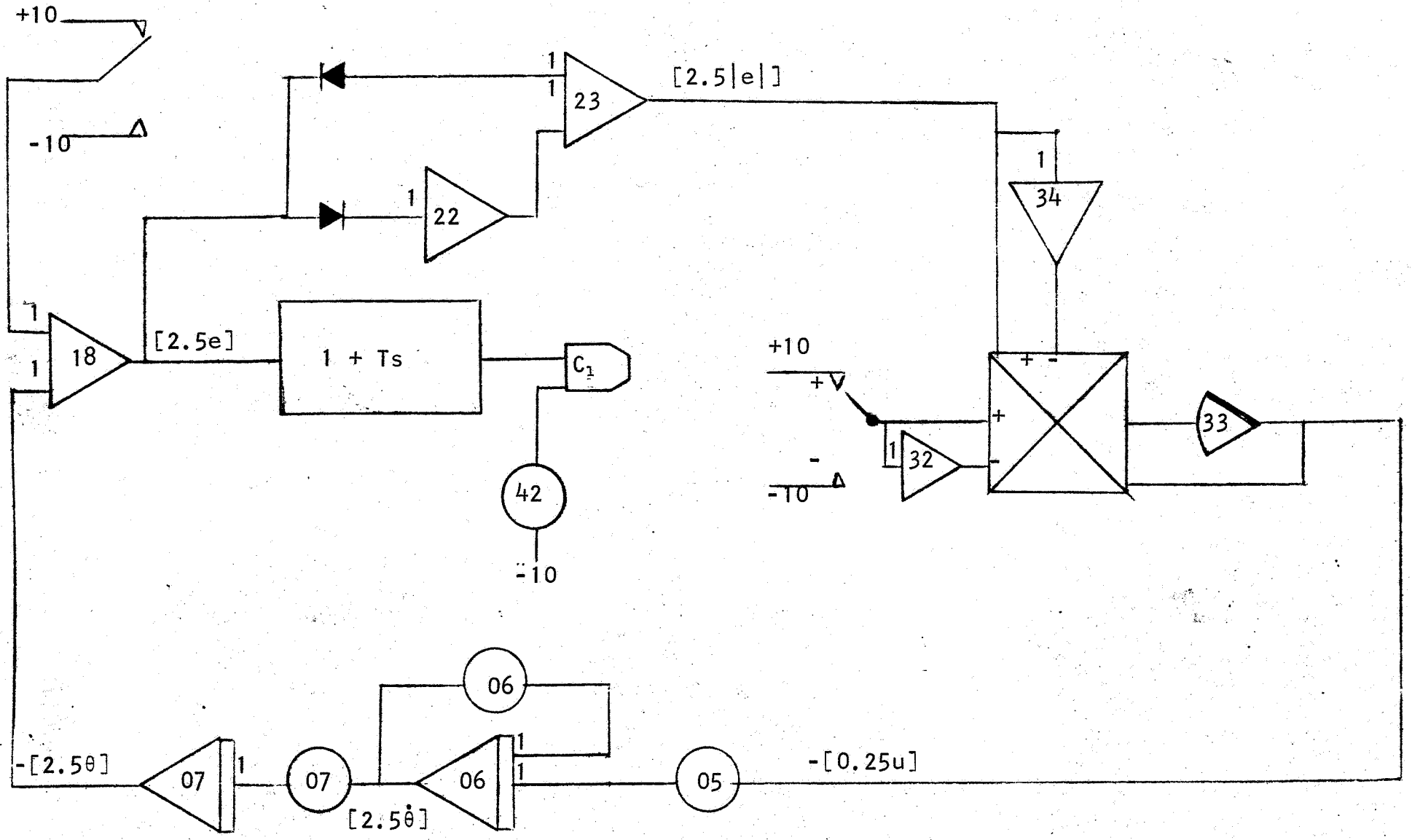

Figure 3.51: Variable Structure Controller, Analog Computer Diagram

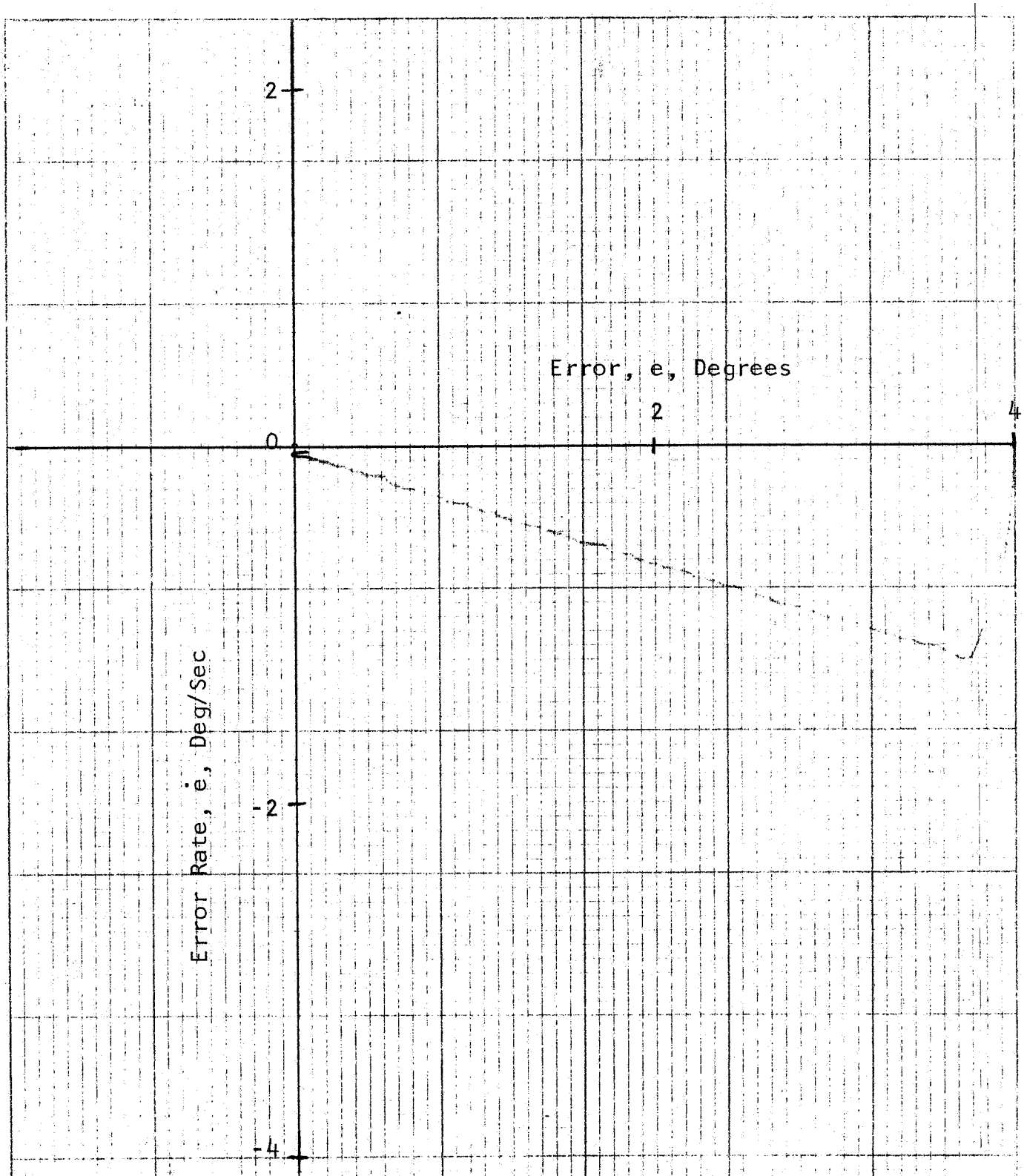

Figure 3.52: Variable Structure Controller, Phase-Plane Portrait, T = 3.2 Seconds

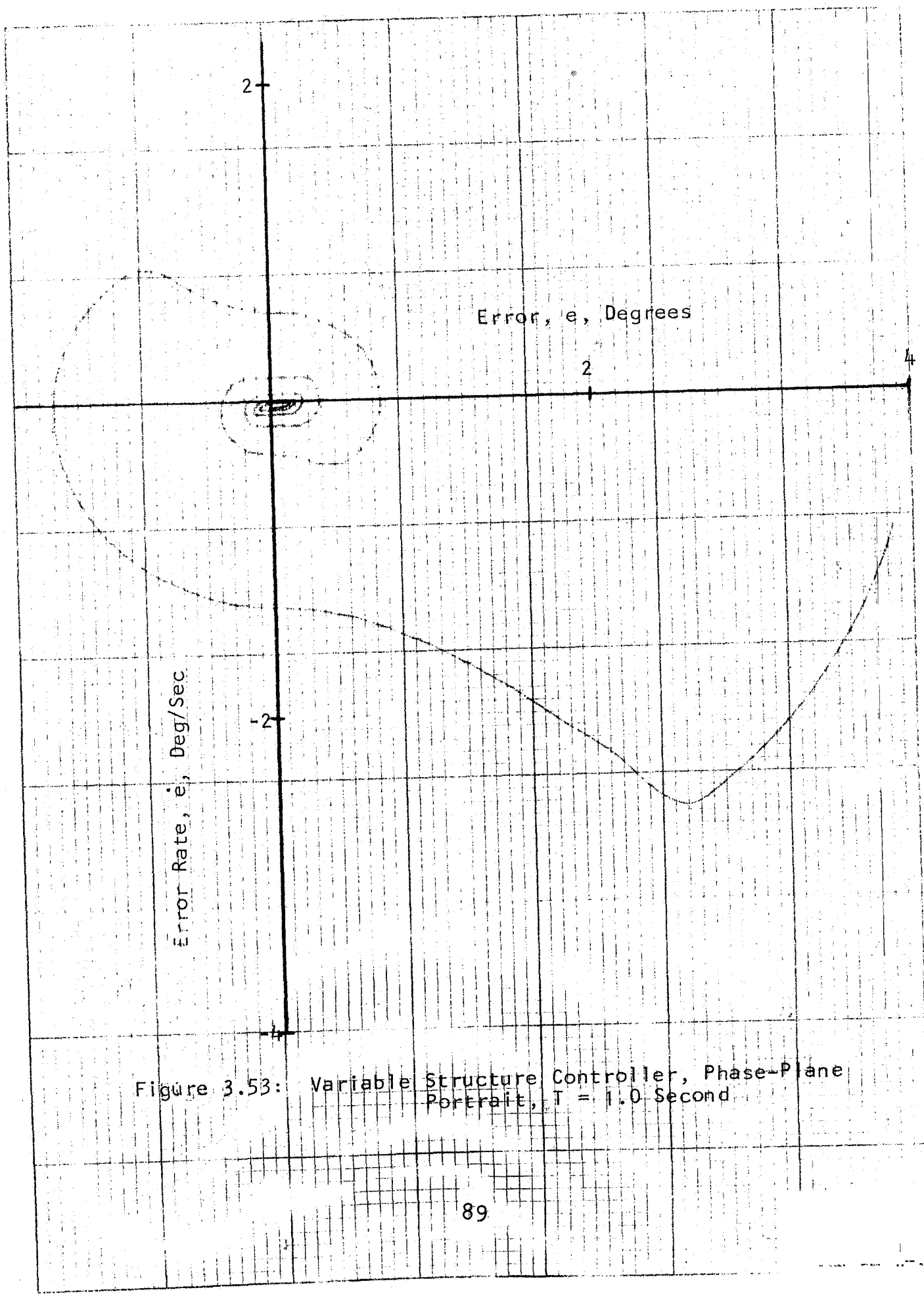

Figure 3.53: Variable Structure Controller, Phase-Plane Portrait, T = 1.0 Second

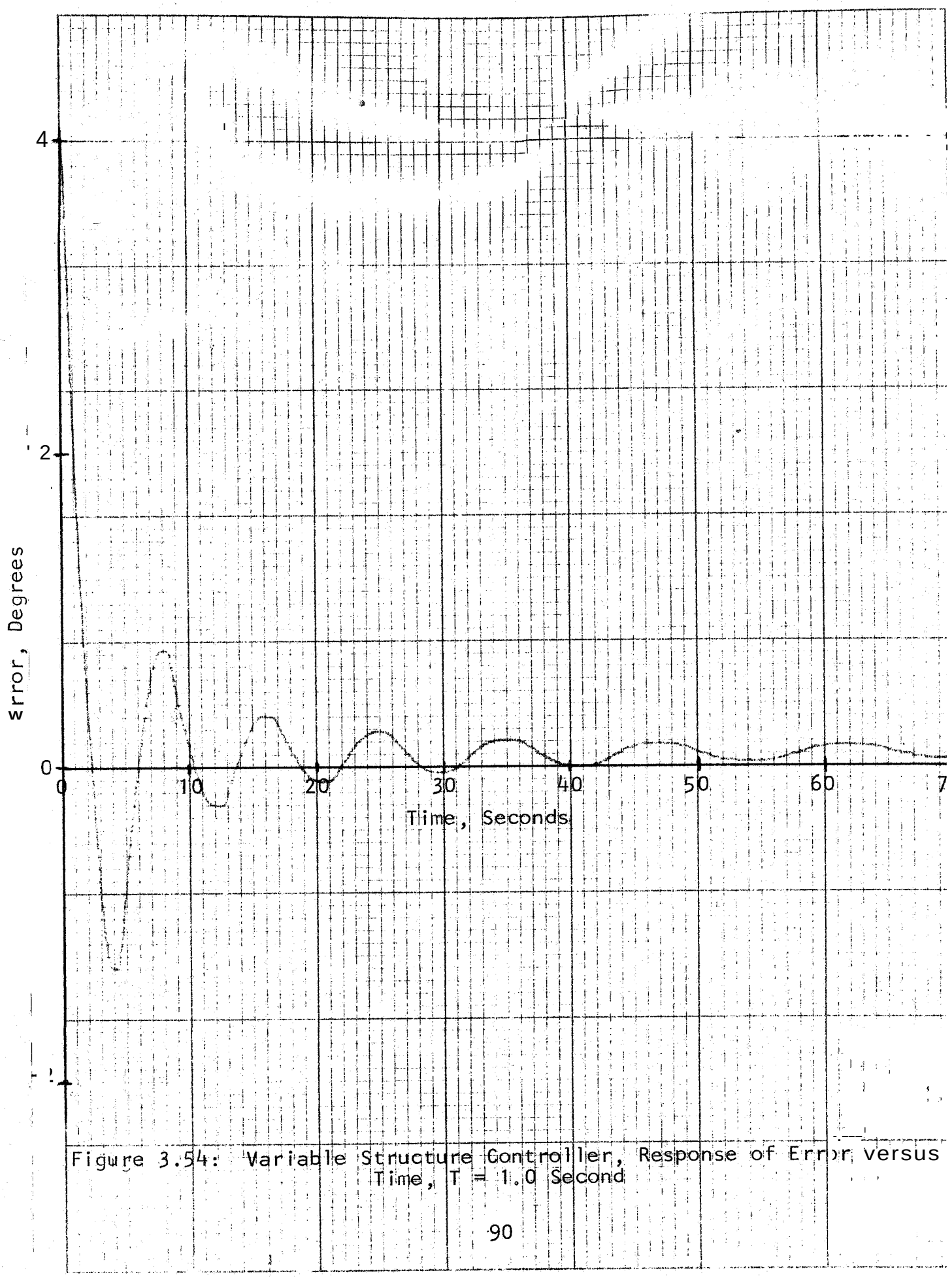

Figure 3.54: Variable Structure Controller, Response of Error versus Time, T = 1.0 Second

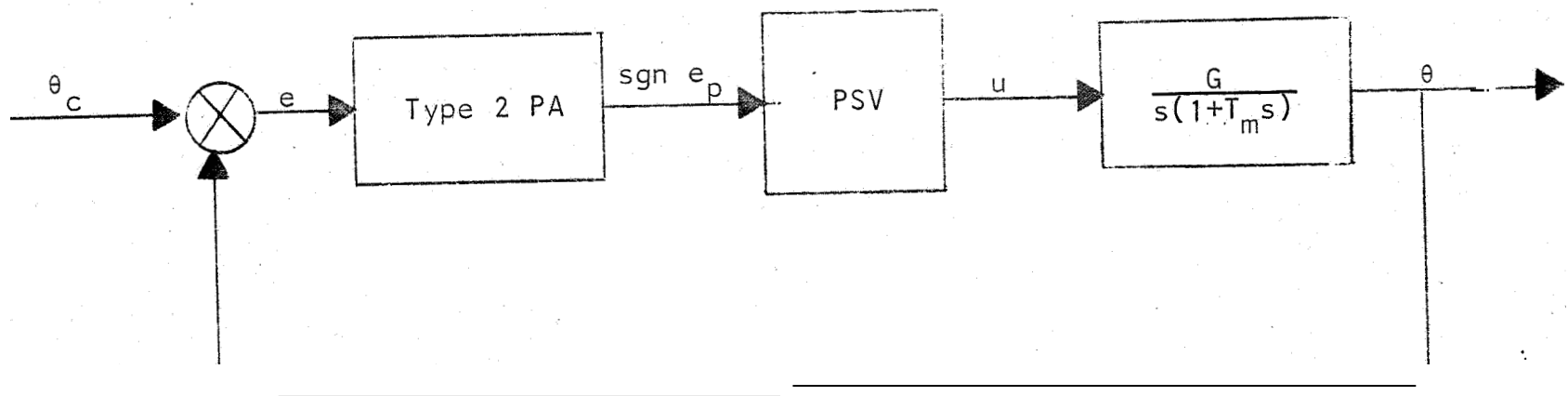

Figure 3.55: Simulation with Elementary SOC

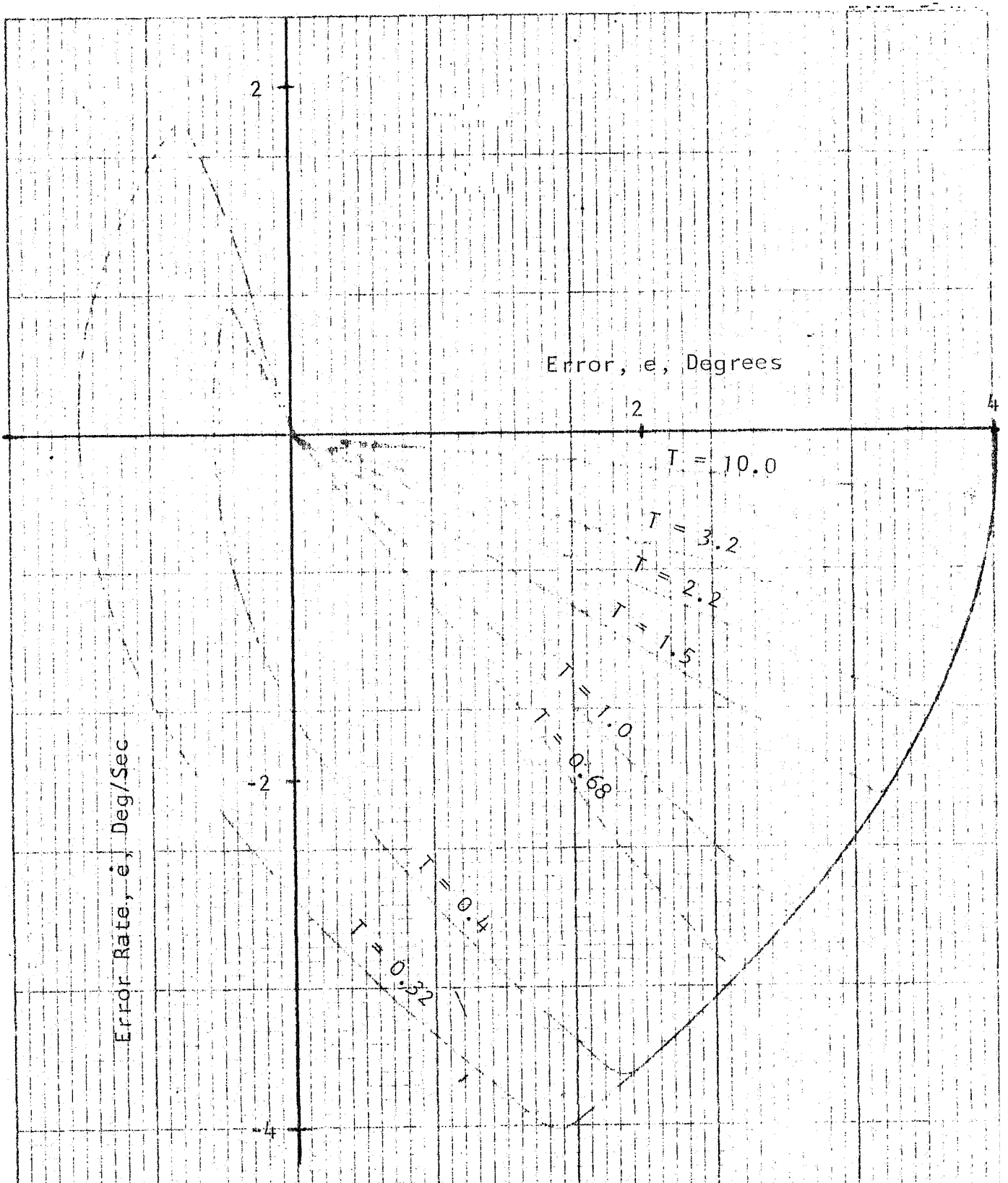

Figure 3.56. Elementary SOC, Phase-Plane Portraits

run for T = 3.2 seconds, the response is smooth for all T values.* As can be seen from the diagram, the SOC reaches the origin of the phase-plane without oscillations.

(b) Type 2 PA/General Purpose PSV Controller

For this experiment, the general purpose PSV was used in conjunction with Type 2 PA hardware, as shown in the block diagram, Figure 3.57. The phase-plane response curves for T = 0.4 second is given in Figure 3.58, and Figure 3.59 is the phase-plane diagram obtained using T = 3.2 seconds. In each case, the SOC exhibits smooth, stable, non-oscillatory response.

3.3 Comparisons of Results

The results for the PSV model and the PSV hardware operating open loop are given in Section 3.1. The model open-loop results show close similarity to those of the hardware if the noise generator output is set to about 2.5 volts RMS or less ("lean" setting). At low input frequencies, the model and hardware sgn Au recordings exhibit essentially identical results. The u(t) response of the PSV model when used with Type 2 PA hardware is also similar to the hardware u(t) for the same configuration when both are subjected to similar e(t) inputs.

The final comparison between the PSV hardware and PSV model will now be made in the closed-loop configuration with T = 1.5. Figure 3.60 is the phase-plane diagram for the

*Figure 3.59 is a better indication of true SOC response characteristics with T = 3.2 seconds.

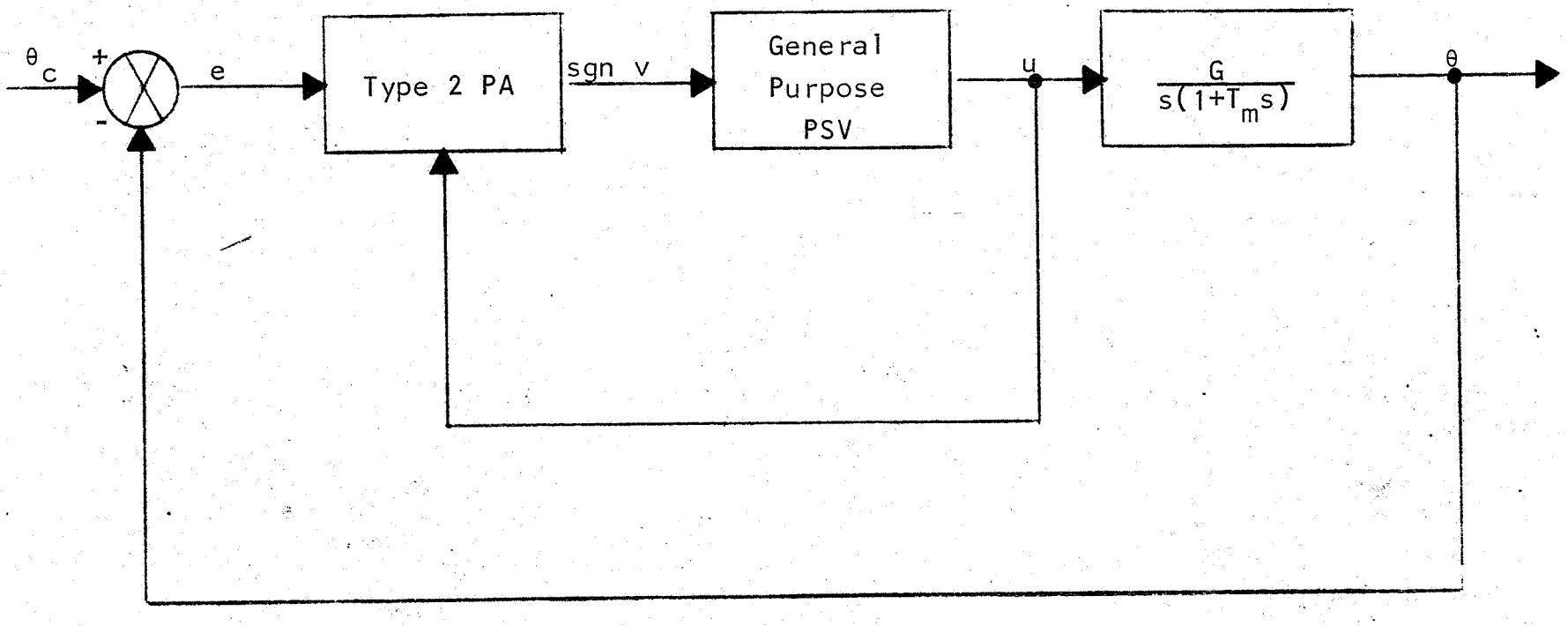

Figure 3.57: Simulation with Type 2 PA/General Purpose PSV Controller

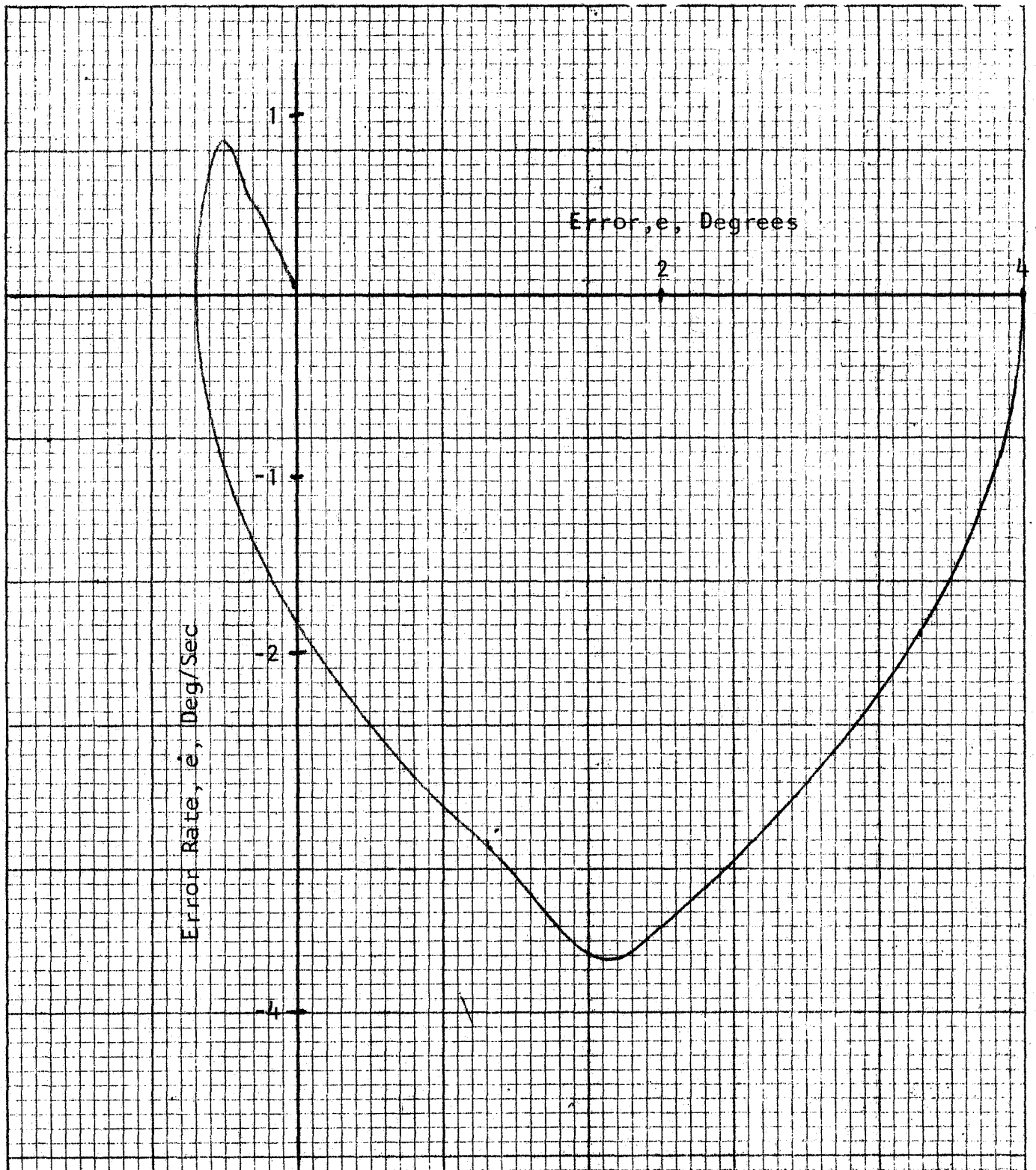

Figure 3.58: Type 2 PA/General Purpose PSV Hardware, Phase-plane Portrait, T = 0.4 Second

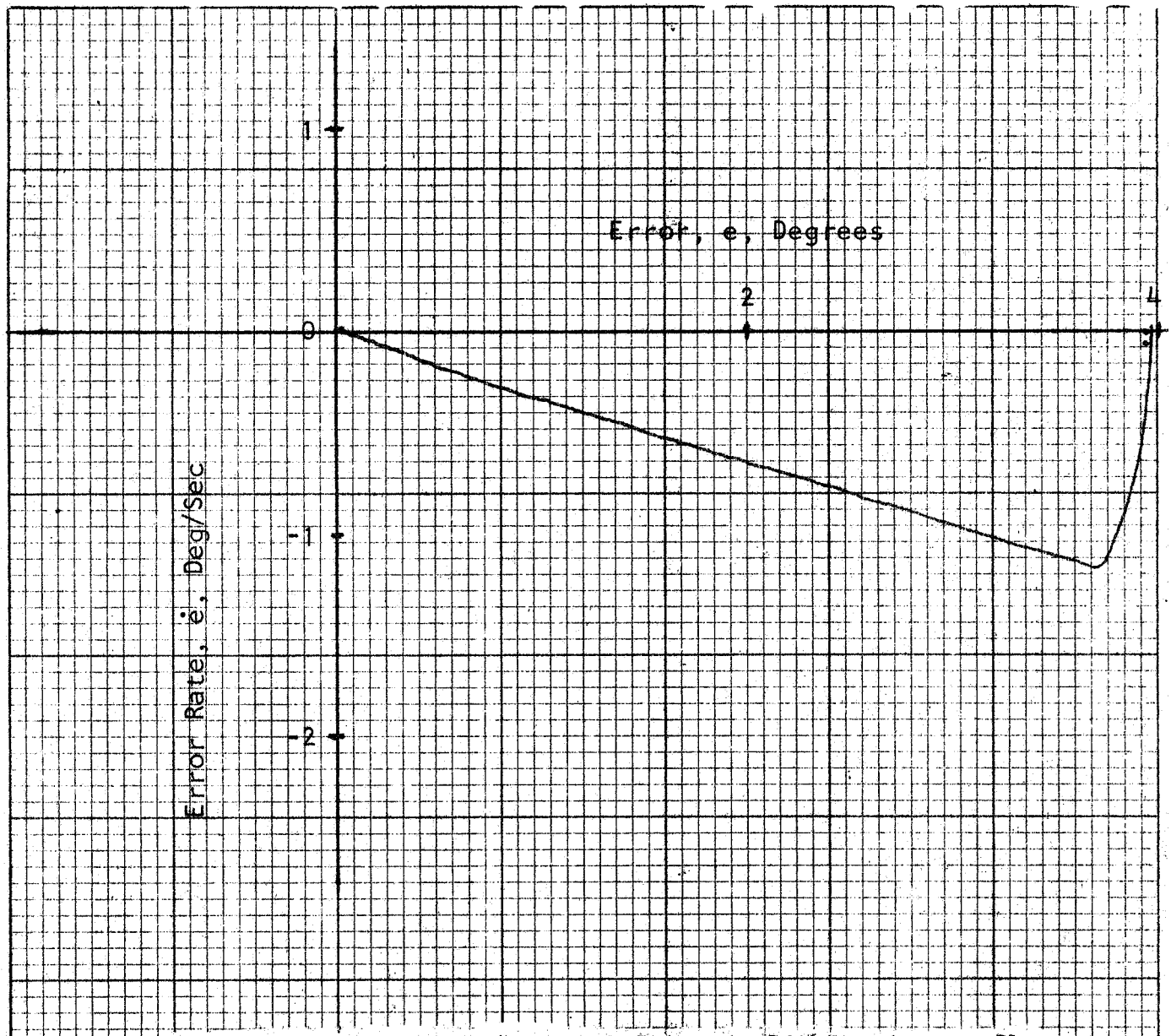

Figure 3.59: Type 2 PA/General Purpose PSV Hardware, Phase-Plane Portrait, T = 3.2 Seconds

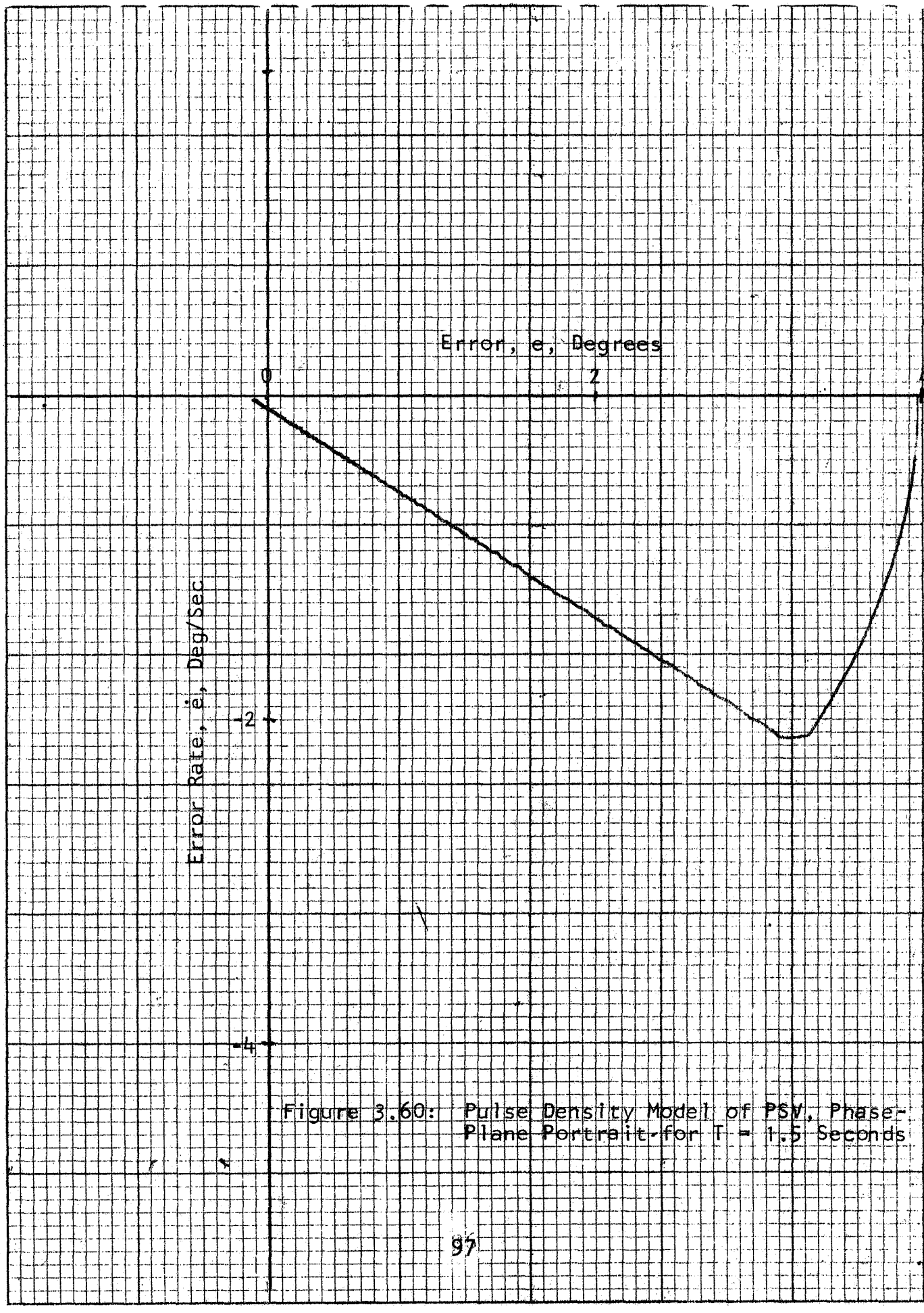

Figure 3.60: Pulse Density Model of PSV, Phase-Plane Portrait for T = 1.5 Seconds

pulse density model and Figures 3.61 and 3.62 are comparative phase-plane portraits for the Elementary SOC hardware and the Type 2 PA/General Purpose PSV controller hardware configurations, respectively. The three results are almost identical, giving further proof of model validity. The family of error time-response histories also verifies the model and hardware similarity. The time response of the model error function for T = 1.5 seconds was presented in Section 3.2.2 (Figure 3.42). The time response of the error function for the Elementary and Type 2 PA/General Purpose PSV controller is given in Figures 3.63 and 3.64, respectively. Again, the resul'ts are nearly identical.

Of the other models, the proportional controller with limiting comes closest to reproducing the PSV hardware responses. Figure 3.65 is the phase-plane diagram for the proportional controller with limiting, for T = 3.2 seconds. The Variable Structure Controller exhibits a damped oscillatdry motion when T = 1.5 seconds, as shown by Figure 3.66. The bang-bang controller phase-plane graph for T = 3.2 seconds exhibits oscillations about the switching line (Figure 3.67), and the deadzone is easily detected in the phase plane for the bang-bang controller with deadzone (Figure 3.68).

It is concluded from these data that the pulse density model is a satisfactory representation of the PSV hardware and is a better model than any of the empirical models with the possible exception of the proportional'controller with 1imiting.

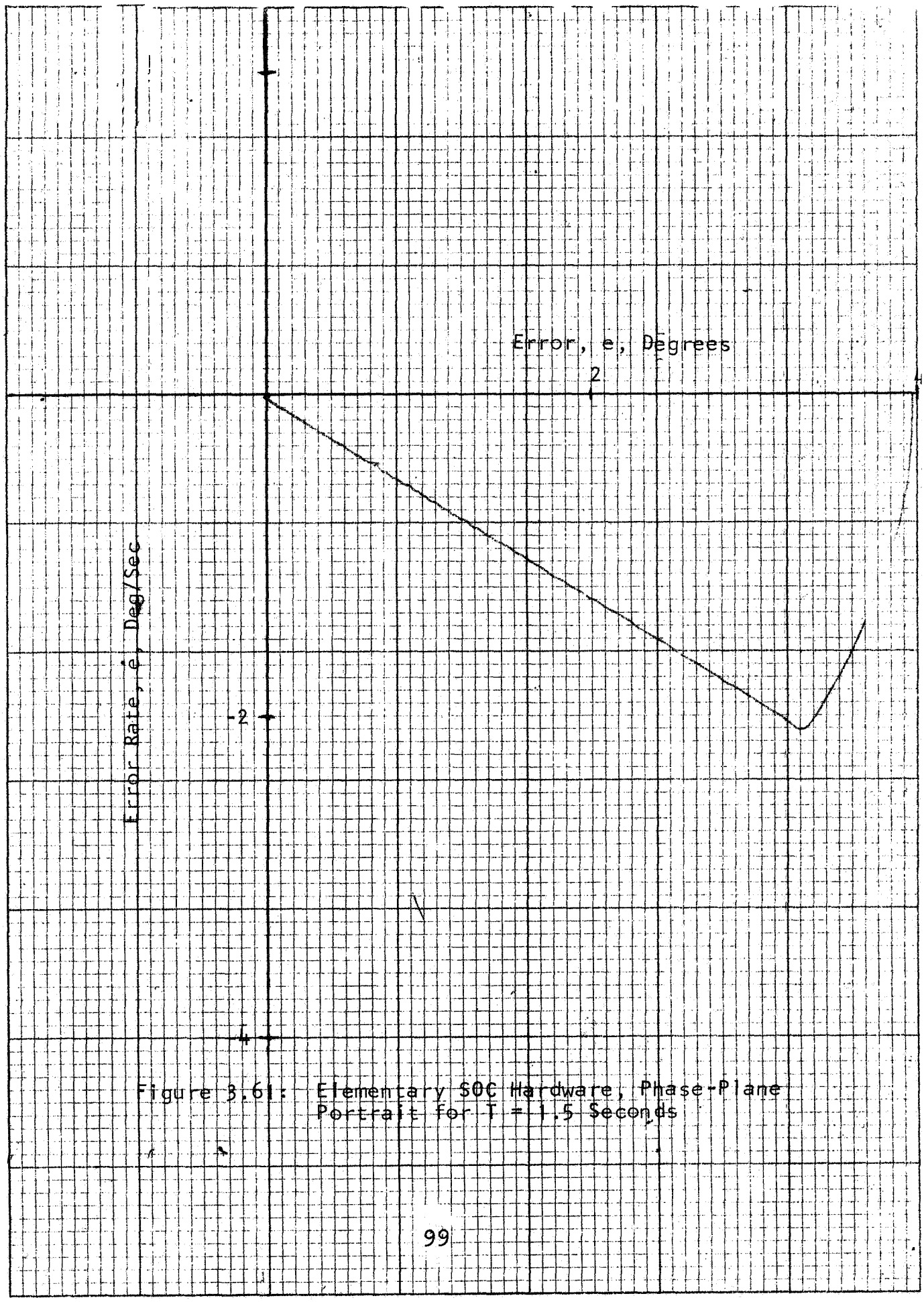

Figure 3.61: Elementary SOC Hardware, Phase-Plane Portrait for T = 1.5 Seconds

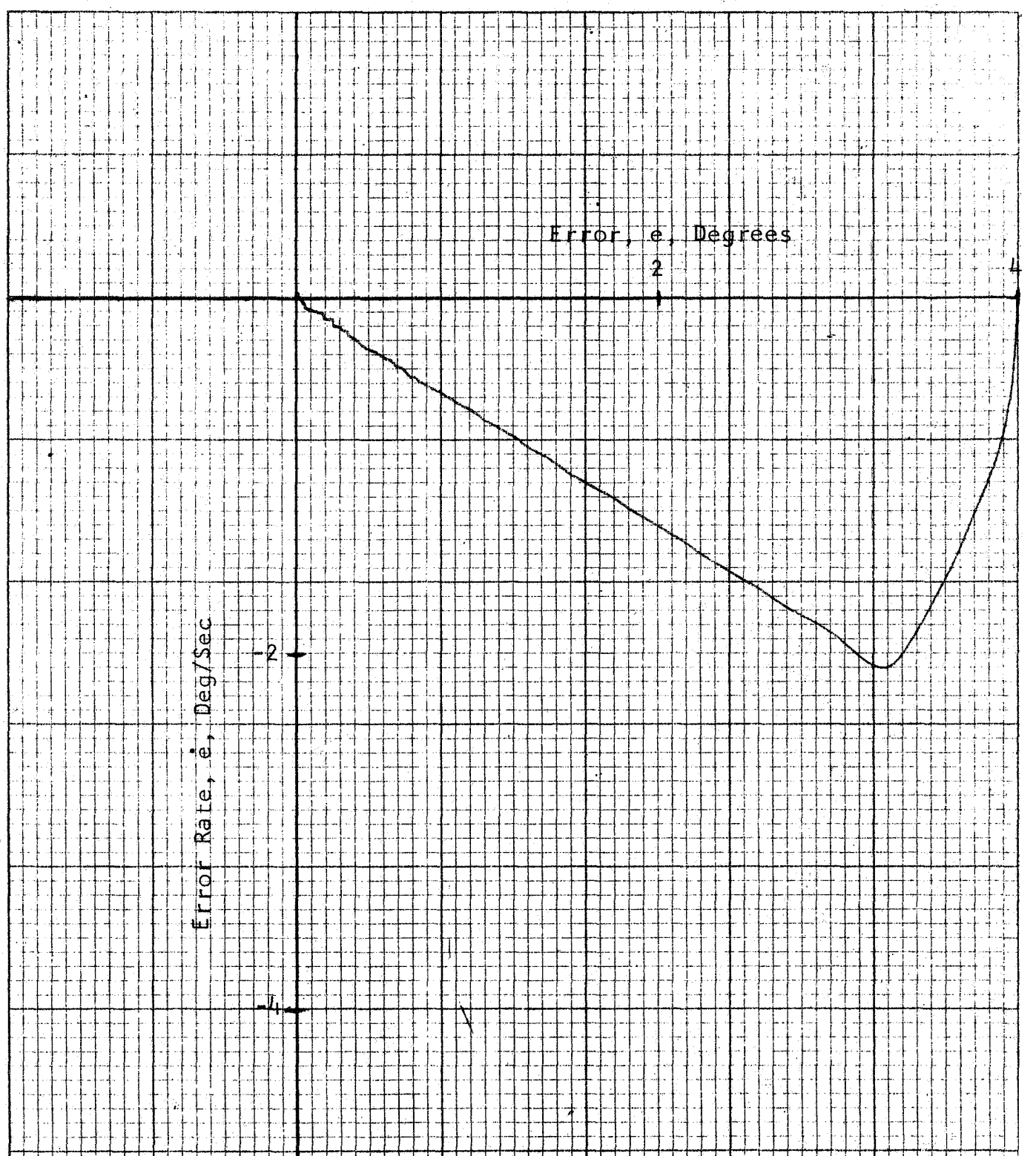

Figure 3.62: Type 2 PA/General Purpose PSV Hardware, Phase-Plane Portrait for T = 1.5 Seconds

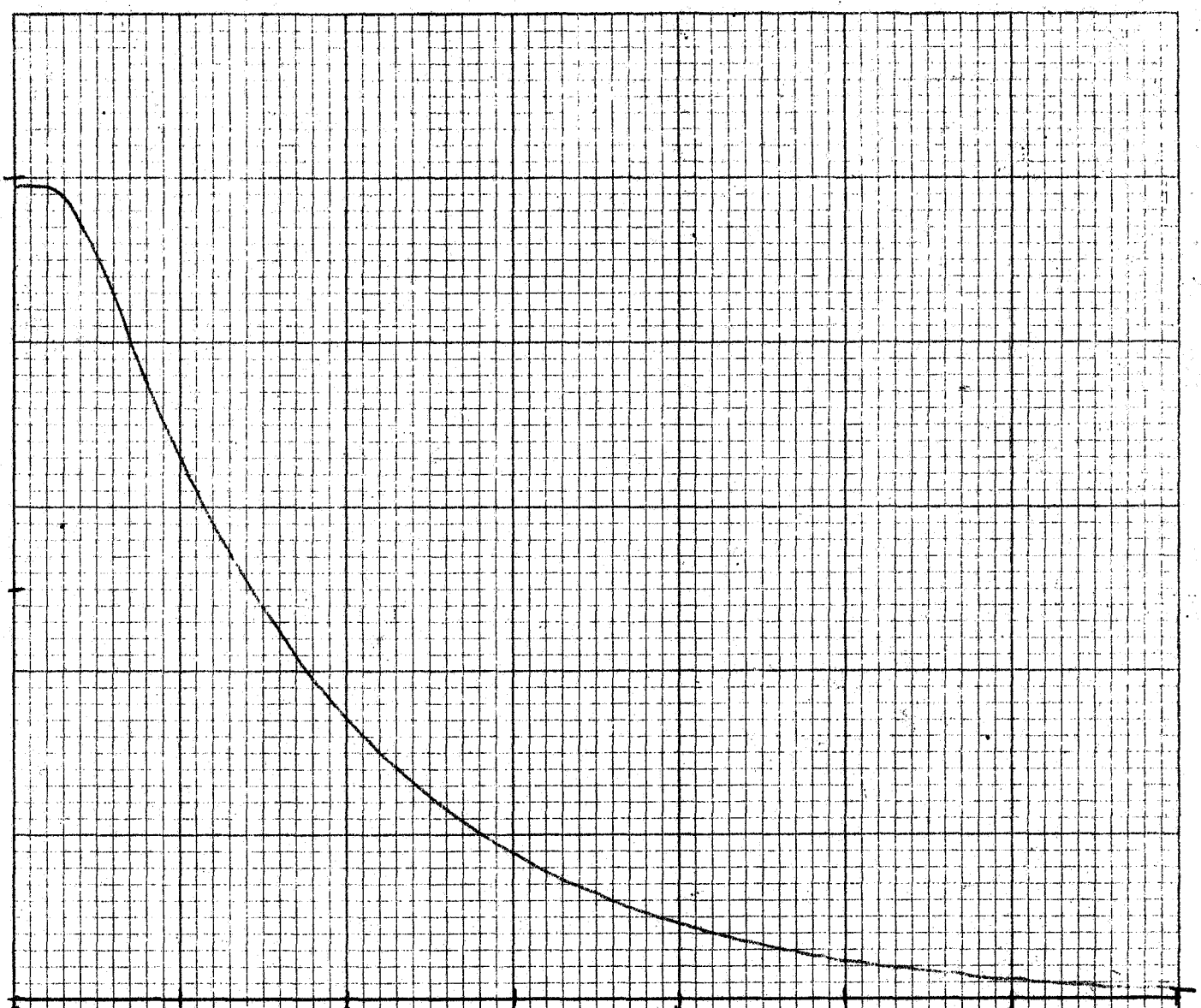

Figure 3.63: Elementary SOC Hardware Configuration, Response of Error Versus Time, T = 1.5 Seconds

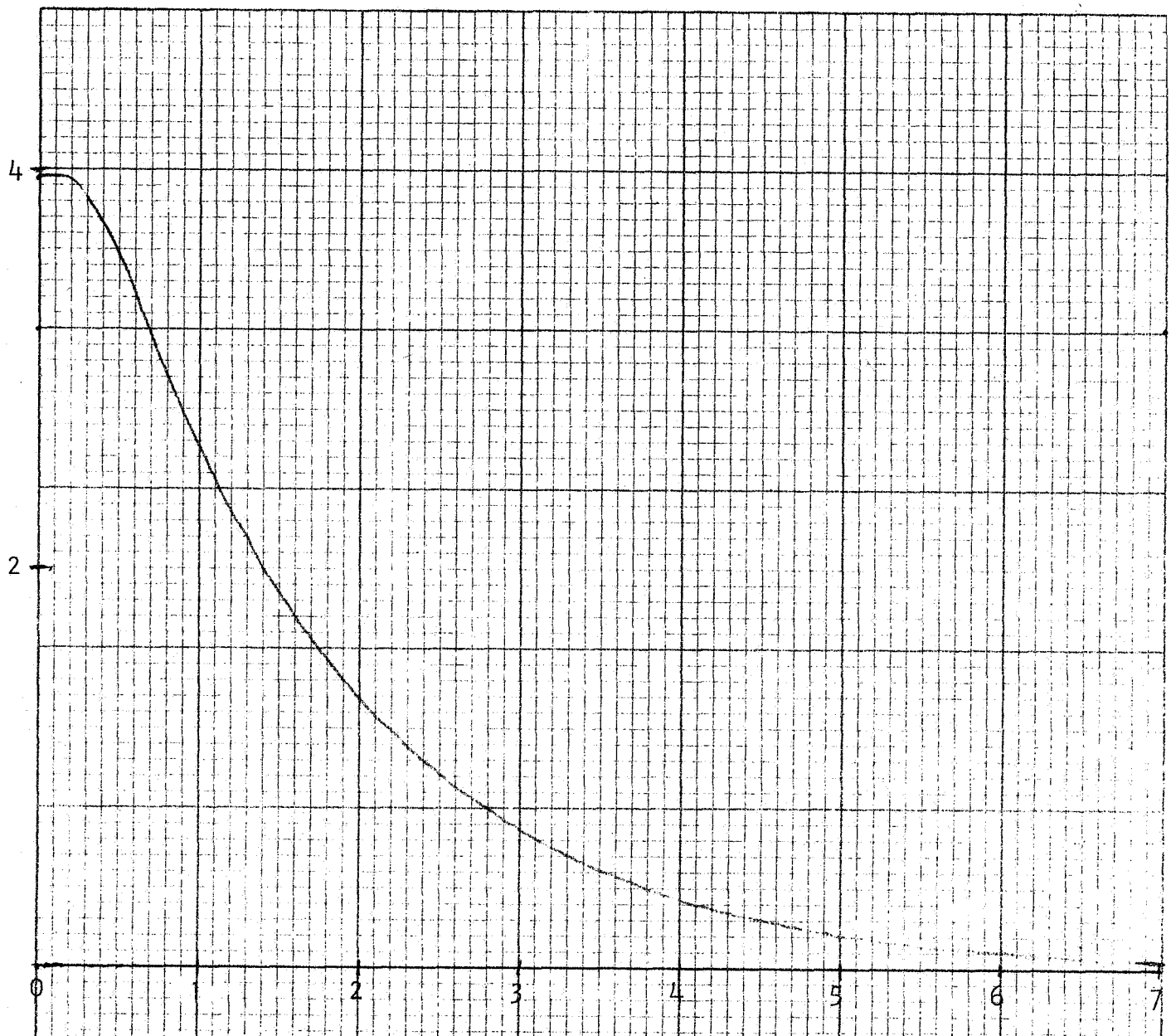

Figure 3.64: Type 2 PA/General Purpose PSV Controller Hardware, Response of Error Versus Time, $\tau = 1.5$ Seconds

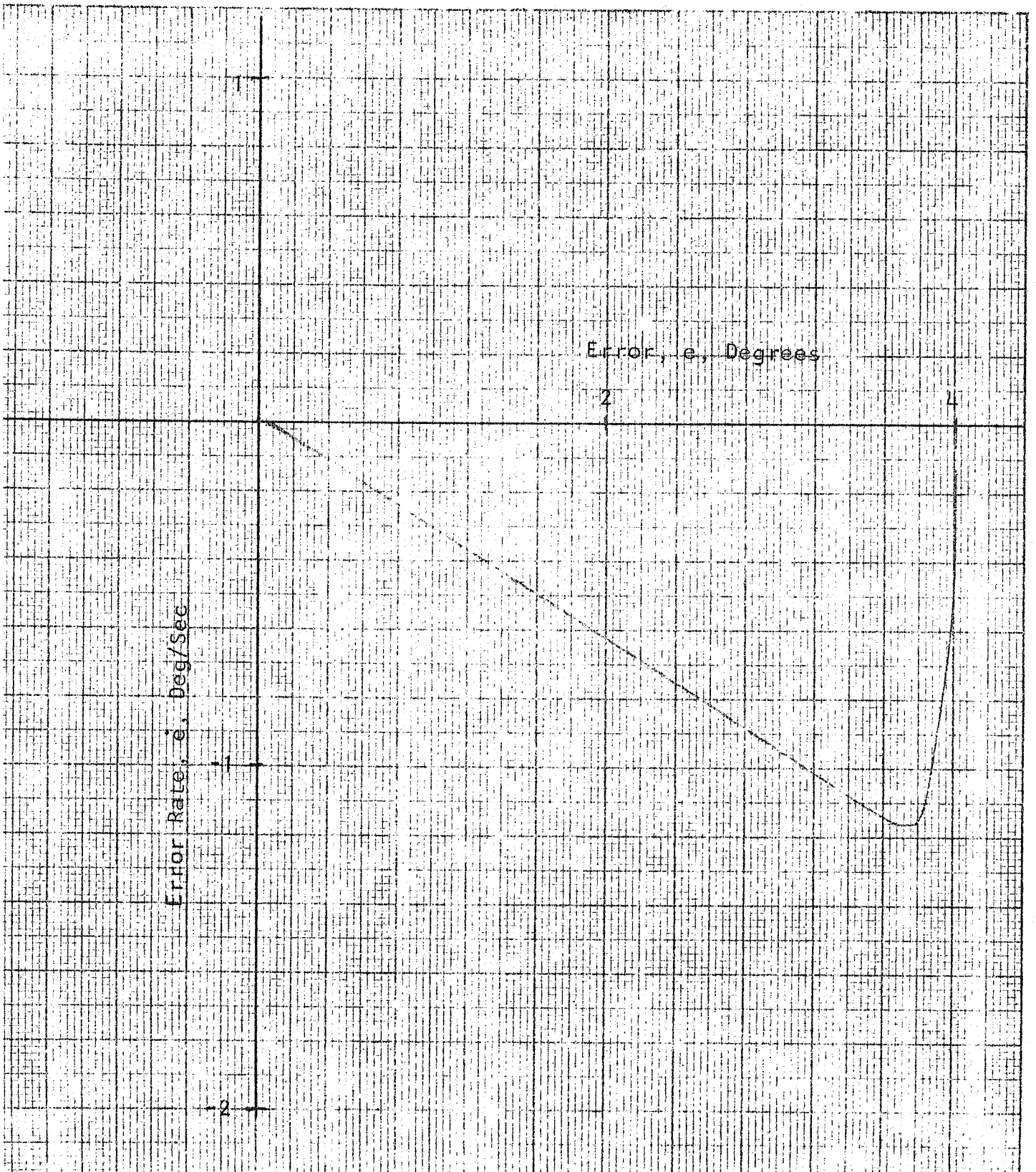

Figure 3.65: Proportional Controller with Limiting, Phase-Plane Portrait for T = 3.2 Seconds.

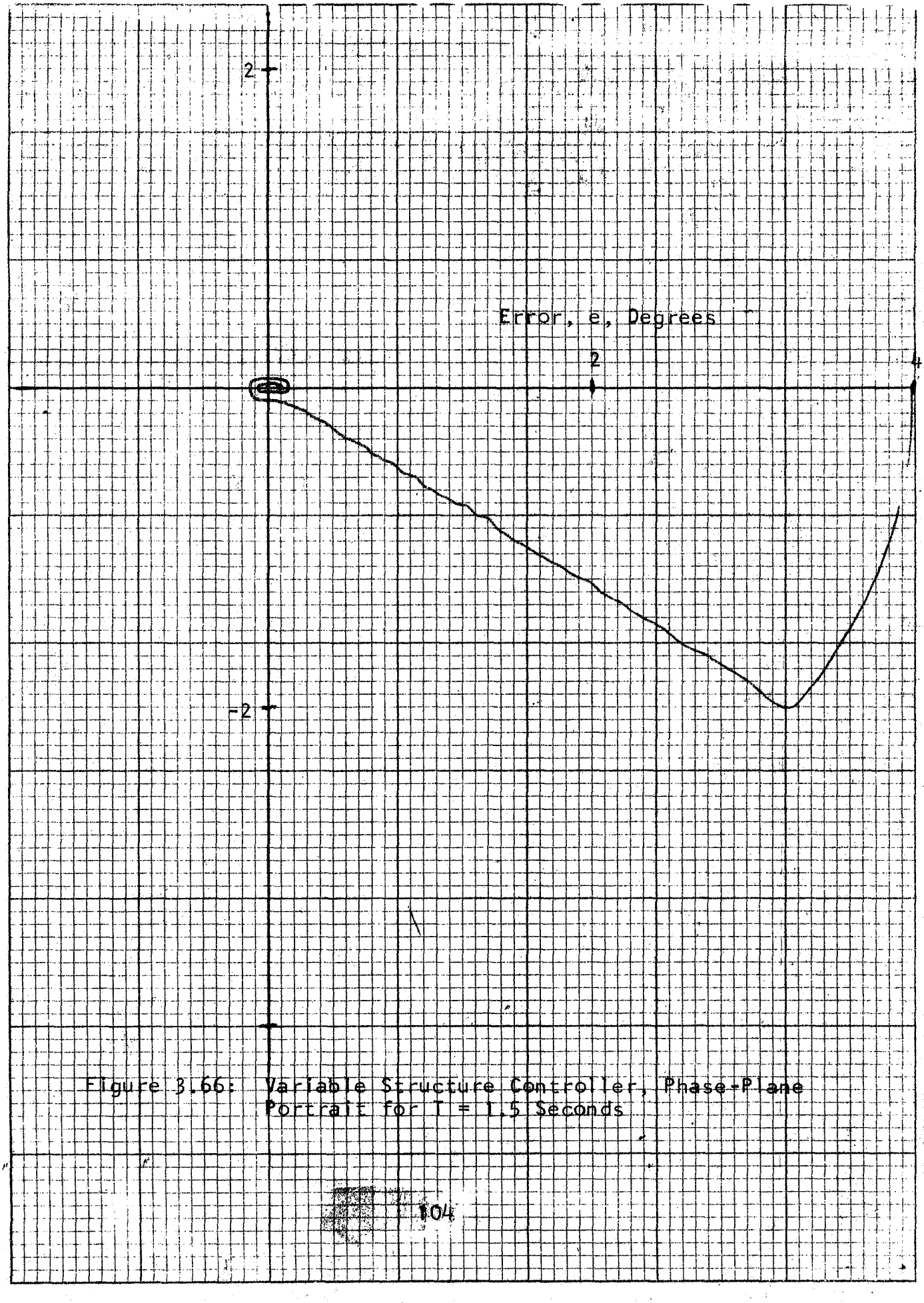

Figure 3.66: Variable Structure Controller, Phase-Plane Portrait for T = 1.5 Seconds

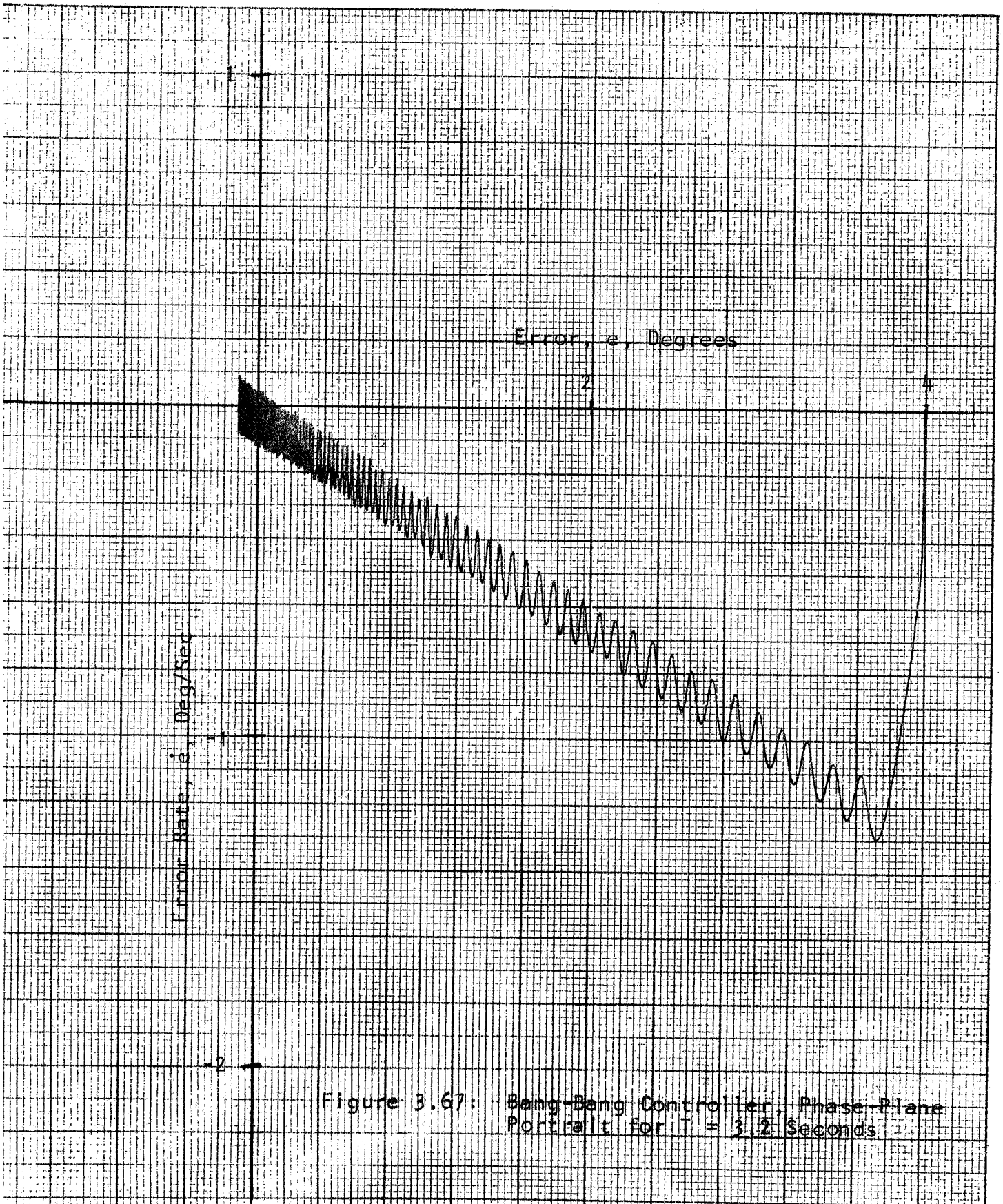

Figure 3.67: Bang-Bang Controller, Phase-Plane Portrait for T = 3.2 Seconds

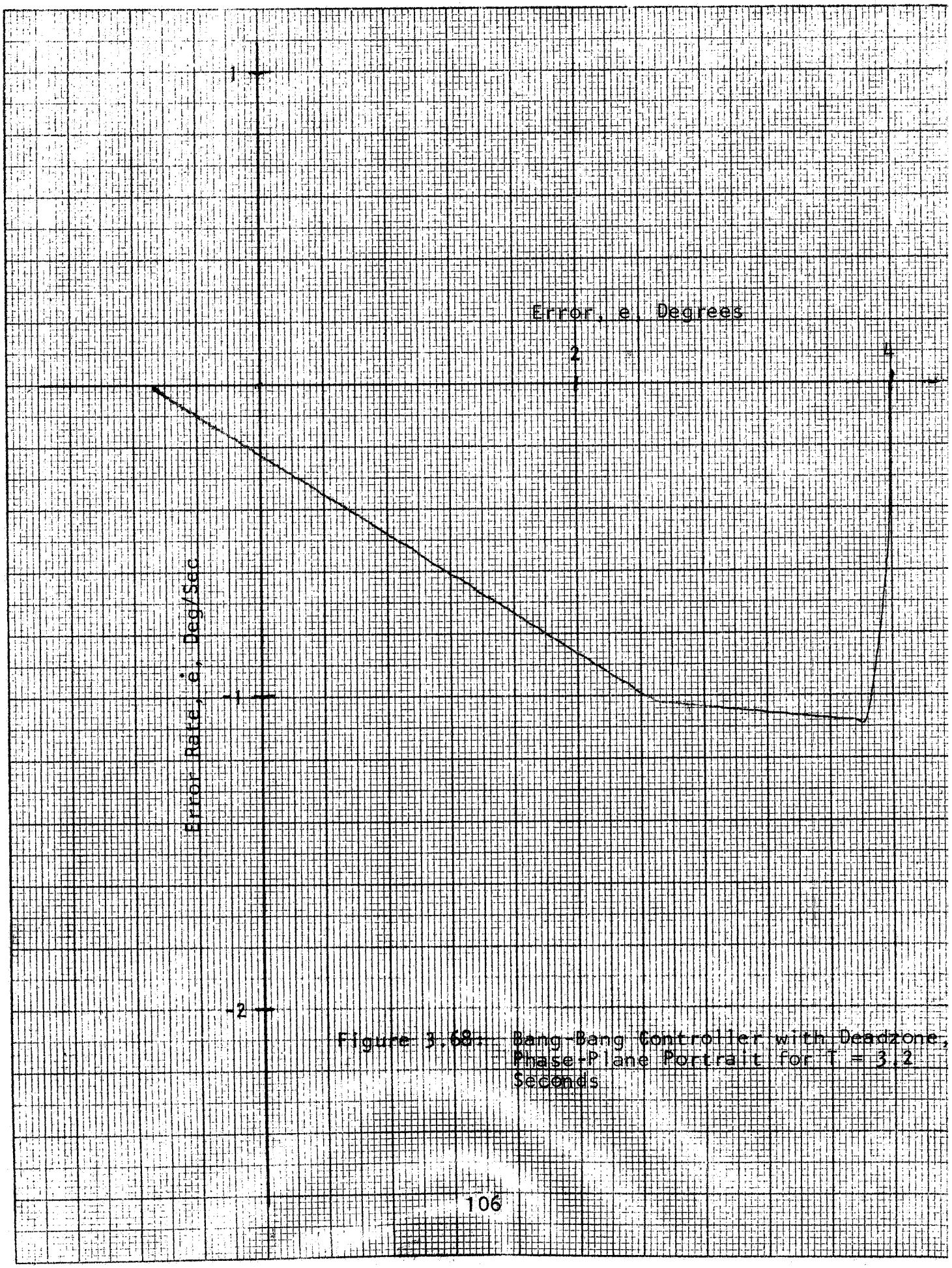

Figure 3.68: Bang-Bang Controller with Deadzone, Phase-Plane Portrait for T = 3.2 Seconds

4. THE STATISTICAL SOURCE

Although the statistical nature of PSV operation was considered in derivation of the theoretical model previously described, development and use of the model for comparative simulation studies did not stress the random output characteristics of the PSV or their effects on control system performance. Since these effects are of central importance in the application of SOC techniques to more complex systems, e.g., distributed actuation in a multiple actuator magnetic torquer system, statistical characteristics of the PSV have also been analyzed during this Phase I study.

The theory of pulse density signals enables us to model the transfer function of the statistical source in a direct manner. However, we would like to be able to view the behavior of the p register and statistical source as a decision-making process to check on the efficiency of the information acquisition or "learning" behavior. While statistical decisions can be made on the basis of several criteria, such as maximum likelihood or minimax, Bayes' Theorem has been used in the following material. Although there are some theoretical limitations on the use of Bayes' Theorem, the present work can serve as a basis for further exploration of the decision process in the PSV and it provides us with qualitative and quantitative results which can be used to evaluate the PSV decision process.

In addition to results of analyses on the use of Bayesian statistics for the design of statistical source characteristics, the following also summarizes work done to identify the role of the statistical source in the PSV

for single-PSV and multiple PSV-applications, results of some digital simulations of the statistical source, and bench test data, using existing PSV hardware, stressing statistical performance aspects.

4.1 Application of Bayes' Theorem to Analysis and Design of Statistical Source

The motivation for exploring the application of statistical decision theory to the modeling of the PSV stems from some striking similarities between the Bayesian approach for relating *a priori* and *a posteriori* probabilities of a hypothesis and the changing probabilities of the PSV output polarity based upon observations of preceding events. We will first summarize pertinent aspects of Bayes' formula for the probabilities of hypotheses and then apply the formula to analysis of the PSV unit.

4.1.1 Bayes' Formula

Consider two events A and B having the following characteristics. Event A can assume only one of two forms which we denote as A_+ and A_-, and only one of these can occur on any one trial. Thus, A_+, A_- form a set of exhaustive and mutually exclusive events and

$$p(A_+) + p(A_-) = 1 \qquad \text{.....} \qquad 4:1$$

where $p(A)$ denotes the probability of A occurring.

B is another event which occurs only if A occurred, i.e., it is conditional on A. We have two forms for the probability of the occurrence of B, viz., $p(B|A_+)$ and $p(B|A_-)$ denoting the probability of the occurrence of B given that A_+ or A_- has occurred.

In view of Equation 4:1, we can restrict the analytical development to either $p(A_+)$ or $p(A_-)$. We will use $p(A_+)$ and refer to it as the a priori probability of the event A+, i.e., before having observed the occurrence of event B. Bayes' formula is intended to provide an updated estimate of $p(A_+)$ based on the observation of event B. The latter is the conditional probability $p(A_+|B)$ and is referred to as the a posteriori probability of A+. The formula is readily derived from fundamental probabi1ity relationships.

The joint probability of the two events B and A+, $p(BA_+)$, can be written in either of the following two forms:

$$p(BA_+) = p(A_+)\, p(B|A_+) \quad \ldots\ldots\ldots\ldots\ldots\ldots \quad 4:2$$

$$p(BA_+) = p(B)\, p(A_+|B) \quad \ldots\ldots\ldots\ldots\ldots\ldots \quad 4:3$$

Equating the right hand sides of 4:2 and 4:3 we obtain

$$p(A_+|B) = \frac{p(A_+)p(B|A_+)}{p(B)} \quad \ldots\ldots\ldots\ldots\ldots\ldots \quad 4:4$$

Since B can occur either jointly with A+ or with A_-, we also have

$$p(B) = p(A_+)\, p(B|A_+) + p(A_-)\, p(B|A_-) \quad \ldots\ldots\ldots \quad 4:5$$

Combining Equations 4:4 and 4:5 yields Bayes' formula for the up-dated probability of A+:

$$p(A_+|B) = \frac{p(A_+)p(B|A_+)}{p(A_+)\, p(B|A_+) + p(A_-)\, p(B|A_-)} \quad \ldots\ldots\ldots \quad 4:6$$

In sequential estimation, the quantity of interest is the change to be made in the a priori probability $p(A_+)$

based on the use of Equation 4:6 for the *a posteriori* $p(A_+|B)$. We denote this difference as $\Delta p(A_+)$. Thus,

$$\Delta p(A_+|B) = p(A_+|B) - p(A_+) \quad \ldots\ldots\ldots\ldots\ldots\ldots \quad 4:7$$

Combining Equations 4:7 with 4:6 and 4:1, we obtain

$$\Delta p(A_+|B) = \frac{1 - p(A_+)}{1 + \frac{1}{p(A_+)(r-1)}} \quad \ldots\ldots\ldots\ldots\ldots \quad 4:8$$

where

$$r = \frac{p(B|A_+)}{p(B|A_-)} \quad \ldots\ldots\ldots\ldots\ldots \quad 4:9$$

Equation 4:8 gives the required change in the prior value of $p(A_+)$ as a result of observing the event B, provided r is known. The latter involves the conditional probabilities of B on A. Ref. 7 describes Bayes' theory in further detail.

4.1.2 PSV Model

To relate the various events and their probabilities as they appear in Equations 4:8 and 4:9 to the PSV unit operation, reference is made to Figure 4:1. v is the output from the Performance Assessment unit and can assume either the value +1 or -1. The output of interest here is the sign of the u-register increment. We therefore define the output as Au and associate with it one of two possible values, viz., either +1 or -1. We also separate the functional elements of the PSV as shown in Figure 4.1 to distinguish the part in which the product $\text{sgn } v \cdot \text{sgn } \Delta u(t - \Delta t)$ is taken. The block marked "Statistical Device" includes the p register, random noise source

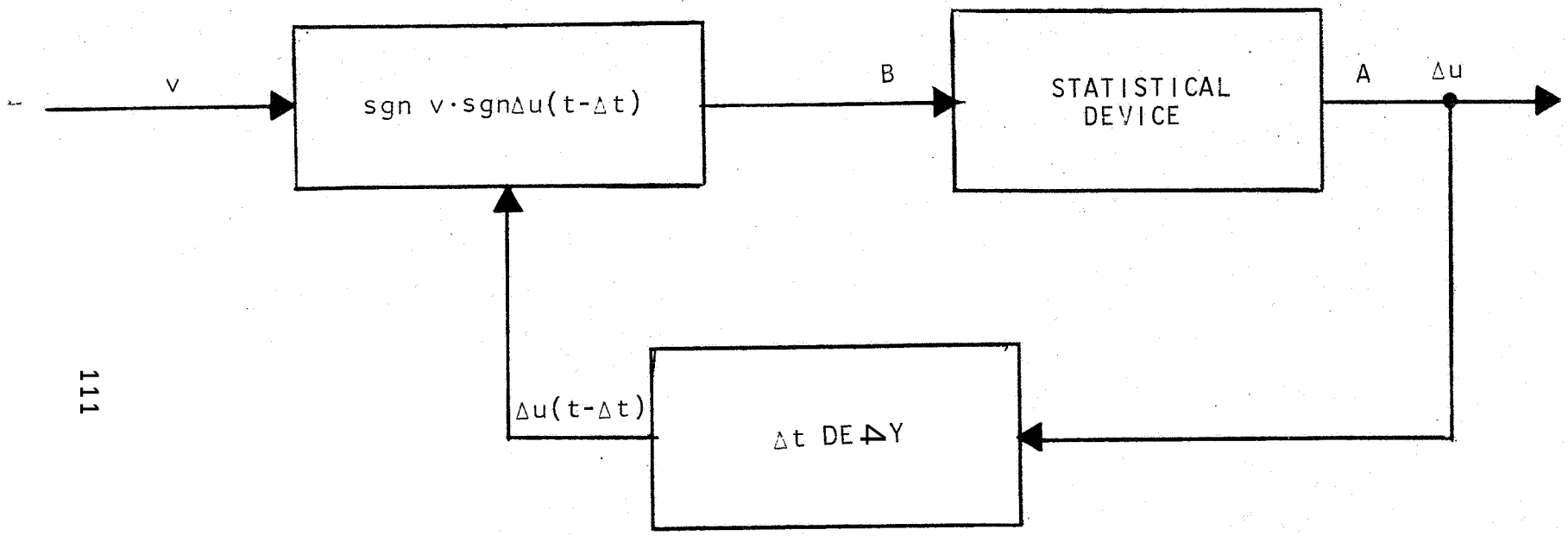

FIGURE 4.1: PSV LOCK DIAGRAM

and the comparator. The input to the statistical device is thus a +1 or -1 signal which determines the direction of the increment of the p register.

The event A in the preceding section is the sign of the output Au. A_+ thus corresponds to a positive Au and A_- to a negative Au. Clearly, only one of these can occur but one must occur on any one clock pulse. A_+ and A_- therefore meet the requirement that they form an exhaustive set of mutually exclusive events.

The event B in the development of Bayes' formula is the input to the Statistical Device. However, this input can be either +1 or -1 and we therefore have two events. We will denote these as B_+ and B_-, respectively. We must therefore apply Bayes' formula twice to define the needed change in $p(A_+)$ when the observed event is B_+ and also when it is B_-. This is readily done by replacing B in Equations 4:8 and 4:9 by B_+ and B_-. We will distinguish the two equations resulting from 4:9 by using r_+ and r_- corresponding to B_+ and B_-, respectively. Thus,

$$\Delta p(A_+|B_+) = \frac{1 - p(A_+)}{1 + \frac{1}{p(A_+)(r_+ - 1)}} \qquad \text{..... 4:10a}$$

where

$$r_+ = \frac{p(B_+|A_+)}{p(B_+|A_-)} \qquad \text{..... 4:10b}$$

and

$$\Delta p(A_+|B_-) = \frac{1 - p(A_+)}{1 + \frac{1}{p(A_+)(r_- - 1)}} \qquad \text{..... 4:11a}$$

where

$$r_- = \frac{p(B_-|A_+)}{p(B_-|A_-)} \qquad \text{.....} \qquad 4:11b$$

Referring to Figure 4.1, it is noted that the product sgn v·sgn Δu(t - At) produces the event B which is being observed and this event is conditional upon the sign of Δu(t - At). But the latter is the event A+ or A_-, which is understood to be, by definition, the prior event in the Au sequence. Thus, the probability, say, that B will be negative, given that Δu(t - At) is negative depends entirely on the probability that the input v will be positive; this probability is, in turn, a function of the way in which the controlled plant and the Performance Assessment react to the event A+ or A_-. Denoting the probability that v will be positive by $p(v_+)$, we can write

$$p(B_-|A_-) = p(v_+) \qquad \text{.....} \qquad 4:12$$

By similar reasoning, we also have

$$p(B_-|A_+) = p(v_-) \qquad \text{.....} \qquad 4:13$$

$$p(B_+|A_+) = p(v_+) \qquad \text{.....} \qquad 4:14$$

$$p(B_+|B_-) = p(v_-) \qquad \text{.....} \qquad 4:15$$

Using Equations 4:12 through 4:15, we can define r_+ and r_- in 4:10b and 4:11b as

$$r_+ = \frac{p(v_+)}{p(v_-)} \qquad \text{.....} \qquad 4:16$$

$$r_- = \frac{p(v_-)}{p(v_+)} \qquad \text{.....} \qquad 4:17$$

and we note that

$$r_+ = \frac{1}{r_-} \qquad \text{.....} \qquad 4:18$$

Furthermore, v_+ and v_- also form an exhaustive set of mutually exclusive events, since only one can occur but one is always present. Therefore,

$$p(v_+) + p(v_-) = 1 \qquad \text{.....} \qquad 4:19$$

Equations 4:10a and 4:11a, with the corollary Equations 4:16, 4:17, and 4:19 (to be referred to as the defining equations) provide an analytical basis for further understanding of PSV operation. Thus $p(v_+)$ defines the input being considered, and $\Delta p(A_+|B_+)$, $\Delta p(A_+|B_-)$ define the manner in which the output probability should be changed, sequentially, depending upon whether B_+ or B_- is observed at the input to the statistical device.

The above equations can be summarized in a single equation using the notation and conventions established in Section 2 of this report. By simple substitution and algebra, all the equations for $\Delta p(A|B)$ become expressed as ΔZ_5:

$$\Delta Z_5 = \frac{1}{4} \frac{\sigma(Z_2) Z_1 (1 - Z_5^2)}{1 + \sigma(Z_2) Z_1 Z_5}$$

where $\sigma(Z_2)$ is the algebraic sign of the p-register input. This difference equation can be used to approximate a differential equation, so that an expression for the Z_5 value for different p-register levels can be obtained. However, for the remaining discussion, the interest will be on the sequential aspect of the problem.

The polarity of Ap relative to the input $p(v_+)$ is of interest since this polarity must be established in the PSV, i.e., the PSV must decide whether Ap will be increased when $B = B_+$ and decreased when $B = B_-$ or vice versa. As may be seen from an examination of the defining equations

$$\Delta p(A_+|B_+) > 0$$

$$\Delta p(A_+|B_-) < 0$$

when $p(v_+) > 0.5$ 4:20

Hence a mechanization in which the polarity of incrementing $p(A_+)$ matches the sign of the observed signal B at the input to the statistical device implies an input $p(v_+)$ having a higher probability of being positive than negative. If the opposite were expected, i.e., $p(v_+) < 0.5$, it would be necessary to invert the Δp polarity, i.e., to decrease Ap when B_+ occurred. Since the relationship between the Ap and B polarities can only be one or the other of the above two possible mechanizations, $p(v_+) = 0.5$ becomes an intractable input. Indeed, as may be seen from the defining equations

$$\Delta p(A_+|B_\pm)\Big|_{p(v_+) = 0.5} = 0 \qquad \text{..... 4:21}$$

In view of the symmetry of Ap for $0 < p(v_+) < 0.5$ and $0.5 < p(v_+) < 1$, and since the latter is of greater practical interest, we will restrict further consideration to this range. We will thus be concerned with the class of inputs, v, which are more likely to be positive than negative. Note that for the upper limit of this range, i.e., when $p(v_+) = 1$

$$\Delta(A_+|B_+)\Big|_{p(v_+) = 1} = 1-p(A_+)$$

and

$$p(A_+|B_+)\Big|_{p(v_+)\,=\,1} = 1$$

The above simply says that when we are certain to always have a plus at the input, i.e. $p(v_+) = 1$, we should follow this input on a one-to-one basis. This obviously eliminates the PSV. The range of practical interest is therefore when v is neither certain to be positive nor is it completely random, i.e. there is some bias toward a positive polarity in the PSV input.

4.1.3 Desiqn Considerations

Figure 4.2 is a plot of the absolute value of Ap as a function of $p(A_+)$, for $p(v_+)$ as a parameter in the range $0.5 < p(v_+) < 1$. This form of presentation has been chosen to facilitate comparisons of the magnitude of Ap for opposite signs of B. It is thus noted that pairs of curves correspond,-ing to a given value of $p(v_+)$ are mirror images of each other when the mirror is located at $p(A_+) = 0.5$.

It is evident from Figure 4.2, as well as from the defining equations, that mechanization of the analytical model must exclude the extremes $p(A_+) = 0$ and $p(A_-) = 1$. At this point Ap is always zero, regardless of the observed polarity of B, and the system would therefore become in-operative. Actual PSV units have used a range $0.05 \leq p(A_+) \leq 0.95$ for this and related reasons.

Figure 4.2 can serve as a basis for constructing statistical source transfer functions if we assume $p(v^+)$ to be known. Although the analytical model defines the change in $p(A_+)$ for any random sequence of plus and minus

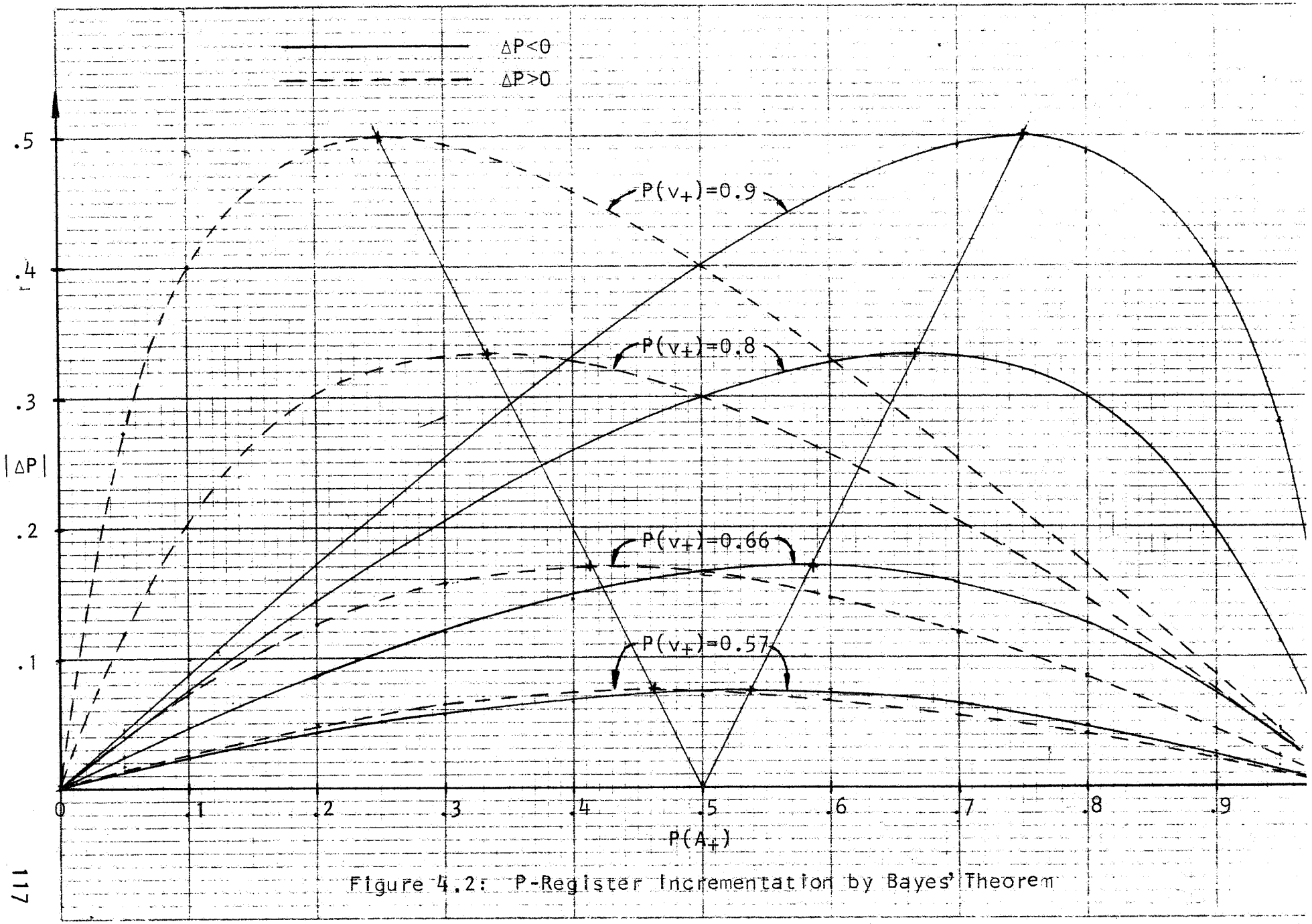

Figure 4.2: P-Register Incrementation by Bayes' Theorem

v signals at the input, it is constructive to pose the following problem. Assume that $p(A_+)$ is at one or the other of its limits, i.e.

$$p(A_+) = 1-\epsilon$$

or

$$p(A_+) = \epsilon$$

where E is the small positive quantity needed to avoid the theoretical limits of $p(A_+) = 0$ and $p(A_+) = 1$, as discussed above. Depending upon the actual polarities of v and their time sequence, $p(A_+)$ will progress from one of these limits to the other and assume particular values in between,

Since a change in $p(A_+)$ is accomplished with each clock pulse, the sequential change $p(A_+)$ corresponds to its variation with time. The minimum time to traverse the range of $p(A_+)$ will be obtained when there is a consecutive sequence of B inputs of sufficient length (and of the appropriate polarity). To illustrate this and to show the effect of $p(v_+)$ on this minimum reversal time, assume that we start at $p(v_+)_0 = \epsilon$ and we set E = 0.01. For any fixed value of $p(v_+)$ we can obtain the required Δp from Figure 4.2 and compute the next value, $p(A_+)K=1$, i.e., the value of $p(A_+)$ at the end of the first step (K=1). We can thus proceed to take a sufficient number of steps to attain the upper limit $p(A_+) = 1-E$. Figure 4.3 has been produced in this manner and shows the minimum time needed to change $p(A_+)$ from one extreme to the other for each of the assumed values of $p(v_+)$.

This analytical development treats the PSV as a separate element having a $p(v_+)$ input and p(A+) output, and the relationship between the two is considered as though the input is known independently from the output. This

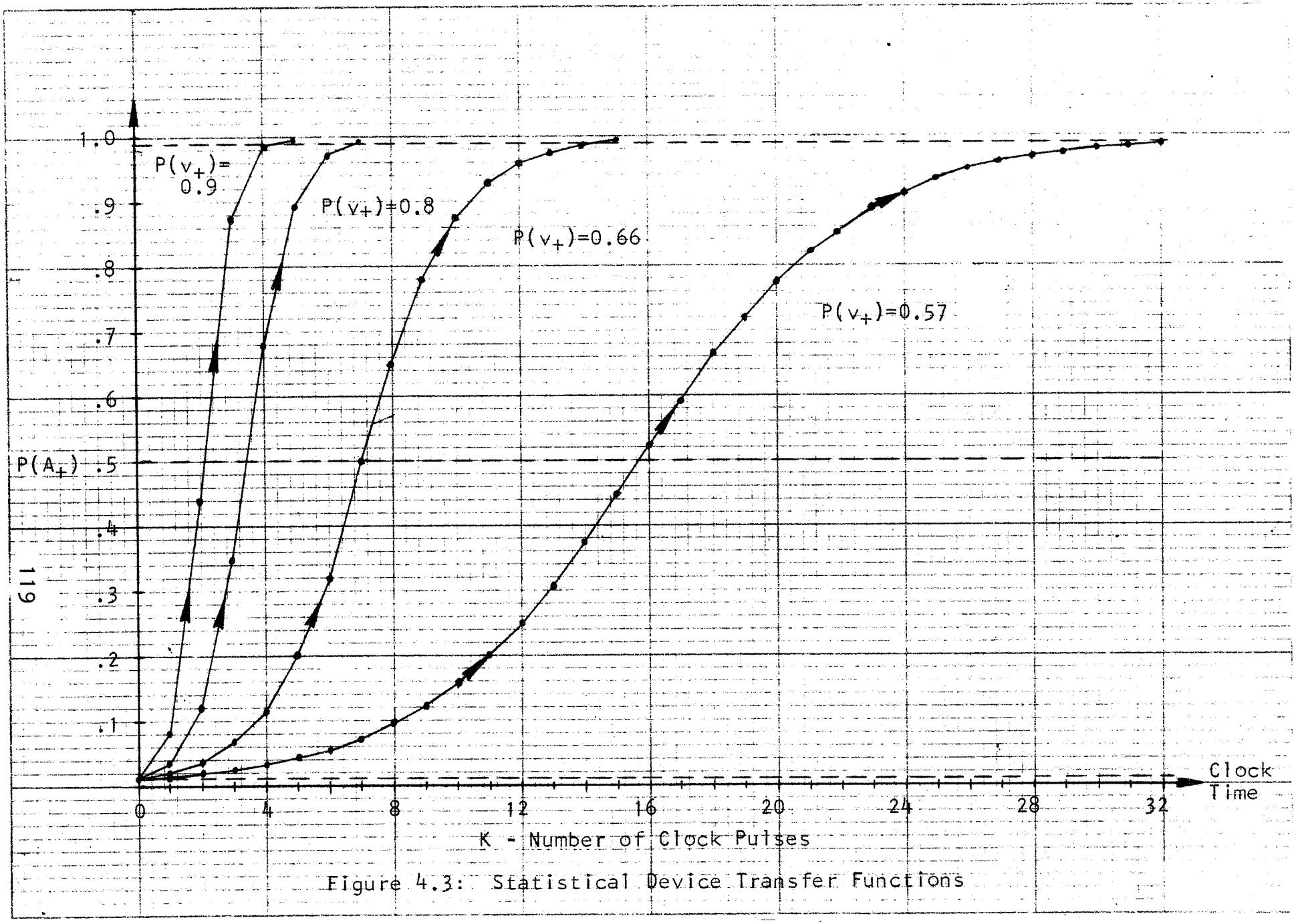

Figure 4.3: Statistical Device Transfer Functions

is useful in gaining a better understanding of the internal operation of the PSV. For example, the curves in Figure 4.3 can facilitate design of the p register both with regard to the number of steps and the selection of clock rates. However, it is well known from application studies that the input, v, to the PSV is dependent upon the previous output, A. indeed in the simplest case, v is the result of directly assessing the output and, in more general cases, additional factors enter the assessment to make the dependence more comp1ex.

That the PSV input and output must be dependent events can also be demonstrated by again using the analytical framework developed in this section. Thus, consider once more the PSV module element in which the product sgn v·sgn $\Delta u(t-\Delta t)$ is taken (Figure 4.1). We will assume that v and A are independent events and prove that this assumption is not valid. First, we express the probability $p(B_+)$ based on the assumption of independence and obtain

$$p(B_+) = p(A_+)\, p(v_+) \quad \ldots\ldots\ldots\ldots\ldots\ldots \quad 4{:}22$$

or

$$p(B_+) = p(A_-)\, p(v_-) \quad \ldots\ldots\ldots\ldots\ldots\ldots \quad 4{:}23$$

Equating the right-hand sides of 4:22 and 4:23 and expressing the result in terms of $p(A_+)$ and $p(v_+)$ only, we obtain

$$p(v_+) + p(A_+) = 1 \quad \ldots\ldots\ldots\ldots\ldots\ldots\ldots \quad 4{:}24$$

We can also write the probabilities of B_- as follows

$$p(B_-) = p(A_+)\, p(v_-) \quad \ldots\ldots\ldots\ldots\ldots\ldots \quad 4{:}25$$

or

$$p(B_-) = p(A_-)\, p(v_+) \quad \ldots\ldots\ldots\ldots\ldots\ldots \quad 4{:}26$$

Combining as above, we obtain

$$p(v_+) = p(A_+) \quad \text{.....} \quad 4:27$$

Accordingly, from 4:24 and 4:27 we have

$$p(v_+) = 0.5$$

But this last corresponds to the intractable case previously discussed, for which the PSV, and the analytical formulation of it, have no physical meaning. The assumption of independence between the PSV input and its output must therefore be excluded from consideration. Thus the ideal first step, in applying the analytical techniques as evaloved herein to system design, is that of defining the dependence of the input to the PSV unit on its output (this output is, of course, reacted to and transformed by the outer loop, i.e., by the plant and the Performance Assessment unit). Additional effects, such as the expected degree of noise on sensor signals, should then be considered in design of the statistical source transfer characteristics.

4.2 Role of Statistical Sources in Single-PSV Systems

The preceding section dealt with the methods which might be used to design the statistical source when $p(v_+)$ is assumed to be constant for all values of $p(A_+)$. Past designs of the PSV, although not based on the above formal methods, nevertheless produced statistical source transfer functions somewhat similar to the ones shown in Figure 4.3 for values of $p(v_+)$ in the range of 0.8-0.9. We now wish to consider the nature of system operation when such a PSV is incorporated in the controller design, using the "Elementary SOC" (defined in Section 3).

As discussed in earlier parts of the report, it is illuminating to compare a single-PSV SOC system with relay controllers. Because of the u-register characteristics, the controller output is restricted to the range between $+u_{max}$ and $-u_{max}$, which is a characteristic also common to relay controllers. It is therefore of interest to establish the form in which switching occurs from one extreme of u to the other in a PSV controller, as compared to a variety of relay controllers, e.g., relays with a proportional range, deadzone, delay, hysteresis, or combinations of these characteristics.

To facilitate the comparative analysis, we will use the system configurations shown in Figure 4.4. The essential feature of configuration (B) in the figure is that the PSV and u-register combination replace the relay controller. The sgn e_P operation can be viewed as a signal-conditioning process aimed at providing the binary form required by the PSV. However, this operation will be seen to influence greatly the switching function of the PSV. To define the switching function, we assume that u is initially at its positive limit, u_{max}, and that this is the desired direction of control, i.e., sgn e_P is positive and the system is driving toward the switching line defined by the slope 1/T. Let us denote this phase as I and establish the correspdnding PSV operation. If the phase persists long enough, $p(A_+)$ will reach its limiting value $1 - \epsilon$, and the probability of obtaining positive Au, so as to maintain u at $+u_{max}$, will become very nearly unity. That this condition will be sustained is readily seen from the fact that, in the absence of noise in the system (outside the PSV), the probability of v_+ is essentially unity, since it is determined only by the polarity of predicted error. Since the probability of A+ is controlled by the sign of B, the input to the statistical device, we are interested in $p(B_+)$. But

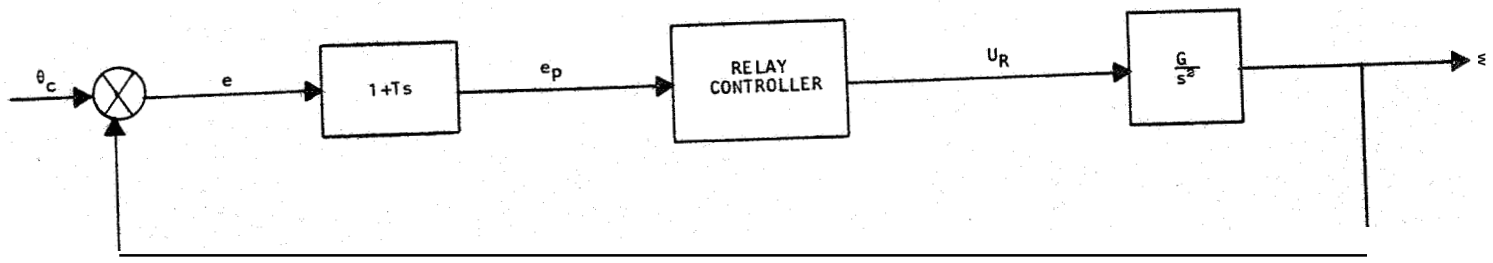

(A) RELAY CONTROLLER

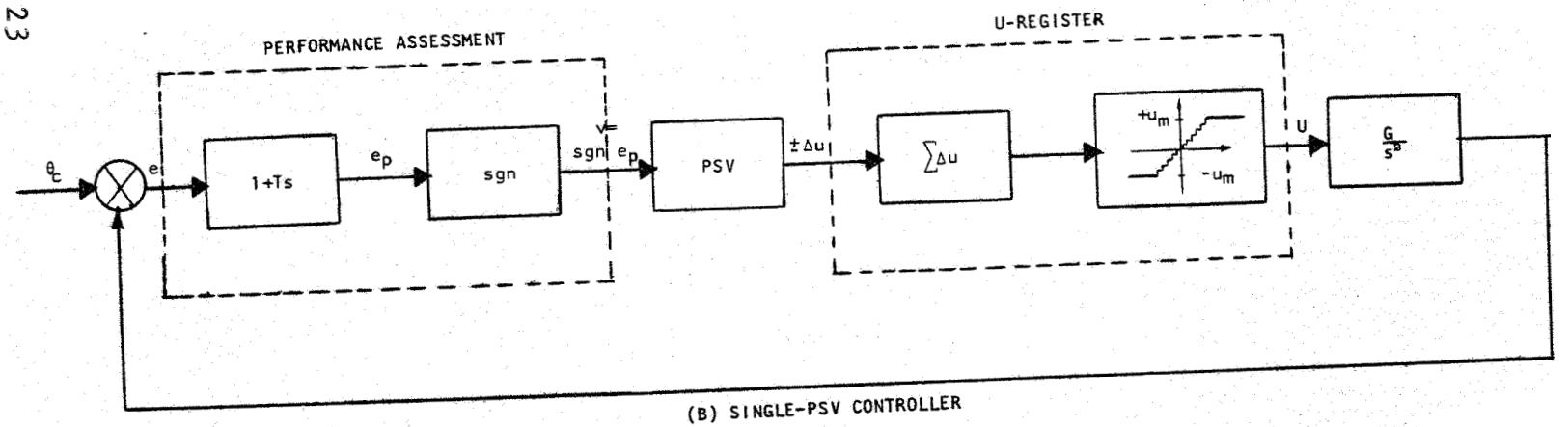

(B) SINGLE-PSV CONTROLLER

FIGURE 4.4: COMPARATIVE RELAY AND SINGLE PSV CONTROL CONFIGURATIONS

$$p(B_+) = p(A_+)p(B_+|A_+) + p(A_-)p(B_+|A_-) \quad \ldots\ldots\ldots \quad 4:28$$

Also, as previously shown,

$$p(B_+|A_+) = p(v_+) \quad \ldots\ldots\ldots\ldots\ldots\ldots \quad 4:14$$

$$p(B_+|A_-) = p(v_-) \quad \ldots\ldots\ldots\ldots\ldots\ldots \quad 4:15$$

Combining the above, and replacing $p(v_-)$ and $p(A_-)$ by their complements

$$p(B_+) = p(A_+)p(v_+) + [1 - p(A_+)][1 - p(v_+)] \quad \ldots \quad 4:29$$

For the conditions of phase I described above

$$p(B_+)_I = 1 - \epsilon = p(A_+)_I$$

which is very nearly unity, and therefore u will remain at $+u_{max}$ with only occasional decrements, $-\Delta u$, at a probability E.

We now consider the sequence of events following a change in sgn e_P. This implies a crossing in the switching line and a need to reverse the polarity of u. Since the u register must go through at least half its full range to achieve the change in polarity, it is evident that, regardless of the sign of Au, v will be v_- during this interval of reversing. Identifying this phase as II, we have

$$p(v_-)_{II} \approx 1$$

But $p(A_+)$ remains initially at $p(A+)I = 1 - \epsilon$, and a computation of $p(B_+)_{II}$ at the beginning of the phase, using Equation 4:28, gives

$$p(B_+)_{II} = \epsilon$$

The probability of B_- is therefore nearly unity and $p(A_+)$ is nearly certain to start decreasing. This ihitiates decrements in u based on the transfer function of the statistical source. The resulting change of u with time is nonlinear even if the average value of $p(A_+)_{II}$ is used. In addition, a random variation is superimposed on this nonlinear function of time as sketched in Figure 4.5.

It is of interest to consider the terminal point of phase II, since this deals with relative sizes of the p and u registers. In current designs, the p register has about half the number of u-register steps, i.e. 7 vs. 15. The effect of this choice is to assure the change of $p(A_+)$ from one extreme to the other while the u register is largely in its initial (positive) polarity. Thus, in the case considered above, v remains negative for at least 7 steps of the u register, but this corresponds to the minimum number of steps in Ap needed to change $p(A_+)$ from 1 - E to E. The time delay associated with the change of u from its maximum positive value to zero therefore depends upon the shape of the transfer function in the statistical device, the number of steps in each register, and the clocking rate(s) for the registers.

The remainder of phase II, in which u goes from the vicinity of zero to $-u_{max}$, is then accomplished with approximately minimum delay, i.e., it takes little more than the minimum time required to step through half the u register. This is also sketched in Figure 4.5.

The above illustration is intended to describe the general character of the PSV when viewed as a switching device in a single-axis controller. The PSV is seen to produce a delayed switching action, where the shape of the delayed

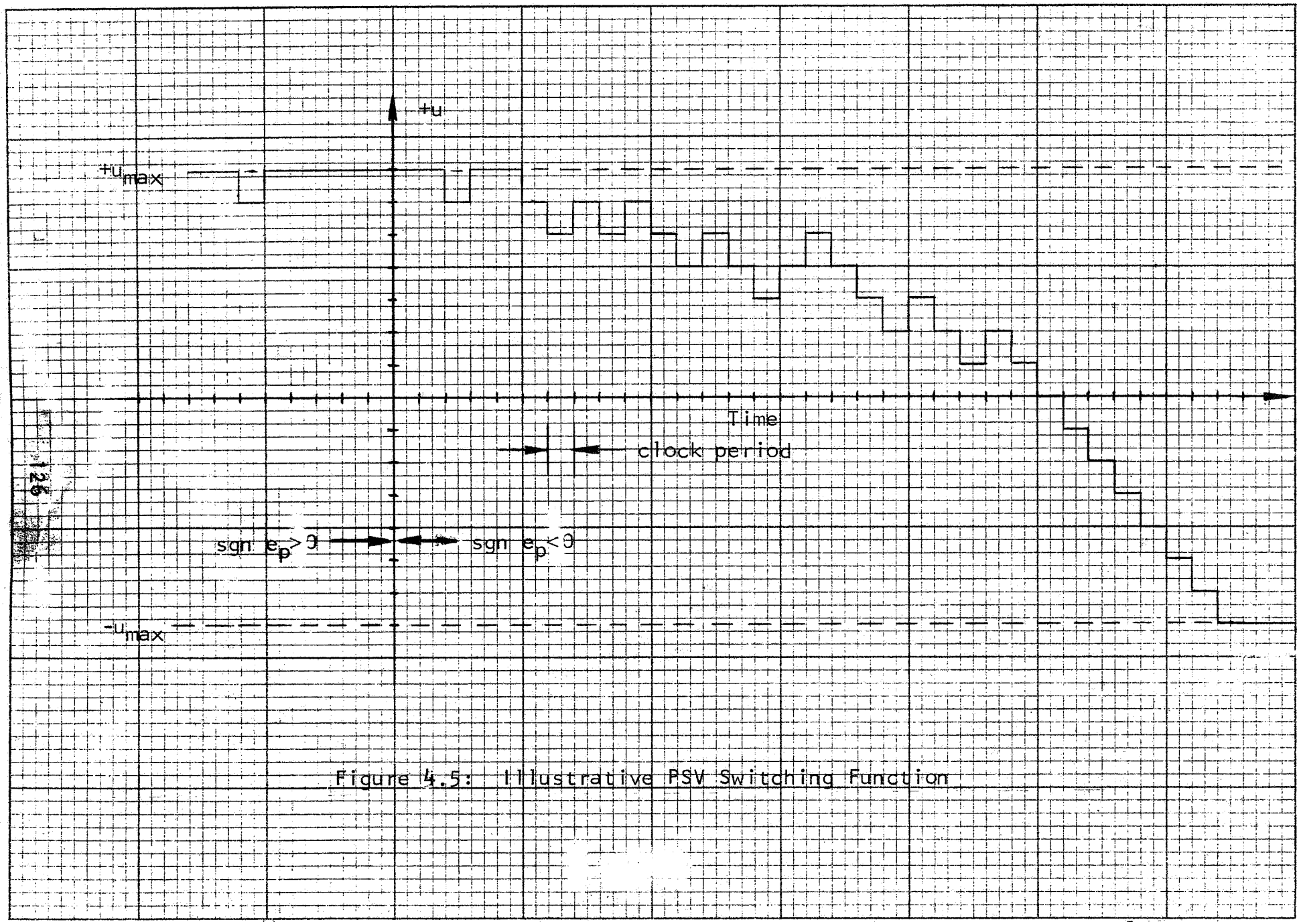

Figure 4.5: Illustrative PSV Switching Function

values of u as a function of time is controlled by the relative sizes of the u and p registers, the shape of the statistical source transfer function, i.e., $\Delta p(A_+)$ as a function of $p(v_+)$, and the register clocking rate(s). The PSV cannot be itself produce properties which are symmetrical about $e_P = 0$, as usually occurs in relay controllers, because of the sgn e_P operation. The switching action of the PSV begins when e_P changes sign, but not before.

The nature of the delayed switching in a PSV controller is such as to produce a bias favoring the initial polarity of u, i.e., the PSV hesitates to change polarity. However, once the change in polarity is accomplished, this change proceeds with essentially minimum delay to the limiting u value having the required polarity. Note that the delayed switching contains considerable variability, especially during the initial phase, due to the random aspects of its operation, and the frequency of switching will therefore also have a random element in it. This tends to prevent sustained excitation of system high-order resonant frequencies, should the frequency of switching and the resonant frequencies be of comparable magnitudes,

It is well established that relay controllers with a time delay are characterized by an undesirable limit cycle in the steady state. It is to be emphasized, therefore, that the delay produced by the PSV *is* not of the same nature as that found in conventional relays, since u achieves intermediate values while switching. (Perhaps a better characterization for the PSV switching action would be that of delay, plus proportional control with limiting.) Furthermore, limit cycles are produced by a repetitive pattern in the control process (resulting in a fixed pattern in the phase plane), whereas the random characteristics of the PSV

switching function preclude a fully repetitive control pattern. For this reason, and as has been verified with hardware tests of single-axis SOC's, and as shown in Section 3 of this report, PSV controllers do not usually exhibit a limit cycle.

The preceding discussion assumed the absence of corrupting noise. In the presence of noise, the delayed switching function of the PSV controller takes on a different light. If noise were present to corrupt the v input, i.e., to give wrong assessments of required control polarities, the p register would serve as a noise filter, the threshhold of which would be given by half the number of steps in the p register. However, suppose there is no statistical source in the system. The p register would then, depending on the amount of noise present in v, have to be viewed as a simple delay within the context of normal relay controllers, and system operation would then be characterized by limit cycling.

The effect of the statistical source noise in single-PSV operation might be placed on more analytical bases, using the techniques described in this section, This effort has not as yet been completed, but general performance characteristics in the presence of noise are quite evident. Thus, one *of* the functions of the delayed change in output polarity is to provide assurance that the change is not being triggered'by noise. The more likely it is that noise can corrupt the known dependence of $p(v_+)$ upon $p(A_+)$, the more time should be taken before u is made to reverse polarity. However, while this decision process is taking place, action is also taking place, since u is being reduced in magnitude in accordance with the weight which the statistical source gives to the accumulating evidence.

The above feature of simultaneous learning and action, where the latter is based on the best estimate to date, is central to self-organizing control. In the case of a single-PSV system, it does not come into view until the control problem incorporates sufficient complexity, which in this discussion meant the inclusion of noise in the v input. Thus, a conventional controller can readily be configured to provide desirable performance in the absence of noise. It can also be configured to handle noise. However, it can not be made to handle both extremes, or gradations in between, in an optimum fashion. Thus, with the p-register filter alone, u would follow the corrupted input with a simple transport delay. In PSV Control, u is changing in the required direction and the rate of the change is determined by the accumulating evidence as to the validity of the v input signals. Furthermore, the PSV controller randomizes its "sliding mode" (Refs. 5,6) and steady-state operation, with or without noise in the v input, and thus avoids limit cycling. The p register alone, on the other hand, may have a satisfactory steady-state behavior if there is enough noise in the system. In the absence of noise, however, it would produce a limit cycle.

4.3 Role of Statistical Source in Multiple-PSV Systems

To show the unique functions performed by the statistical source in a single-PSV system, it was necessary to include noise as an element of the problem and consider performance in its presence. Although noise can, obviously, be a part of any system, it is not necessary to invoke its presence when considering PSV functions in multiple-PSV configurations, since the latter contain other complexities which can draw upon the functional capabilities of the PSV. Although Phase I of this study did not include multiple-PSV configurations, the potential use of the PSV in such

systems during Phase II formed a background for qualitative projections of Phase I results into multiple-PSV usage. The purpose of this section is to summarize the present thinking concerning the nature of multiple-PSV systems as it relates to statistical source functions. Since this presentation is necessarily a qualitative one, it is best done through a specific example.*

Figure 4.6 (A) shows an illustrative multiple-PSV configuration which maintains as much similarity as is feasible to the single-PSV system considered throughout this report. Thus, we are still dealing with a single-axis system as exemplified by the $\frac{1}{Is^2}$ plant, controlled by a torque T. However, this torque is the sum of two components, each due to a separate actuator. For the sake of specificity, we have assumed the actuators to be magnetic torquers and the coil inputs u_1 and u_2 are therefore currents. The two torquers are assumed to be orthogonal and to have outputs which vary with time, due to, say, motion of a satellite vehicle in a polar orbit around the Earth. An assumed time variation is also illustrated in Figure 4.6(B). The polarities of T_1 and T_2 are understood to relate to the same polarities of input current, i.e. sgn u_1 = sgn u_2.

It is emphasized that the torque curves in Figure 4.6 are taken to be representative of operational conditions but that the controller does have the benefit of knowing the specific time dependence (phase) of such curves, Specifically, the controller is to be designed to produce the desired control characteristics without (a) knowing a priori the polarity of either of the two torquers or (b) the relative

*Suggested by J. A. Gatlin, GSFC.

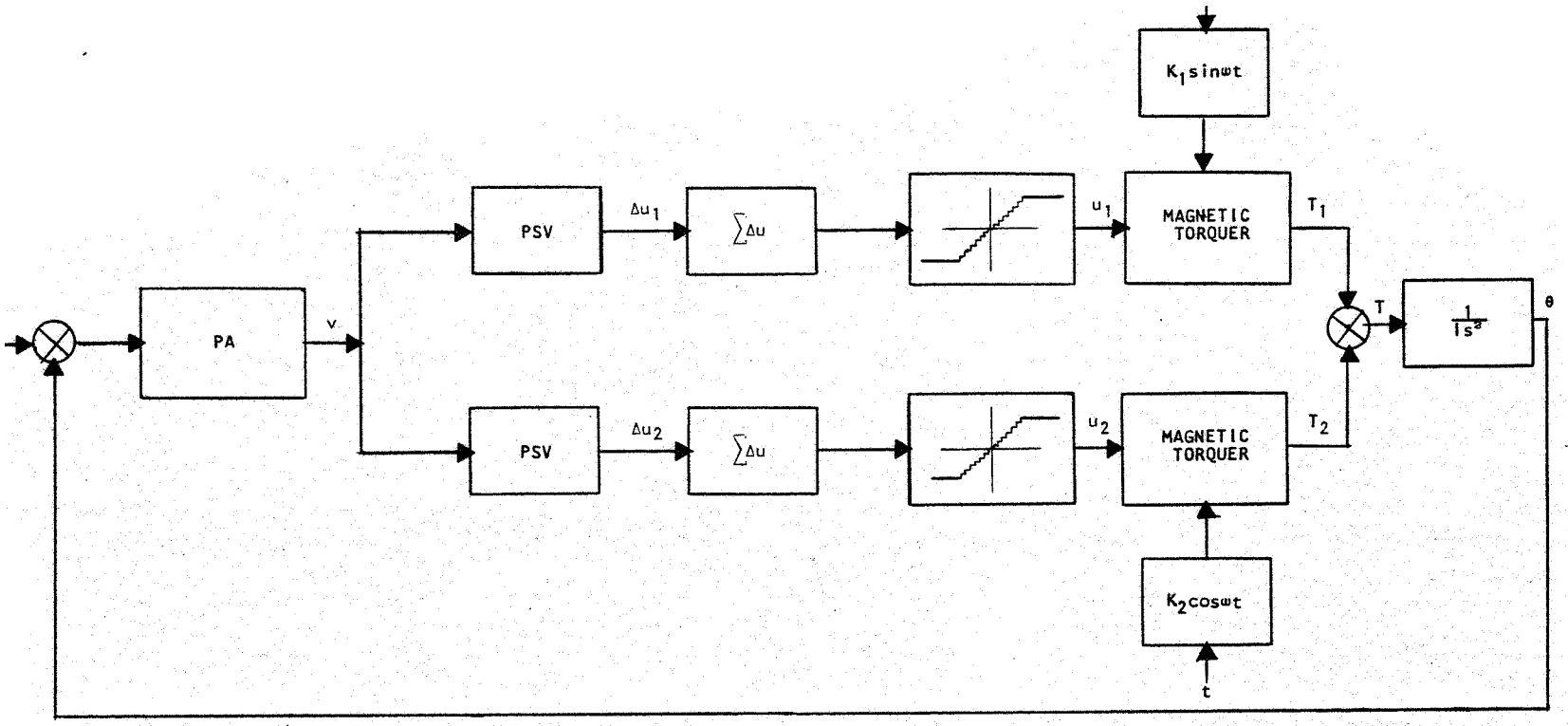

(A) FIGURE 4.6: ILLUSTRATIVE MULTI-PSV CONFIGURATION (Continued)
(A) SYSTEM BLOCK DIAGRAM

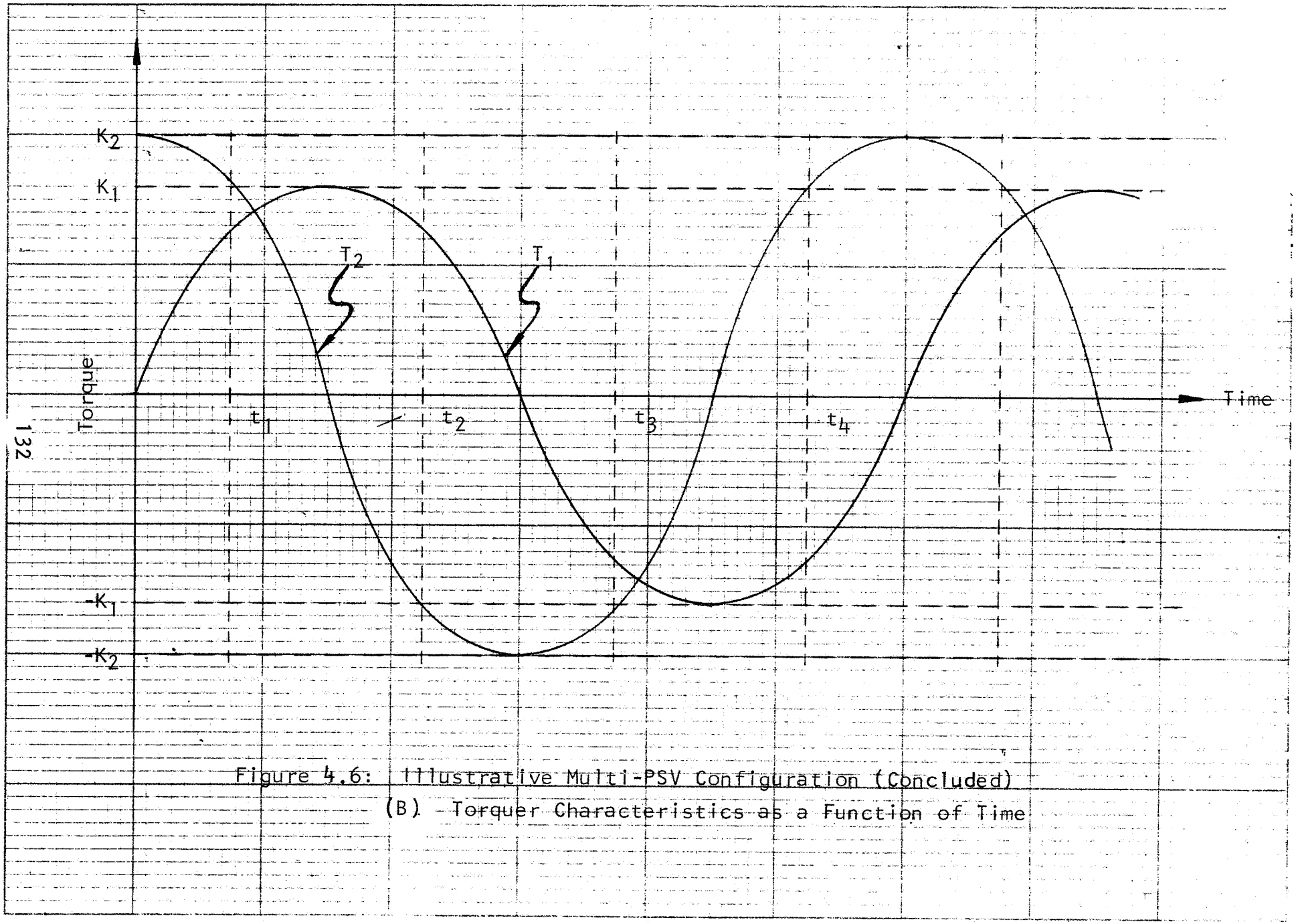

Figure 4.6: Illustrative Multi-PSV Configuration (Concluded)
(B) Torquer Characteristics as a Function of Time

magnitudes of T_1 and T_2. The controller should strive for the best performance possible under any set of conditions on the torquers. This problem clearly involves the performance assessment criterion; however, although some mention of this aspect will be made, we wish to focus on the PSV role in such a design.

In general, the control process can be viewed as that of acquiring a specified trajectory in the phase plane, e.g. the switching line, and following this line into the origin of the phase plane. In this sense the configuration of Figure 4.6 is not different from the other single-axis controllers considered in this report, and we can think of the output v from the Performance Assessment unit in Figure 4.6 as being a measure of the polarity of T relative to the required polarity of control. However, whereas in the single-PSV system there may not have been any question about how to achieve the maximum torque in the required direction, such is not the case here.

Referring to Figure 4.6(B), consider the torque capabilities of the two actuators at times t_1 and t_2 in relation to a requirement for maximum positive torque. At t_1 the input currents u_1 and u_2 should obviously both be positive. However, at t_2, u_2 should be negative and u_1 should be positive. Including the times t_3 and t_4, the four combinations which would at different times produce the desired result are

time	sgn u_1	sgn u_2	state
t_1	+	+	(a)
t_2	+	-	(b)
t_3	-	-	(c)
t_4	-	+	(d)

Note that at any one t, there is for each of the above states a different combination in which the torque cannot be maximum but will have the required polarity. Denoting this as a secondary state, we have, for example, (d) as a secondary state for (a) when $t = t_1$, i.e., since $T_2 \geq T_1$, a negative u_1 will reduce the total applied torque but still permit a net positive torque.

The first question which can be posed in relation to the above would deal with the performance assessment criterion. Since actuator polarities are not known, a criterion of the form sgn v = sgn $e_p \cdot$ sgn u_p would not be adequate. We therefore assume that a second-order criterion is used, of the form sgn v = -sgn $e_p \cdot$ sgn $\ddot{e}_p$. Such a criterion would, in effect, rank the four possible states and produce a positive assessment whenever a change has occurred from a less to a more desirable state. For $t = t_1$, for example, the ascending order of desirable states would be

$$(c) \rightarrow (b) \rightarrow (d) \rightarrow (a) \quad \ldots\ldots\ldots\ldots\ldots\ldots \quad 4:30$$

The role of the PSV units in the system of Figure 4.6 becomes evident when it is noted that, although the Performance Assessment unit can make the proper judgment as to changes of state, it cannot induce all of the possible alternatives because, at their inputs, the two PSV's are synchronized with respect to a single v signal. The PSV units must themselves generate all the alternative modes and rapidly proceed to the maximum values of T at the polarities of T_1 and T_2 which give the primary state.

The above is a simple illustration of the more general parameter space search function of the PSV. It is intended to highlight two important aspects: (1) the

ability of the PSV, in conjunction with a suitable performance assessment criterion, to distinguish between two or more extrema so as to choose the true optimum state, and (2) the ability to produce a rapid search so as to make control possible in a changing environment. The latter is accomplished through the same process previously discussed for single-PSV applications, i.e., to delay the final decision long enough to permit a progressive accumulation of evidence as to the nature of the incoming control signal, but to continuously apply control, the magnitude of which is weighted by the confidence in the currently available evidence.

4.4 Monte Carlo Experiments Using Statistical Decision Device

The purpose of the Statistical Decision Device (SDD), consisting of the p register and statistical source, is to accept a binary input signal which has been corrupted by noise and generate at its output a binary signal consistent with the recent *a posteriori* bias (if any) in the input. It is apparent that a device which responds to trends must introduce some lag in its response. Further, the introduction of probabilistically-controlled noise might seem, at least initially, to compound rather than solve the problem. The purpose of this section is to offer evidence that the action of the SDD is consistent with the desired results, and that the techniques used do not result in any significant loss of information or degradation of performance.

To demonstrate this, a G-15 digital computer program was written to implement the flow chart shown in Figure 4.7. This program iterates indefinitely through successive integer values of N, generating the outputs A, B, and C. The simulation of the SDD is open loop, with a noise generator furnishing a random series of positive and negative inputs.

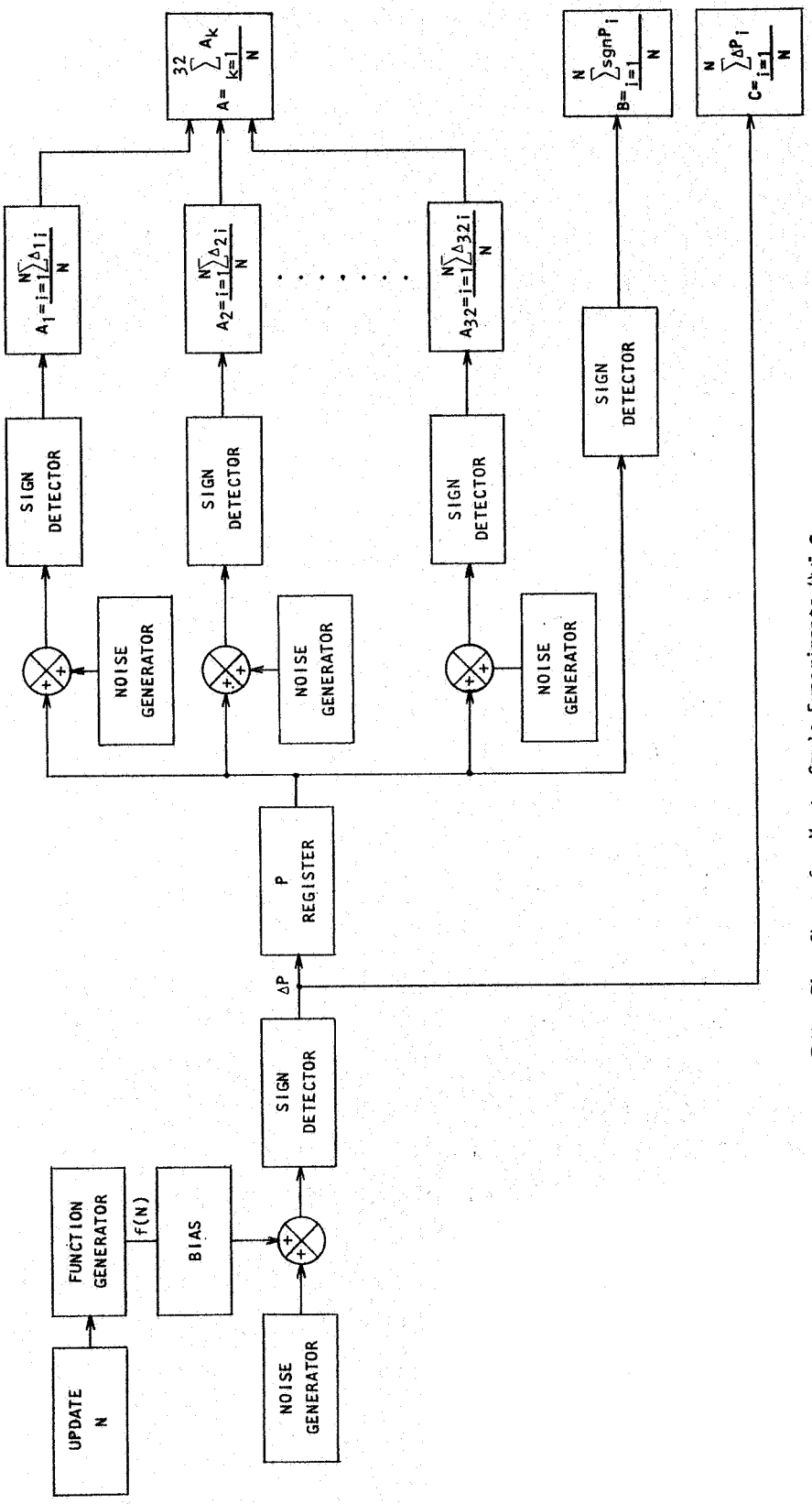

Figure 21 Flow Chart for Monte Carlo Experiments With Statistical Decision Device

This is accomplished by using a classical Random Number Subroutine which provides an output, $-50 < RN < 50$. The sign of this output is determined, and corresponding positive or negative increments are added to the p register and to the C calculator.

$$C = \frac{\sum_{i=1}^{N} \text{sgn } \Delta p_i}{N}$$

The sign of the p register is monitored to provide input for the B calculator.

$$B = \frac{\sum_{i=1}^{N} \text{sgn } p_i}{N}$$

In addition, the contents of the p register bias the generation of each of the increments in the A Channels. In each A Channel,

$$A_K = \frac{\sum_{i=1}^{N} \Delta A_i}{N}$$

There are 32 such channels (to provide a statistically meaningful sample for each iteration) from which a grand mean, A, is derived. Provision was made for the insertion of a steady-state or periodic bias into the Ap generation.

Runs were made with a seven-level p register, except for one comparison run, which used a three-level register.

Figures 4.8 through 4.11 show the results of typical runs. Figure 4.8 shows response to a steady a priori bias of 0.1. Figure 4.9 has a steady a priori bias of -0.5.

Figure 4.10 has no a priori bias, but shows the effect of reducing the p register to three levels. Figure 4.11 shows the result of a periodically varying bias.

4.5 Hardware Tests of Statistical Decision Device

Hardware Tests of the Statistical Decision Device (SDD) have been performed so as to relate actual operation of this circuit to its theoretical performance. This testing has been conducted using the p register, noise generator, and statistical source logic in the SDD configuration shown in Figure 4.12. Table 4.1 sets forth the test program. Equipment used for these tests was described in Section 3 above.

4.5.1 Definitions

The definitions presented in Section 3.1 of this report will again be used.

4.5.2 Experimental Configuration

The Statistical Decision Device, Figure 4.12, is composed of a 7 level p register, a noise generator, and statistical source logic. sgn Δp is the p-register digital input, the probability control voltage (PCV) is the p-register analog output, and sgn Δu is the SDD digital output.

The SDD was tested open loop using two types of input pulse trains, one of which contained noise. In each case, the sgn Δu output was recorded photographically to determine:

(i) time for the sgn Δu output to equal the sgn Δp input with essentially unity probability,

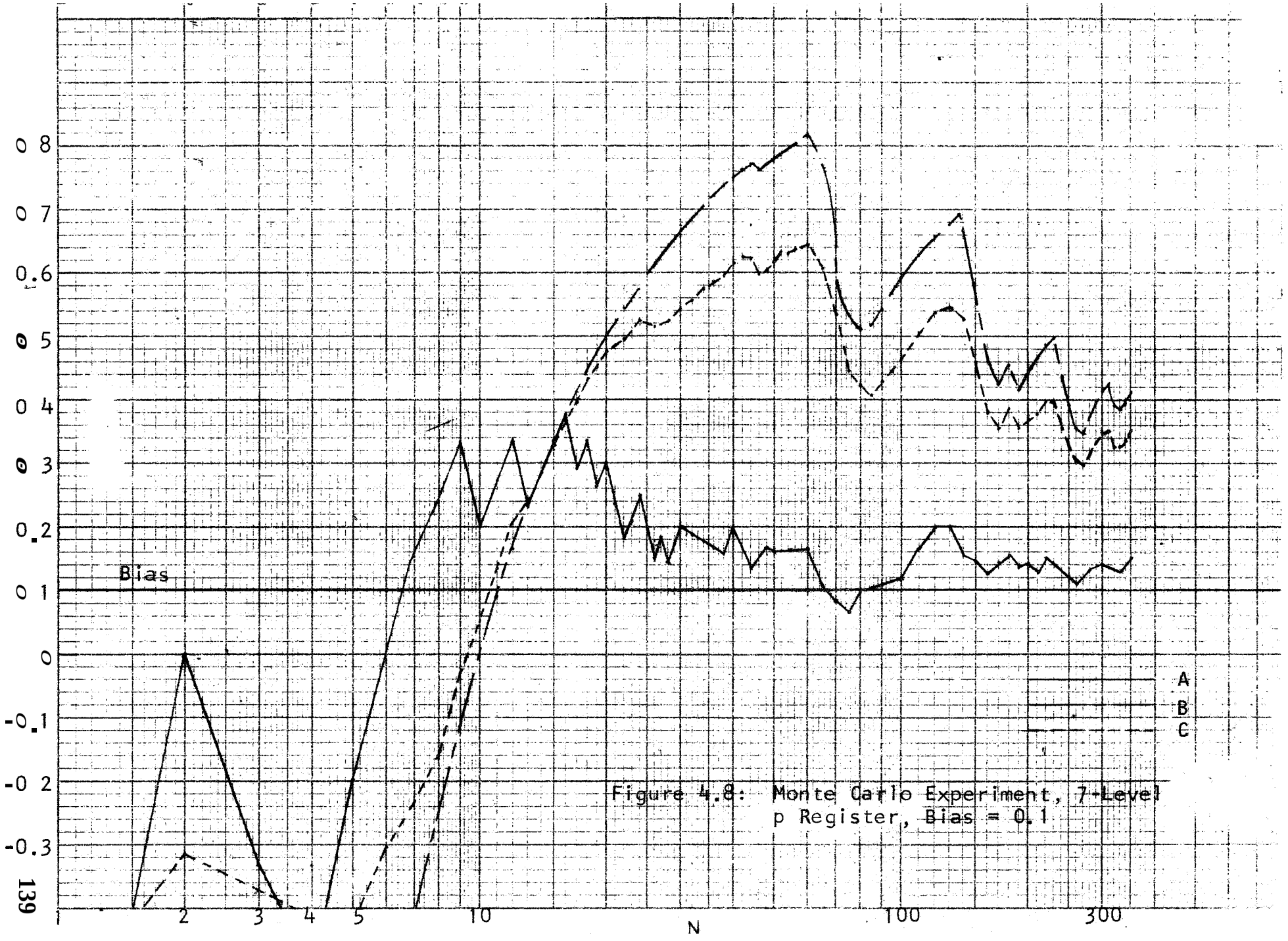

Figure 4.8: Monte Carlo Experiment, 7-Level p Register, Bias = 0.1

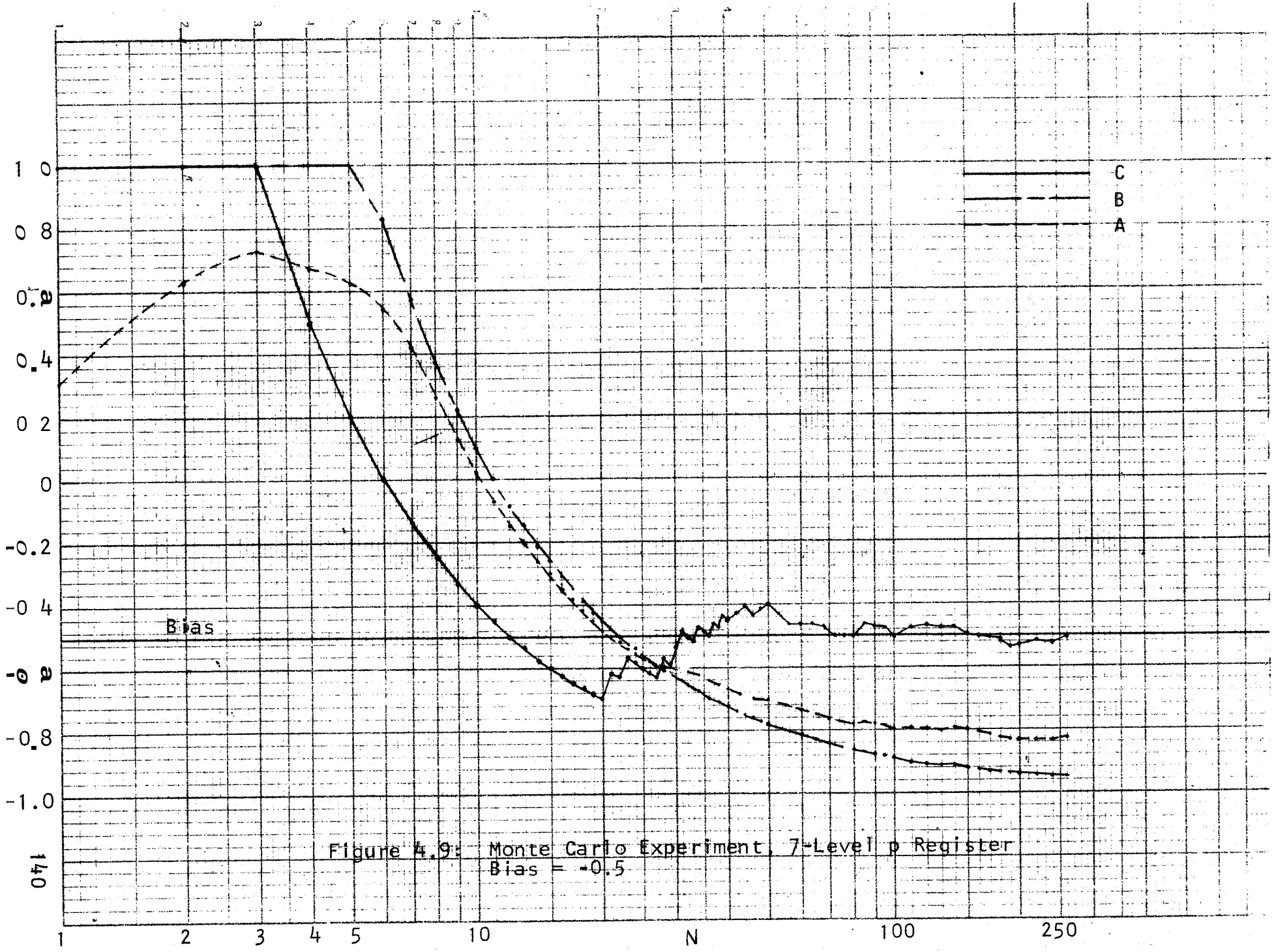

Figure 4.9: Monte Carlo Experiment, 7-Level p Register
Bias = -0.5

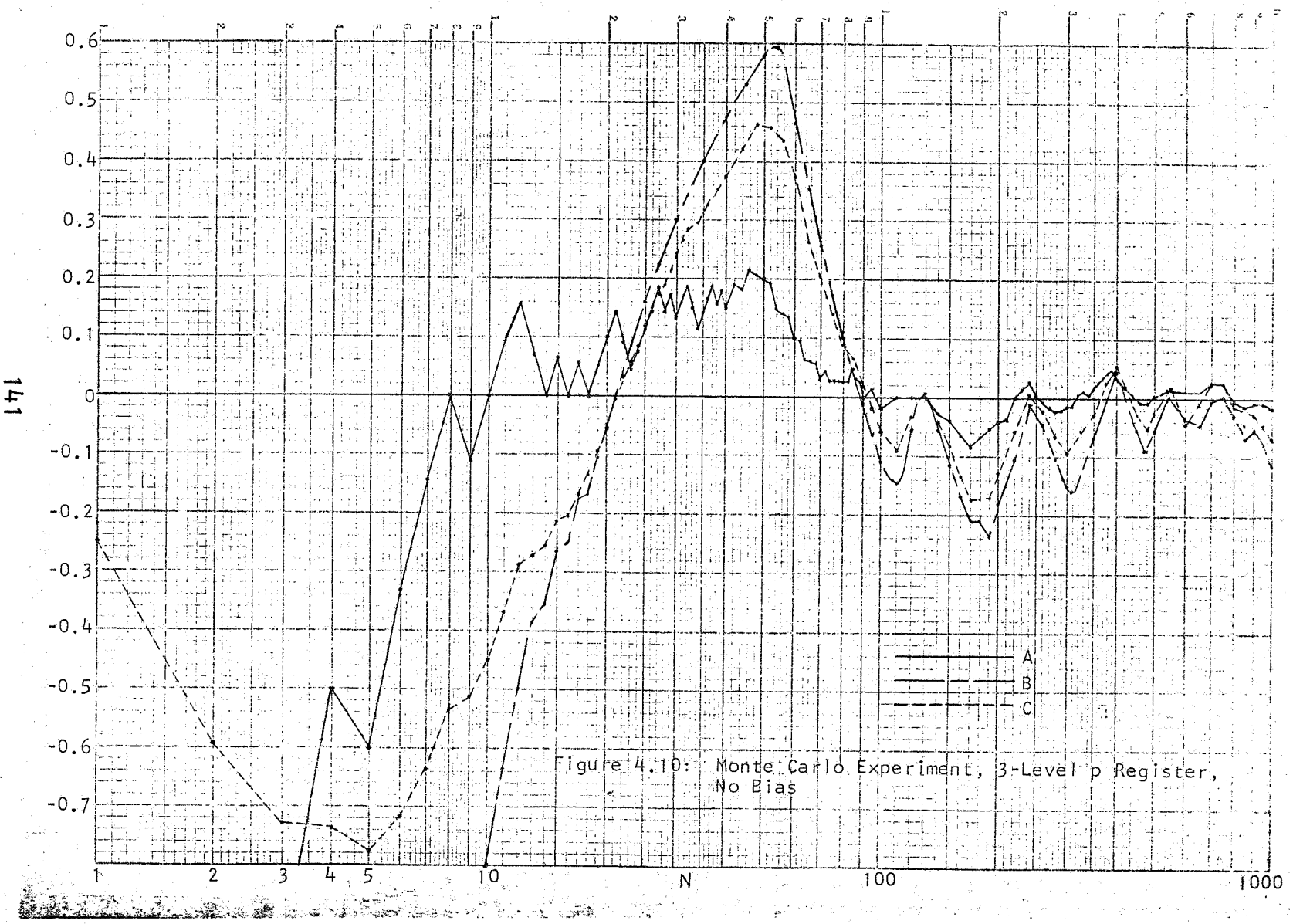

Figure 4.10: Monte Carlo Experiment, 3-Level p Register, No Bias

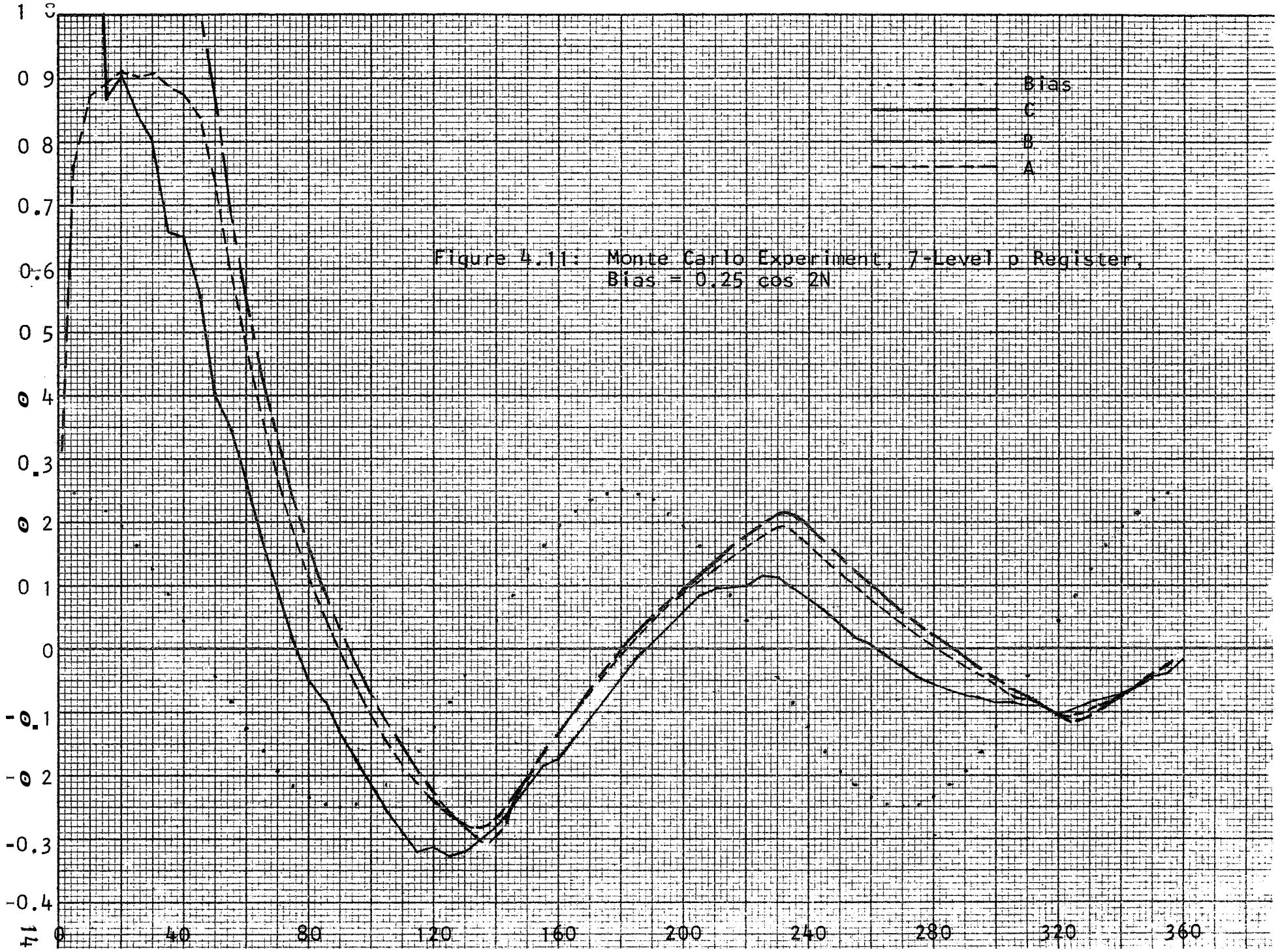

Figure 4.11: Monte Carlo Experiment, 7-Level p Register, Bias = 0.25 cos 2N

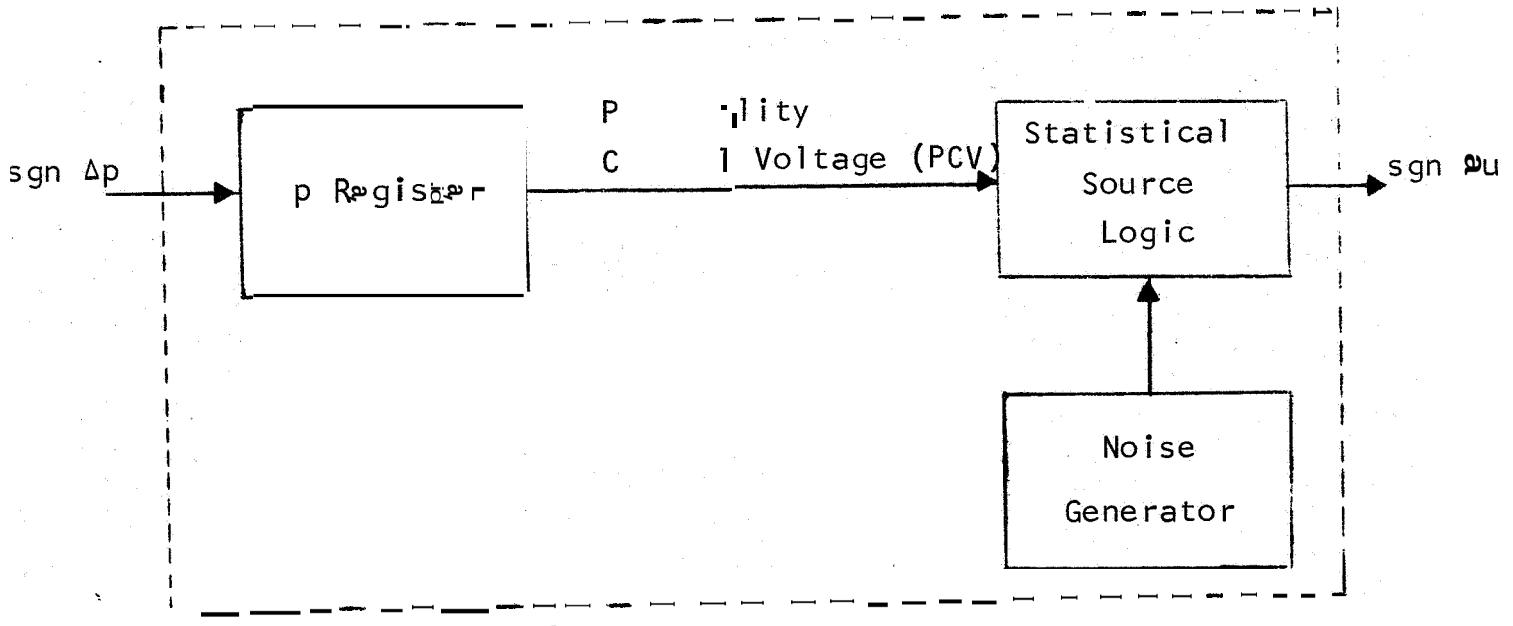

Figure 4.12: Statistical Decision Device

Input	Output	Looking For
Pure Pulse Train	Mixed Pulses	Time for output $\cong$ input
Pure Pulse Train with Noise	Mixed Pulses	Degree of correspondence in steady state
		Effects of various $\lvert E_n \rvert$ & $\lvert P_{max} \rvert$ "rich"-vs-"lean" settings of source

(ii) degree of correspondence between sgn Au and sgn Ap in the steady state,

(iii) effects of various noise-generator voltage levels and PCV levels.

4.5.3 Expected Results

The time requited for sgn Δu to follow sgn Ap with a probability of approximately unity can be calculated for various SDD internal signal-to-noise ratios. These results are easiest to obtain for s/n ratios of 1.0 and ∞, since in reality the points between these limits display the effects of circuit nonlinearity. Assuming that the p register is at one of its limits and the sgn Δp signal does not contain noise, it is easily calculated for R = ∞ that sgn Δu follows sgn Δp in three clock periods. When R = 1.0, it takes six clock periods, using the same assumptions.

4.5.4 Test Results

Due to the many conditions tested, only a fraction of the oscilloscope pictures can be presented. Figure 4.13 shows the sgn Au response to a sgn Ap with an input s/n ratio of ∞, with R = ∞ in the SDD, Figure 4.14 shows the sgn Au response for an input s/n ratio of ∞, with R = 1.18, and Figure 4.15 shows the sgn Δu response for an input s/n of 3, with R = 2.82. Table 4.2 summarizes the conditions tested.

Test results are shown in Figure 4.16, for a pure pulse train input, and Figure 4.17, which shows the results obtained for inputs with input signal-to-noise ratios of 1,2,3,4 and ∞.

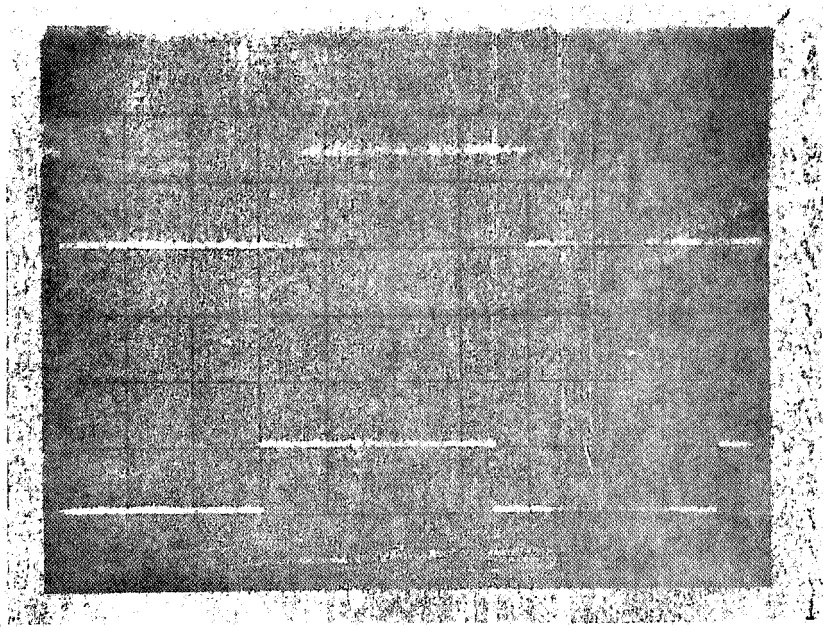

Figure 4.13 : SDD Response, R = ∞, S/N = ∞

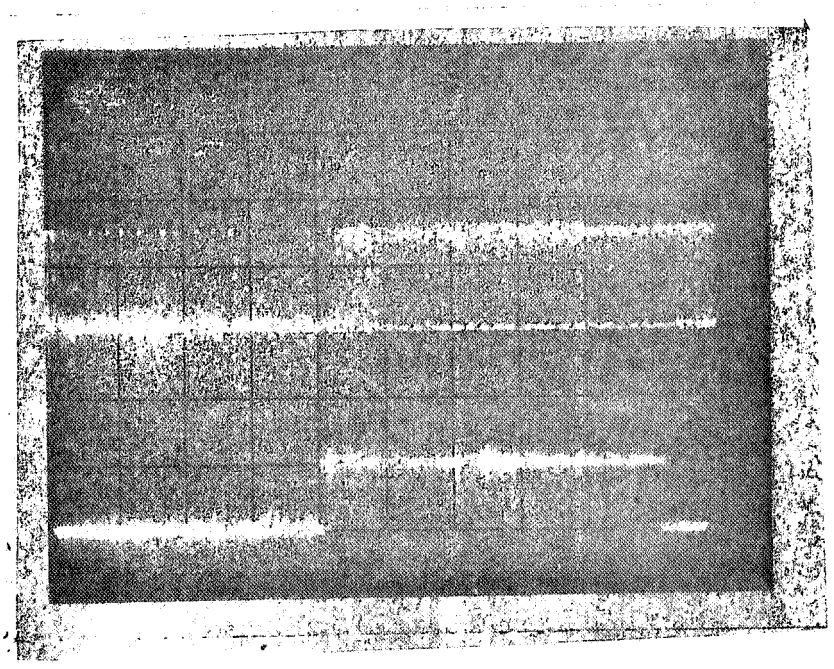

Figure 4.14 : SDD Response, R = 1.18, S/N = ∞

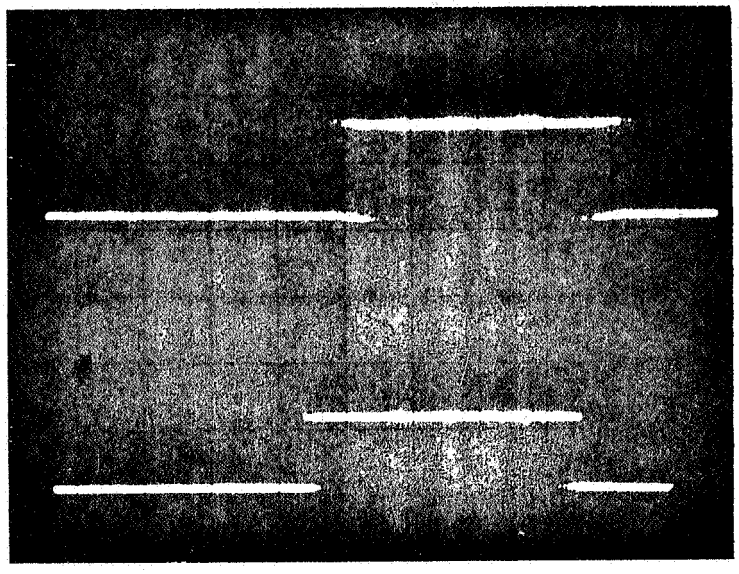

70 msec.

Figure 4.15: SDD Response, R = 2.82, S/N = 3

4.5.5 Comparison of Experimental and Calculated Results

The actual and expected results are identical for an input signal-to-noise ratio of ∞, using R = 1 and R = ∞ in the SDD. For R = ∞, three clock periods are required for the sgn Δu output to follow a (constant) sgn Δp input, while for R = 1, six clock periods are required. The tests where the input signal-to-noise ratio is less than ∞ also follow the expected results, since input noise does delay proper identification of the signal; but in all cases (including s/n = 1) the SDD is able to find the signal in the noisy environment.

Table 4.2: Test Conditions for Statistical Decision Device (SDD)

SDD R	Input S/N Ratio ∞	4	3	2	1
0.58	x	---	x	---	---
0.67	x	---	---	---	---
0.78	x	x	x	x	---
0.88	---	x	x	x	---
1.0	x	---	---	---	---
1.18	x	x	x	x	x
1.43	x	x	---	---	---
1.57	x	x	x	x	x
2.14	x	---	---	---	---
2.82	x	x	x	x	x
∞	x	---	x	x	x

x = conditions tested

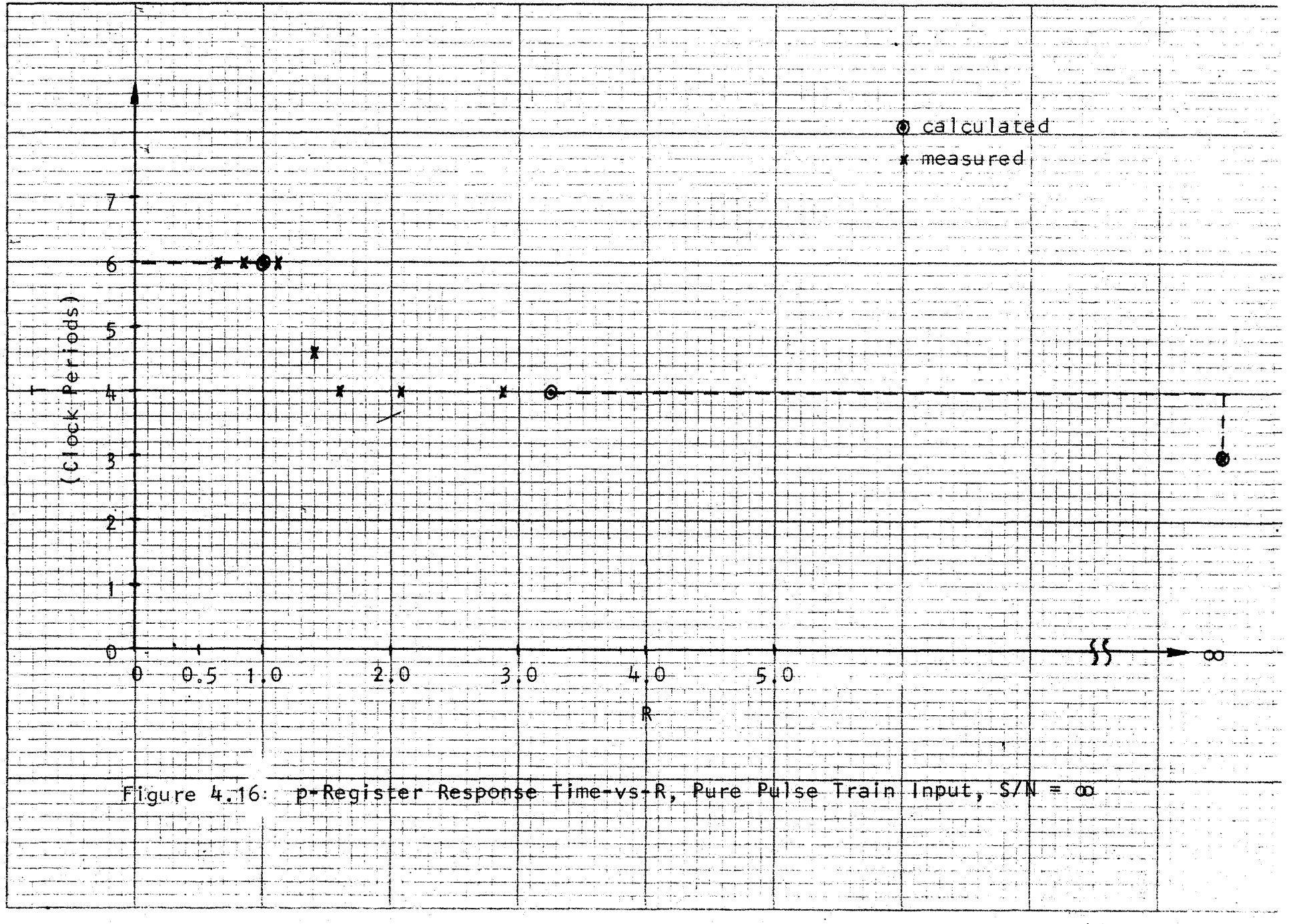

Figure 4.16: p-Register Response Time-vs-R, Pure Pulse Train Input, S/N = ∞

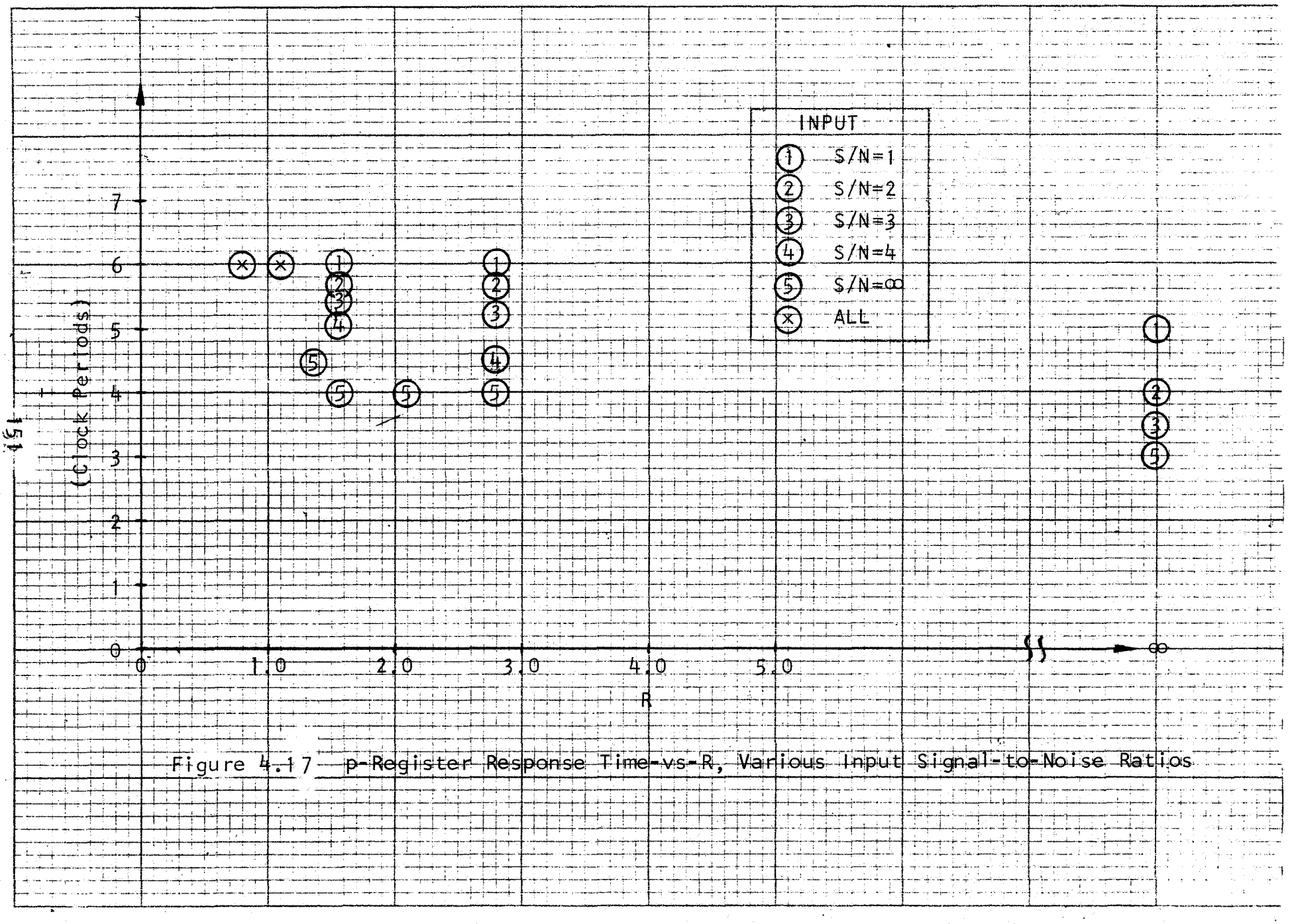

Figure 4.17 p-Register Response Time-vs-R, Various Input Signal-to-Noise Ratios

5. CONCLUSIONS

It is concluded that:

1. Pulse density signal theory provides the conceptual link between digital pulse trains and analog signals. This link has led to development of a mathematical model of the PSV, resulting in simple simulations of the PSV self-organizing control system using conventional, but nonlinear, control elements.

2. The mathematically predicted input-output behavior of the PSV is in excellent agreement with the actual behavior of PSV hardware and computer simulation of the PSV model. The closed-loop responses obtained with the simulation and the actual hardware are also in excellent agreement for a representative plant.

3. For the case of single-axis control investigated, the pulse density model simulation generally provides a better match with PSV hardware behavior than do several empirically-derived models, including a bang-bang controller (with and without relay deadzone), a proportional controller with limiting, and a variable structure controller.

4. The present study has provided further verification of the known characteristics of single-degree-of-freedom PSV control, including the fact that the PSV system produces essentially minimum-time acquisition of the phase-plane switching line without the limit cycle characteristic of bang-bang controllers. In the limiting condition of near zero error, the PSV controller exhibits a very low amplitude (almost within limits of resolution of signals) search which has a random

component that tends to prevent pure cyclic action. Furthermore, it is not necessary to compromise the PSV design if high levels of controller input noise are expected.

6. RECOMMENDATIONS

It is recommended that investigations begin for representative applications of the PSV to distributed-actuation (multiple actuator) self-organizing control systems. This work should consider multiple performance assessment criteria, including the problems of control which minimizes electrical power consumption.

It is also recommended that some theoretical studies continue, with the research including, but not being limited to, investigation of alternative types of conditioning logic, the object being to compare performance of various possible decision rules that use on-line performance assessment information.

7. REFERENCES

1. Self-Organizing Control of Aircraft Pitch Rate and Normal Acceleration, R. L. Barron, R. M. McKechnie, III, S. Schalkowsky, J. M. Davies and R. F. Snyder, Adaptronics, Inc. Final Technical Report under Contract AF 33(615)-2908, AFFDL-TR-66-41, AF Flight Dynamics and Avionics Laboratories, AD # , March 1966.

2. Analysis and Synthesis of Advanced Self-Organizing Control Systems, R. L. Barron, S. Schalkowsky, R. M. McKechnie, III and L. O. Gilstrap, Jr., Adaptronics, Inc. Interim Technical Report under Contract AF 33(615)-3673, AF Avionics Laboratory, May 1966.

3. Self-Organizing and Learning Control Systems, R. L. Barron, invited paper presented at 1966 Bionics Symposium, 2-5 May 1966, Dayton, Ohio.

4. Random Processes in Nonlinear Control Systems, A. A. Pervozvanskii, Trans.Ed. I. Herzer, Columbia University, N. Y., from State Press for Physical and Mathematical Literature, Moscow, U.S.S.R. (1962), R. Bellman, Ed., Academic Press, New York, 1965.

5. "Motion of Variable Structure Systems in the Sliding State", M. A. Bermant et al., Avtomatika i Telemekhanika, Vol. 26, No. 8., (U.S.S.R.), August 1965, pp. 1316-1326.

6. "Design Principles in Variable Structure Systems for Control of Non-Stationary Plants", S. V. Yemelyanov et al., paper presented at IFAC, June 24, 1966.

7. Optimal Control Systems, A. A. Fel'dbaum, Trans. by A. Kraiman, Academic Press, New York, 1965.

APPENDIX I

DESCRIPTION OF ADAPTRONICS, INC. PSV CONDITIONING LOGIC AND RELATED PERFORMANCE ASSESSMENT FUNCTIONS

The Probability State Variable (PSV) Conditioning Logic circuitry developad by Adaptronics, Inc. may be described, in conjunction with either Type I or Type II Performance Assessment (PA) circuitry, as a signal generator whose output signal magnitude and sign are based on a continuous dynamic assessment of actual plant performance versus desired plant performance. The PSV conditioning logic uses a value signal generated by the PA circuitry and an internal sgn Au feedback signal representing the direction of the most recent change in the plant control variable, u(t), to generate the plant control variable. The characteristics of the plant control variable thus generated are such as to drive the system toward and maintain a minimum (ideally zero) system error signal.

The main functions of the PSV conditioning logic circuitry are depicted in Figure 1. The primary functional blocks within the PSV conditioning logic are: a u register which, with its associated control logic, digital-to-analog output conversion, and buffer amplifier, increments, stores, converts, and buffer amplifies the plant control variable; a statistical source whose random pulse output signal with controlled bias governs the direction in which the u register is incremented; a p register which, with its associated control logic and digital-to-analog output; conversion, generates a voltage which controls the bias on the statistical source in accordance with the value signal generated by the PA circuitry and with the delayed sgn Au feedback signal, the latter representing the direction of a recent change in the plant

control variable; a sgn Δu delay register; and a time base generator which regulates the sequence of events associated with each incremental change in the plant control variable. In summary, the operation of the PSV conditioning logic circuitry is such that the probabilities associated with alternative directions of change in the plant control variable are biased in favor of changes which produced desirable results, as indicated by the value signal generated by the PA circuitry. The sequence of main events occurring during each plant control variable update period is: (1) the p register is incremented in accordance with the value and sgn Δu feedback signals, thus changing the output statistics of the statistical source, *(2)* the u register is incremented in accordance with the new probabilities, and (3) the direction of the u register increment is transferred to the delayed sgn Δu feedback loop.

The variation of control system probabilities, as expressed by the statistical source output, is accomplished by the p-register control logic which generates an ADD or a SUBTRACT signal to determine the direction in which the p register is incremented. The p-register control logic bases its decision regarding a positive or a negative increment of the p-register contents upon an instantaneous correlation of the value signal, v, from the PA circuitry and the delayed sgn Δu feedback signal representing that change in the plant control variable, $u(t)$, which resulted in the then-existing v ("reward-punish") signal. The nature of this correlation is such that a positive increment to the p-register contents is ordered if the value signal is positive ("reward") and if, furthermore, the delayed sgn Δu feedback signal indicates the associated change in the plant control variable was a

---

*logical one

positive increment; or if the value signal is negative*** ("punish") and the delayed sgn Δu feedback signal indicates the associated change in the plant control variable was a negative increment. Conversely, a negative increment to the p-register contents is ordered if the value signal is positive and the delayed sgn Δu feedback signal indicates the associated change in the plant control variable was a negative increment, or if the value signal is negative and the delayed sgn Au feedback signal indicates the associated change in the plant control variable was a positive increment. The resultant ADD or SUBTRACT signals delivered to the p register may be expressed as the Boolean functions

$$\text{ADD} = V \cdot \text{sgn } Au \cup \overline{V} \cdot \overline{\text{sgn } Au}$$

and

$$\text{SUB} = V \cdot \overline{\text{sgn } Au} \cup \overline{V} \cdot \text{sgn } Au$$

The p register consists of an N-stage up-down counter with the number of stages determined by the degree of resolution desired in governing the control system probabilities; i.e., by the number of intermediate levels desired between the minimum and maximum probabilities that the plant control variable will change by a positive increment.*** A convenient rule of thumb in design is to limit the number of stages in the p register to one less than the number of stages in the u register (assuming these registers are clocked at approximately the same frequency). The p register incorporates limit gates to prevent)'end-around" operation. When the p register has

---

*** logical zero

*** In the Type 1507 PSV module of the Mark III Self-organizing Controller, a three-stage (seven level) p register is used.

been incremented to either of its limit states, it will remain in that state until the p-register control logic reverses its directional instructions. The rate at which the p register is incremented is determined by the time base generator. This rate may be chosen to be greater than the rate at which the u register is incremented."* A continuous digital-to-analog conversion is performed on the p-register contents to derive the probability-bias control voltage for the statistical source. This D/A conversion is accomplished via a binary-weighted precision resistor summation network.

The statistical source consists of an analog random noise generator with essentially a Gaussian distribution of output voltage probabilities, a threshold circuit for comparing the output of the noise generator with the analog signal representing the p-register contents, and an output buffer which shapes the comparator output and shifts it to the desired logical one and logical zero levels. The action of the statistical source is such that when the P register is at its maximum limit the source output has approximately a 95 percent probability of being at the logical one level, when the p register is at its minimum limit the source output has approximately a 95 percent probability of being at the logical zero level, and when the p register is at its midpoint the source has approximately a 50 percent probability of being at either the logical one or logical zero level.

The u-register control logic determines the direction in which the plant control variable will be changed, based solely upon the instantaneous state of the statistical source output at the occurrence of a sequence pulse from the time base generator. A positive increment to the u-register

---

*In the Type 1507 PSV module of the Mark III Self-organizing Controller, identical increment rates are used.

contents is ordered if the statistical source output is a logical one, while a negative increment to the u-register contents is ordered if the statistical source output is a logical zero. The u register consists of an N-stage up-down counter with the number of stages dependent upon the desired size of incremental change in the plant control variable, u(t).* The u register incorporates limit gates to prevent "end-around" operation. When the u register has been incremented to either of its limit states, it will remain in that state until the u-register control logic reverses its directional instructions, The rate at which the u register is incremented is determined by the time base generator and is, in theory, a function of the response time of the plant being controlled. A continuous digital-to-analog conversion is performed on the u-register contents to generate the conditioning logic output signal, which is operated on by a buffer amplifier to obtain a plant control signal at the required power level. D/A conversion is accomplished via a binary-weighted precision resistor summation network. The delayed sgn Δu feedback signal may be generated by transferring the u-register control logic ADD-SUBTRACT signals into a tapped shift register.** The amount of delay is a function of the tap selected by the user. Usually, the polarity of the delayed sgn Au feedback signal is chosen to be that of the last preceding change in the plant control variable,

Two main types of performance assessment circuitry have been developed by Adaptronics, Inc. for use in self-organizing control systems. The main functions of these

---

*In the Type 1507 PSV module of the Mark III Self-organizing Controller, a four-stage (fifteen level) u register is used.

**In the Type 1507 PSV module of the Mark III Self-organizing Controller, the sgn Au feedback signal is obtained by detecting the slope of the plant control variable.

two types of PA circuitry are depicted in Figures 2 and 3. Both types of performance assessment employ a predicted-error function to generate the value signal. However, the value signal generated by the Type I PA circuitry is based on the predicted error and its second derivative, while the value signal generated by the Type II PA circuitry is based on the predicted error and a predicted value of the plant control variable.

In the Type I performance assessment circuitry, Figure 2, the error signal, $e(t)$, is operated on, approximately per the Laplace transform $(1 + Ts)$, to yield the predicted error signal, $e_P = e(t) + Te(t)$. The second derivative, $\ddot{e}_P$, of the predicted error is then obtained, and sign information is extracted from both e_P and $\ddot{e}_P$. This sign information is then operated on by value logic to generate a v signal of the form

$$\text{sgn } v = -\text{sgn } e_P \cdot \text{sgn } \ddot{e}_P.$$

The Type II performance assessment circuitry also generates a predicted error signal, $e_P = e(t) + Te(t)$. But, the Type II circuitry also operates on the plant control variable, $u(t)$, approximately per the Laplace transform $(k + T_1 s)$, to obtain its predicted value, $u_P = ku(t) + T_1 u(t)$. Sign information is extracted from both e_P and u_P. This sign information is then operated on by value logic to generate a v signal of the form

$$\text{sgn } v = \text{sgn } e_P \cdot \text{sgn } u_p.$$

The Type II performance assessment circuitry has the advantage of being less sensitive to plant lags and sensor noise, because it eliminates the second derivative of e_p, but the

Type II PA requires that plant polarity (viz, $\partial \ddot{e}_P / \partial u_P$) be known a priori.

Adaptronics, Inc. has a patent pending (Application No. 535,551, entitled "Self-Organizing Control System") which covers the PSV conditioning logic and both types of performance assessment discussed here.

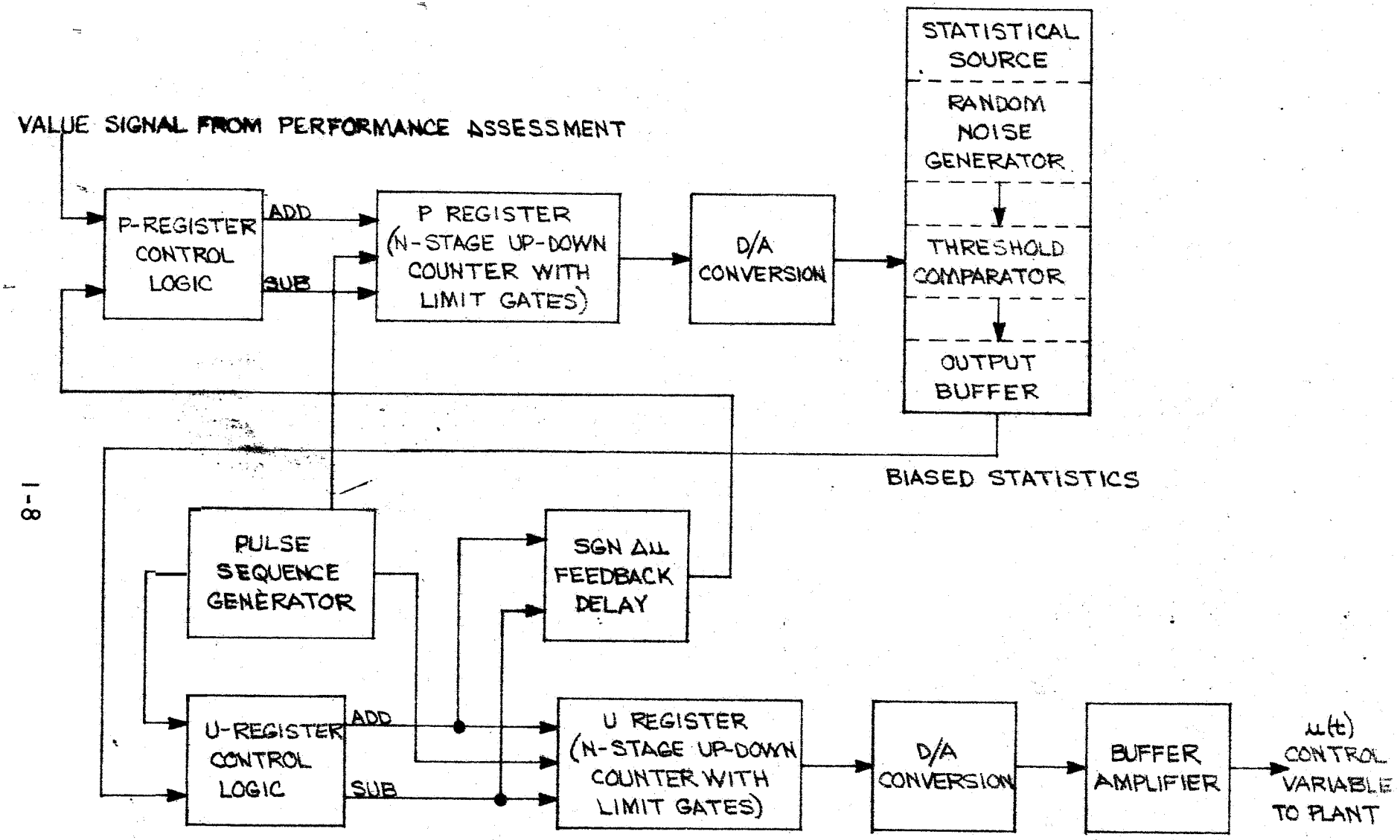

FIGURE 1: FUNCTIONAL DIGRAM - PSV CONDITIONING LOGIC

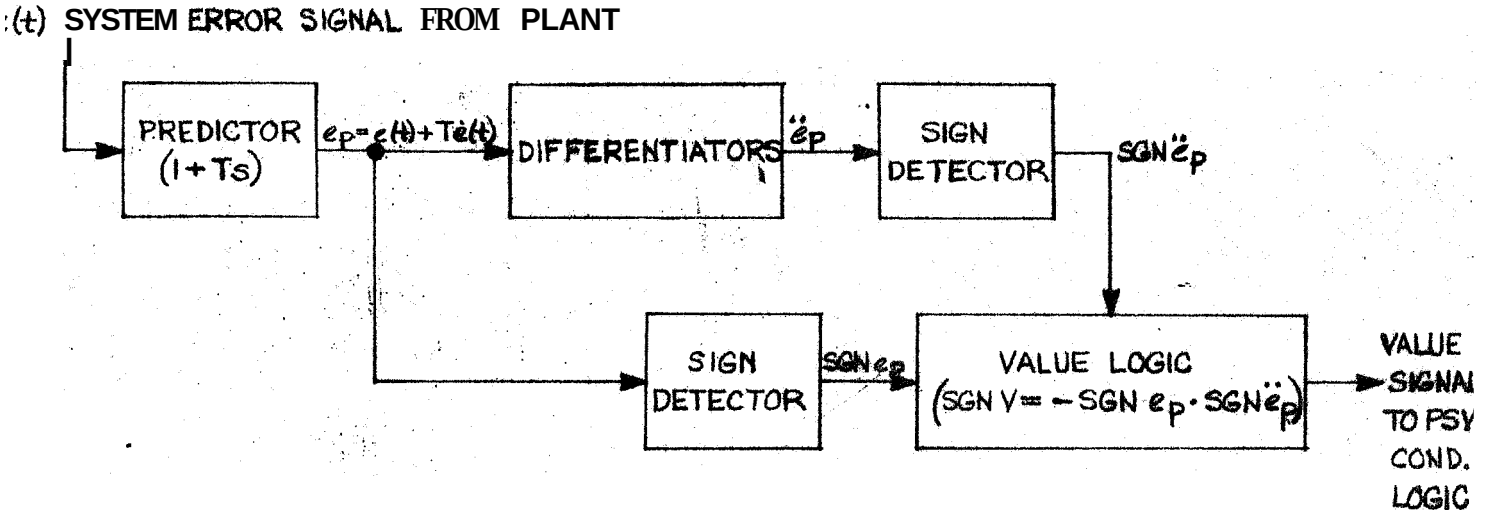

FIGURE 2: FUNCTIONAL DIAGRAM – PERFORMANCE ASSESSMENT, TYPE I

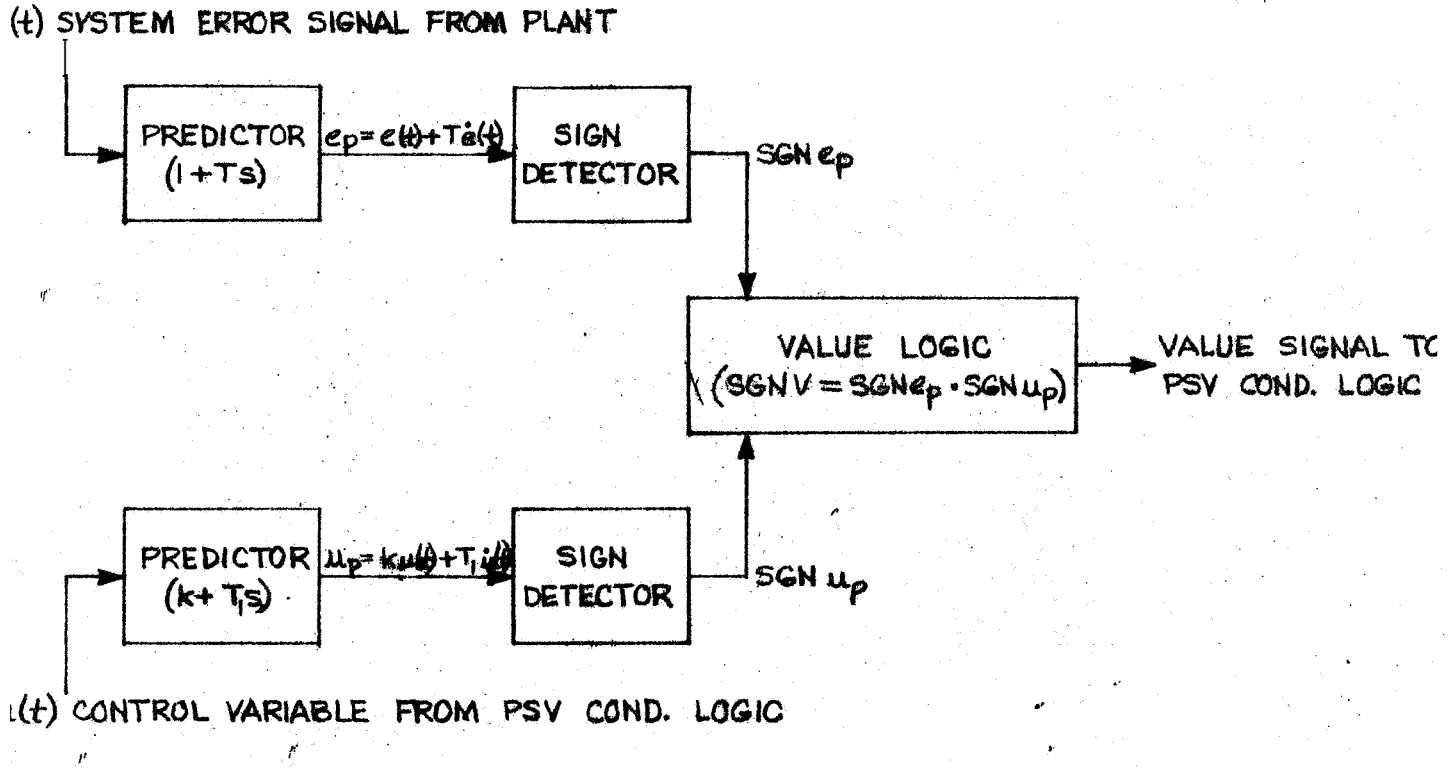

FIGURE 3: FUNCTIONAL DIAGRAM – PERFORMANCE ASSESSMENT, TYPE II

APPENDIX II

THEORY OF PULSE DENSITY CODES AND OPERATIONS ON PULSE DENSITY SIGNALS

by

Lewey O. Gilstrap, Jr.
ADAPTRONICS, INC.

1. INTRODUCTION

Pulse density signals are pulse trains that encode analog signals as the density or number of pulses per unit time of a train of pulses. Mathematically, encodings of this type are forms of numbers to the base or radix 1.

The objective in studying pulse density signals is to relate the density of the signal to the logic gates, counters, and other elements of the logic circuitry used to transmit and operate on the signals. With these relationships established, it is a relatively simple matter to analyze the behavior of such devices as the PSV unit of a self-organizing controller or to obtain approximations to the PSV behavior in new applications.

2. PARAMETERS OF PULSE TRAINS

2.1 Basic Definitions

Single, rectangular pulses have pulse width, pulse height, rise time, and fall time as the basic parameters of interest. To simplify the analysis of pulse trains, we will assume that all pulses have unit height and zero rise and fall times. Although this idealized pulse cannot be mechanized, we can approach it to a satisfactory degree.

The fundamental parameters of pulse trains are

$f \equiv$ pulse repetition rate (or frequency)

$\tau \equiv$ pulse width of an individual pulse.

Just as fundamental, but not an inherent parameter of a pulse train is the period of time over which we observe a pulse train to determine f. For a pulse train with constant f and τ, the observation period is arbitrary, except that it should be an integral multiple of $\frac{1}{f}$ for accurate determination of f. However, if f is changing as a function of time, we should select an observation interval that is long enough to permit us to count a sufficient number of pulses to get f accurately but not so long that f has changed appreciably in the counting interval. Depending on the circumstances of the application, the observation interval may be either a design parameter of a pulse system or an environmental parameter fixed by the application. This point will be discussed further in the section on encoding and decoding variables.

We define

$T \equiv$ observation interval

from which we get the number, n, of pulses occurring during T must be

$$n = IT \qquad \text{2:1}$$

and, obviously

$$f = \frac{n}{T} \qquad \text{2:2}$$

We further assume that physical devices for realizing pulse trains all have a practical maximum frequency, f_m, that they can produce. This assumption implies a maximum number, n_m, of pulses that can be observed in any given observation interval:

$$n_m = f_m T \qquad \text{2:3}$$

Dividing Equation 2:1 by Equation 2:3, we get

$$X = \frac{n}{n_m} = \frac{fT}{f_m T} = \frac{f}{f_m} \qquad \text{2:4}$$

This ratio, which is the normalized pulse repetition frequency averaged over the observation interval, is termed the absolute pulse density of a pulse train. Since this ratio is a parameter of any signal composed of pulses, we will use functional notation to indicate the operations required to determine this ratio. It will be denoted by X( ) in this paper. Thus, if x is a pulse signal, then X(x) is the absolute pulse density of the signal x. If x_1 and x_2 are two different signals, then $X(x_1)$ and $X(x_2)$ are their respective absolute pulse densities. When no ambiguity can arise, we will drop the functional notation and subscript X for brevity's sake. Thus,

$$X_1 = X(x_1)$$

$$X_2 = X(x_2)$$

and so on.

From the absolute pulse density, we get Y, the relative pulse density of a pulse train:

$$Y = 2X - 1 = 2\left(\frac{n}{n_m}\right) - 1 = 2\left(\frac{f}{f_m}\right) - 1 \quad \ldots\ldots\ldots\ldots\ldots 2:5$$

It can be observed that X must vary between 0 and 1, while Y varies between -1 and +1. Hence, the relative pulse density could be used as a means for encoding suitably normalized analog signals. When no ambiguity can arise, X or Y will be referred to as pulse densities.

Letting x(t) be a signal consisting solely of pulses, where

$$x(t) = \begin{cases} 1 \text{ if a pulse is present} \\ 0 \text{ otherwise} \end{cases}$$

we can define other parameters of a pulse train. Let

$$W = \frac{1}{T}\int_o^t x(t)dt \quad \ldots\ldots\ldots\ldots\ldots\ldots\ldots\ldots\ldots 2:6$$

We will define W as the absolute duty cycle of a pulse train averaged over the period, T. Following the procedure for pulse density, we also define the relative duty cycle of a pulse train and denote it by Z[x(t)] or Z(x), if the dependence of x on t is understood. The relative duty cycle is

$$Z = 2W - 1 \quad \ldots\ldots\ldots\ldots\ldots\ldots\ldots\ldots\ldots 2:7$$

We can now relate these parameters of pulse trains to one another. Since W is the duty cycle of a pulse train, we have, for constant or average pulse width, τ,

$$W = \frac{n\tau}{T} \equiv \frac{n}{n_m} \cdot \frac{n_m}{T}\tau = Xf_m\tau \quad \ldots\ldots\ldots\ldots\ldots\ldots 2:8$$

Since we have established the relationships of absolute to relative pulse density and absolute to relative duty cycle, then Equation 2:8, which relates absolute pulse density to absolute duty cycle completes the links.

Summarizing, we have

f = pulse repetition frequency

τ = pulse width

T = observation interval

n = fT = the number of pulses in an observation interval

X = the absolute pulse density

Y = the relative pulse density

W = the absolute duty cycle

Z = the relative duty cycle

We also have

$$X = \frac{Y+1}{2} = f_m \tau = \frac{W}{\tau} = \frac{Z+1}{2 f_m \tau} \quad \text{.....2:9}$$

$$Y = 2X - 1 = \frac{2W}{f_m \tau} - 1 = \frac{Z+1}{f_m \tau} - 1 \quad \text{.....2:10}$$

$$W = X f_m \tau = \frac{Y+1}{2} f_m \tau = \frac{Z+1}{2} \quad \text{.....2:11}$$

$$Z = 2X f_m \tau - 1 = (Y+1) f_m \tau = 2W - 1 \quad \text{.....2:12}$$

where

$f_m \equiv$ maximum pulse repetition frequency attainable in the system

$n_m \equiv$ maximum number of pulses that can be observed during an observation interval.

2.2 Two Major Types of Pulse Train Modulation

By holding either τ or f fixed, we can obtain the two major types of pulse trains (without decoding reset). These two types of signals are termed, respectively, pulse density modulated signals and pulse width modulation signals. If

$$f = .5\frac{1}{\tau} + g(t) \text{ and } \tau = \text{const.} \qquad \text{.....2:13}$$

then

$$Y = 2\tau g(t),\ Z = 0 \qquad \text{.....2:14}$$

This is clearly a matter of modulating the pulse density. If

$$\tau = .5\frac{1}{f} + g(t) \text{ and } f = \text{const.} \qquad \text{.....2:15}$$

then

$$Z = 2fg(t),\ Y = 0 \qquad \text{.....2:16}$$

This is pulse width modulation.

2.3 Extracting Pulse Train Parameter Values

2.3.1 Continuous and Reset Decoding

As noted above, the pulse repetition rate in a pulse train can be a carrier of information. To "decode" or demodulate the density of a pulse train requires that the number of pulses per unit of time be determined. While a counting procedure using a reset to zero at the end of each counting interval can be used to obtain the number of pulses per unit time, it is sometimes desirable to have a continuous decoding method. A lag filter will provide a continuous measure proportional to the number of pulses in a train of uniform shaped pulses, provided that the number of pulses per unit time is not changing rapidly with respect to the filter time constant. The lag filter is convenient as a decoder in another way: for the case of slowly varying pulse density, the lag filter with time constant, τ, gives the same pulse density measure as does the counting process carried out over a time interval equal to the constant, τ, of the filter.

Strictly speaking, the lag filter does not so much "decode" a pulse density coded signal as it does transform the pulse signal into an analog signal, Likewise, a counter converts the density into a binary (or other) coded number. In transmitting information from one point to another it is always necessary to employ a carrier of some kind. In this report we are primarily concerned with carriers in the form of pulse trains and with the process of recovering the information contained in some parameter of the pulse train. In general, physical devices operate on analog signals, so we have investigated the several decoding possibilities. From an abstract point of view, it is just as reasonable to be concerned with transforming analog signals or binary coded digital signals into pulse density signals, and some of these transformations will be noted in later sections of this appendix.

We shall distinguish between the two decoding methods by referring to them as "counting with reset" and "continuous". The counting with reset allows us to decode a pulse number code as well as a pulse density code. The pulse number code is simply that in which a magnitude of interest is directly encoded as a number of pulses. For example, the number 119 could be encoded by a train of pulses containing exactly 119 pulses. A unary pulse number code of the above type would be properly decoded by a counting-with-reset decoder for its singular occurrence, assuming proper synchronism of the pulse train and decoder. Hence, a unary pulse number code can be made into a pulse density code by allowing a fixed amount of time to send a number and restarting the number at the beginning of each successive time interval. These codes have a fixed number which is the largest that can be so transmitted; this largest number is equal to the maximum system transmission rate multiplied by the allotted transmission interval.

Pulse density codes based on unary pulse codes are generally clocked and are therefore usually correlated. Repetitive number codes can be operated on by appropriate algorithms to obtain arithmetic operations, and, in fact, the digital differential analyzer uses these codes to great advantage. However, we are interested in this study primarily in uncorrelated pulse density signals and do not plan to pursue the pulse number codes.

2.3.2 Analog and Digital Decoding

As discussed above, decoding pulse density signals can be accomplished using either digital counters or filters.

If a counter of sufficient capacity to contain the number n_m is driven by a pulse density signal for a period of time, T, then the contents of the counter at the end of that time must be

n. Knowing n_m, then the absolute pulse density can be readily determined. If the counter is reset at the end of each T interval of time, then the register contents are n, but if the counter continues to run, the register contents at time, t, must be

$$\int_0^t x(t)dt$$

As a variation on counting, suppose we sample the incoming pulse train at a frequency $f_c < f$, incrementing the counter if there is a pulse present and decrementing the counter in the absence of a pulse. The number of "ones" seen by the sampling device must be proportional to the duty cycle, W, of the pulse train, and, during the interval T, we must have

no. of samples = f_cT

no. of "ones" in sample = Wf_cT

no. of "zeros" in sample = $(1 - W)f_cT$

Therefore, counter contents = f_cTZ . If the counter continues to run and Z varies, then the counter contents will approximate

$$\int_0^t f_cZdt$$

Decoding with a lag filter, whose Laplace transform is

$$\frac{G}{1+Ts}$$

produces much the same result as decoding with counters. If the "one" level of a pulse code is set to +V volts and the "zero" level set to 0 volts, then the filter output will be WV, provided that W is not changing rapidly compared to T. If the "one"

is set to +V volts and the "zero" set to -V volts, then the filter output will be ZV, again, provided Z is not varying rapidly with respect to T.

2.3.3 Variation of Decoding Frequency

If a square wave of duty cycle W and frequency $f << \frac{1}{T}$ is fed to a decoder, very little change in the waveform is noted except for a rounding of the corners. As $f_o = \frac{1}{T}$ is gradually reduced, a definite filtering action becomes noticeable. The square wave becomes more nearly a rounded sawtooth which varies between two voltage levels which lie between the "zero" and "one" voltage level of the square wave. Finally, when $f_o << f$, f becomes decoded and appears as a d.~.level which is directly proportional to duty cycle, W. At the point of equality, $f = f_,$, the square wave has some of the characteristics of a pulse density code.

In general, we should design pulse density circuits such that $f >> f_o$ to avoid inappropriate decoder response. However, it is not always possible to do this. In dynamic problem environments, it sometimes happens that the environment response time constitutes a natural decoding. This is indeed the case in the Adaptronics self-organizing controller (Ref. 1). If the environment is to "decode" ouputs, it can happen that conditions will arise that correspond to the ambiguous situation is which $f = f_o$ or to the other complex case in which $f >> f_,$, but the duty cycle itself is changing at a rate close to f_o. While these cases should be avoided, it may not always be possible, and studies of these conditions are planned in future work.

2.4 Uncorrelated Signals

The absolute duty cycle of a pulse train can be formally

equated to the probability that there will be a pulse at a given sample time, since it satisfies the frequency definition of a probability. Using this interpretation, we can ask what the probability is that two distinct signals will be at the "one" level at a given instant. Thus, if we have signals, x_1 and x_2, we know from the definition of conditional probabilities that

$$p(x_1 \cdot x_2) = p(x_1 | x_2)p(x_2) \quad \ldots\ldots\ldots\ldots\ldots 2:17$$

$$= p(x_2 | x_1)p(x_1) \quad \ldots\ldots\ldots\ldots\ldots 2:18$$

We now define two pulse density signals: x_1 and x_2, to be uncorrelated if

$$p(x_1 | x_2) = p(x_1) \quad \ldots\ldots\ldots\ldots\ldots 2:19$$

$$p(x_2 | x_1) = p(x_2) \quad \ldots\ldots\ldots\ldots\ldots 2:20$$

Since an "AND" gate has an output when and only when both inputs are at the "one" level, we see that if

$$y = x_1 \cdot x_2 \quad \ldots\ldots\ldots\ldots\ldots 2:21$$

then

$$p(y) = p(x_1 | x_2)p(x_2) = p(x_1)p(x_2) \quad \ldots\ldots\ldots\ldots\ldots 2:22$$

Hence, for an "AND" gate

$$W(y) = W(x_1)W(x_2) \quad \ldots\ldots\ldots\ldots\ldots 2:23$$

or $$W_3 = W_1 W_2 \quad \ldots\ldots\ldots\ldots\ldots 2:24$$

. To be precise, Equation 2:24 holds for all pairs of signals that are uncorrelated at frequencies below $\frac{1}{T}$. This includes signals, such as those from statistical sources, which are uncorrelated at all frequencies (strictly uncorrelated) as well as those which are correlated at frequencies above $\frac{1}{T}$.

We can also note that sampling of the complement or logical inverse of a given pulse density signal can also be expressed in probability terms:

$$p(\bar{x}) = 1-p(x) = 1-W \qquad \text{..... 2:25}$$

With the intersection and complementation operations, it is possible to obtain any arbitrary Boolean function and, correspondingly, we can obtain the parameters of pulse trains that are obtained by logic gating of multiple signals.

A measure of caution is necessary in computing the parameters of pulse trains obtained from gates. Intermediate signals fed into a gate will be correlated if they contain a common term derived from a common signal. For example, consider the case of two signals, x_1 and x_2, fed into an "AND" gate. The output of the "AND" gate is correlated with both x_1 and x_2. If the product term, $x_1 x_2$, is fed to an "AND" gate with either x_1 or x_2, the output of the second "AND" gate is $x_1 x_2$, and the absolute duty cycle of the second "AND" gate is the same as the first. If the product signal were uncorrelated with its two constituent terms, we would get $x_1^2 x_2$ or $x_1 x_2^2$ as the "AND" gate output, whereas, in fact, we get $x_1 x_2$.

3. OPERATIONS ON PULSE DENSITY SIGNALS

The ultimate utility of pulse density signals depends on whether we can operate on the various parameters of a given signal and on whether we can combine two pulse density signals to produce a third signal whose parameters are a specific mathematical function of the corresponding parameters of the two given signals, With methods of performing addition, subtraction, multiplication, division, integration, differentiation, and sign testing, it should be possible to perform in pulse density any calculation that can be per'formed with an analog computer. Of course, the desirability of performing analog computations with pulse density signals would depend on such factors as attainable precision and relative costs. These other factors will not be discussed here.

3.1 Gating Logic

Assuming uncorrelated signals, we can compute the output of various logic gates using the formulas for intersection and complementation which were developed in Section 2.4 and de Morgan's law. We have compiled in Table 1 the results of feeding two pulse density signals into all 16 of the possible types of two-input gates. These gates correspond to the 16 possible Boolean functions of two variables. Results are shown only for the two duty cycle parameters. Pulse densities corresponding to these can be obtained using formulas 2:9 and 2:10. For Table 1, we have assumed that signal x_1 is fed to the a side of the gates and signal x_2 is fed to the b side of the gates. The left hand column of the table is the equivalent binary state vector, $S = (s_{11}, s_{10}, s_{01}, s_{00})$, obtained by expanding the Boolean functional $s_{ij} x_1^{\,i} x_2^{\,j}$ according to the convention established earlier by Gilstrap (Ref. 2). The second column gives the gating function in familiar Boolean notation.

Table 1. Pulse Density Code Signal Mixing Produced by Two-Input Gating Logic

Binary Logic State	Gating Logic	Output of Gates	
$S=(s_1, s_2, s_3, s_4)$	$s_{ij} a^i b^j$	W-parameter	Z-parameter
0000	ϕ	0	- 1
0001	$\overline{a \cup b}$	$1-W_1 - W_2 + W_1 W_2$	$\frac{1}{2}(Z_1 Z_2 - Z_1 - Z_2 - 1)$
0010	$\bar{a}b$	$W_2 - W_1 W_2$	$\frac{1}{2}(-Z_1 Z_2 - Z_1 + Z_2 - 1)$
0011	$\bar{a}$	$1-W_1$	$-Z_1$
0100	$a\bar{b}$	$W_1 - W_1 W_2$	$\frac{1}{2}(-Z_1 Z_2 + Z_1 - Z_2 - 1)$
0101	$\bar{b}$	$1-W_2$	$-Z_2$
0110	$a\bar{b} \cup \bar{a}b$	$W_1 + W_2 - 2W_1 W_2$	$-Z_1 Z_2$
0111	$\bar{a} \cup \bar{b}$	$1-W_1 W_2$	$\frac{1}{2}(-Z_1 Z_2 - Z_1 - Z_2 + 1)$
1000	ab	$W_1 W_2$	$\frac{1}{2}(Z_1 Z_2 + Z_1 + Z_2 - 1)$
1001	$ab \cup \bar{a}\bar{b}$	$2W_1 W_2 - W_1 - W_2 + 1$	$Z_1 Z_2$
1010	b	W_2	Z_2
1011	$\bar{a} \cup b$	$1 - W_1 + W_1 W_2$	$\frac{1}{2}(Z_1 Z_2 - Z_1 + Z_2 + 1)$
1100	a	W_1	Z_1
1101	$a \cup \bar{b}$	$1 - W_2 + W_1 W_2$	$\frac{1}{2}(Z_1 Z_2 + Z_1 - Z_2 + 1)$
1110	$a \cup b$	$W_1 + W_2 - W_1 W_2$	$\frac{1}{2}(-Z_1 Z_2 + Z_1 + Z_2 + 1)$
1111	1	1	+1

3.2 Proportional Signal Mixing

There is a simple and very useful generalization of the logic gating that was developed above. The state vector above was assumed to be a constant, binary number. If we take a completely general, programmable two-input gating logic and introduce four independent pulse density signals instead of the four constants for the state vector, then we can obtain a large family of algebraic functions of the pulse width parameters.

Thus, for the gating shown in Figure 1, we see that

$$W = s_1 W_1 W_2 + s_2 W_1 (1-W_2) + s3 (1-W_1) W_2 + s_4 (1-W_1)(1-W_2)$$

$$= (s_1 - s_2 - s_3 + s_4) W_1 W_2 + (s_2 - s_4) W_1 + (s_3 - s_4) W_2 + s_4 \quad \ldots 3:1$$

Letting

$$s_4 = A_0$$

$$s_2 - s_4 = A_1$$

$$s_3 - s_4 = A_2$$

$$s_1 + s_2 + s_3 + s_4 = A_3$$

we obtain

$$W_3 = A_0 + A_1 W_1 + A_2 W_2 + A_3 W_1 W_2 \quad \ldots\ldots\ldots\ldots\ldots 3:2$$

Similarly, for the Z-parameter of the two input signals, we obtain

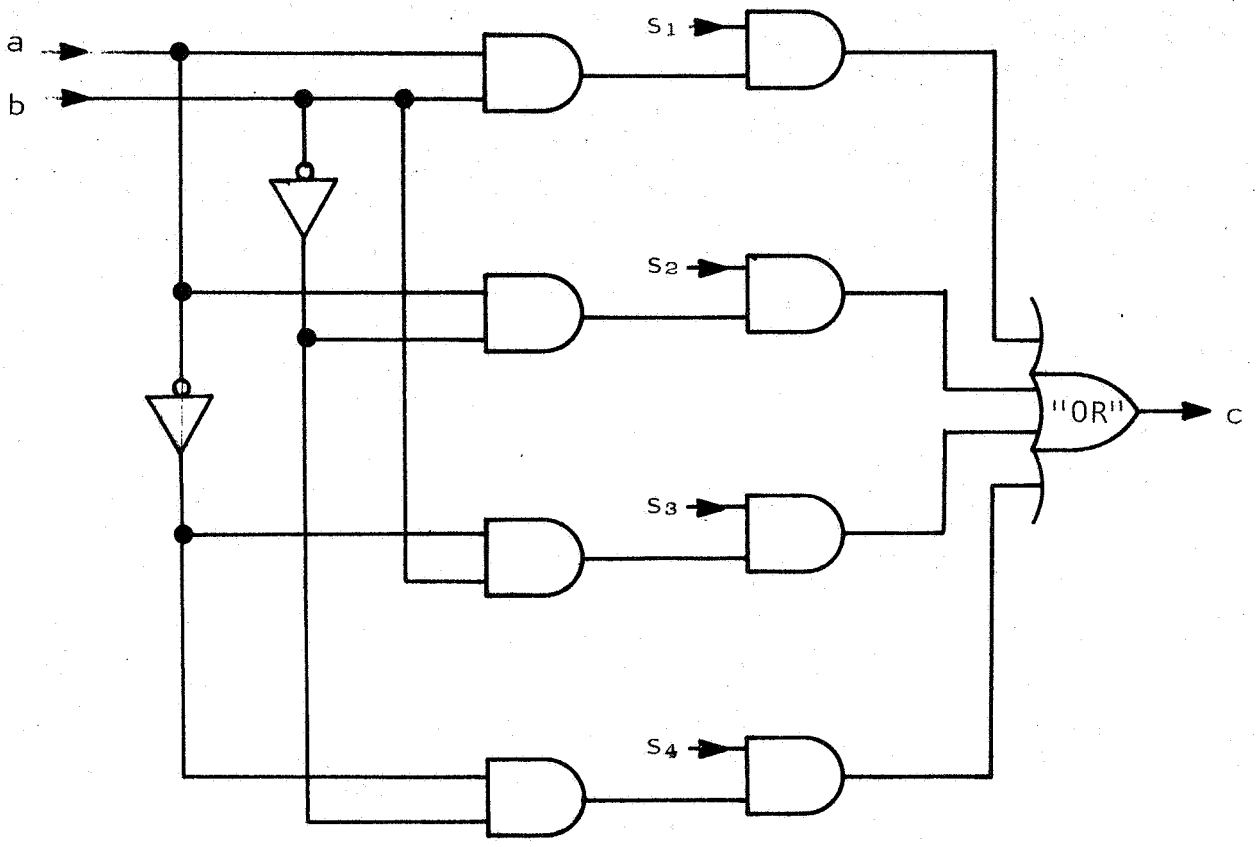

(a) Logic Diagram

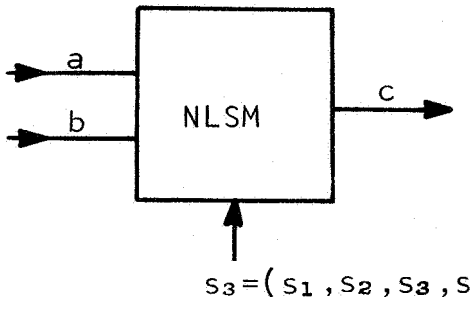

(b) Block Diagram Notation for

Figure 1. Nonlinear Signal Mixer Gating

$$Z_3 = \tfrac{1}{2}s_1(-Z_1Z_2+Z_1+Z_2-1) + \tfrac{1}{2}s_2(Z_1Z_2+Z_1-Z_2-1) +$$
$$\tfrac{1}{2}s_3(Z_1Z_2-Z_1+Z_2-1) + \tfrac{1}{2}s_4(-Z_1Z_2-Z_1-Z_2-1)$$
$$= \tfrac{1}{2}\left[(-s_1+s_2+s_3-s_4)Z_1Z_2 + (s_1+s_2-s_3-s_4)Z_1 + \right.$$
$$\left.(s_1-s_2+s_3-s_4)Z_2 - (s_1+s_2+s_3+s_4)\right] \quad \text{..... 3:3}$$

Letting

$$a_0 = -\tfrac{1}{2}(s_1+s_2+s_3+s_4)$$

$$a_1 = \tfrac{1}{2}(s_1+s_2-s_3-s_4)$$

$$a_2 = \tfrac{1}{2}(s_1-s_2+s_3-s_4)$$

$$a_3 = \tfrac{1}{2}(-s_1+s_2+s_3-s_4)$$

we obtain

$$Z_3 = a_0 + a_1Z_1 + a_2Z_2 + a_3Z_1Z_2 \quad \text{..... 3:4}$$

Thus, we can observe that the operations necessary for non-linear signal mixing are obtained directly from the gating logic that was referred to in an earlier report as "the Neurotron Main Logic Gating", with the proviso that all variables lie in the -1 to +1 range. (Ref. 1)

3.3 Counters

A counter can be used to count or integrate pulses in a pulse train. There are several ways to employ counters in this capacity:

1. The pulses in the signal can be fed directly to a counter which can be set either to
   a. run continuously, incrementing the counter by one for each occurrence of a pulse, or

b. be reset at the end of each observation interval, T:

2. the pulses can be sampled during an interval of time that is very short in comparison *to* the minimum expected pulse width; the counter may then be:

a. run continuously, incrementing the counter with each joint occurrence of a clock pulse and a signal pulse.

b. incremented at each clock pulse if the signal level is "one" and decremented if the signal level is "zero".

The above methods of using counters to count or integrate pulses have varying counter contents as a function of time. Since the maximum number of pulses that can be seen in an observation interval is n_m (by previous assumption), we can normalize the counter contents to obtain a quantity on the same scale as the input pulse train parameters. Thus, if we let $n(t)$ = number in the counter at time t, and n_s = maximum number of steps in the counter, then n/n_s has the same scale as the Z-parameter of the input, provided we have a two-way counter and are sampling as in Case 2b, above. With appropriate normalization for the four cases, above, we can obtain the parameters of the counter contents.

Letting W_o and Z_o be the W- and Z-parameters of the output signal (i.e. the counter contents), respectively, and letting X_i, W_i, and Z_i be the X-, W- and Z-parameters, respectively, of the input to the counter, we obtain:

1a. $$W_o = \left(\frac{n_m}{n_s}\right) \cdot \frac{1}{T} \int_c^t X_i \, dt \quad \text{.....} \quad 3:5$$

Set $\left(\frac{n_m}{n_s}\right) = k_1$, then

$$W_o = k_1 \cdot \frac{1}{T} \int_o^t X_i \, dt \text{ or } \dot{W}_o = k_1 \left(\frac{1}{T}\right) X_i \quad \text{.....} \quad 3:6$$

1b. $W_o = k_1 X_i$, at end of each interval T 3:7

2a. $W_o = \frac{k_1 k_2}{T} \int_o^t W_1 \, dt$ or $\dot{W}_o = \frac{k_1 k_2}{T} W_1$ 3:8

2b. $Z_o = \int_o^t \frac{k_1 k_2}{T} Z_1 \, dt$ or $\dot{Z}_o = \frac{k_1 k_2}{T} Z_1$ 3:9

Figure 2. shows the block diagram of functional blocks which perform equivalent functions of the finite counter in Case 2b.

It is clear that further utilization of counter contents may require conversion of the binary count to a pulse density signal. This conversion can be accomplished by first converting the normalized counter value to an analog signal? which can then be used to control a statistical source. The statistical source is a device which puts out pulses at random times. The pulse density or duty cycle of the device are determined by an input control signal.

The combination of sampling logic and necessary clock signal, finite counter, and statistical source is termed a statistical decision device (SDD). The SDD is so named because: the algebraic sign of the counter contents is the same (most of the time) as the algebraic sign of the input signal, and the relative duty cycle of the statistical source is a measure of how confident we are of the correctness of the equivalence of sign.

There is a simpler alternative in recoding counter contents as a pulse train. If the counter contents are fed to a digital to analog converter and the upper limit level set to correspond to the "one" voltage and the lower limit level set to correspond to the "zero" voltage, then the resulting analog signal can be viewed as a multilevel pulse density code. The Z-parameter of the resulting signal bears a relationship to the Z-parameter of the input signal which depends on the variations in the input Z.

For example, suppose that the Z-parameter of the input signal can be expressed as

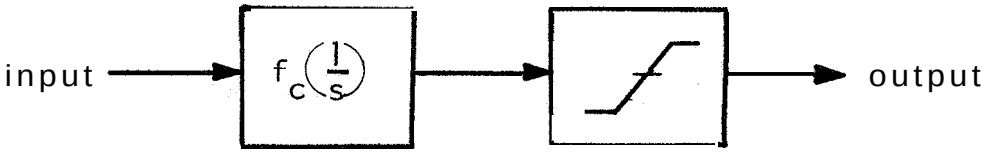

(Note: Limiter cut-off determined by number of stages in counter and by parameters of counter-to-pulse density converter)

Figure 2. Equivalent Functions for the Finite Counter

$$Z_1 = a_o + a_1 \sin 2\pi f_z t \quad \ldots\ldots\ldots\ldots\ldots\ldots\ldots \quad 3:10$$

Further, let a_o vary slowly with time:

$$a_o = a_o(t)$$

To be explicit, assume that T is the observation interval, f is the frequency of the pulse density signal, and f_a the frequency at which a_o varies. Then, let

$$\frac{1}{f} << T << \frac{1}{f_z} << \frac{1}{f_a}$$

The ratio of successive time constants is, say, 10 or 100 to 1. Under these assumptions, we can easily show that the Z-parameter of the output becomes

$$Z_o = \frac{2}{\pi} \sin^{-1} (a_o/a_1) \quad \ldots\ldots\ldots\ldots\ldots\ldots\ldots\ldots 3:11$$

Proof follows readily from the fact that the duty cycle of the output is equal to the ratio of the time the signal is positive to the total time it is observed. For simplicity, this interval can be set exactly to one cycle of the f_z signal. Then the time the signal is positive depends on the bias level, a_o, and on the amplitude of the sine wave:

$$W = \frac{\pi + 2 \sin^{-1} (a_o/a_1)}{2\pi} = \frac{1}{2} + \frac{1}{\pi} \sin^{-1}(a_o/a_1) \quad \ldots\ldots 3:12$$

From this we get

$$Z = 2W - 1 = \frac{2}{\pi} \sin^{-1}(a_o/a_1) \quad \ldots\ldots\ldots\ldots\ldots\ldots \quad 3:13$$

Equations 3:12 and 3:13 do not hold for complex waveforms and no general rule can be devised for the slow variation case.

if the input to a counter is varying in sign at a speed greater than the reciprocal of the observation interval, then the counter acts as a transport lag.

$$Z_o(t) = Z_i(t-\Delta t) \quad \text{3:14}$$

where Δt is approximately equal to the total number of steps in the counter times the sampling period.

3.4 Mathematical Function Mechanization

Since pulse density codes are, in engineering terms, merely carriers of analog-variable information, one is immediately directed toward possible methods of achieving ordinary, mathematical operation on the information conveyed by a pulse density code. The two "natural" operations on pulse codes are rnultiplication and integration, in that these two operations can be achieved with relatively few components. The following is a summary of digital circuit mechanizations of the basic mathematical operations of addition, subtraction, rnultiplication, division, integration, and differentiation. In addition to these basic mathematical operations, the logical operation of sign detection is frequently desirable. This latter operation is the same as a threshold detector and is often used in adaptive systems. The elementary threshold detector is a special case of the statistical decision maker (Ref. 3). Together, these operations of (+, -, x, $\div$, $\int$, $\frac{d}{}$,) constitute a very powerful repertoire from which almost any desired linear or nonlinear function, mathematical or logical, can be constructed.

3.4.1 Addition and Subtraction

Addition can be derived directly from the generalized Boolean function of two variables. For an arbitrary Boolean function of two variables, we know that

$$y = s_{ij} x_i^i x_j^j \quad \text{3:15}$$

The decoding theorem for pulse density is that the density W_3 is equal to the number of "ones" over a unit time. Since the four minterms, $x_1^{i} x_2^{j}$, are independent, it is clear that the $s_{ij} x_1^{i} x_2^{j}$ are likewise independent. Hence, we can properly add the individual minterms multiplied by their respective coefficients. To this we must add that if $x_2 = x_1'$, then in terms of pulse density

$$W_2 = 1 - W_1 \qquad \text{3:16}$$

Thus, for a pulse density coded signal, we have

$$W_3 = s_1 W_1 W_2 + s_2 W_1 (1-W_2) + s_3 (1-W) W_2 + s_4 (1-W_1)(1-W_2) \qquad \text{3:17}$$

where

$$s_1 \rightarrow s_{11}$$

$$s_2 \rightarrow s_{10}$$

$$s_3 \rightarrow s_{01}$$

$$s_4 \rightarrow s_{00}$$

and where "→" is read "corresponds to", for an arbitrary functional.

From the above, we have

$$W_3 = (s_1 - s_2 - s_3 + s_4) W_1 W_2 + W_1 (s_2 - s_4) + W_2 (s_3 - s_4) + s_4 \qquad \text{3:18}$$

For a pure addition,

$$s_4 = 0$$

$$s_1 - s_2 - s_3 = 0$$

$$s_2 = s_3$$

or

$$s_2 = s_3, \; s_4 = 0, \; s_1 = -(s_2 + s_3), \; s_1 = 1, \; s_2 = s_3 = \tfrac{1}{2}$$

From these relationships, we have

$$w_3 = \tfrac{1}{2}(W_1 + W_2) \quad \text{3:19}$$

In terms of the Z-parameter, we have

$$Z_3 = \tfrac{1}{2}(Z_1 + Z_2) \quad \text{3:20}$$

And, in terms of gating logic, we have

$$c = ab \cup (\tfrac{1}{2})(ab' \cup a'b) \quad \text{3:21}$$

as shown in Figure 3. Since complementation implies negation for the Z-parameter, we see that subtraction can be achieved by complementing the variable of interest prior to adding. As a matter of detail, we note a $\frac{1}{2}$ for the W-parameter is the same as a "zero" for the Z-parameter.

We summarize addition and subtraction as follows: the logical gating circuitry is as shown in Figure 3a. Addition and subtraction we denote symbolically by means of a box with signed inputs as shown in Figure 3b. In the case of subtraction, the variable must be complemented prior to introduction into the addition or summation box. The extension to n variables is simple, but there appears to be no hardware savings achieved by adding n terms at once over adding them pairwise.

3.4.2 Multiplication

Multiplication of W-parameters is achieved using an ordinary "AND" gate. Multiplication of Z-parameters is achieved with

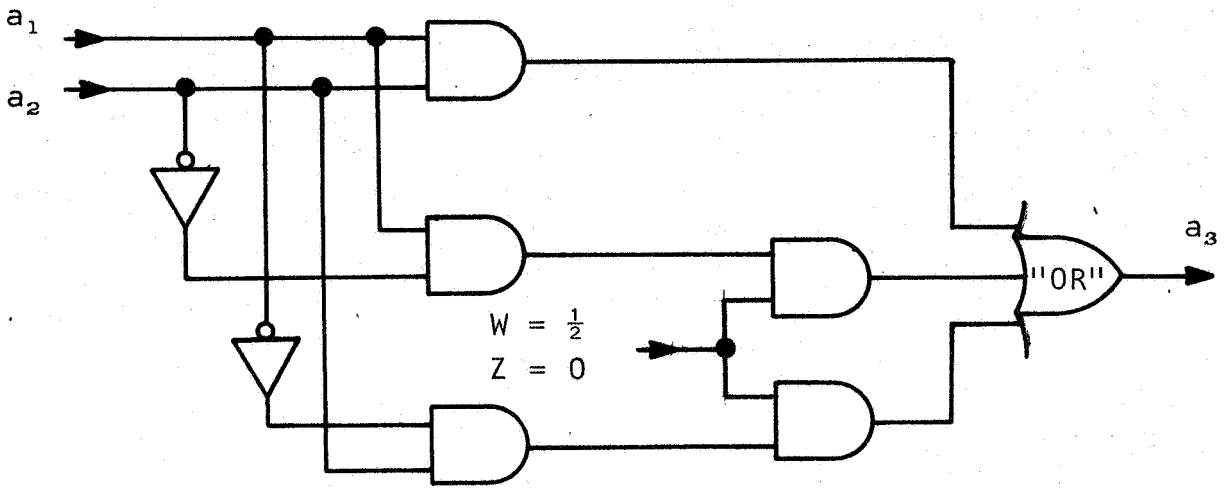

(a) Logic Gating for Addition

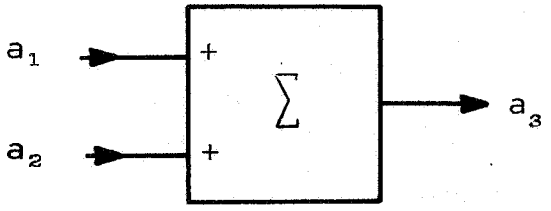

For two inputs: $Z_3 = \frac{1}{2}(Z_1 + Z_2)$

For n inputs; $Z_{n+1} = \frac{1}{n}\left(\sum_{i=1}^{n} Z_i\right)$

(b) Notation for Addition for Block Diagrams

Figure 3. Gating Logic and Block Diagram Symbol for Addition of Pulse Density Signals.

a complemented "exclusive OR", i.e., by gating of the form

$$c = ab + a'b' \quad \text{3:22}$$

Figure 4 indicates the notation for multiplication. The contents of M depend upon whether we choose to multiply the W-parameter or the Z-parameter.

3.4.3 Division

Division cannot be achieved directly by gating logic, since it is nonconservative with respect to the (0, 1) or (-1, +1> range. However we can achieve division by nulling the error of multiplication:

if

$$c = \frac{a}{b} \quad \text{3:23}$$

then

$$a = bc \quad \text{3:24}$$

Hence, after transients have subsided, the circuit in Figure 5a has an output that is the ratio of its two input variables. To prove this, let

$$a = bc^* \quad \text{3:25}$$

if

$$a - bc^* = 0 \quad \text{3:26}$$

then

$$c = c^* \quad \text{3:27}$$

The error, E, drives the register, r, up until the product of its output with b is equal to a. Note that even if the register

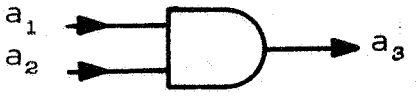

$$W_3 = W_1 W_2$$

(a) Gating Logic for Multiplication of W-parameters of Pulse Codes.

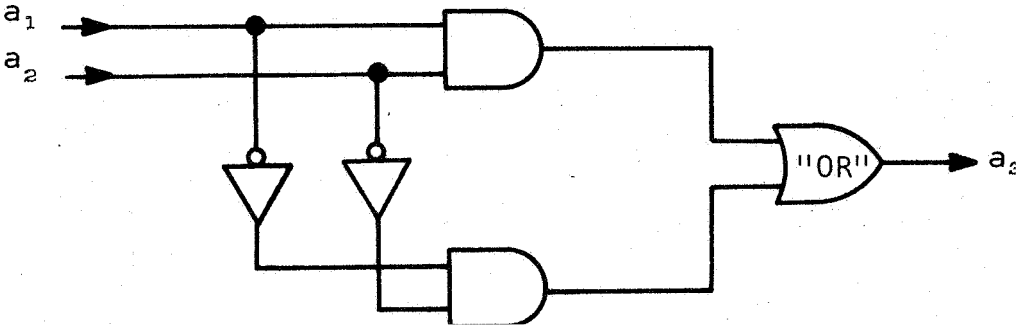

$$Z_3 = Z_1 Z_2$$

(b) Gating Logic for Multiplication of Z-parameters of Pulse Codes.

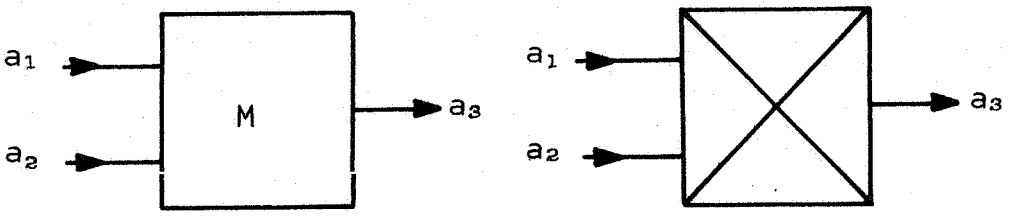

(c) Alternative Block Diagram Notations for Multiplication

(Note: Gating Logic in M depends on desired parameter, as indicated above.)

Figure 4. Gating Logic and Block Diagram Symbols for Multiplication of Pulse Density Signals.

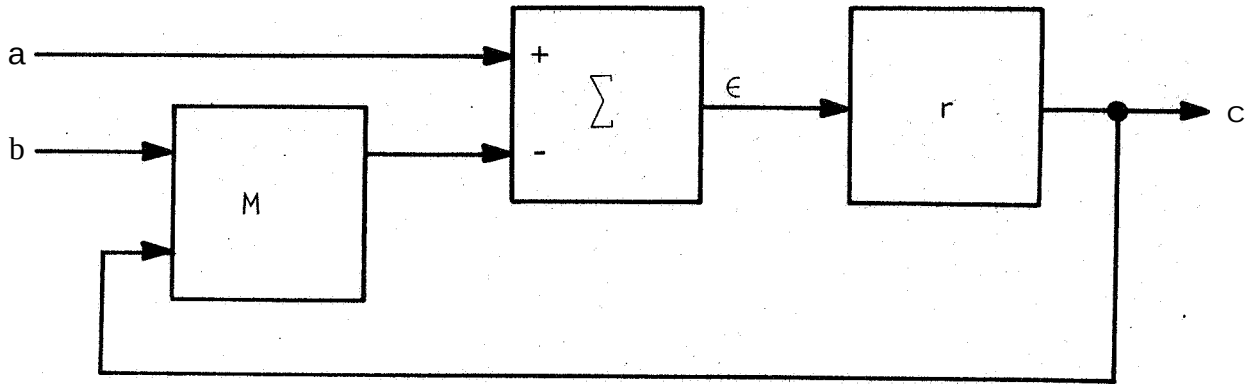

(a) Logic Diagram for Division of Pulse Density Signals

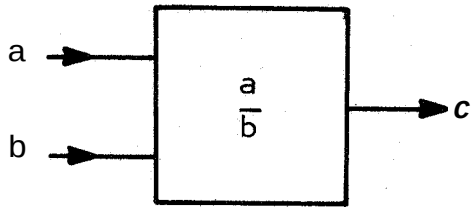

(b) Block Diagram Notation for Pulse Density Signal Divider

Figure 5. Gating Logic and **Block** Diagram **Symbol** for Division of Pulse Density Signals

Is accurate to, say, one part in 16, that the integrated value of c may be more accurate, since r will tend to oscillate between two levels if a lies between these two, provided that the period of integration (decoding period) for the pulse code is much longer than the clock period for the register.

We will denote division by a functional box, as shown in Figure 5b.

3.4.4 Integration

Integration is accomplished naturally by a two-way, up-down counter as we indicated in Section 3.2. However, for a true integration, the sampling clock must run at the same speed as the incoming pulse train. This is difficult to accomplish if the pulse density signal is asynchronous with the clock.

While the content of the counting register is a number equal or proportional to the integral of the incoming signal, it is in number form. Hereafter, we will assume that a binary-to-pulse density converter is always a part of any integrator so that the integral is available as another pulse density signal, as indicated in Figure 6.

It is essential for a true integration that the clock frequency of the counter input logic be equal to the pulse repetition rate of the input signal. Otherwise, the counter value would merely be proportional to, but not equal to, the integral of the input signal. Also it is necessary for the digital-to-pulse density converter to have a linear transfer function, since this function will have as its argument the counter contents

3.4.5 Differentiation

Differentiation cannot be achieved in a direct manner. The simplest method of achieving differentiation is by an inverse

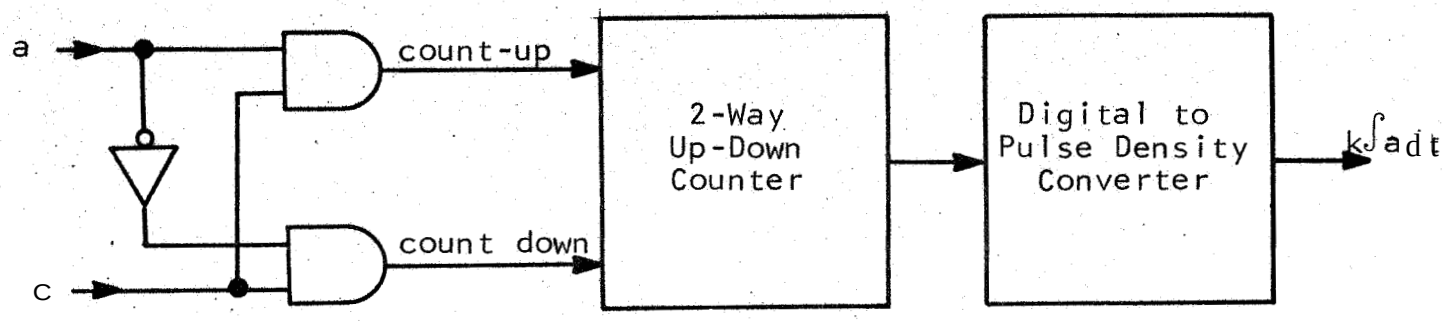

(a) Logic Required for a Pulse Density Signal Integrator

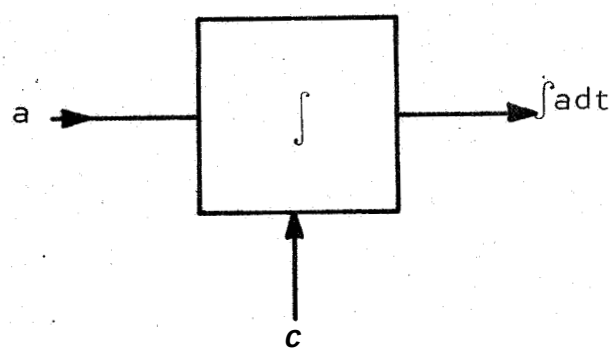

(b) Notation for Integration in Logic Diagrams

Figure 6. Gating Logic and Block Diagram Symbol for integration

integration. From Figure 7, and from the usual rule for feedback systems, we have

$$\frac{\dot{x}^*(s)}{x(s)} = \frac{\frac{k}{s}}{1+\frac{k}{s^2}} \qquad \text{3:28}$$

$$= \frac{ks}{s^2+k} \qquad \text{3:29}$$

or

$$\frac{\dot{x}^*(s)}{x(s)} = \frac{s}{1+\frac{s^2}{k}} \qquad \text{3:30}$$

As k becomes large, for bounded s

$$\frac{s^2}{k} \to 0 \qquad \text{3:31}$$

so that

$$\frac{\dot{x}^*(s)}{x(s)} \simeq s \qquad \text{3:32}$$

or

$$\dot{x}^* \simeq \dot{x} \qquad \text{3:33}$$

It is apparent that there is a relationship between k and an observation period, T. By selecting k sufficiently large, modulation frequencies above $\frac{1}{T}$ will be negligible and the approximation should be fairly good.

3.4.6 Lead-Lag Filtering

The equivalent of lead-lag filtering of input signals can be achieved with a modification of the circuitry required for integration and differentiation. For the filter whose Laplace transform is

$$\frac{1+\tau_1 s}{14\text{-}72 s}$$

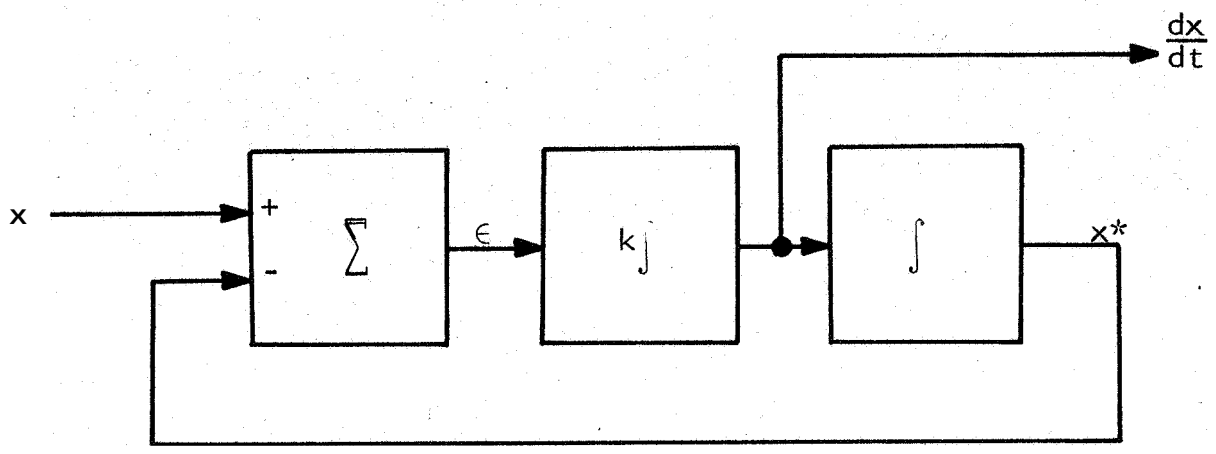

(a) Logic for Differentiation

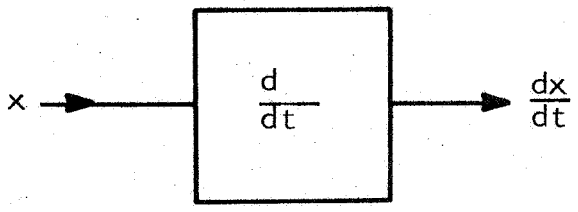

(b) Block Diagram Symbol for Differentiation

Figure 7. Gating Logic and Block Diagram Symbol for Differentiation of Pulse Density Signals.

we know that

$$y(s) = \frac{1+\tau_1 s}{1+\tau_2 s} x(s) \quad \text{..... 3:34}$$

or

$$y + \tau_2 \dot{y} = x + \tau_1 \dot{x} \quad \text{..... 3:35}$$

Integrating both sides of the equation, we obtain

$$\int y dt + \tau_2 y = \int x dt + \tau_1 x \quad \text{..... 3:36}$$

Since the above functions are all easily mechanized, the lead-lag filter can be obtained as shown in Figure 8.

3.4.7 Sign Detection

Sign detection in a pulse density code is complicated by the fact that pulse occurrence is random, rather than regular. Pulse width modulation codes are an exception to this rule, and sign detection in a pulse width code requires conversion to analog with sign detection being performed in the analog domain. However, a counter can be used to detect the sign of a random, pulse density signal as discussed in Section 3.3. Since, on the average, the count rate of a counter fed by a pulse density signal is proportional to the value of the W-parameter, then a counter will, on the average, have as its contents a number of the same sign as the input signal. Short run statistics can, of course, produce a reversal of sign in a counter, but the greater the maximum number the register can hold, the less likely that the counter will have an incorrect sign. We will denote a sign detector as indicated in Figure 9.

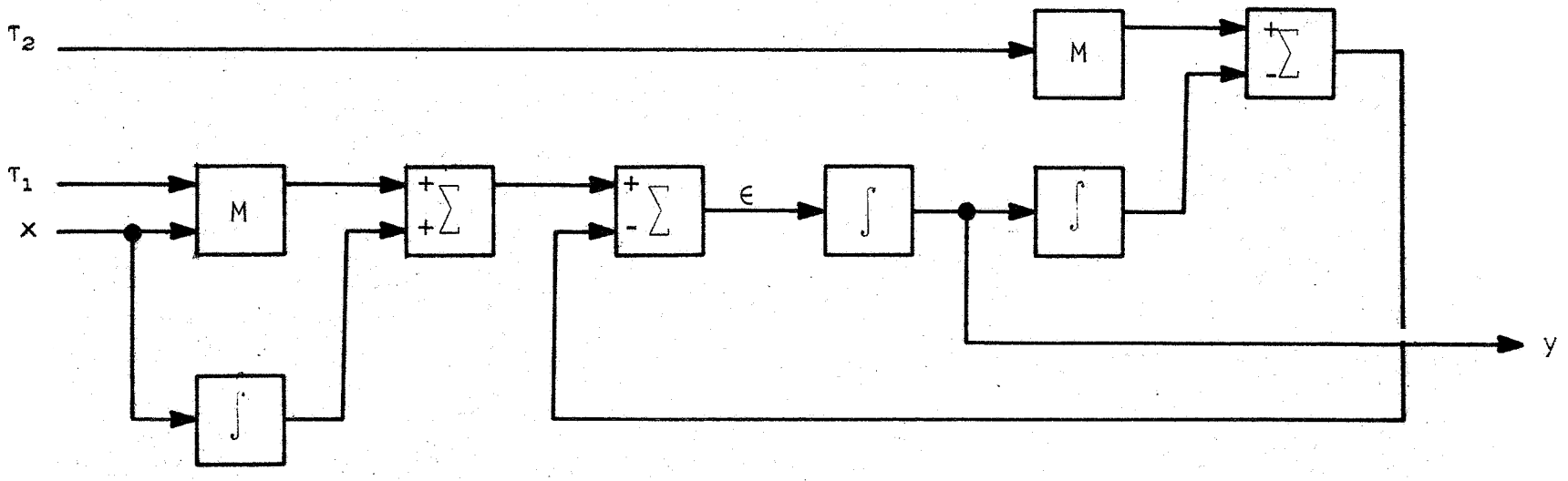

$$y(s) = \frac{1+\tau_1 s}{1+\tau_2 s} X(s)$$

Figure 8. Lead-Lag Filtering with Pulse Density Signals

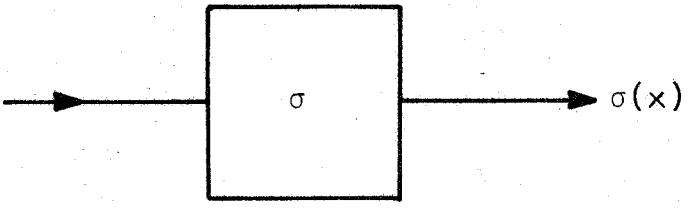

Figure! 9. **Notation** for **a** Sign Detector

4. EFFECTS OF UNBIASED NOISE

We define unbiased noise pulses as a number (per unit time) of "incorrect" pulses with the property that (in Z-parameter terms)

$$\lim_{T\to\infty} \int_0^T n\,dt = 0$$

where

n is +1 if the noise pulse is positive
-1 if the noise pulse is negative

i.e., the average number of incorrect pulses with positive sign equals the average number of incorrect pulses with negative sign, independent of the value of the signal.

If f is the fraction of noise pulses (of either sign) out of the total number of pulses per unit time, then

$$\text{'(signal + Noise)} - \text{'(signal)} \quad (1 - 2f) + f$$

and

$$\text{'(signal + noise)} - \text{'(signal)} \quad (1 - 2f)$$

In other words, noise merely serves to attenuate a signal, but does not change the sign of the Z-parameter, provided the signal-to-noise ratio is less than unity. In terms of signal-to-noise ratio, s/n, we note that

$$f = \frac{n}{s+n} = \frac{1}{1+s/n}$$

$$\text{'(signal + noise)} - \text{'(signal)} \quad \left(\frac{s/n-1}{s/n+1}\right)$$

5. THE PSV ALGORITHM

The algorithm for the incremental **PSV** system is a general scheme among many for learning machines. In this section we will analyze the algorithm under the assumption of infinitely long p and u registers. Although this assumption is not valid for the self-organizing controller, it *is* included here for completeness.

5.1 Differential Equations

The **PSV** algorithm is easily stated in terms of the operations on pulse codes. Figure 10 shows the general flow of signals in the **PSV** module. As it is configured, the logic preceding the p register is the same as the **MULTIPLY** operation for the Z-parameter **of** a pulse density code. Hence, the **PSV** can be described by two equations:

$$\dot{u} = k_2 f(p) \quad \text{.....} \quad 5:1$$

$$\dot{p} = k_1 v\dot{u} \quad \text{.....} \quad 5:2$$

where k_1 and k_2 are proportional to the clock rates in the sampling gates for the counters. The function, $f(p)$, depends on the transfer function of the converter from the binary number, p, to pulse density signals. To a fair approximation, the transfer function of the statistical source *is*

$$f(p) = k \tan\left(p/p_{max}\right) \quad \text{.....} \quad 5:3$$

where

p_{max} = maximum number in the p register

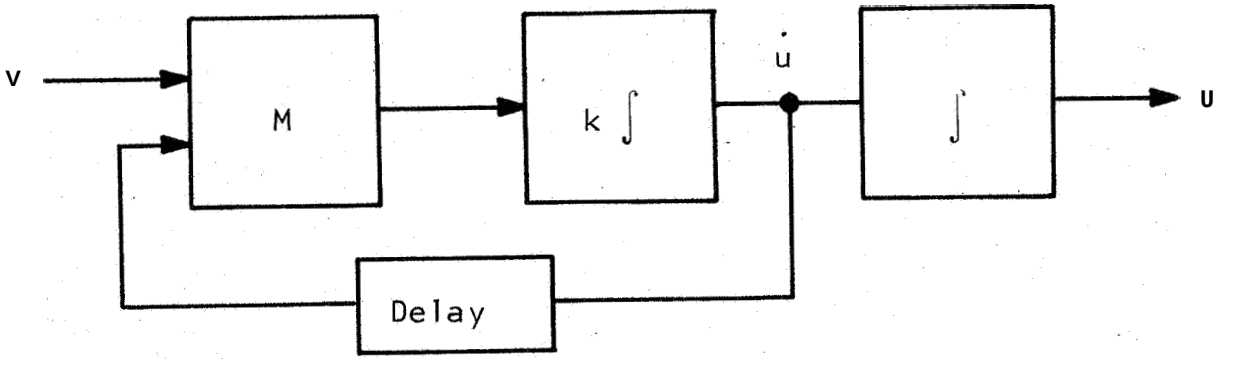

Figure 10. PSV Algorithm Flow Design

. k = scale factor dependent on the bias voltage in the statistical source.

If the statistical source is replaced by a sign detector, then

$$f(p) = \sigma(p) = \sigma\left(p/p_{max}\right) \quad \text{.....} \quad 5:4$$

where $\sigma(\ )$ denotes the signum or sign function. Although not greatly realistic, we could set

$$f(p) = kp/p_{max} \quad \text{.....} \quad 5:5$$

i.e., use a linear function, to get an idea of the general character of the solution.

A variation on the basic PSV algorithm is shown in Figure 11. Tentatively, we have concluded this circuit can be analyzed as follows:

Let $\dot{u}_i$ = count rate for the u register at instant of time i

υ_{i+1} = count rate for the u register at instant of time $i+1$

Assume that the delay is one unit of time. Then

$$\dot{u}_{i+1} = kv_i\dot{u}_i$$

where k is dependent on the clock rate. But

$$\dot{u}_{i+1} = \dot{u}_i + \ddot{u}_i\tau$$

where

τ = delay time

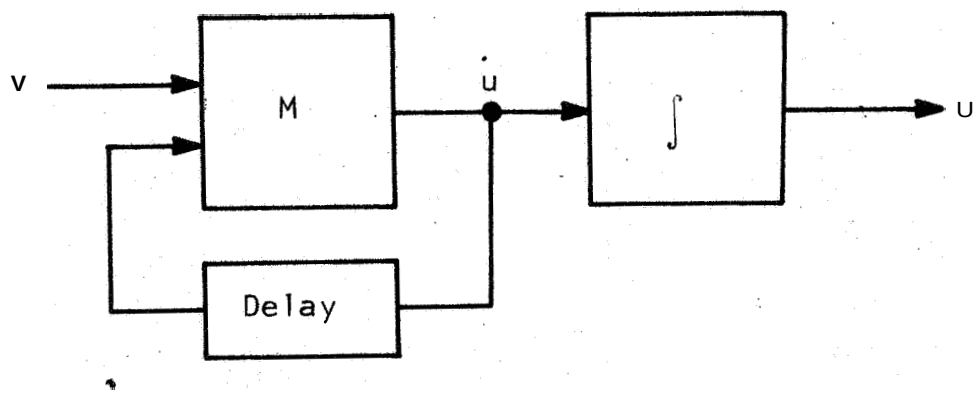

Figure 11. Deterministic Model of the PSV.

Hence

$$\dot{u}_i + \ddot{u}_i \tau = k v_i u_i$$

$$u_i = \frac{k v_i - 1}{\quad} \cdot \qquad 5:6$$

5:2 Open-Loop Solutions

If the dependence of v on u is neglected, we get the open-loop solutions for the PSV. Taking first the linearized PSV, we have from Equations 5:1, 5:2, and 5:5 (assuming long registers)

$$\dot{u} = ka \cdot kp/p_{max} \qquad \ldots\ldots\ldots\ldots\ldots\ldots \quad 5:7$$

$$\dot{p} = k_1 v \dot{u} \qquad \ldots\ldots\ldots\ldots\ldots\ldots 5:8$$

From Equation 7:8

$$p = k_1 v u + p_o \qquad \ldots\ldots\ldots\ldots\ldots\ldots 5:9$$

Hence,

$$\dot{u} = \frac{k_2 k}{P_{max}} (k_1 v u + p_o) \qquad \ldots\ldots\ldots\ldots\ldots\ldots 5:10$$

or

$$\dot{u} = \frac{k k_1 k_2 v}{p_{max}} \left(u + \frac{p_o}{k_1 v}\right) \qquad \ldots\ldots\ldots\ldots\ldots\ldots 5:11$$

$$\frac{u}{u + \frac{p_o}{k_1 v}} = \frac{k k_1 k_2 v}{p_{max}} \qquad \ldots\ldots\ldots\ldots\ldots\ldots \quad 5:12$$

$$\ln\left(u + \frac{p_o}{k_1 v}\right) = \frac{k k_1 k_2 v}{p_{max}} t + \ln u_o \qquad \ldots\ldots\ldots\ldots\ldots 5:13$$

$$u = -\frac{p_o}{k_1 v} + u_o e^{\frac{k k_1 k_2 v}{P_{max}}} \qquad \ldots\ldots\ldots\ldots\ldots 5:14$$

Since v is the sign of a variable, then

$$\frac{1}{v} \equiv v \qquad \text{.....5:15}$$

and, hence

$$u = -\frac{p_o v}{k_1} + u_o e^{\frac{k k_1 k_2 v}{p_{max}}} \qquad \text{..... 5:16}$$

From Equation 5:16 we can observe that us is an exponential function that builds up or decays according to whether v is positive or negative, respectively.

The PSV with a tangent approximation for the statistical source transfer function can also be solved in the open-loop case:

$$\dot{u} = k_2 \tan p/p_{max} \qquad \text{..... 5:17}$$

$$\dot{p} = k_1 v \dot{u} \qquad \text{..... 5:18}$$

or

$$p = k_1 v u + p_o \qquad \text{.....5:19}$$

$$\dot{u} = k_2 \tan\left(\frac{k_1 v u + p_o}{Pmax}\right) \qquad \text{.....5:20}$$

$$\frac{k_1 v \dot{u}/p_{max}}{\tan\left(\frac{k_1 v u + p_o}{p_{max}}\right)} = \frac{k_1 k_2 v}{Pmax} \qquad \text{..... 5:21}$$

$$\ln \sin\left(\frac{k_1 v u}{Pmax} + \frac{p_o}{p_{max}}\right) = \frac{k_1 k_2 v}{Pmax} t + \ln A \qquad \text{.....5:22}$$

$$\frac{k_1 v u}{p_{max}} + \frac{p_o}{p_{max}} = \sin^{-1}\left[A e^{\left(\frac{k_1 k_2 v t}{Pmax}\right)}\right] 1 \qquad \text{.....5:23}$$

$$u = -\frac{p_o v}{k_1} + \frac{p_{max} v}{k_1} s_{in}^{-1}\left[Ae^{\left(\frac{k_1 k_2 v t}{p_{max}}\right)}\right] \quad \text{..... 5:24}$$

The case of $f(p) = \sigma(p) = \sigma\left(p/p_{max}\right)$ can likewise be treated in the open-loop case:

$$\dot{u} = k_2 \sigma\left(p/p_{max}\right) \quad \text{..... 5:25}$$

$$\dot{p} = k_1 v \dot{u} \quad \text{..... 5:26}$$

$$p = k_1 v u + p_o \quad \text{..... 5:27}$$

$$u = k_2 \sigma\left(\frac{k_1 v u + p_o}{p_{max}}\right) \quad \text{..... 5:28}$$

If we set

$$p_o = 0$$

then

$$\dot{u} = k_2 \sigma\left(\frac{k_1 v u}{p_{max}}\right) \quad \text{..... 5:29}$$

Since v is a a-function,

$$\dot{u} = k_2 v \sigma\left(\frac{k_1 u}{p_{max}}\right) \quad \text{..... 5:30}$$

From Section 3.3, we know that the σ function decodes as the time integral of the Y-parameter of the input signal. Hence, the statistical Source merely serves to convert a pulse width modulation to a pulse density. The final u register converts the pulse density back to a multilevel pulse width modulation. Since k_1 and p_{max} are both positive, we have

$$\dot{u} = k_2 v \sigma(u) \quad \text{..... 5:31}$$

and

$$\sigma(u) = \frac{1}{\tau} \int u\,dt = u \qquad \ldots\ldots\ldots\ldots\ldots\ldots \quad 32$$

Hence

$$\dot{u} = k_2 v u \qquad \ldots\ldots\ldots\ldots\ldots\ldots \quad 5:33$$

$$u = u_o e^{k_2 v t} \qquad \ldots\ldots\ldots\ldots\ldots\ldots \quad 5:34$$

Finally, the statistical source removal equation is similar to the linearized case and can **be solved as** follows:

From Equation 5:6 we have (assuming long counters)

$$\ddot{u}_i = \frac{kv_i - 1}{\tau} \dot{u}_i \qquad \ldots\ldots\ldots\ldots\ldots\ldots \quad 5:35$$

Dropping the subscript and integrating once, we obtain

$$\dot{u} = \left(\frac{kv-1}{\tau}\right) u + \dot{u}_o \qquad \ldots\ldots\ldots\ldots\ldots\ldots 5:36$$

$$\dot{u} = \left(\frac{kv-1}{\tau}\right)\left(u + \frac{\dot{u}_o \tau}{kv-1}\right) \qquad \ldots\ldots\ldots\ldots\ldots\ldots 5:37$$

$$\ln\left[u + \frac{\dot{u}_o \tau}{kv-1}\right] = \frac{kv-1}{\tau} t + \ln A \qquad \ldots\ldots\ldots\ldots\ldots\ldots 5:38$$

$$u = -\frac{\dot{u}_o \tau}{kv-1} + Ae^{\left(\frac{kv-1}{\tau} t\right)} \qquad \ldots\ldots\ldots\ldots\ldots\ldots 5:39$$

REFERENCES FOR APPENDIX II

1. See Appendix I of this report for a description of the Adaptronics, Inc. Self-Organizing Controller.

2. Theory of Probability State Variable Systems, Vol. III: Monotype System Theory and Considerations from Automata Theory, by L. O. Gilstrap, Jr. et al., Adaptronics, Inc. Technical Documentary Report, Contract AF 33(657)-7100, ASD-TDR-63-664, AF Avionics Laboratory, AD #428087, December 1963.

3. Self-Organizing and Learning Control Systems, by R. L. Barron, invited paper presented at the 1966 Bionics Symposium, May 2-5, 1966, Dayton, Ohio.